



UNIVERSITY OF TARTU

Understand your data: observational selection effect



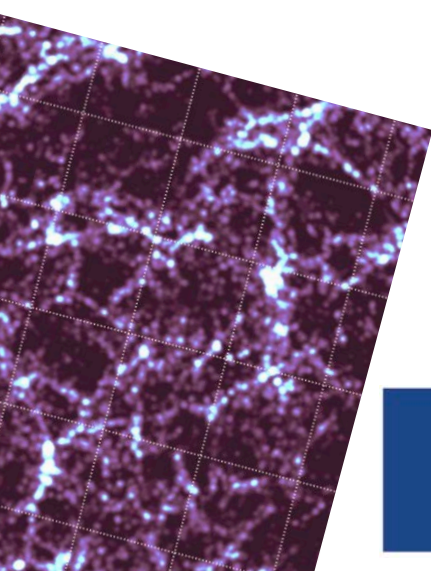
Co-funded by
the European Union



Investing
in your future



Funded by
the European Union





credit: ESA

Perseus cluster, Euclid first images

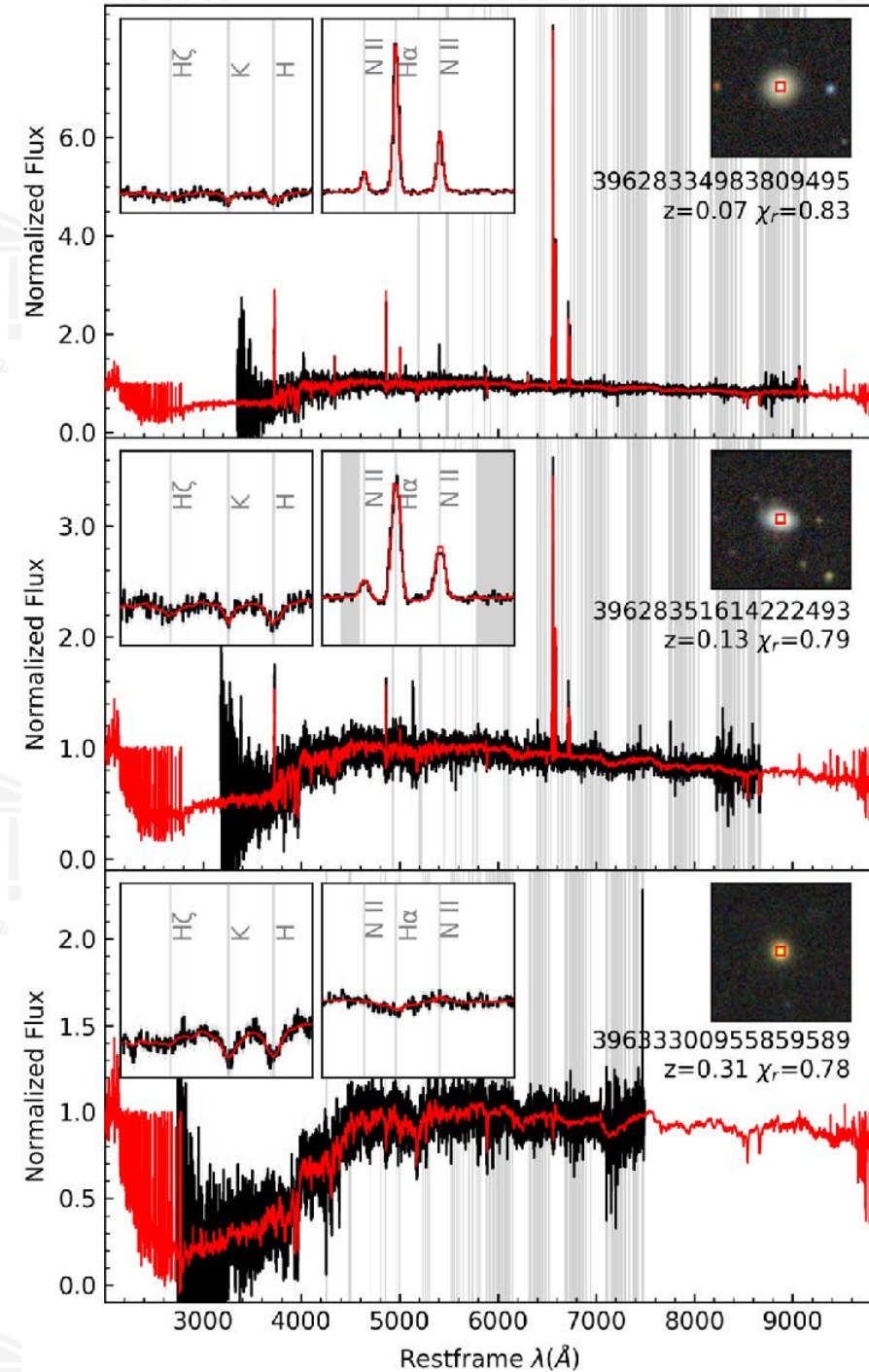
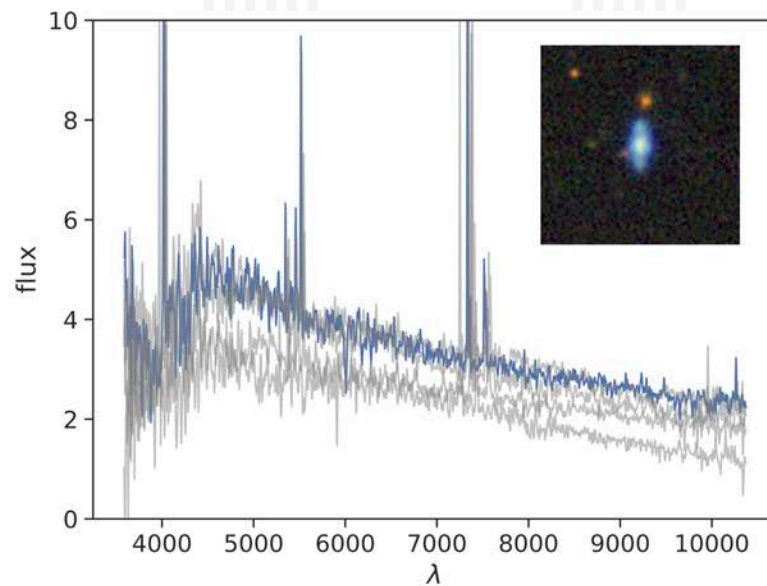
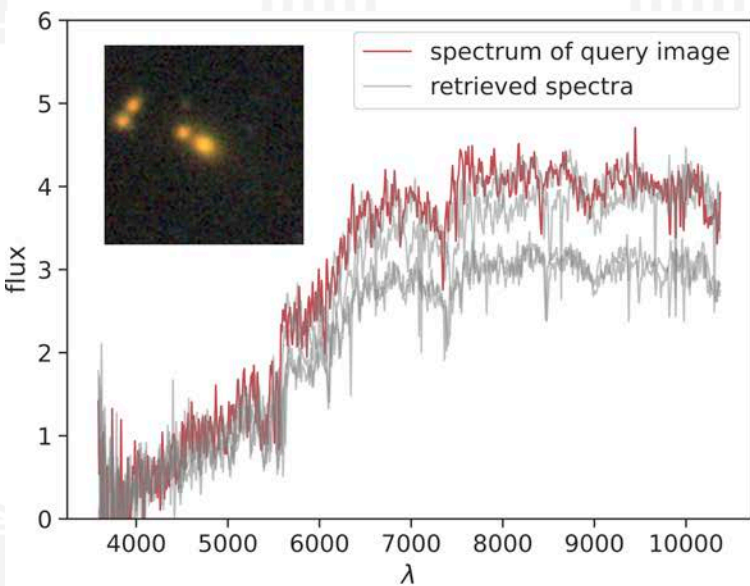
Observed Cosmic Web (Tempel lectures)

- Cosmic Web as revealed in observations
- Galaxy redshift surveys - biased overview
- 4MOST WAVES and 4HS surveys - mapping the Universe
- Preparind a redshift survey - 4MOST example
- Understand your data: observational selection effects
- Galaxy Groups in redshift surveys
- Filaments in the Cosmic Web
- Selected science topics in Tartu Observatory



Disclaimer:

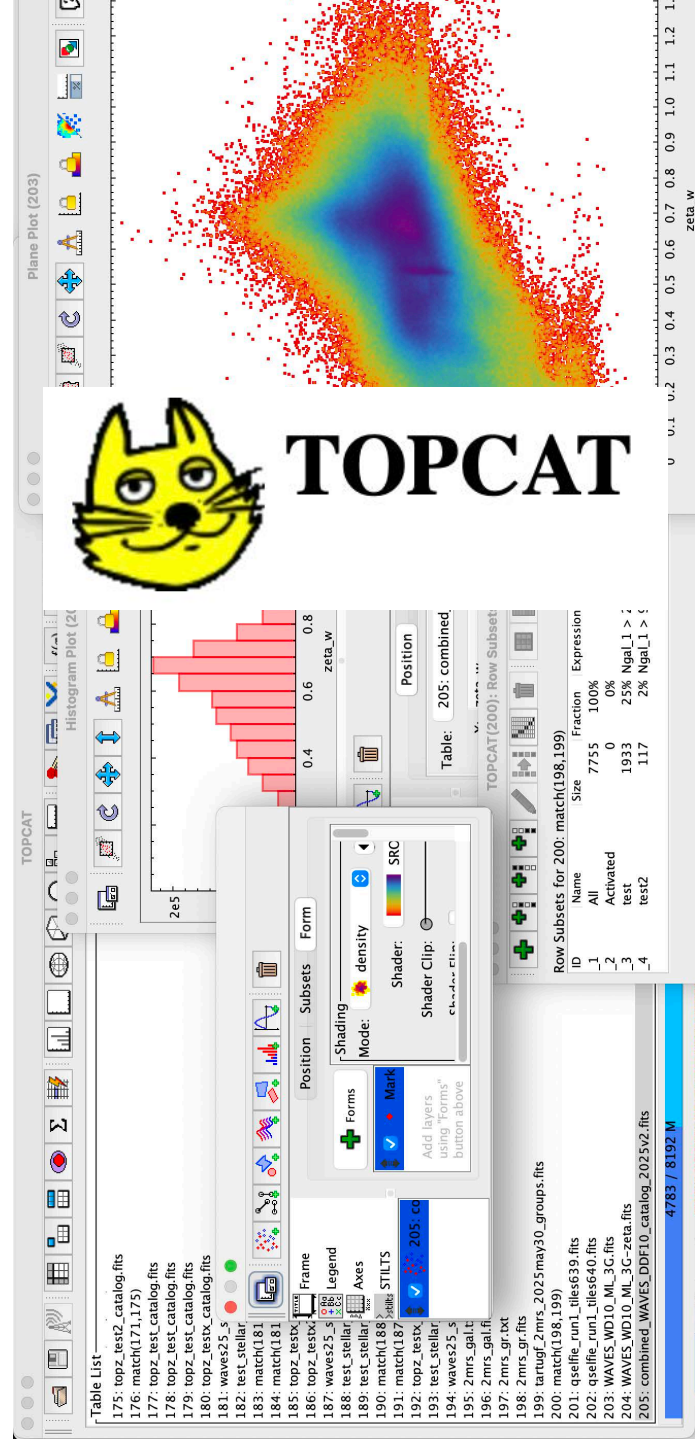
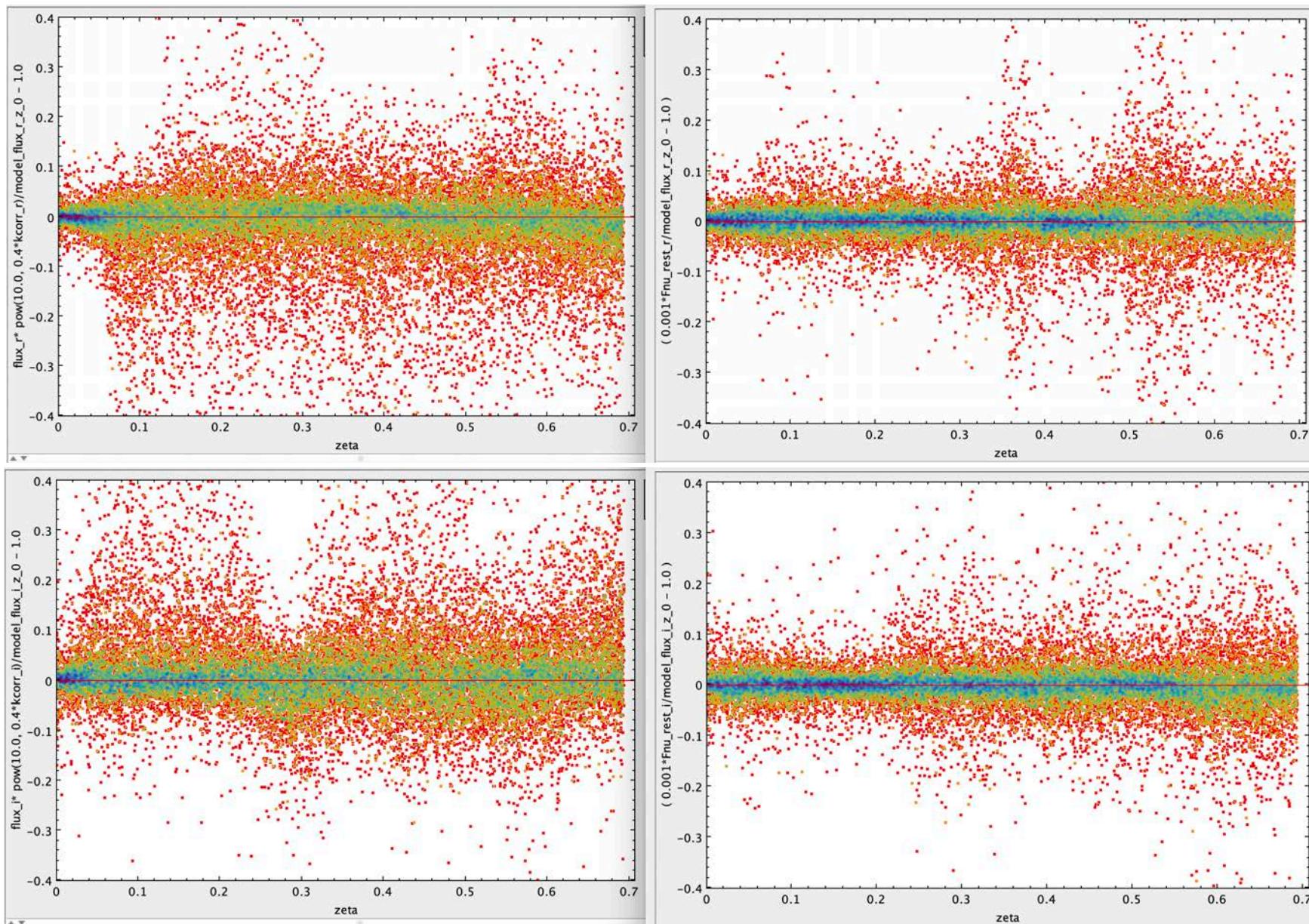
- I'm not a real cosmologist!!
- I'm playing the role of 'observational methods' lecturer.
- I'm focussing on *concepts* more than results.
- I'm showing plots that helped build my understanding, so lots are mine or my friends'.
- Please don't take this as a review!!

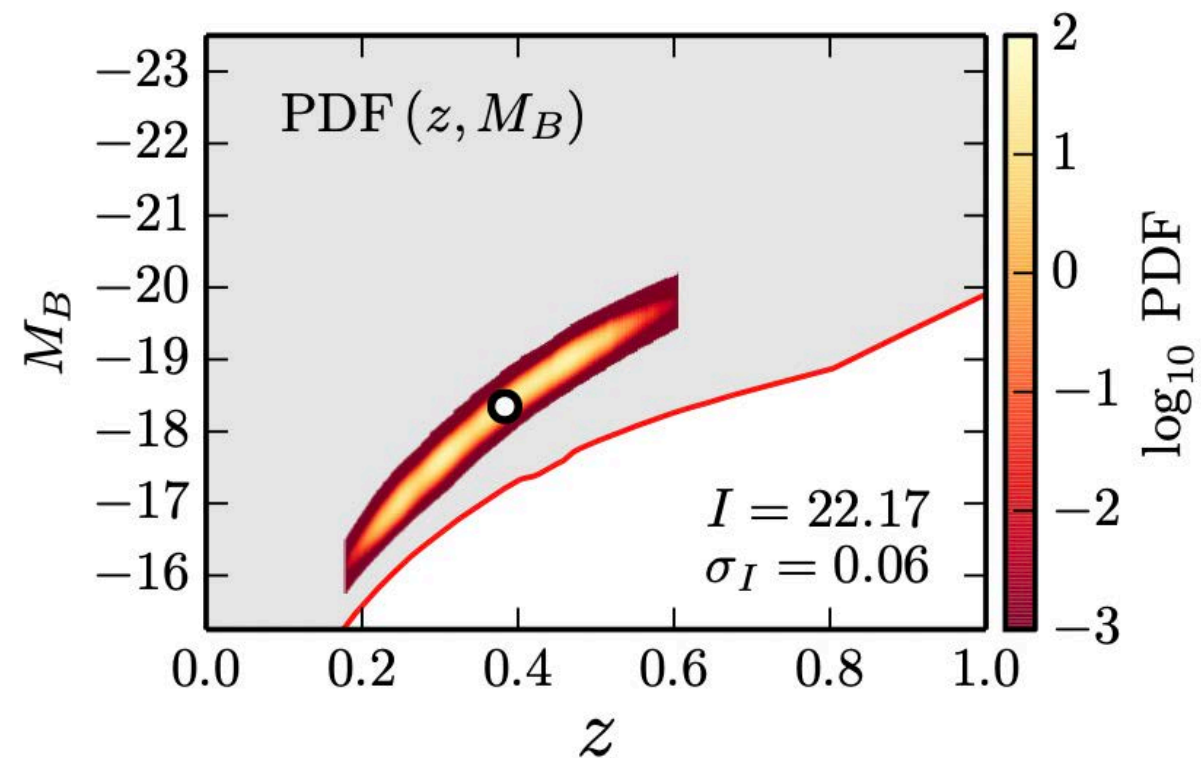
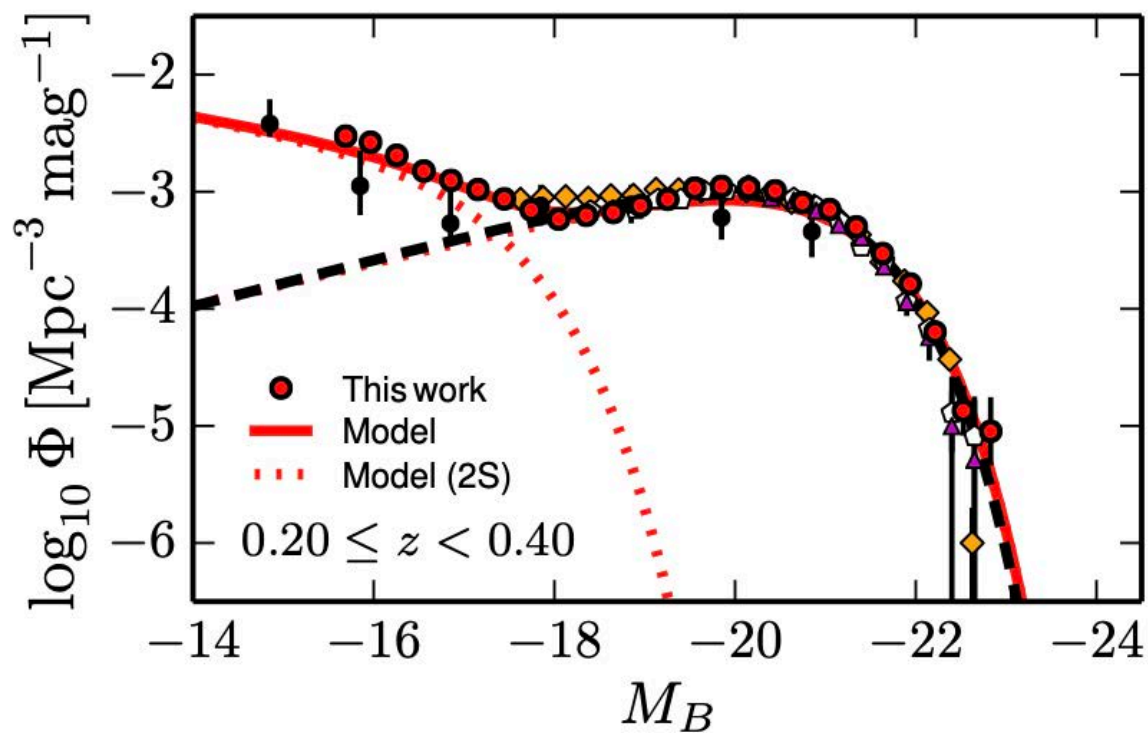


Galaxy spectra

r

i





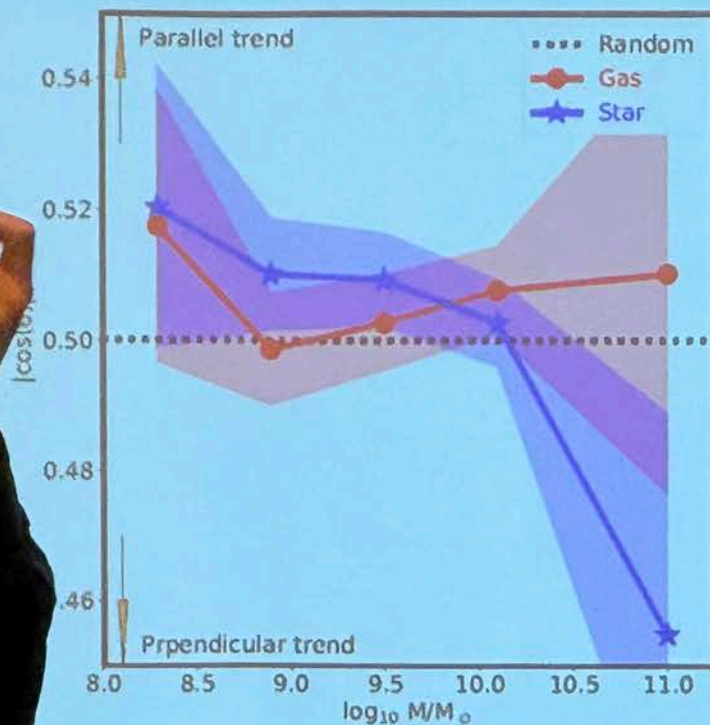
Redshift uncertainty

No one trusts simulations,
except the person who made them!

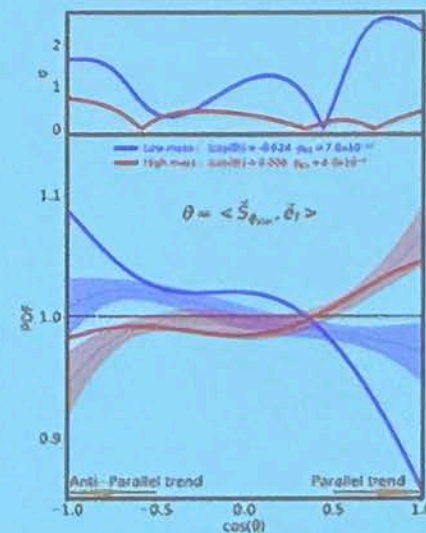
Everyone trusts observations,
except the person who collected the data!



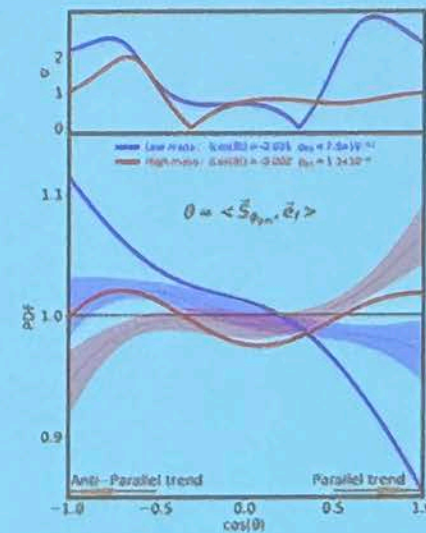
Spinning Filaments – Spinning Gals: parallel vs. anti-parallel ?



stellar comp.

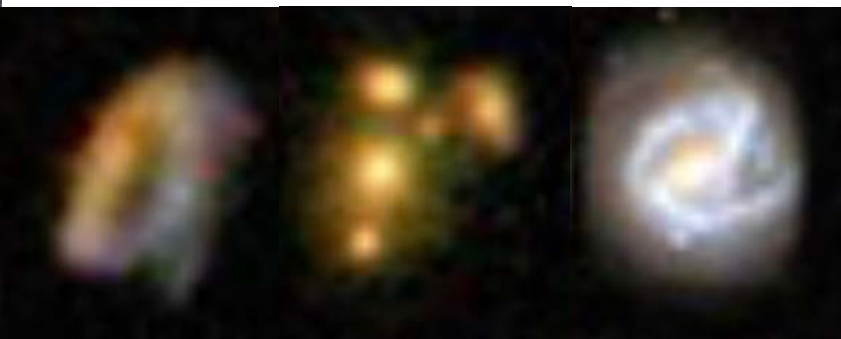


gas comp.

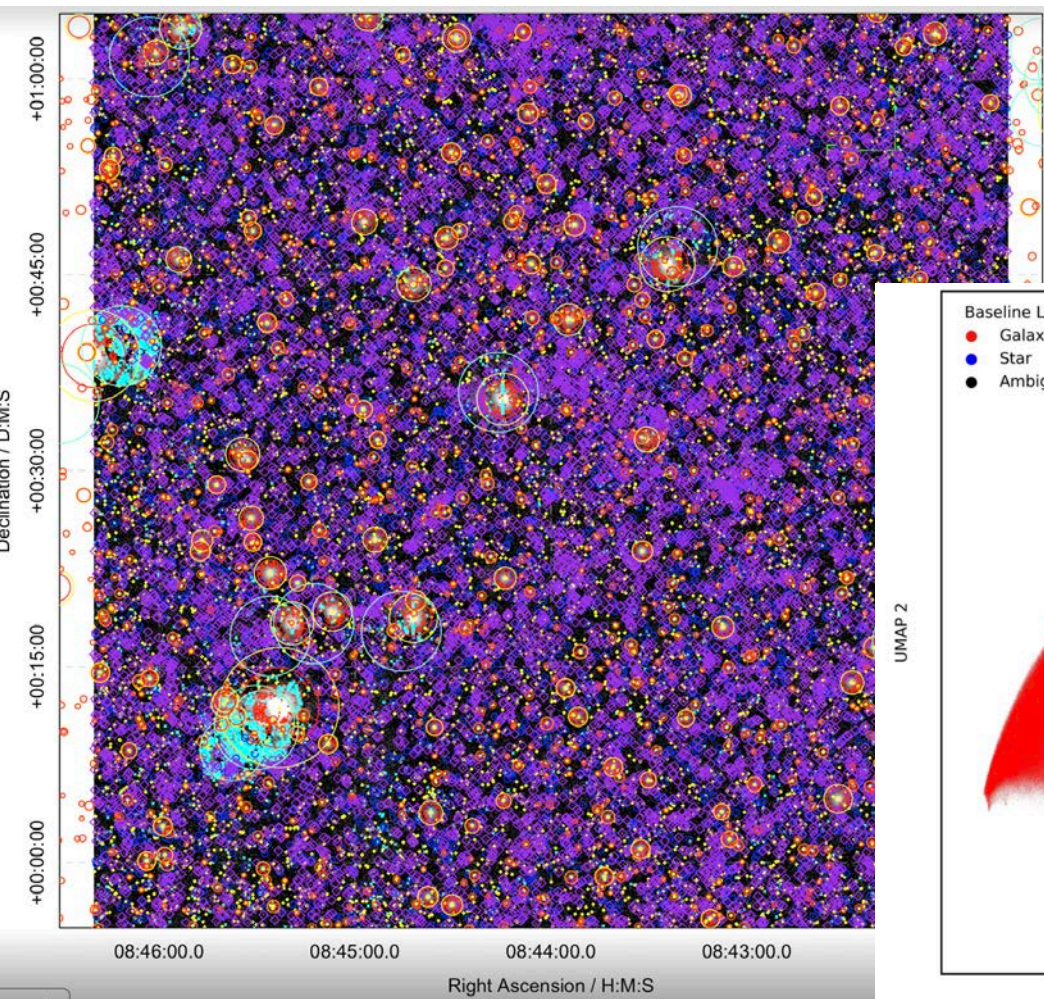


Wang et al. 2025

Sample MaNGA galaxies (IFU)



Masking stars, ghosts, artefacts



Star-galaxy separation

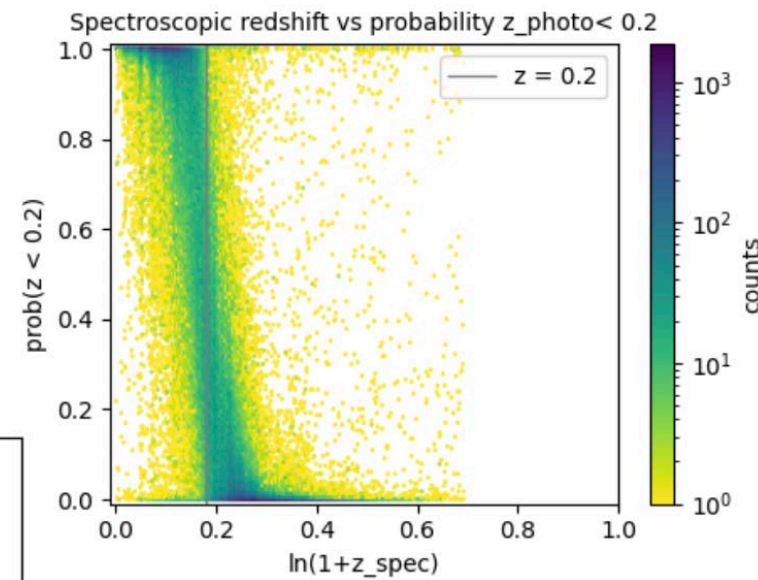
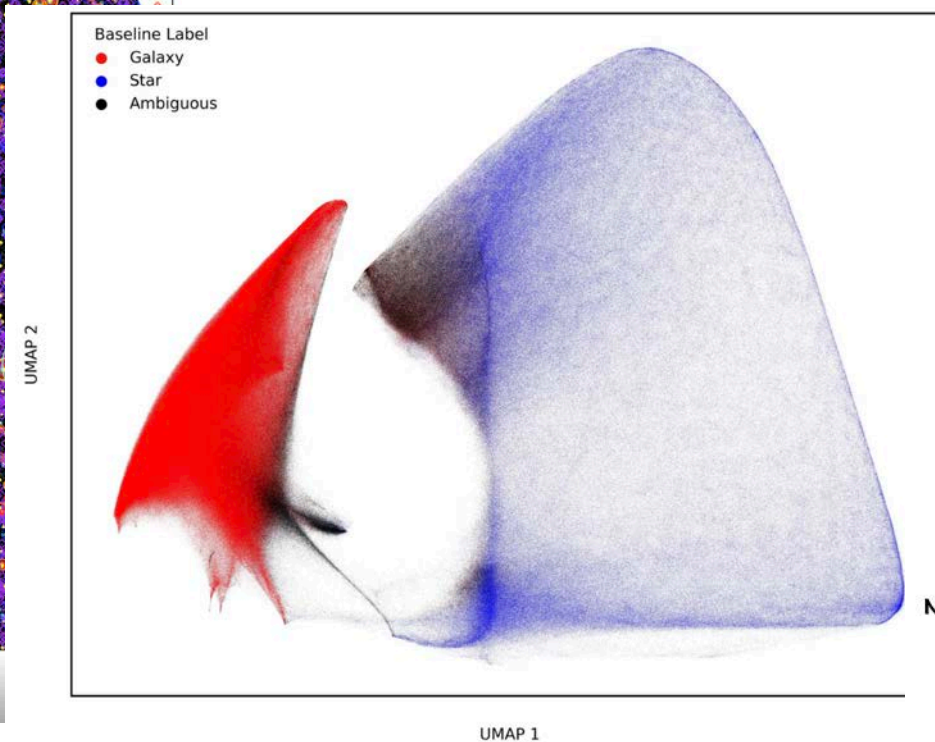
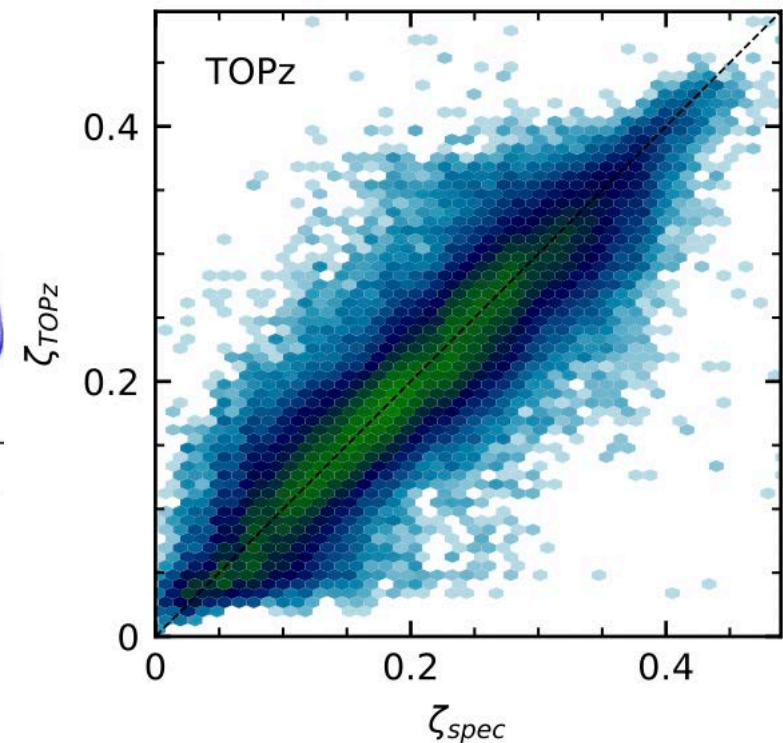
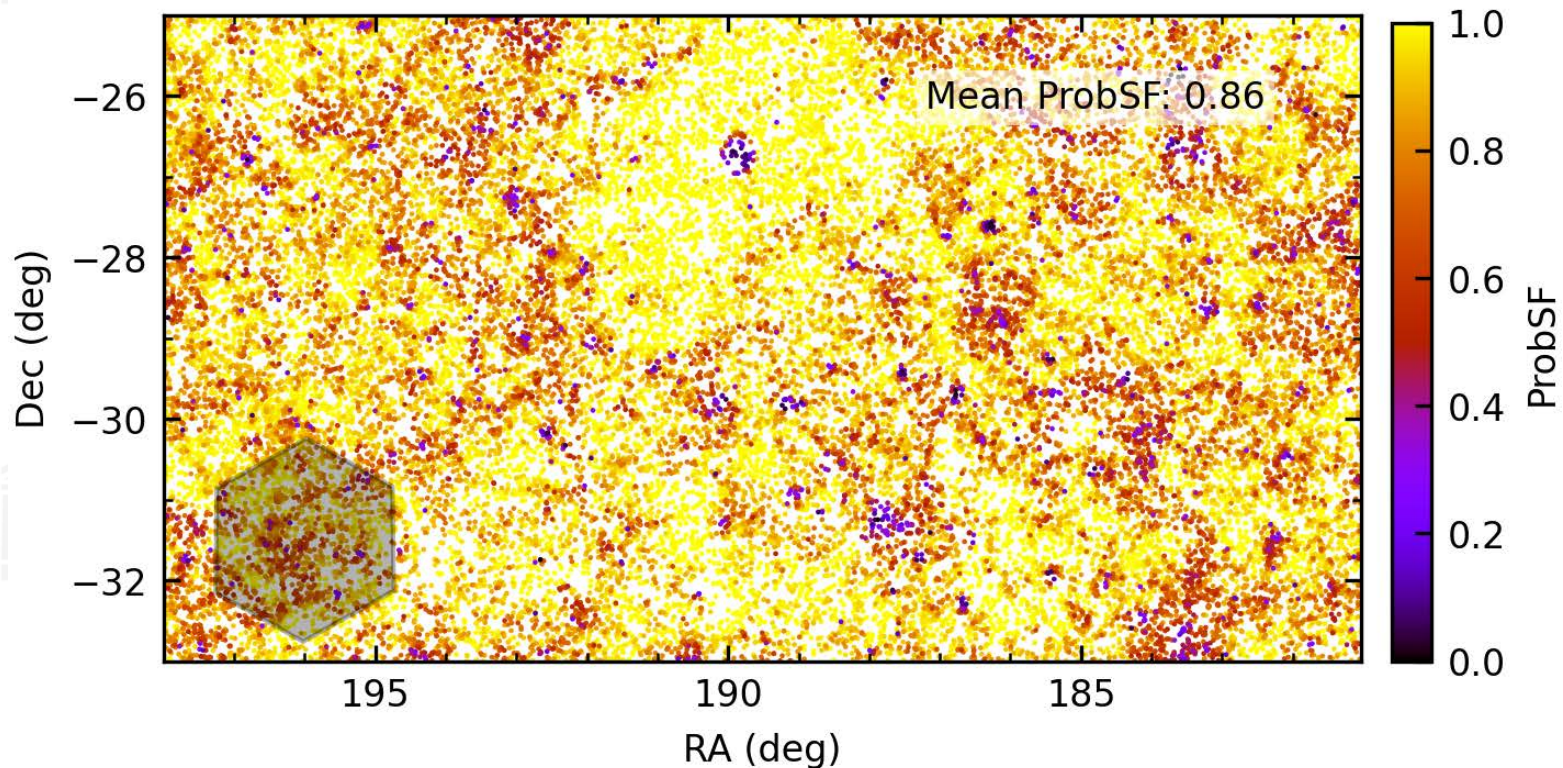
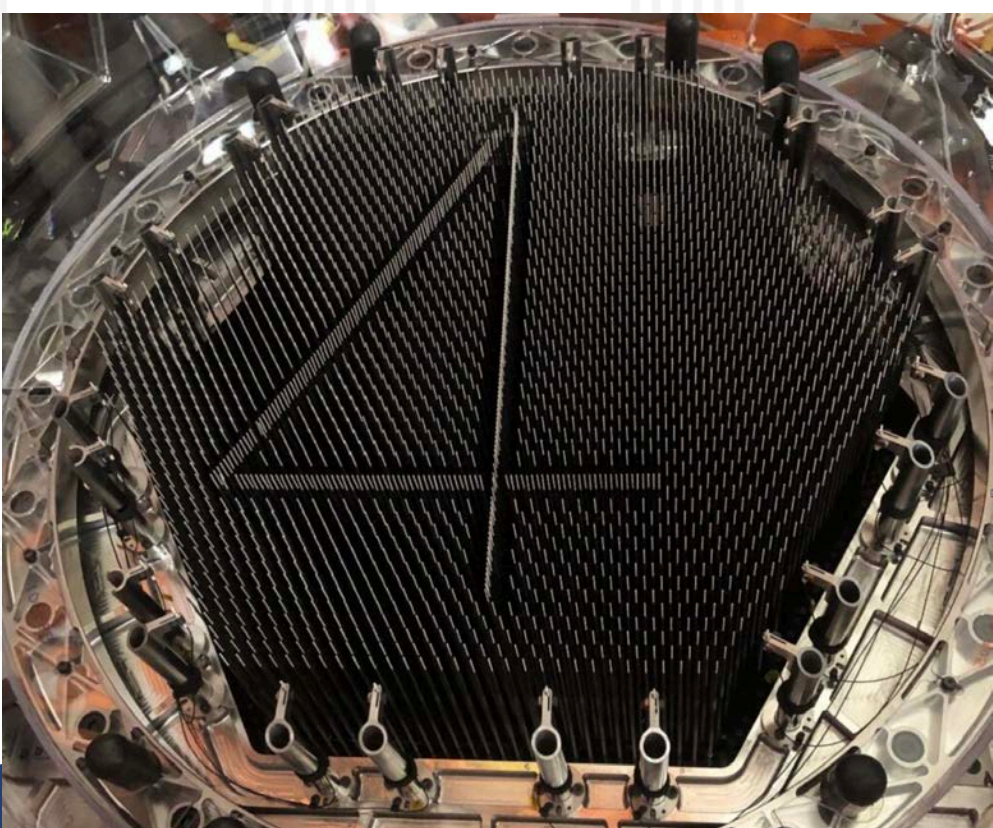


Photo-z preselection



4MOST WAVES survey - target catalogue preparation



Efficiency vs completeness

Fixed fibre pattern

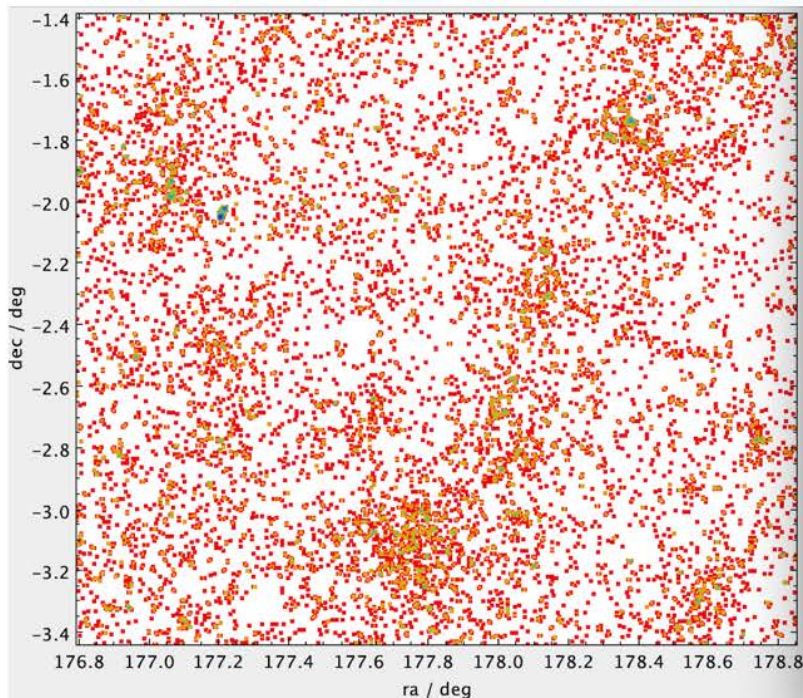
Limited patrol area for each fibre

- all fibres are used
- not all targets are observed

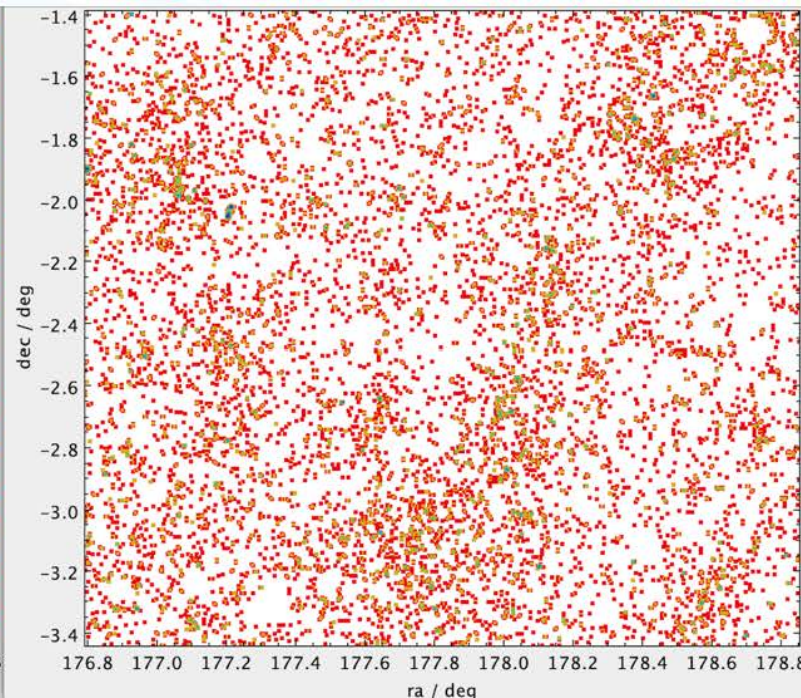
- all targets are observed
- many fibres are empty

Incompleteness in High-Density Areas

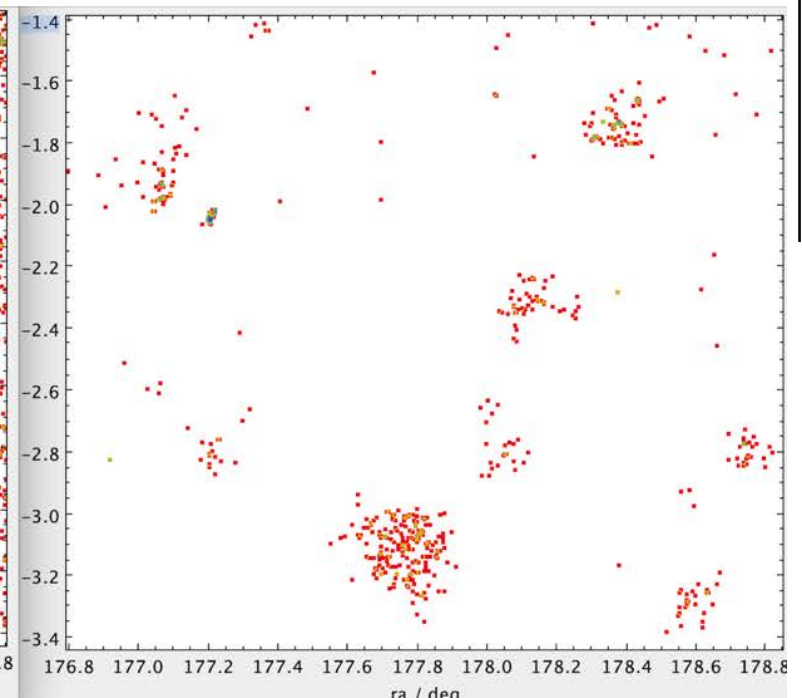
4MOST selection function



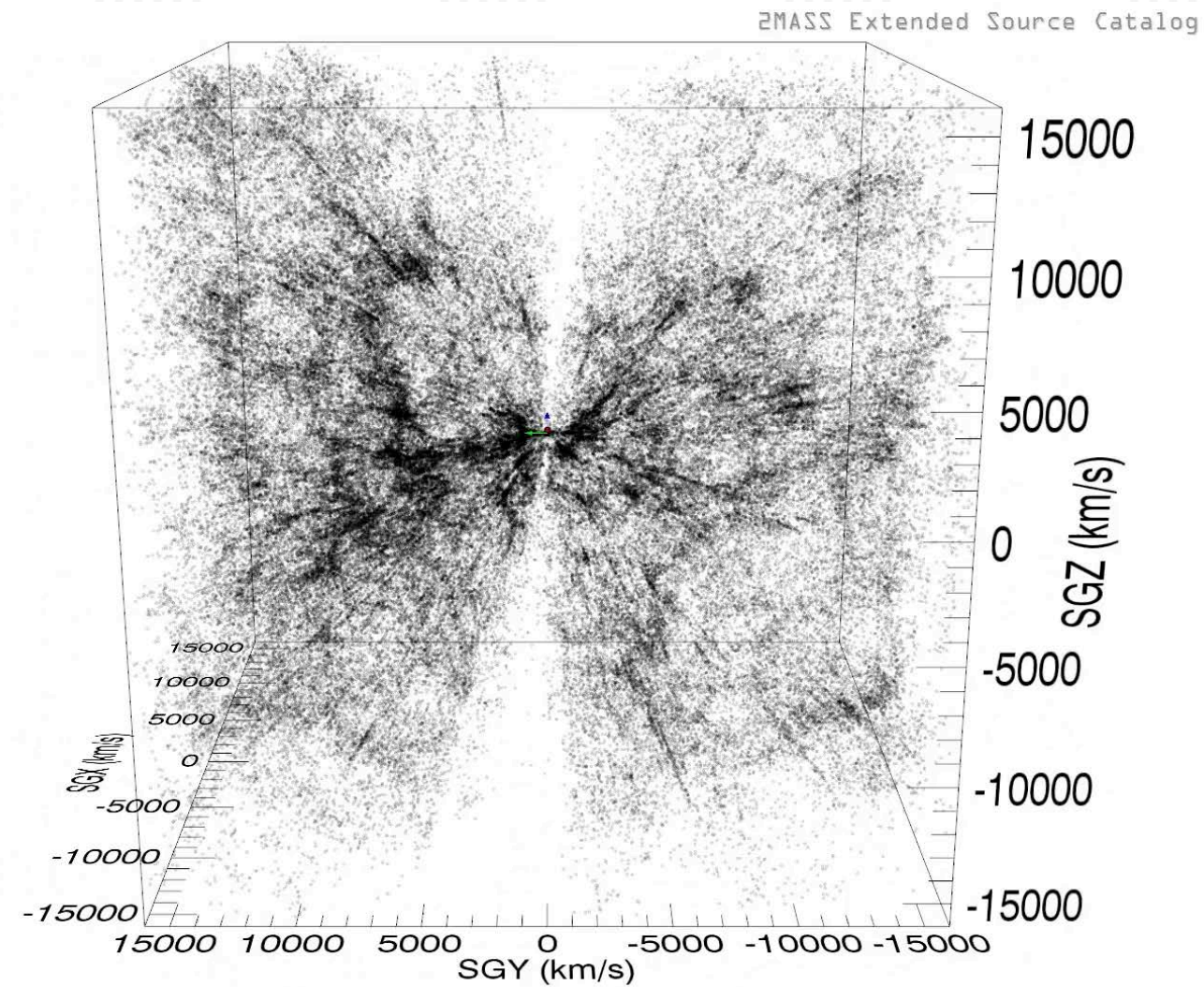
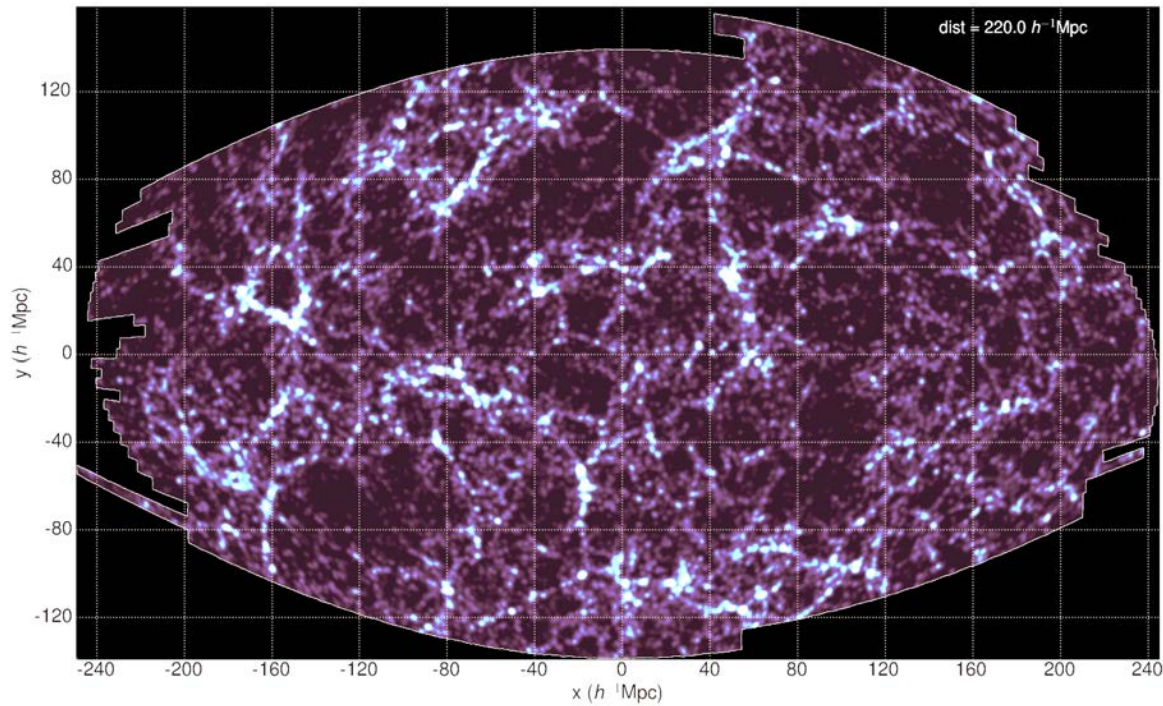
Original catalogue



Observed galaxies



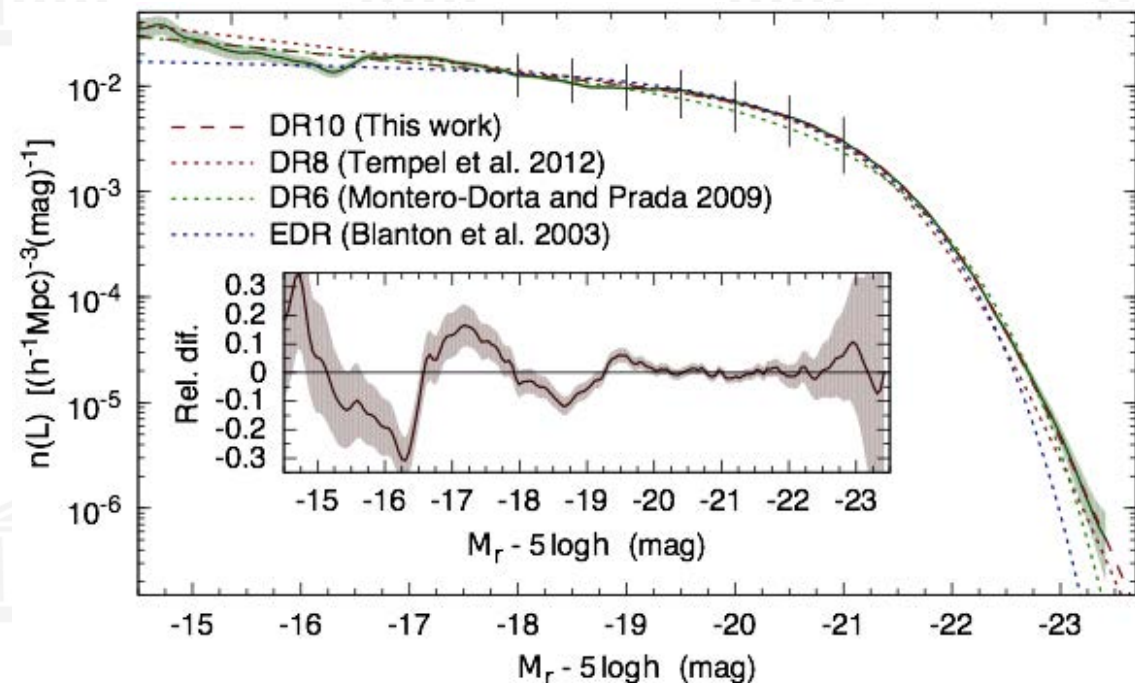
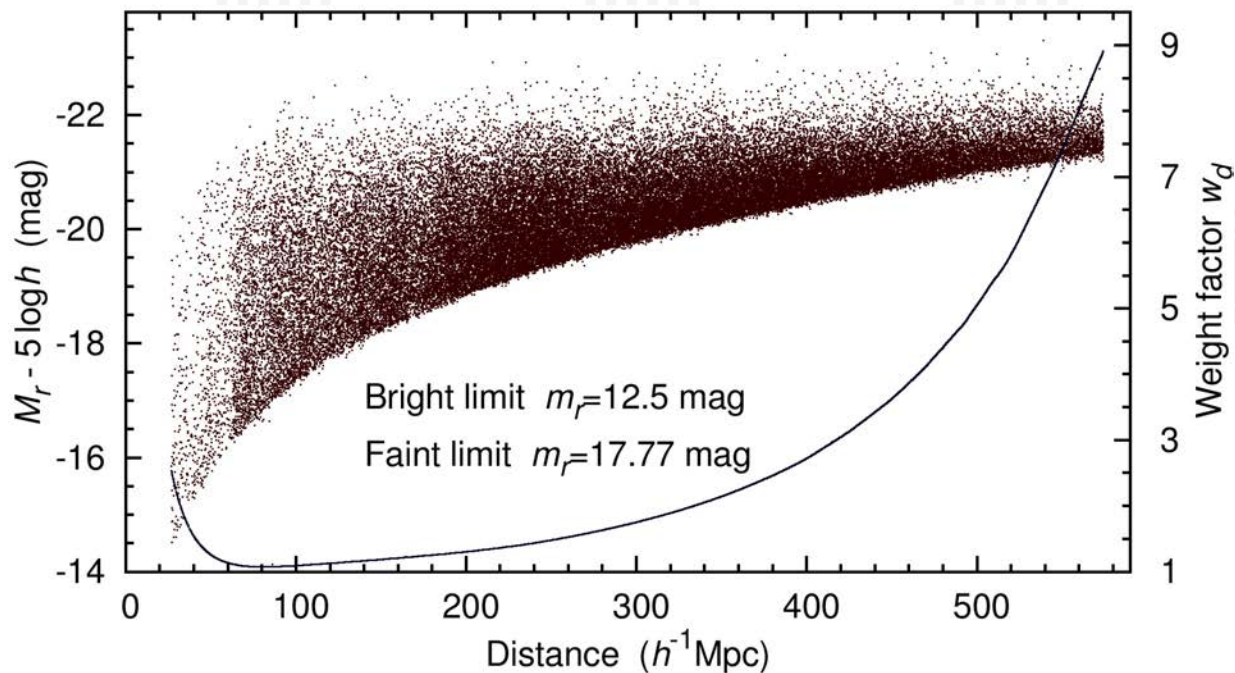
Unobserved galaxies



Fingers of god effect

Tully & Fisher (1978), IAU Symposium 79,
Large Scale Structures in the Universe,
Tallinn, 1977

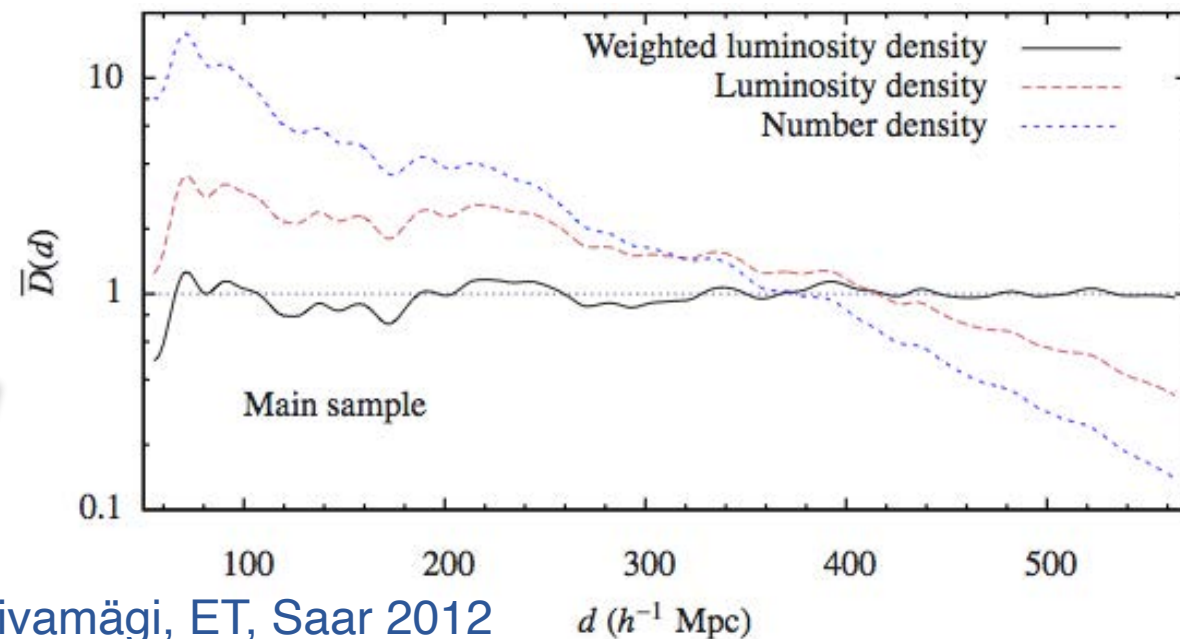
Credit: Tully et al. 2014



ET et al. 2012, 2014

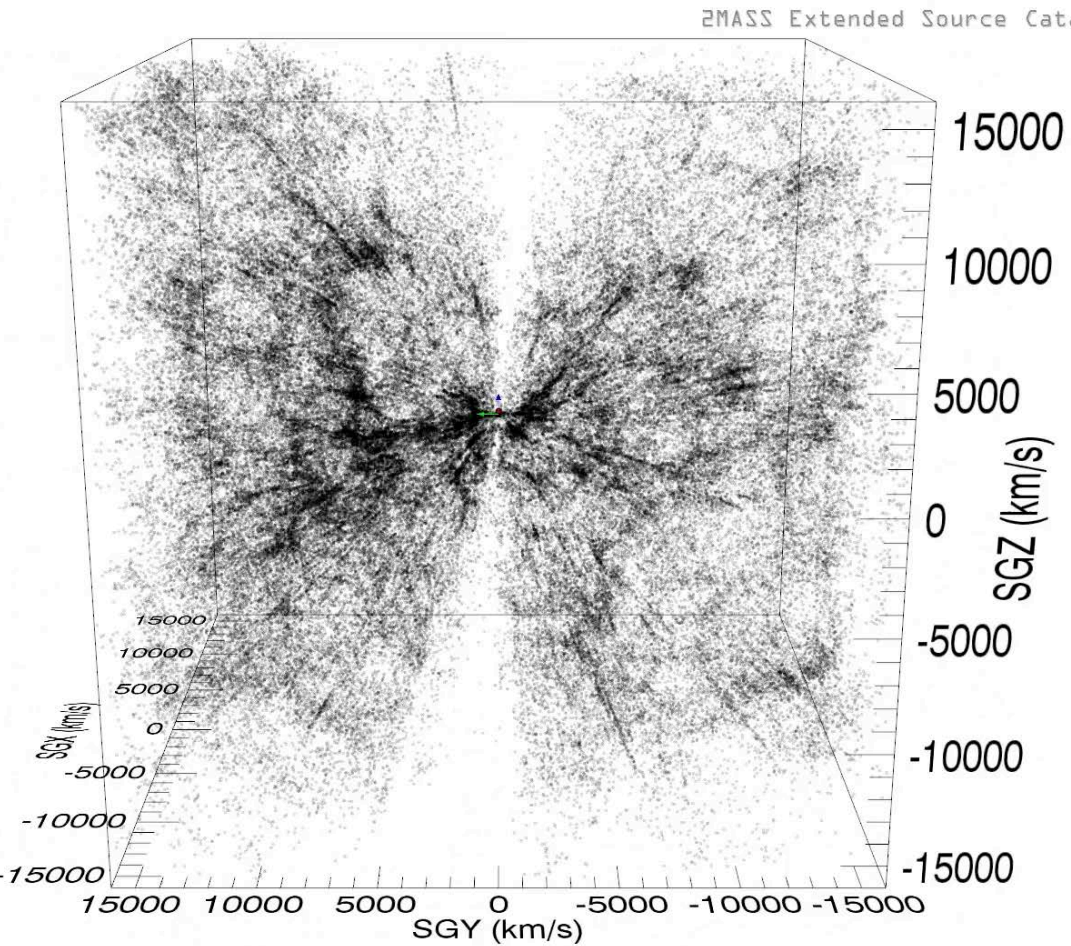
Flux-limited survey effect

Fainter galaxies are missing



Liivamägi, ET, Saar 2012

Observations: selection effects



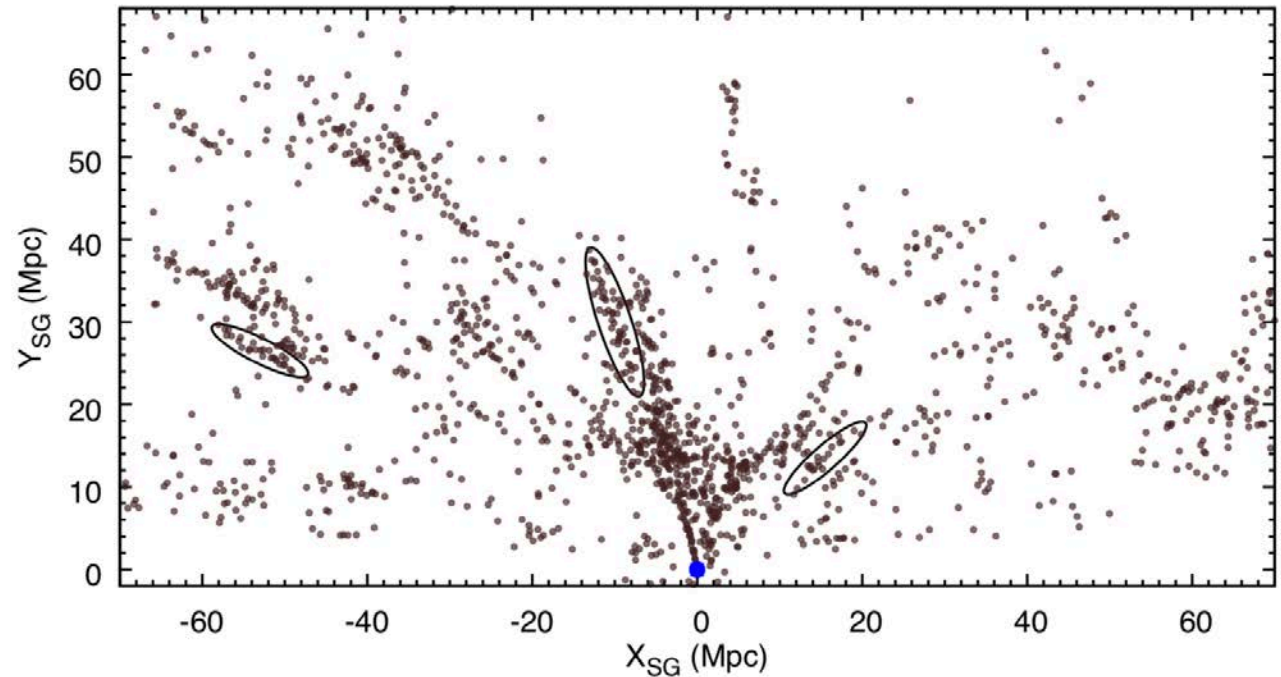
Courtesy: Tully et al. 2014

Fingers-of-god effect:

Tully & Fisher (1978), IAU Symposium 79, Large Scale Structures in the Universe, Tallinn, 1977

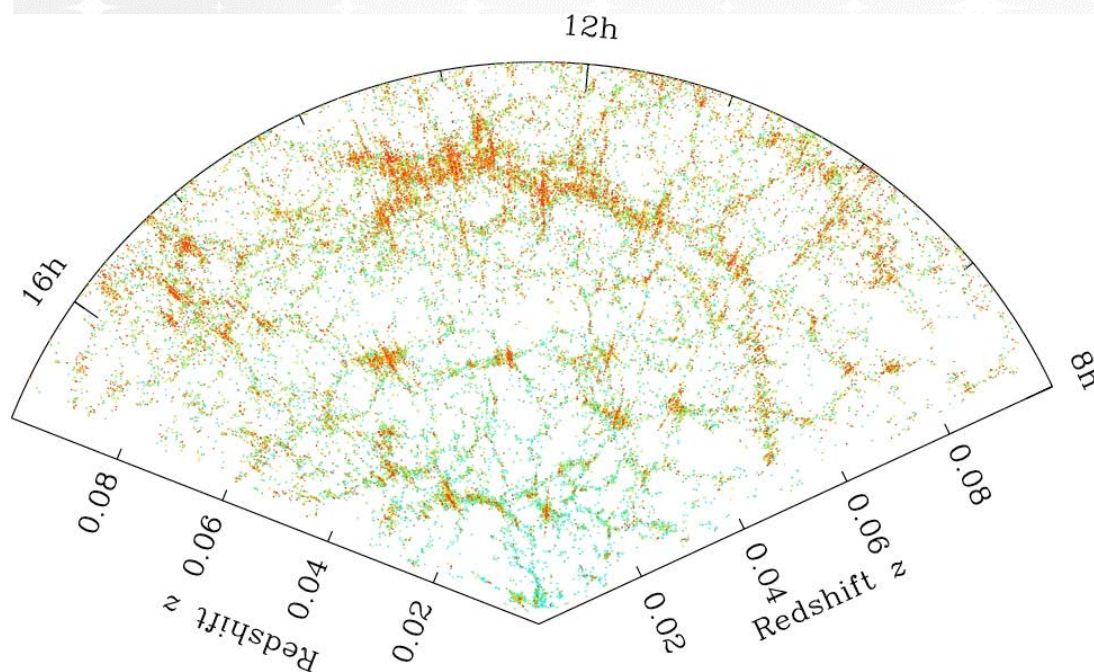
Detecting galaxy groups and clusters:

- Friends of friends
- Marked point processes



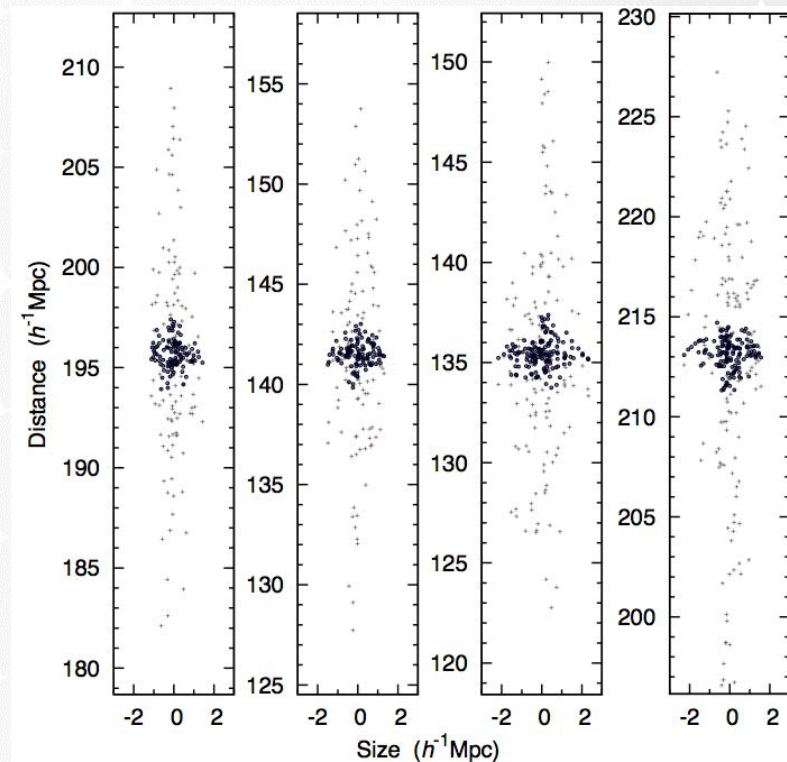
Tempel et al. (2012, 2014, 2017, 2018) 119

Observations: selection effects



Finger-of-god effect:

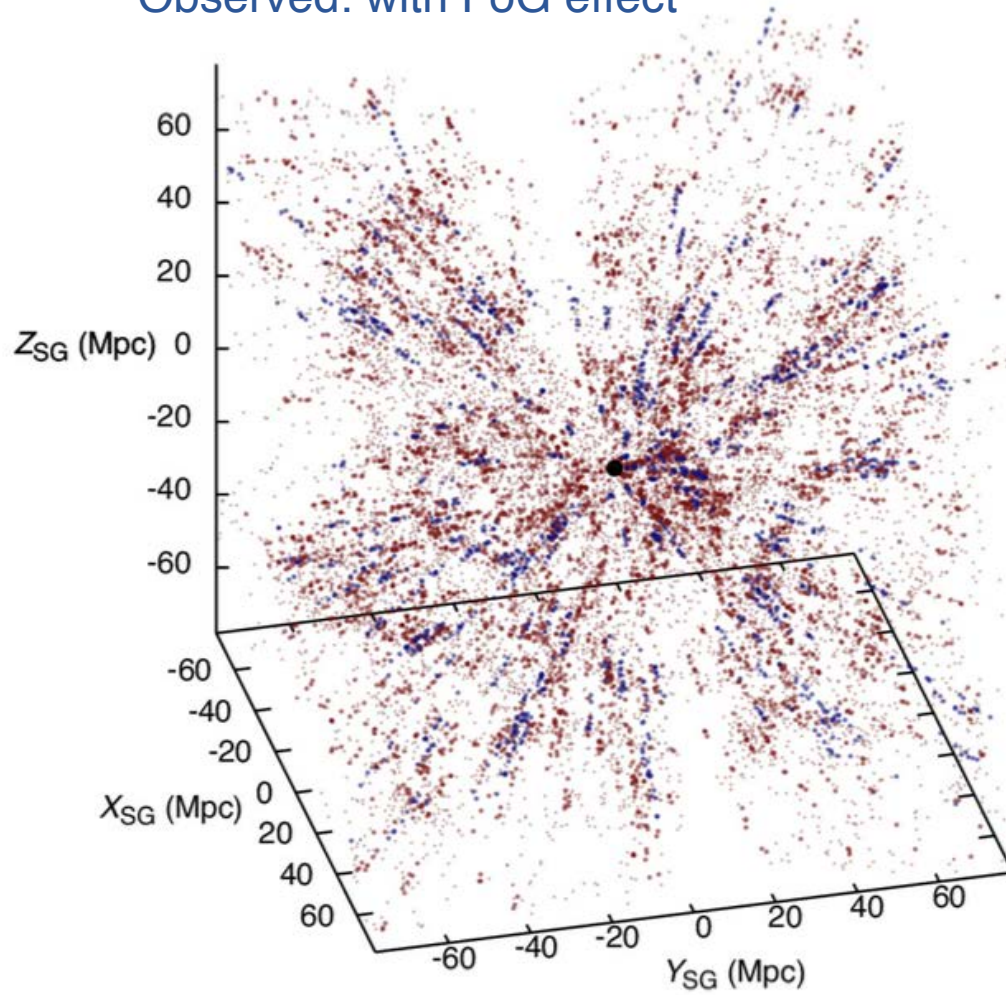
Tully & Fisher (1978), IAU Symposium 79,
Large Scale Structures in the Universe,
Tallinn, September 12-16, 1977



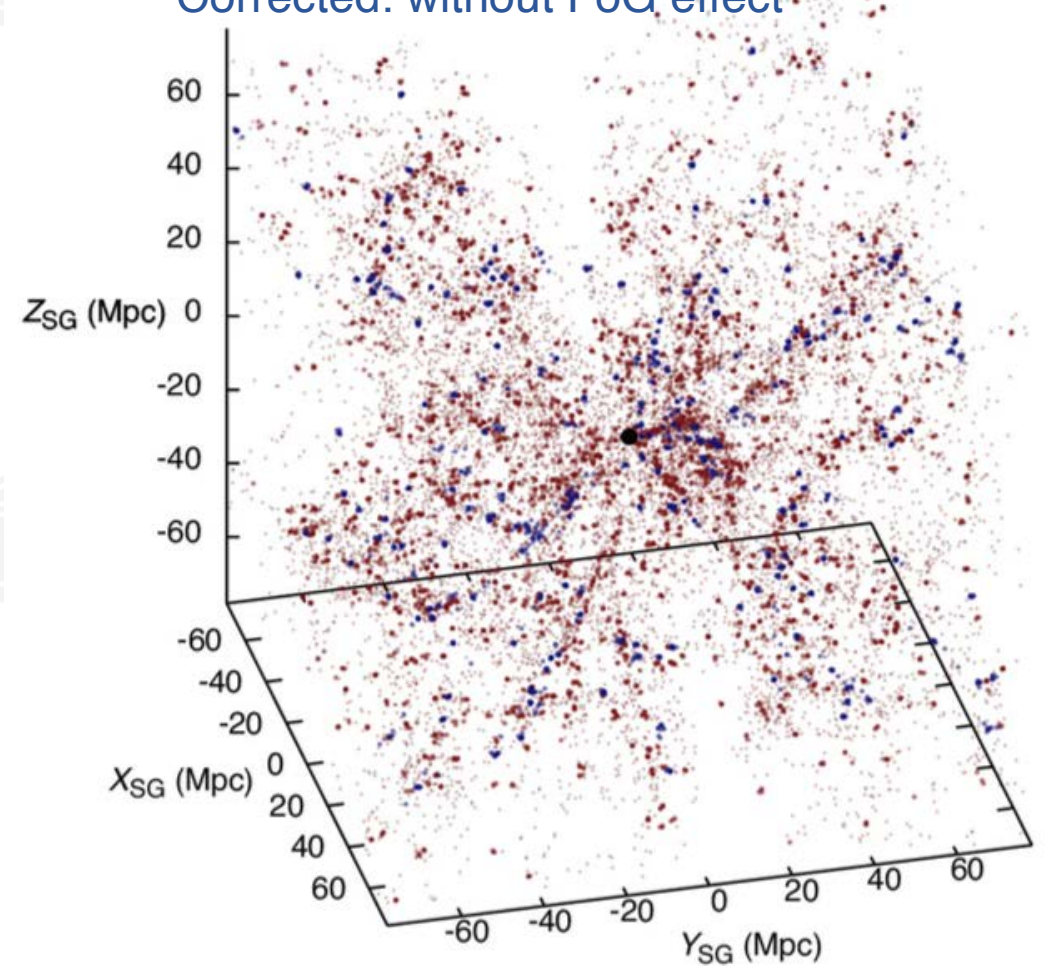
Tempel et al. (2012)

Using friends-of-friends galaxy groups,
we suppress the finger-of-god distortions.

Observed: with FoG effect



Corrected: without FoG effect



Fingers of god effect

Using galaxy groups to spherise groups

Detecting groups in redshift surveys:
ET et al. 2012, 2014, 2016, 2017, 2018

Luminosity function of galaxies

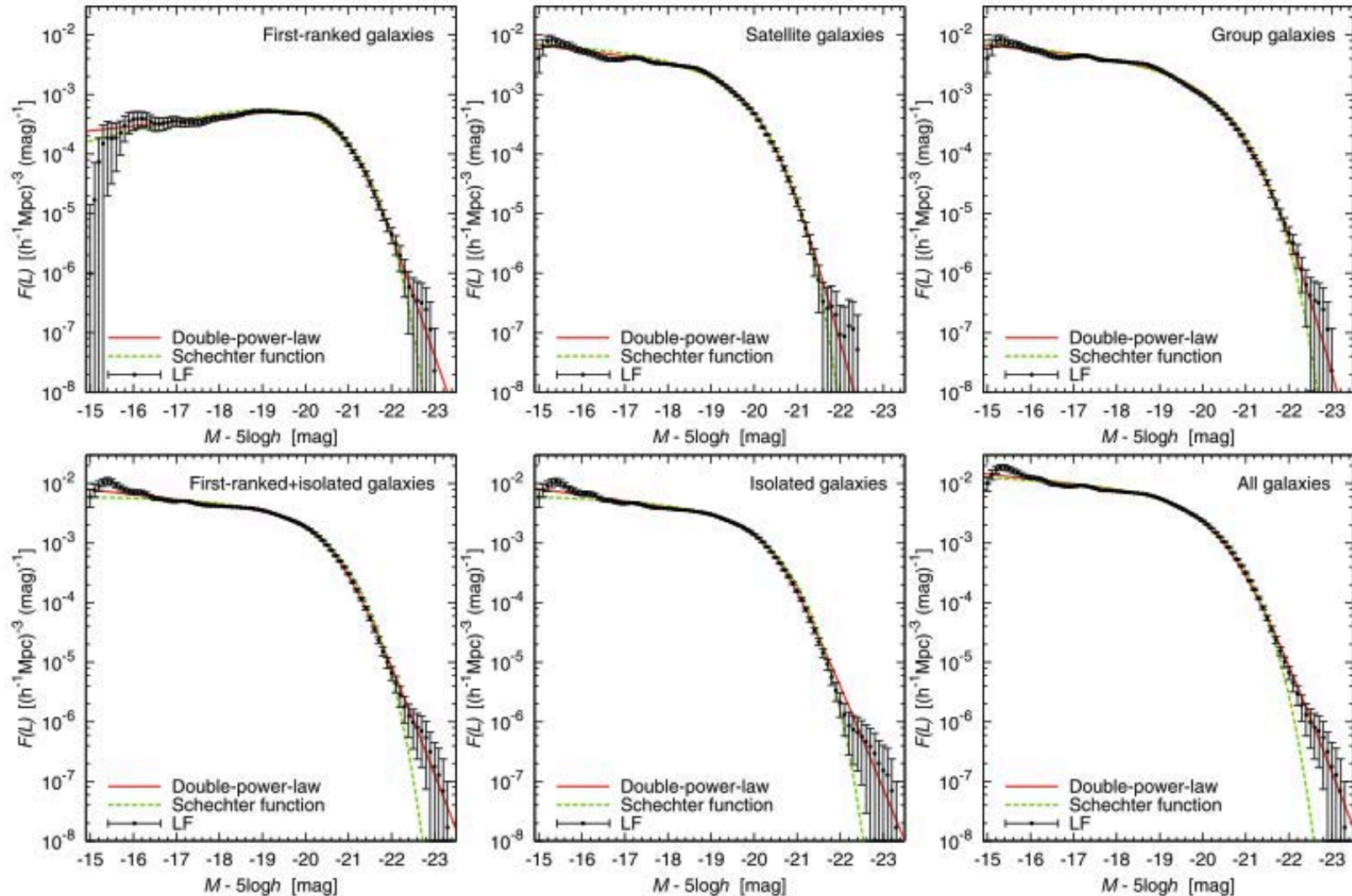


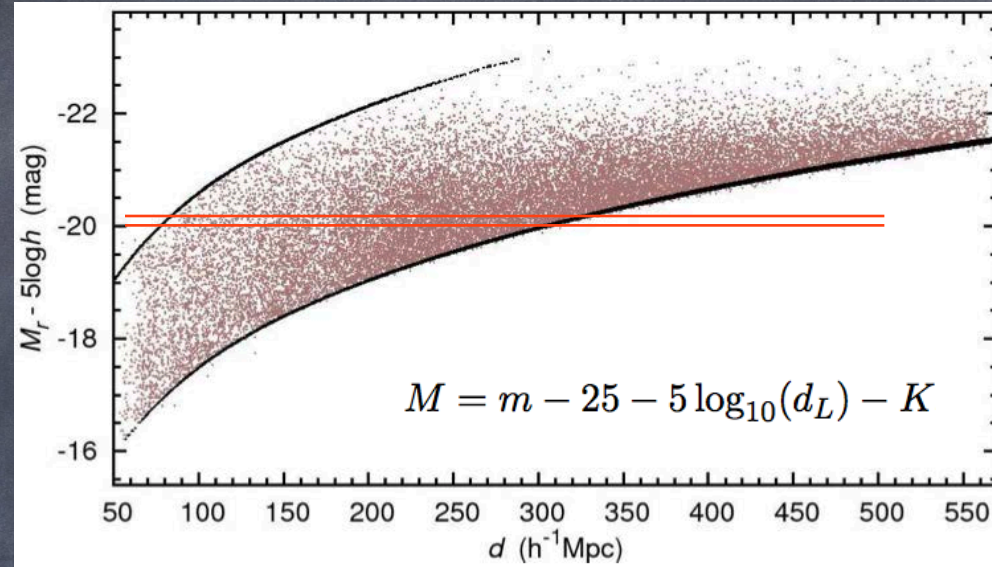
Fig. 13. Differential LFs for various galaxy populations: first-ranked, satellite, first-ranked+satellite (group), first-ranked+isolated, isolated and all galaxies. The points are LFs, using 2dF galaxy catalogue. Error-bars are Poisson $1-\sigma$ errors. The red solid line is the double-power law and the green dashed line is the Schechter function.

Luminosity function – new method

Standard $1/V_{\max}$ method:

$$n(L)dL = \sum_i \frac{\mathbf{I}_{(L, L+dL)}(L_i)}{V_{\max}(L_i)}$$

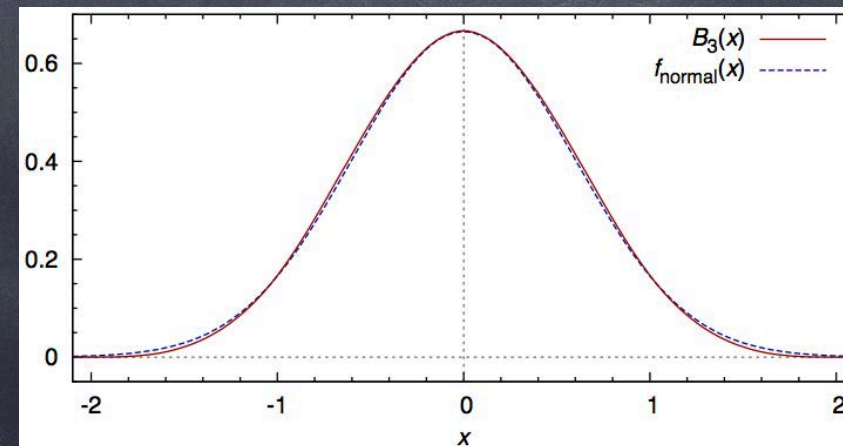
(binned density histogram)



Sum of kernels centered at the data points:

$$n(L) = \sum_i \frac{1}{V_{\max}(L_i)} \frac{1}{a_i} K\left(\frac{L - L_i}{a_i}\right)$$

(adaptive kernel estimation)

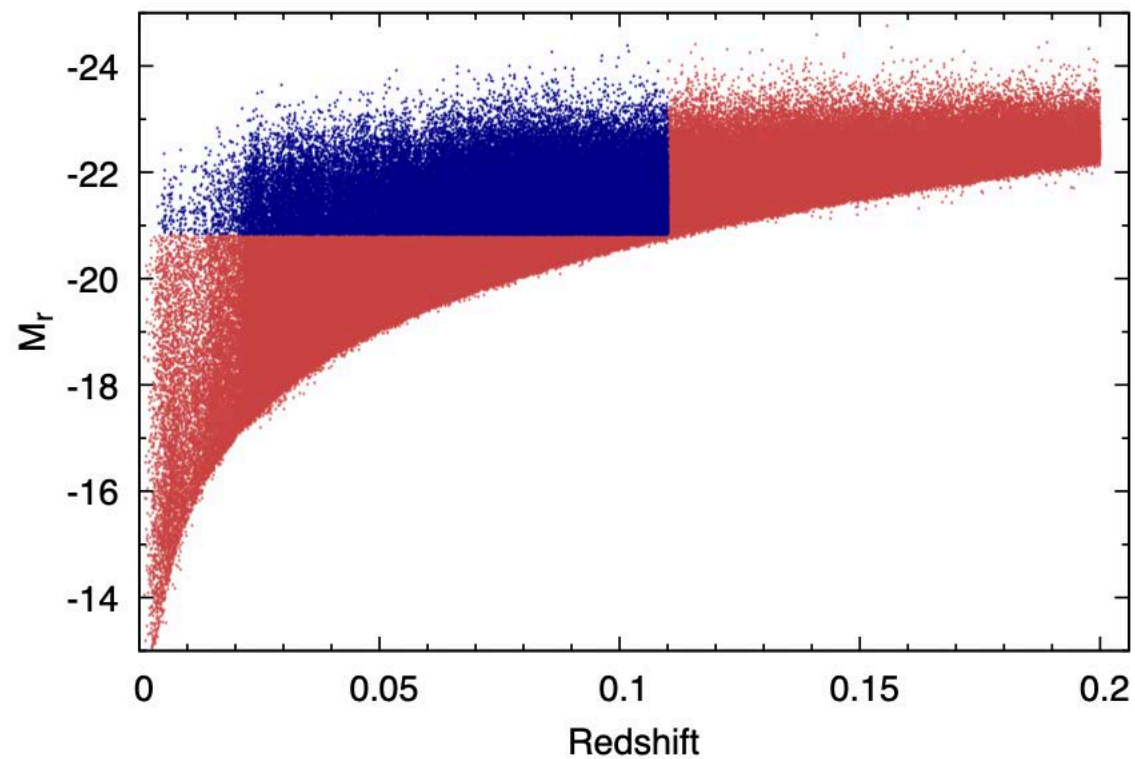
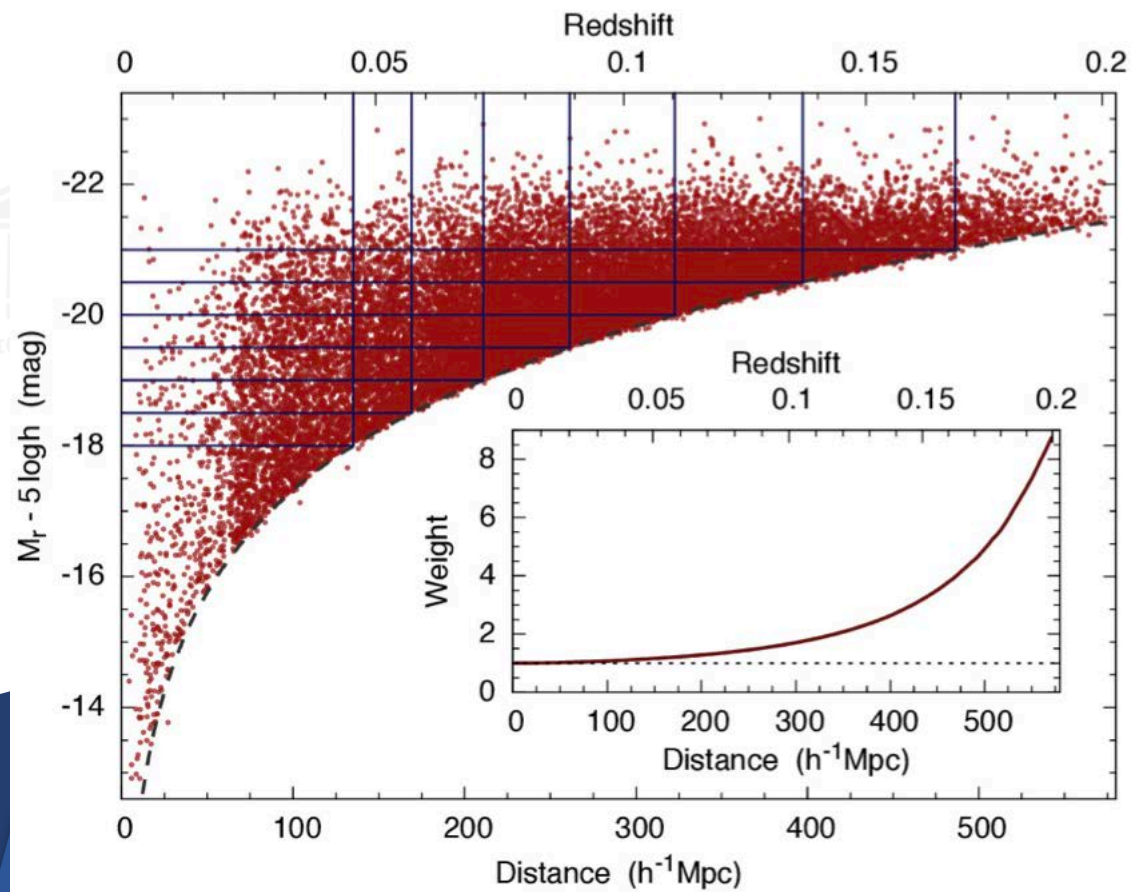


Error bars: smoothed bootstrap

Luminosity function of galaxies

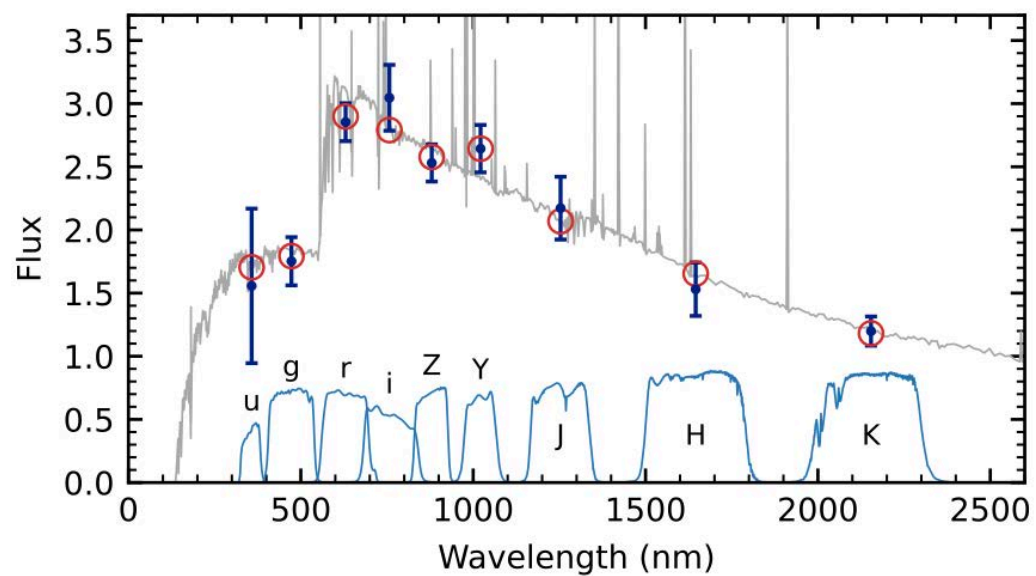
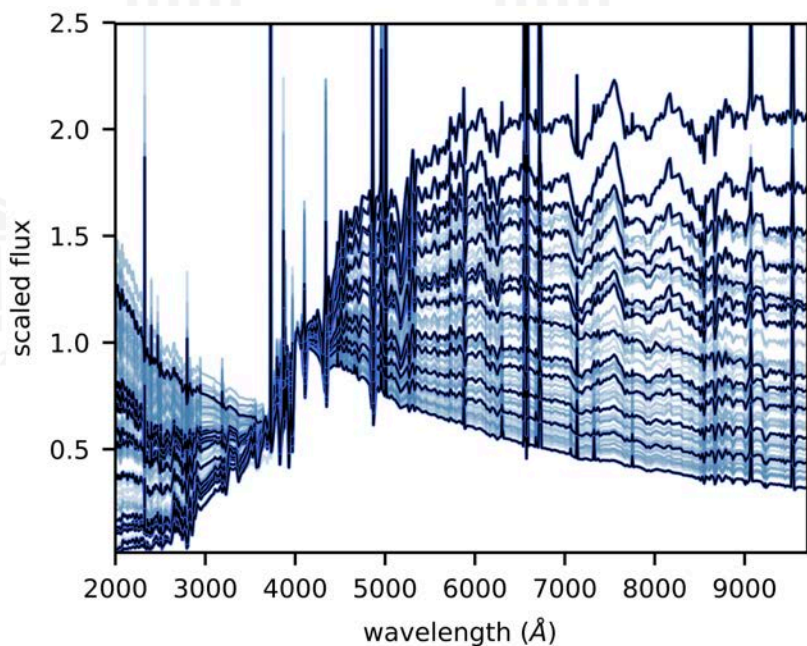
- flux-limited survey
- k-corrections - absolute luminosity
- galaxy dependent limiting distances
- dust effects on luminosity
- inclination angle effects
- surface brightness limitations
- incompleteness in redshift surveys
- redshift to distance conversion (pec vel)



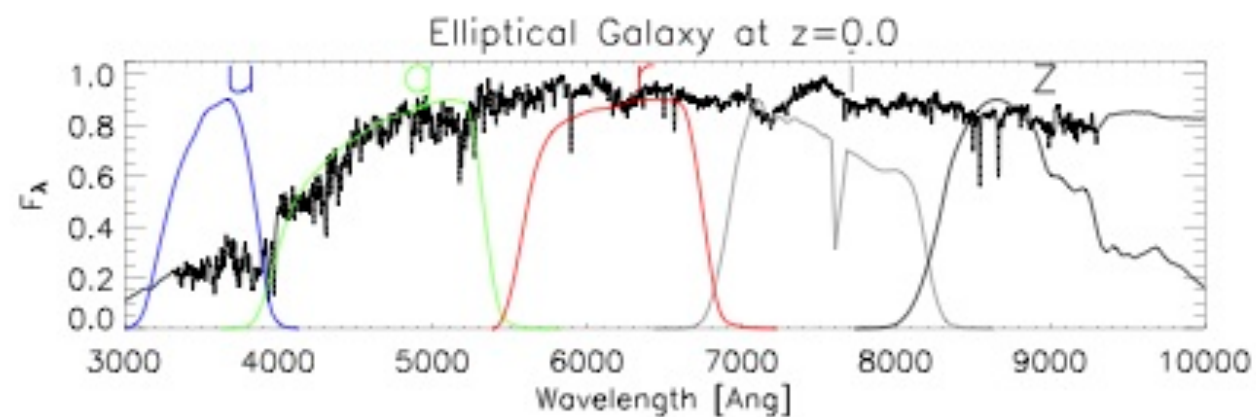
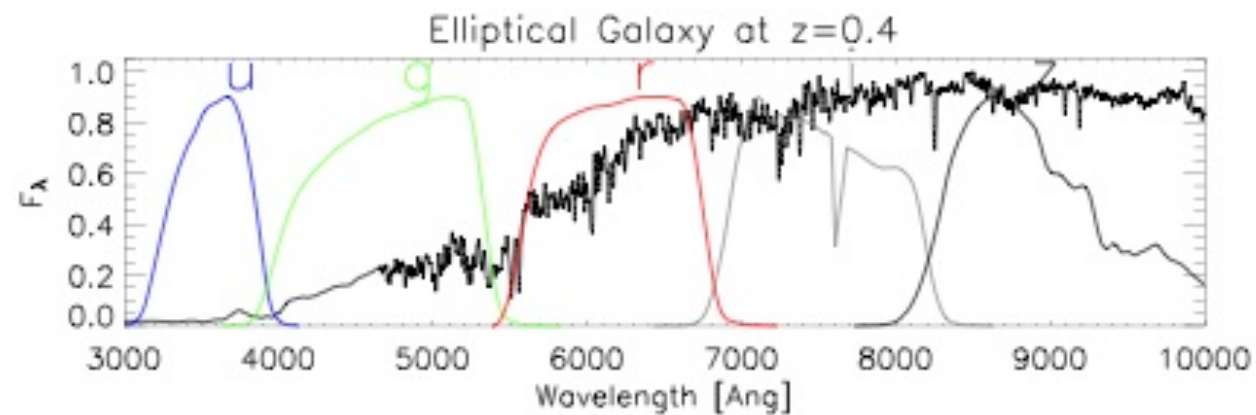
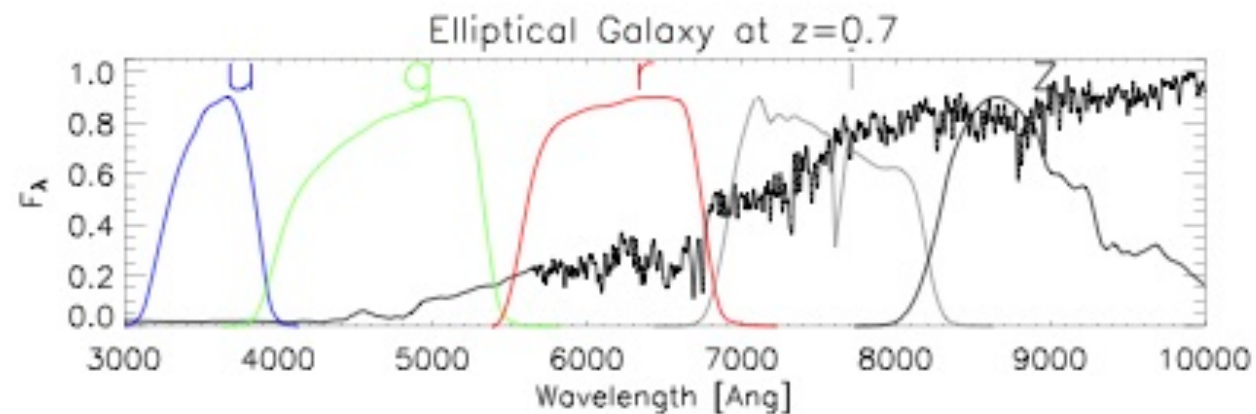


Flux vs volume limited

$$M_\lambda = m_\lambda - 25 - 5 \log_{10}(d_L) - K,$$



Same galaxy at different redshifts



k-corrections



Galaxy modeling

- Simple bulge+disc model...
- ... add dust disc to improve inclination angle estimation
- ... use dust disc to estimate the sign of inclination

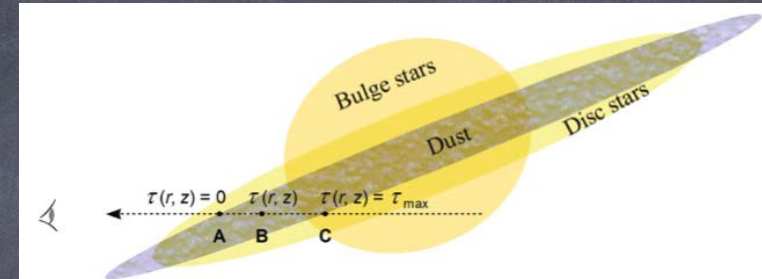
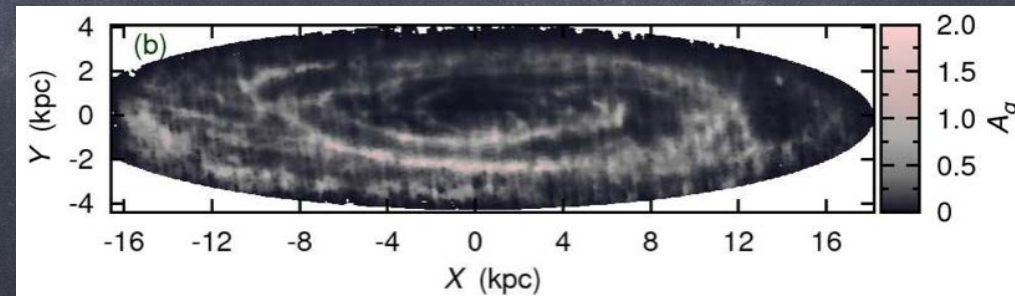
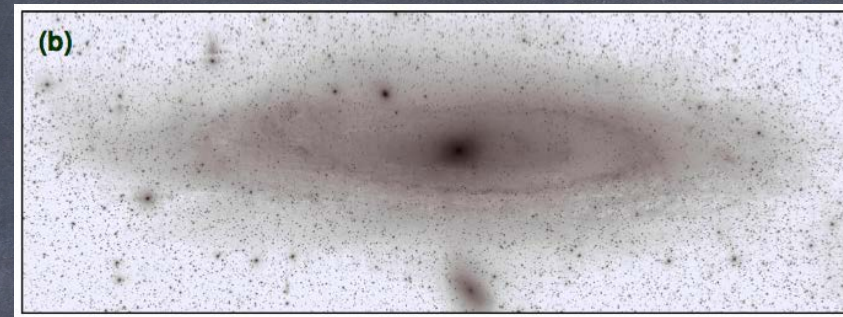


Fig. 1. Geometry of the dust disc model. The line-of-sight optical depth for three positions A–C is indicated. The figure is illustrative only.



Tempel, Tamm, Tenjes (2010)

Tempel, Tuvikene, Tamm, Tenjes (2011)

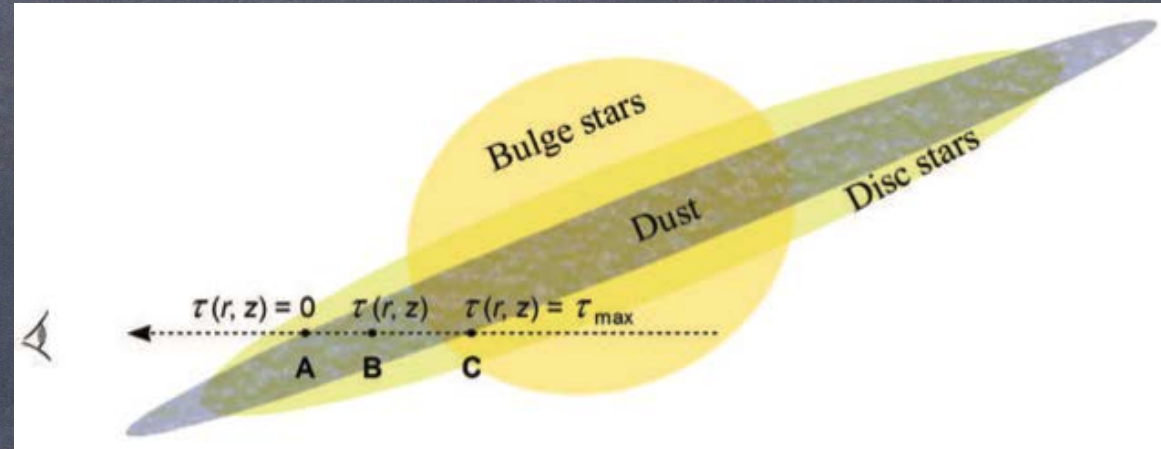
Tamm, Tempel, Tenjes, Tihhonova, Tuvikene (2012)

Dust extinction in spiral galaxies

Model for dust attenuation calculation in galaxies

Attenuation depends on:

galaxy viewing angle,
galaxy stellar structure,
dust disc geometry and
dust properties.



$$l(a) = l(0) \exp \left[- \left(\frac{a}{ka_0} \right)^{1/N} \right]$$

$$L(X, Y) = \int_X^\infty \frac{\sum_{j=1}^2 [l(r, z_j) e^{-\tau(r, z_j)}]}{\sin i \sqrt{r^2 - X^2}} r dr$$

$$z_{1,2} = \frac{Y}{\sin i} \pm \frac{\sqrt{r^2 - X^2}}{\tan i},$$

$$\tau(r, z) = \tau_{\max}(X, Y) \frac{\int_A^B n_{\text{dust}}(s) ds}{\int_A^C n_{\text{dust}}(s) ds}$$

$$n_{\text{dust}}(r, z) = f_{\text{dust}}(r) \cdot n(a)$$

$$\tau_{\max, f}(X, Y) = c_{f, \lambda', T'} F_{\lambda'}(X, Y) \frac{\lambda'^\beta B(\lambda', T')}{(\lambda')^\beta B(\lambda, T(X, Y))}$$

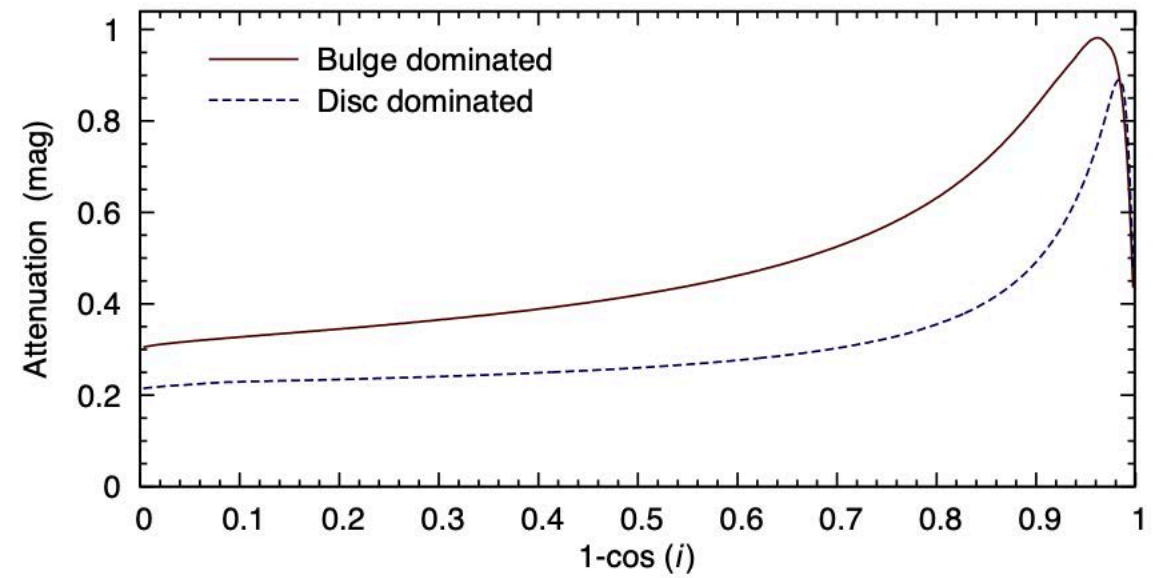
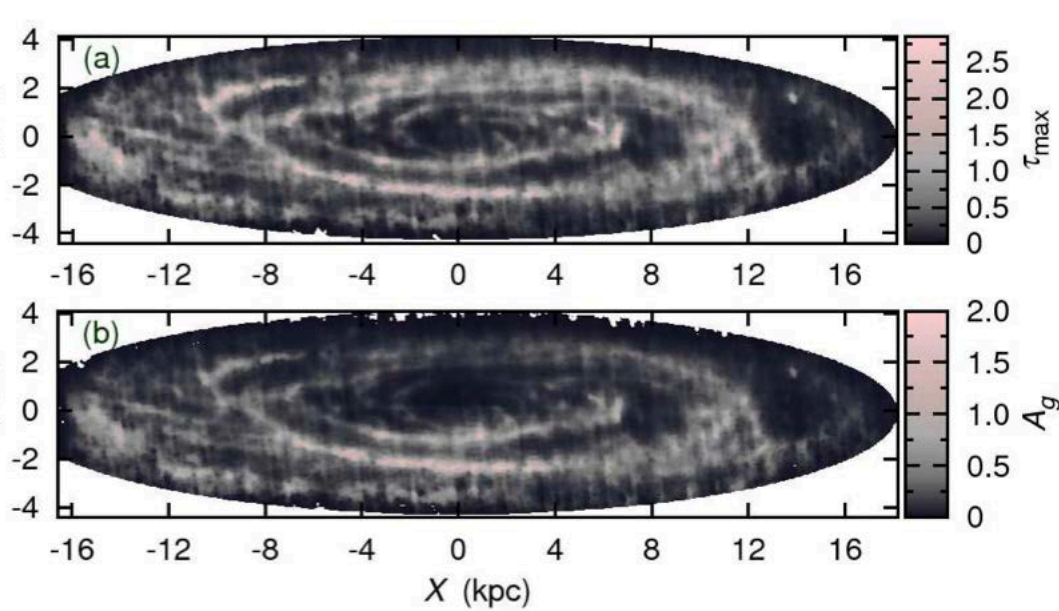
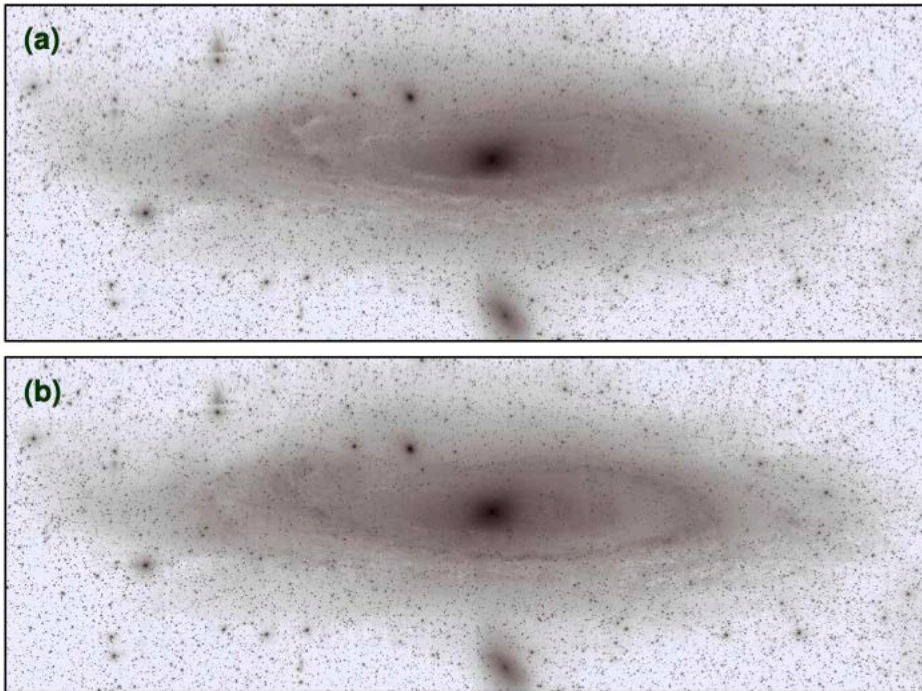


Fig.9. The dependence of attenuation on galaxy inclination for disc-dominated and bulge-dominated spiral galaxies.



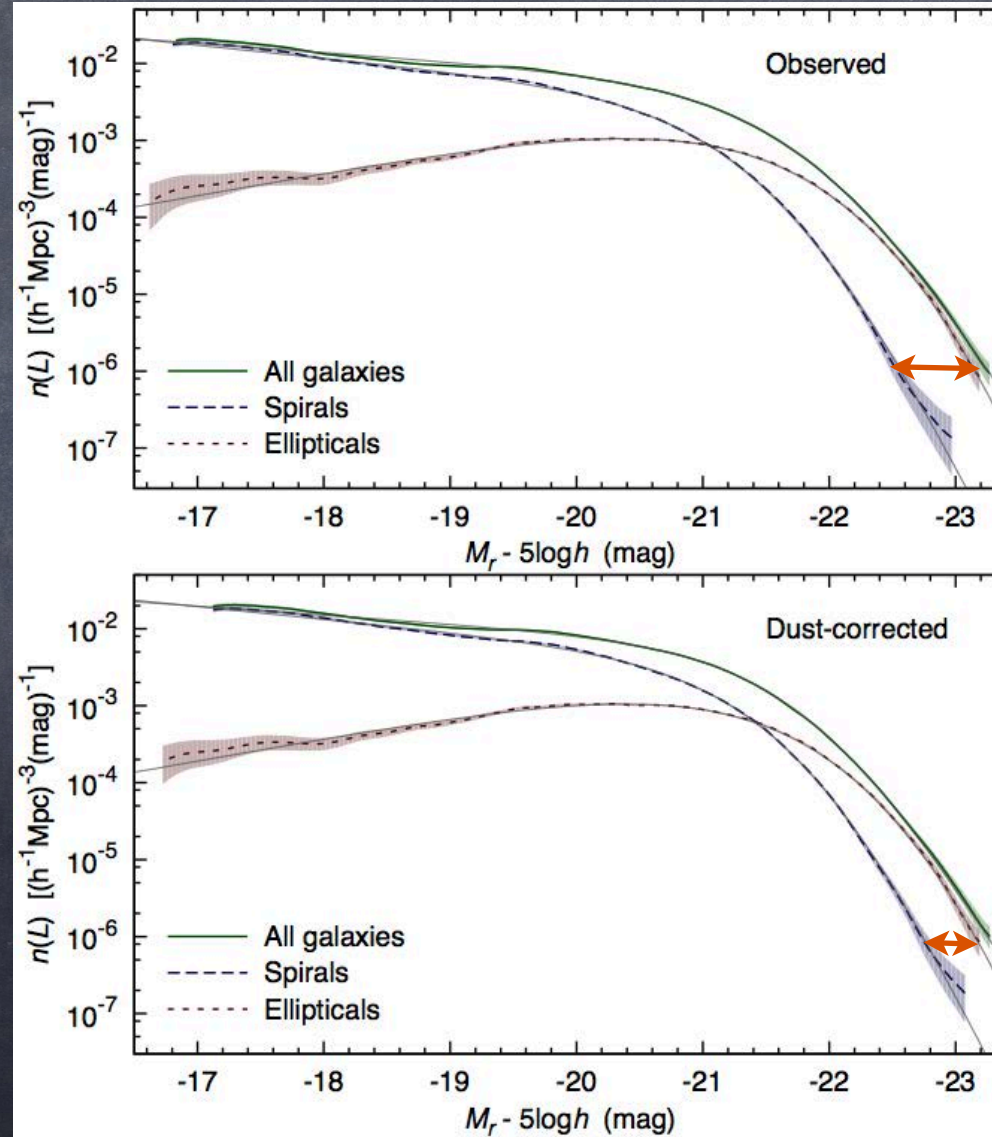
Is 3D modelling necessary?

$$\cos^2(i) = \frac{(a/b)^2 - q^2}{1 - q^2}$$

a/b - visible axial ratio

q - disc flatness (0.1)

Dust extinction: luminosity function



Redshift-space distortion (RSD)

Peculiar motion of galaxies distort the observed (redshift-space) galaxy distribution

$$z_{\text{obs}} = z_{\text{true}} + \delta v/c$$

Linear regime

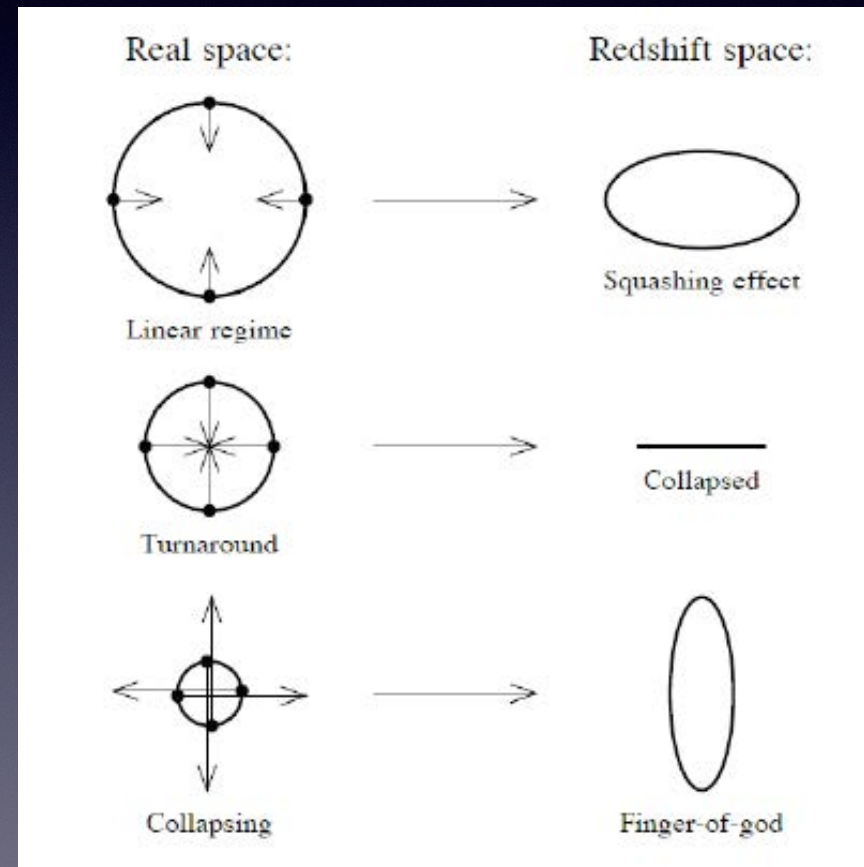
Coherent bulk motion squashes the galaxy distribution along the LOS direction

"Kaiser effect"

Nonlinear regime

Random motion of galaxies elongate the galaxy distribution along the LOS direction

"Fingers-of-God effect"



Hamilton 1992

line-of-sight
direction

Test of Gravity

Redshift-space galaxy power spectra
in linear regime

$$P_g(k, \mu) = (b + f\mu^2)^2 P_m(k) \quad (\text{Kaiser 1987})$$

b : linear galaxy bias $\mu = k_{\parallel}/k$
 f : growth rate

Growth rate is a key probe to test gravity

$$f \equiv \frac{d \ln D}{d \ln a} \simeq \Omega_m(z)^\gamma$$

(Peebles 1976, Lahav et al. 1991)

$\gamma \simeq 0.55$ for Λ CDM

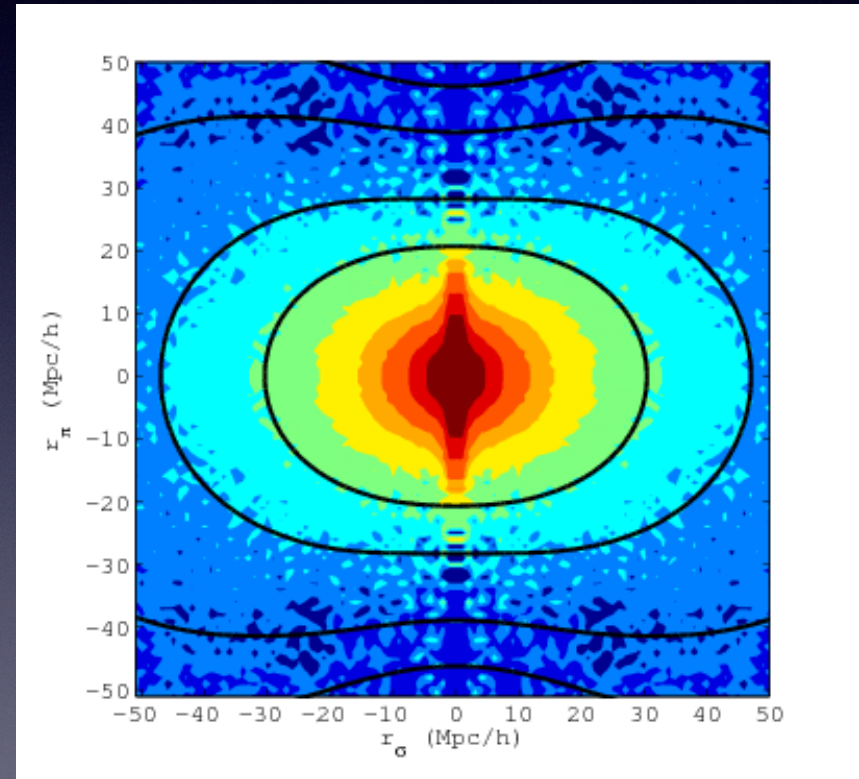
$\gamma \simeq 0.68$ for flat DGP (e.g., Linder & Cahn 2007)

$\gamma \simeq 0.43$ for $f(R)$ (e.g., Hu & Sawicki 2007)

$a = 1/(1+z)$

$D(a)$ - linear
growth factor

2-point correlation functions for
BOSS CMASS samples $\xi(r_p, r_{\pi})$

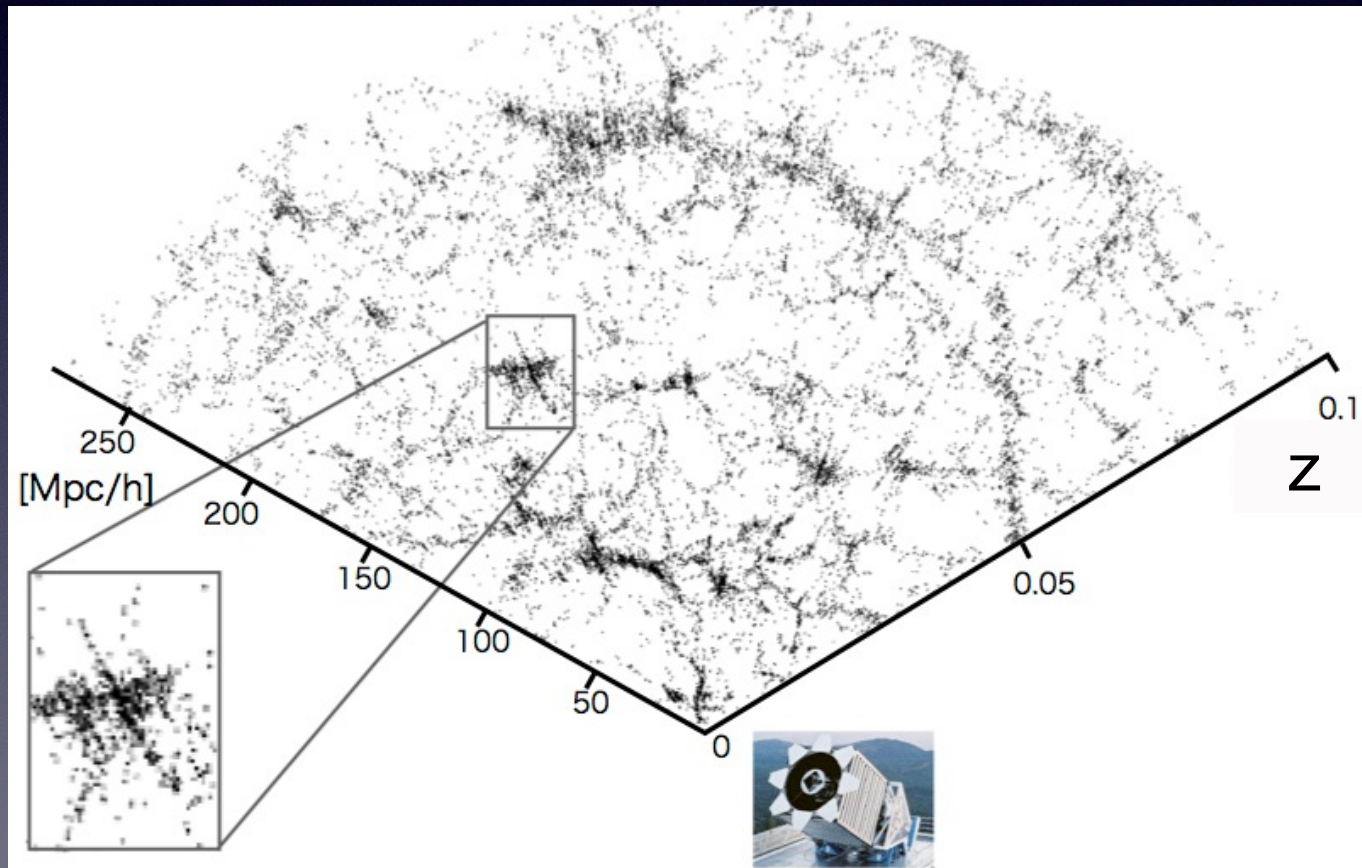


Reid et al. 2012

line-of-sight
direction

Fingers-of-God (FoG) effect

Nonlinear redshift-space distortion due to internal motion of galaxies in the host halos



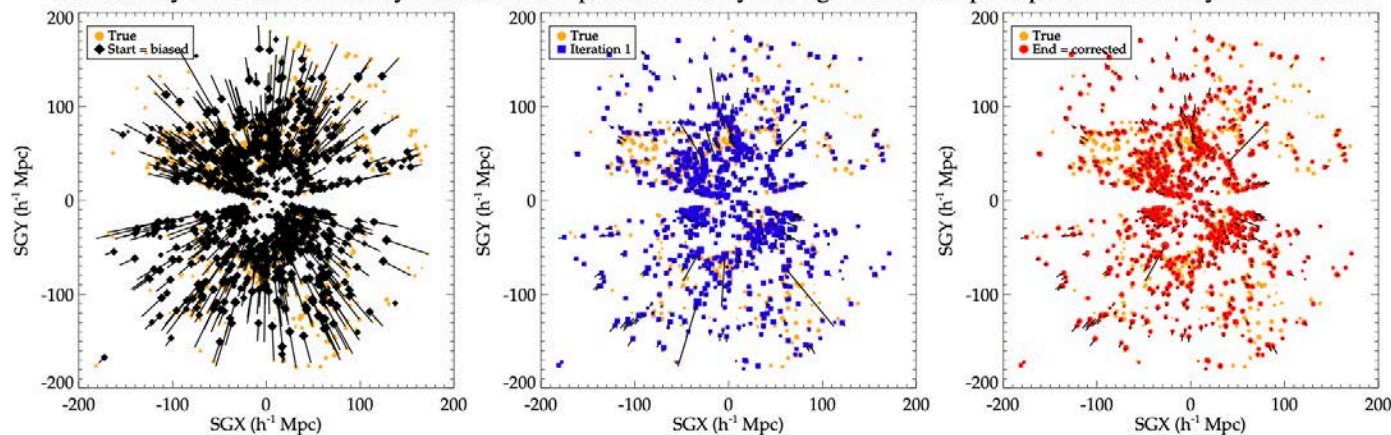
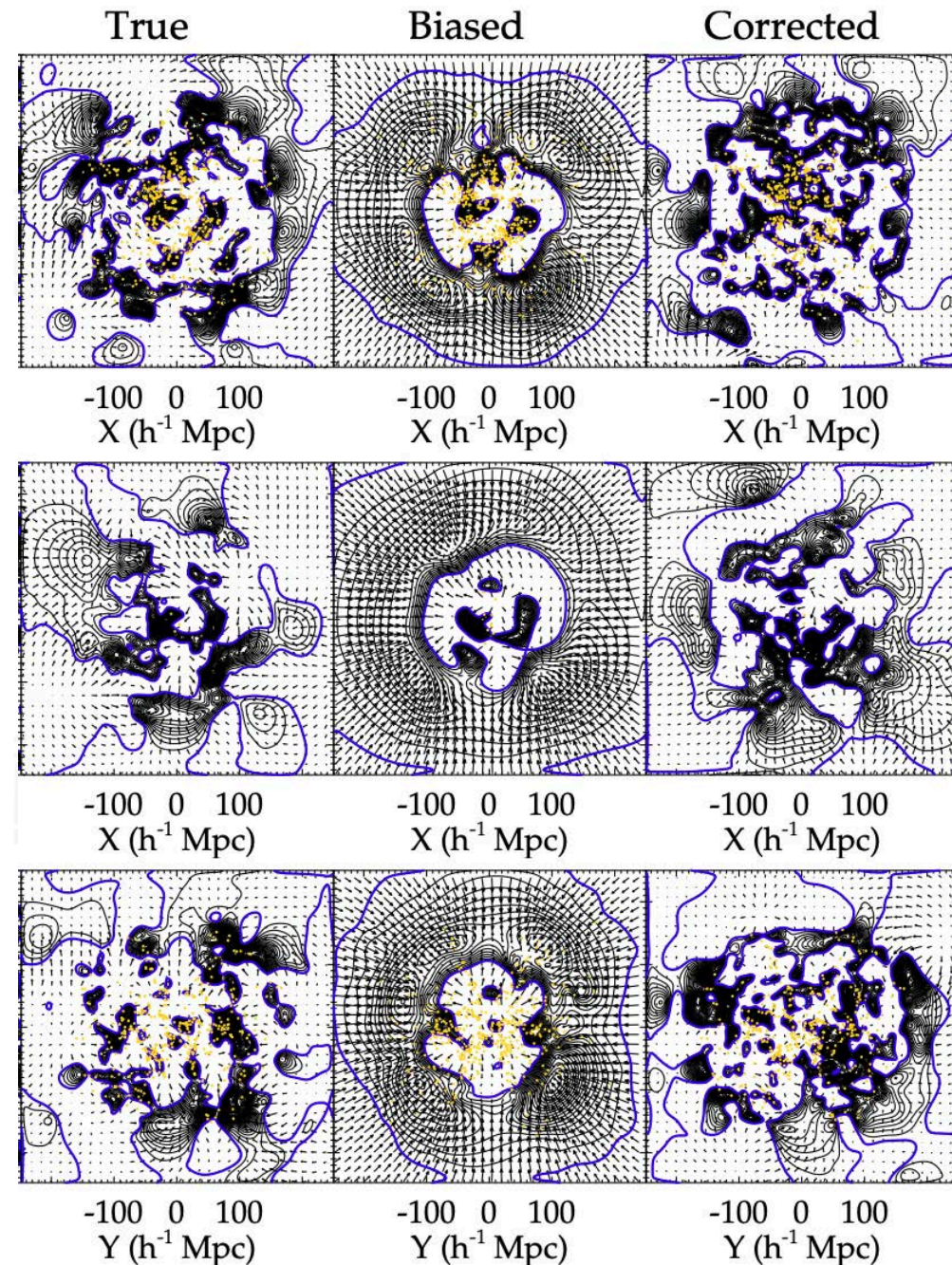


Fig. 4. Galaxies in $5 \ h^{-1}$ Mpc thick slices of the XY supergalactic plane. *From left to right:* Black lines show the projected distances between true (yellow filled circles) and biased (black filled diamonds), after n_{mh} Metropolis Hastings loops but no cooling for the n datapoints (in the text Iteration 1, blue filled square) and, at the end of all loops (red filled circles), datapoint positions. The filled symbol sizes are proportional to velocities on a logarithmic scale. Note that because errors are large in the left panel, yellow filled circles are harder to distinguish. The algorithm reduces on the average errors on datapoint positions thus on their peculiar velocities: on average shorter black lines and by extension better matching filled symbol sizes of different colors.



Biased velocity field

Sorce et al.



UNIVERSITY OF TARTU

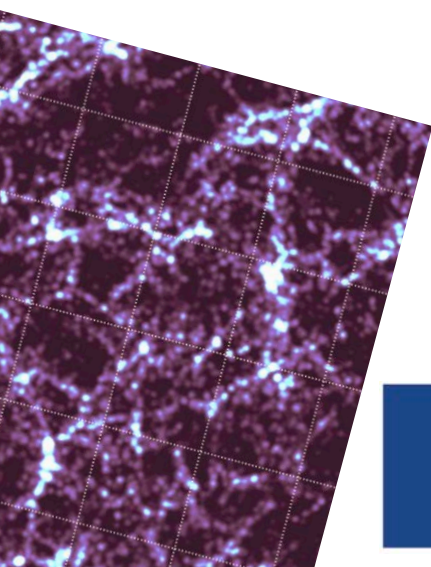


Co-funded by
the European Union



Investing
in your future

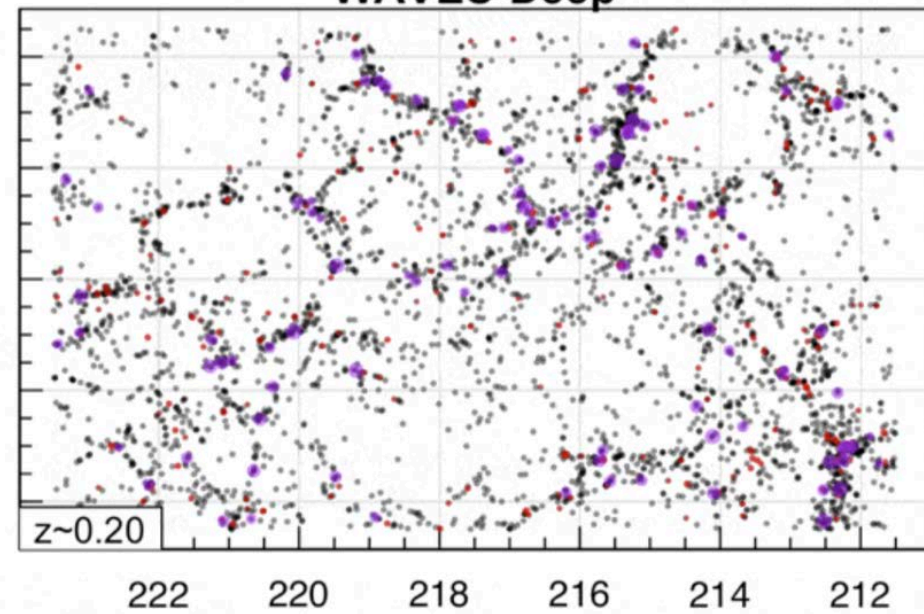
Galaxy Groups in redshift surveys



Funded by
the European Union

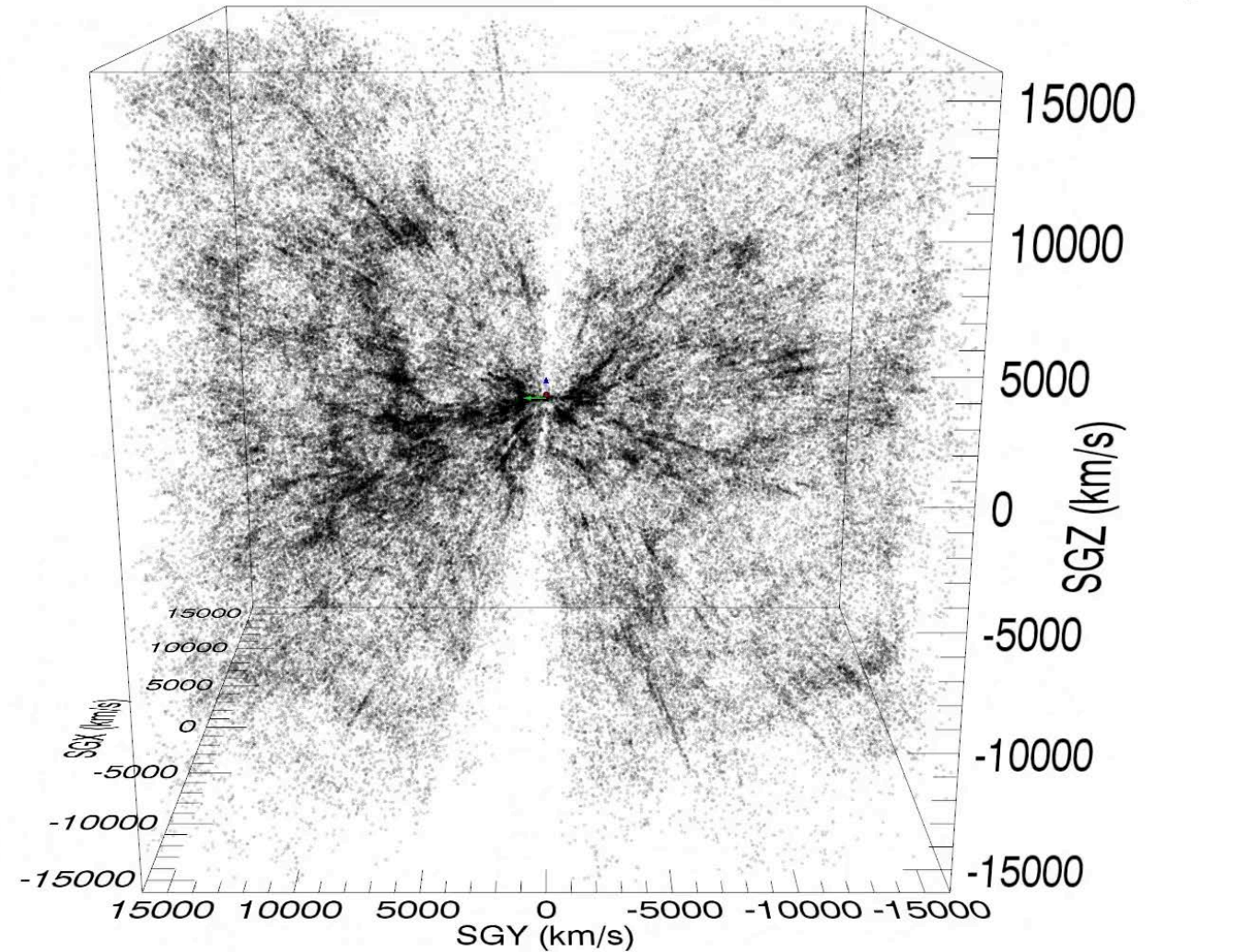


WAVES-Deep



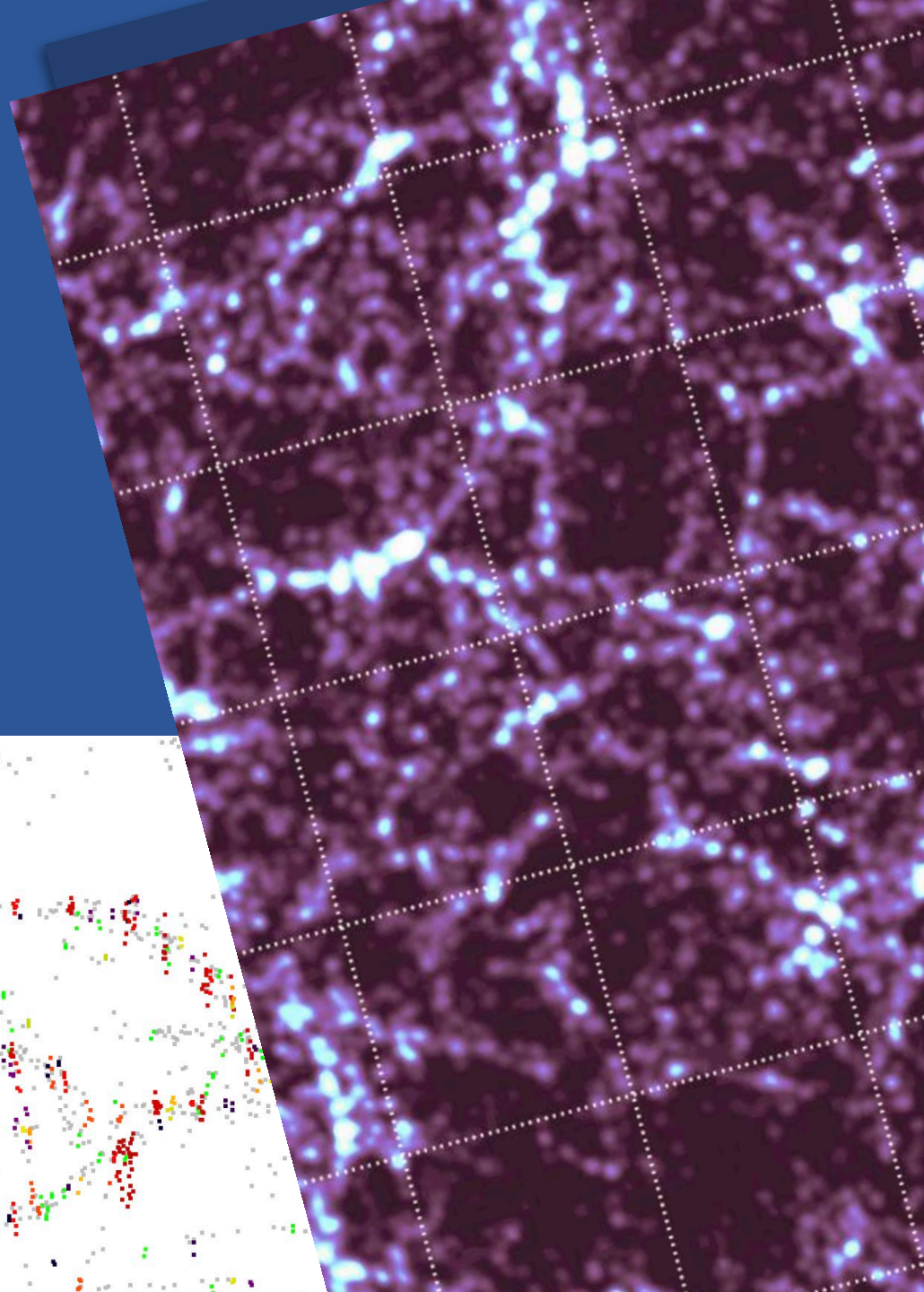
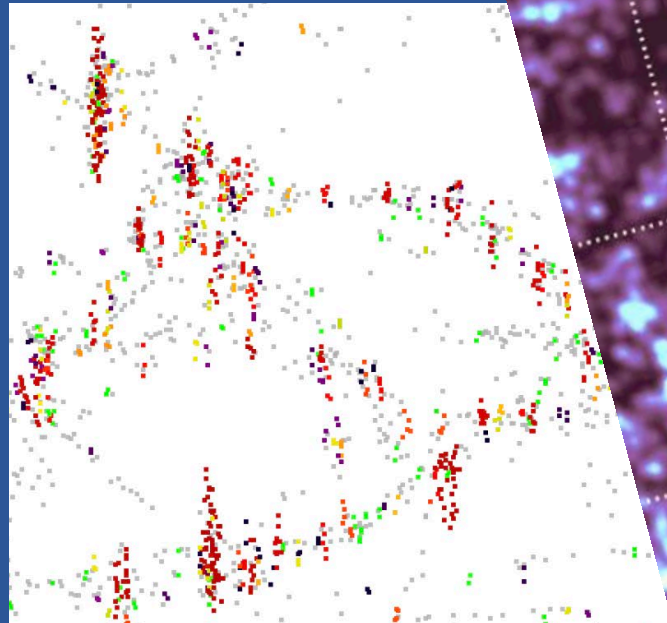
Cosmic Web in 3D

Cosmic web in the Local Universe

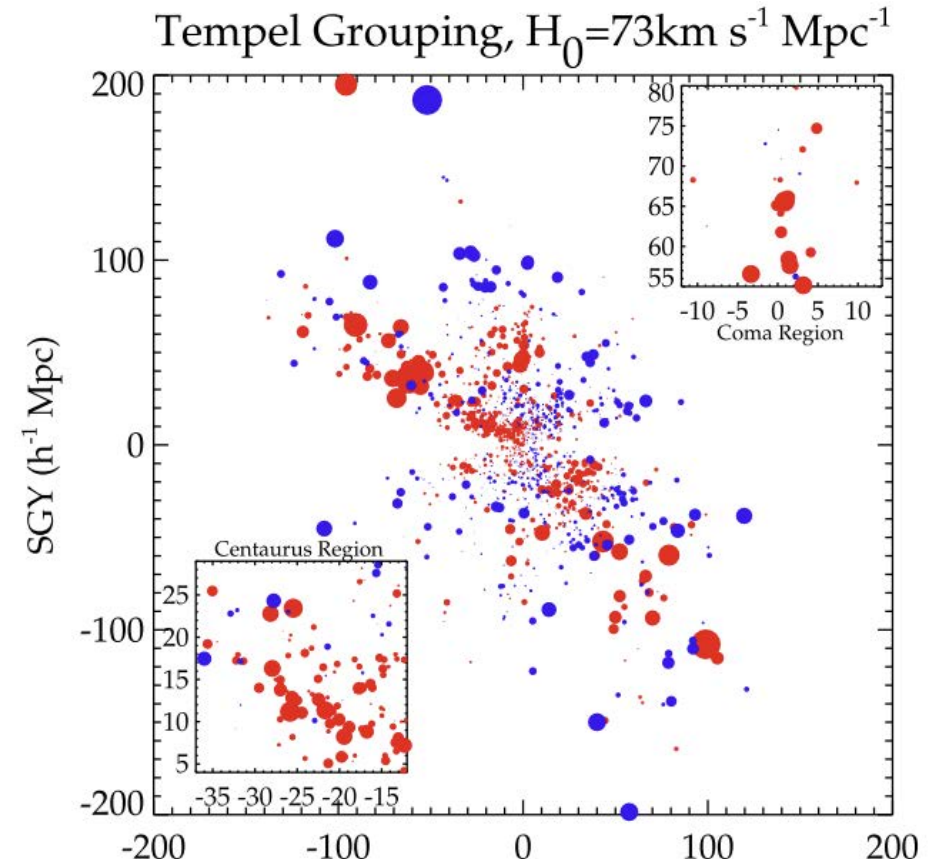
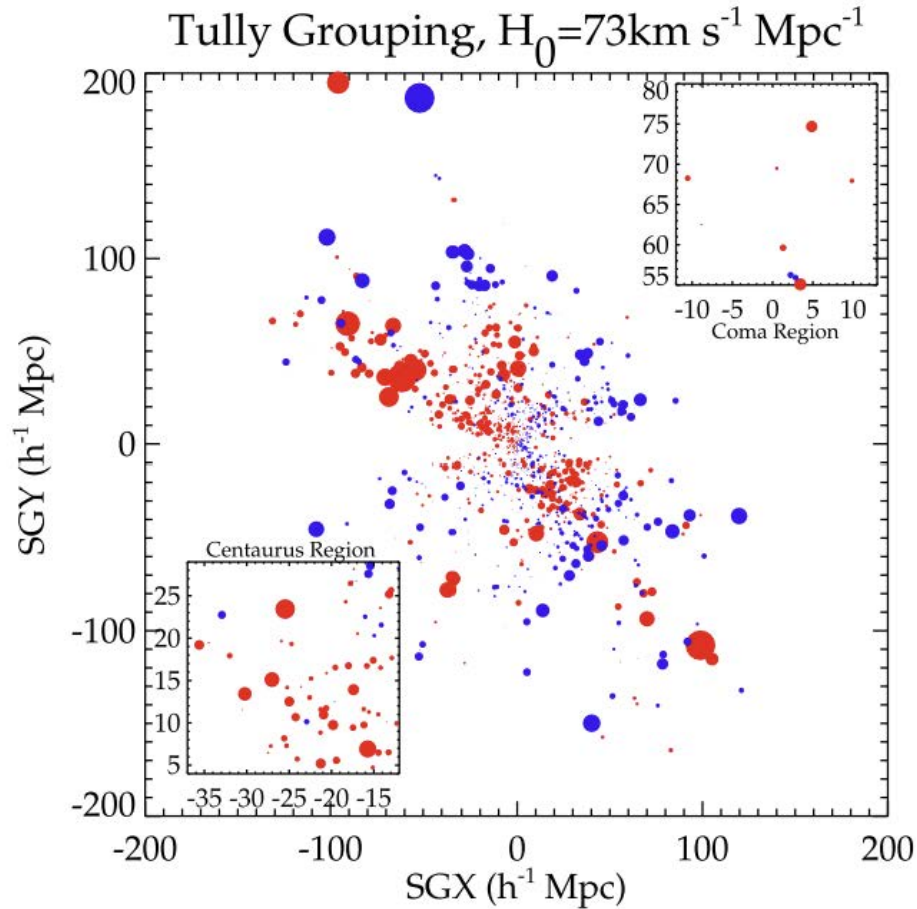


Group finding: three aspects

- Where are the groups?
Finding the group centres
- What galaxies belong to the groups?
Group membership assignment
- Estimating group properties
(i.e. group masses)



Impact of grouping

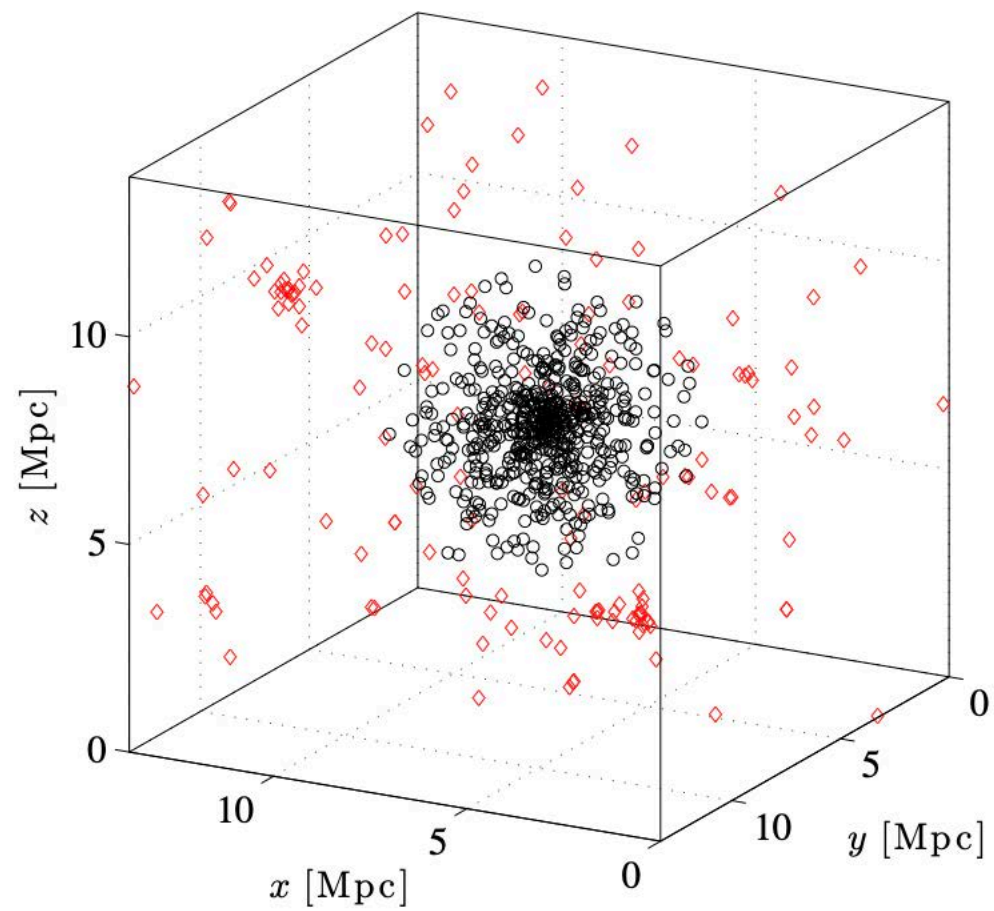


How does the grouping scheme affect the Wiener Filter reconstruction of the local Universe?

Jenny G. Sorce^{1,2★} and Elmo Tempel^{2,3}

¹ CNRS, Observatoire astronomique de Strasbourg, UMR 7550, Université de Strasbourg, F-67000 Strasbourg, France

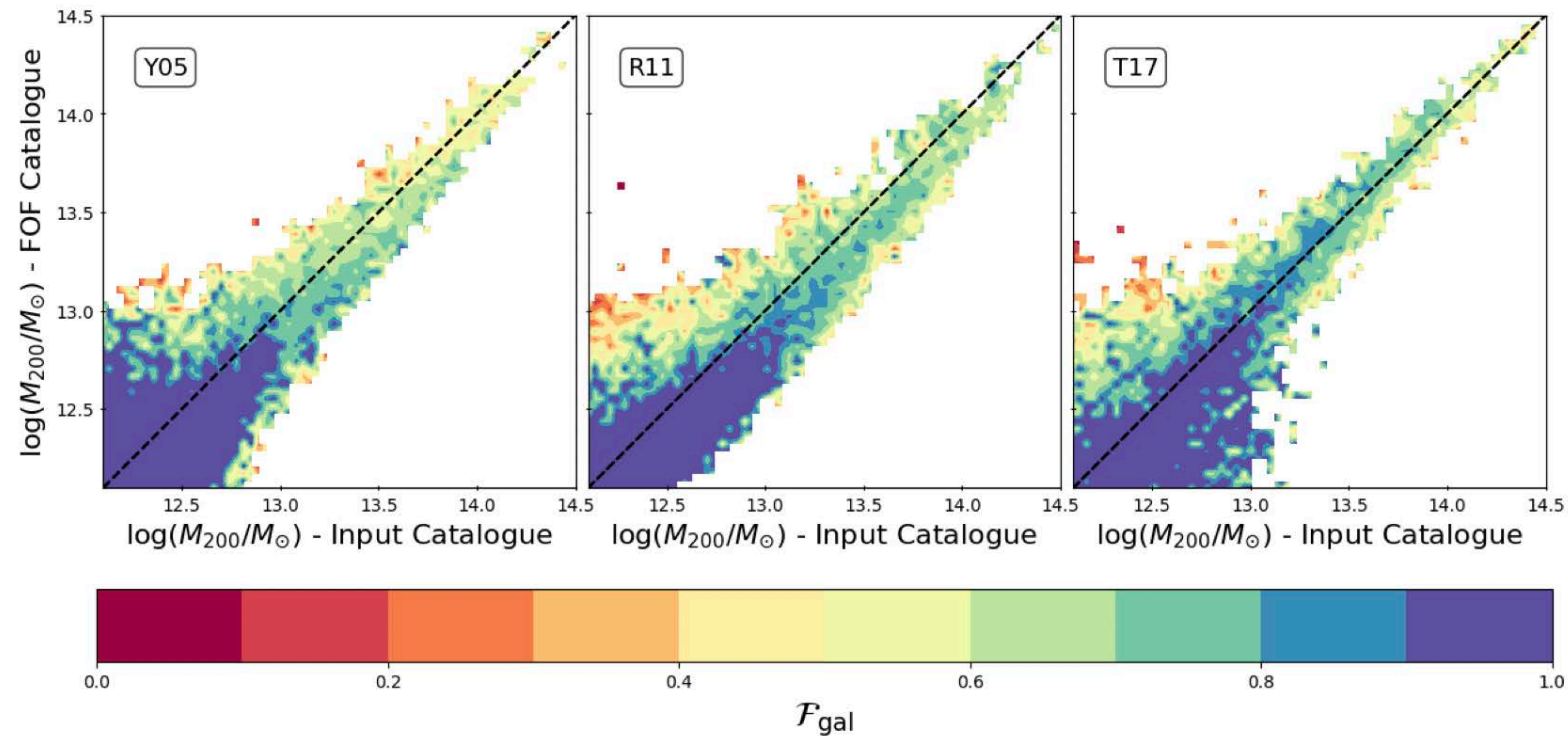
² Leibniz-Institut für Astrophysik, An der Sternwarte 16, D-14482 Potsdam, Germany



Interlopers

Old et al.

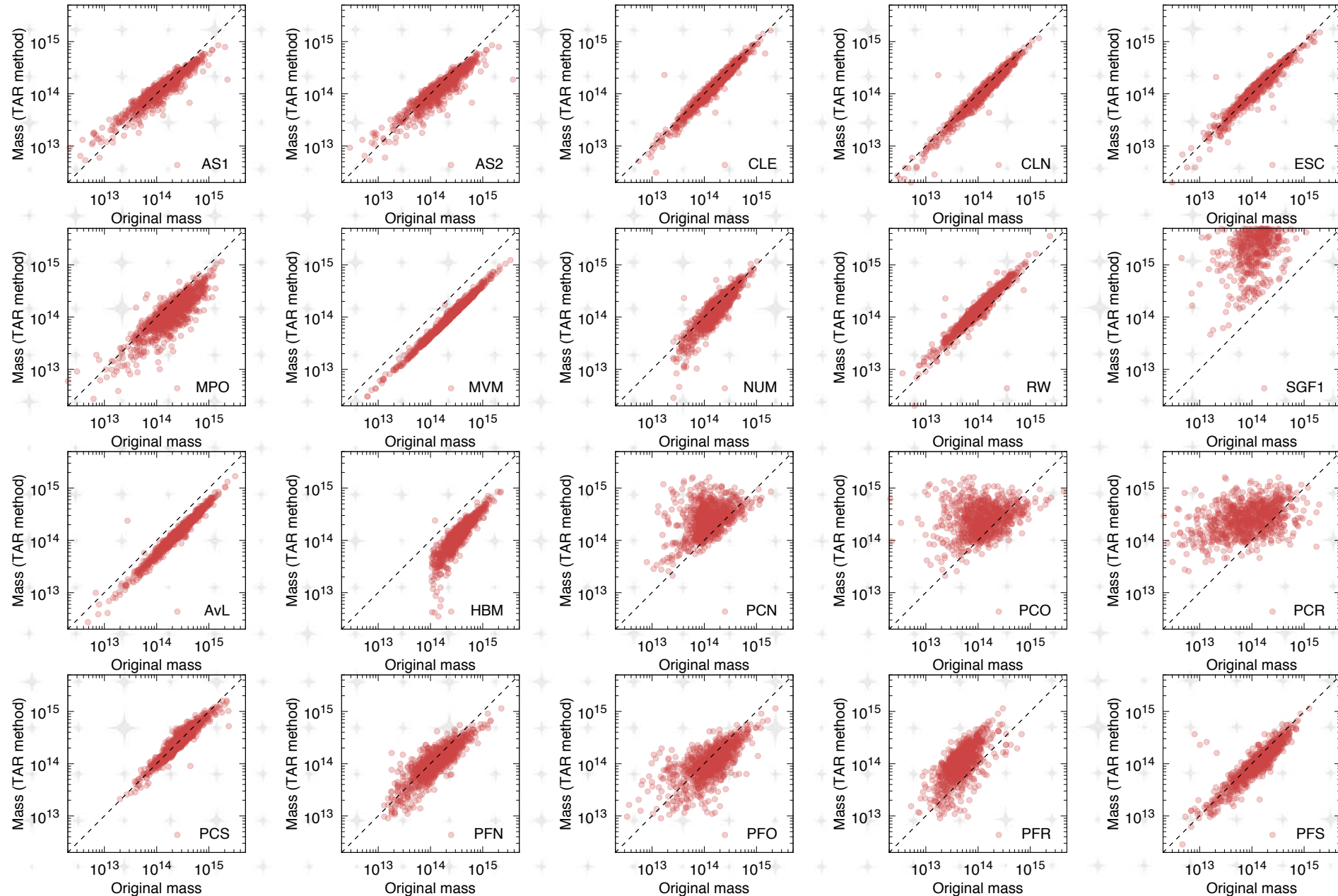
$$\mathcal{F}_{\text{gal}} = \frac{N_{\text{gal}}^2(\text{HALOS} \cap \text{FOF})}{N_{\text{gal}}(\text{HALOS}) N_{\text{gal}}(\text{FOF})},$$

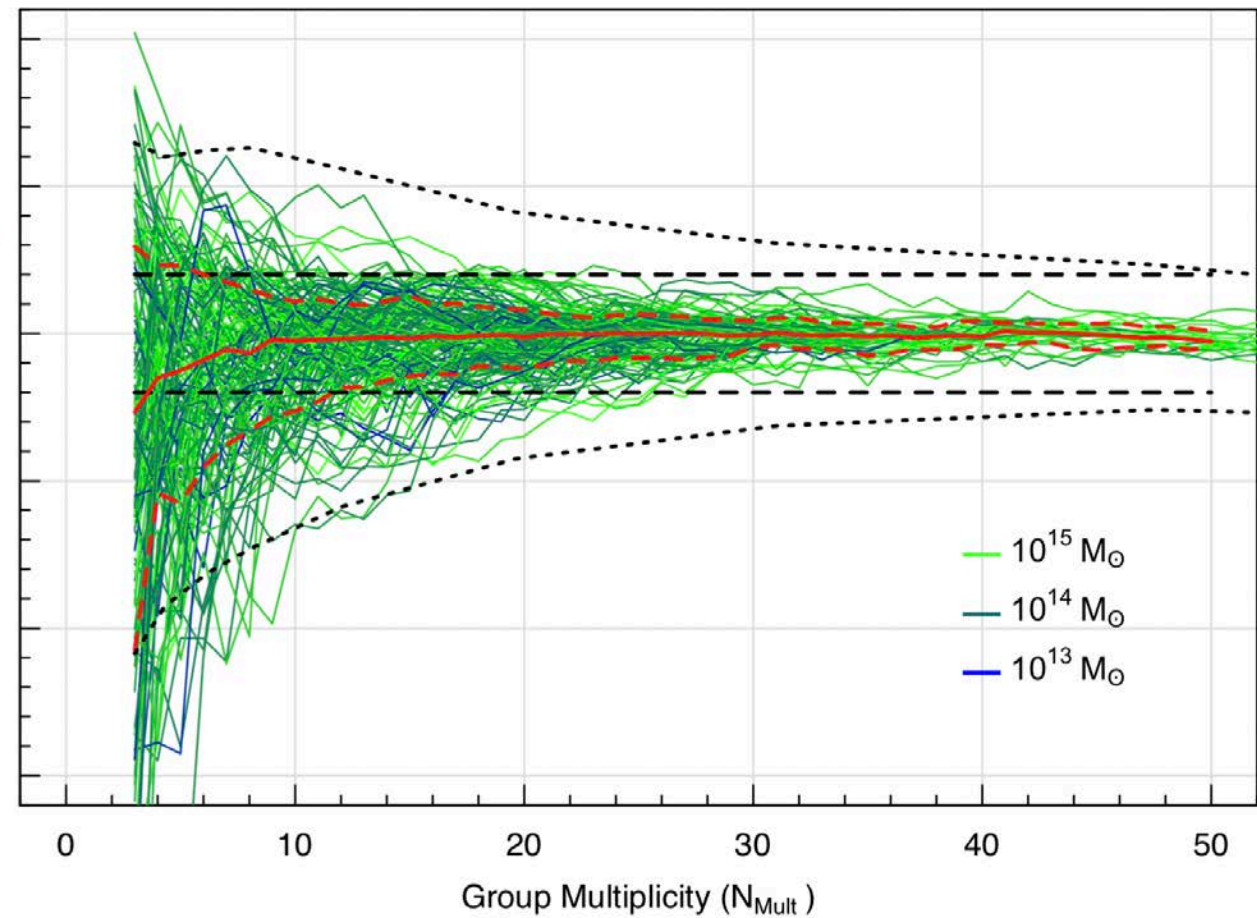
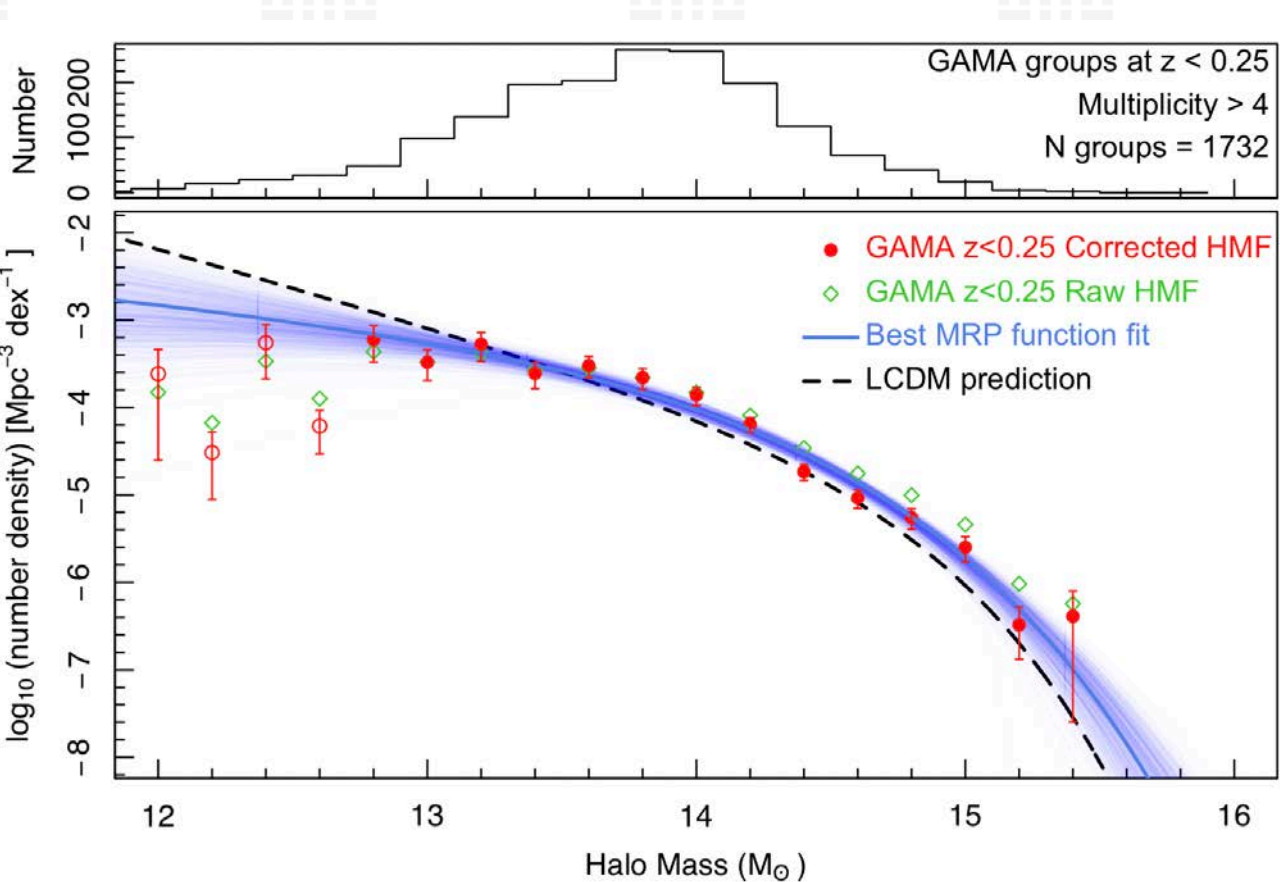


Estimated group masses

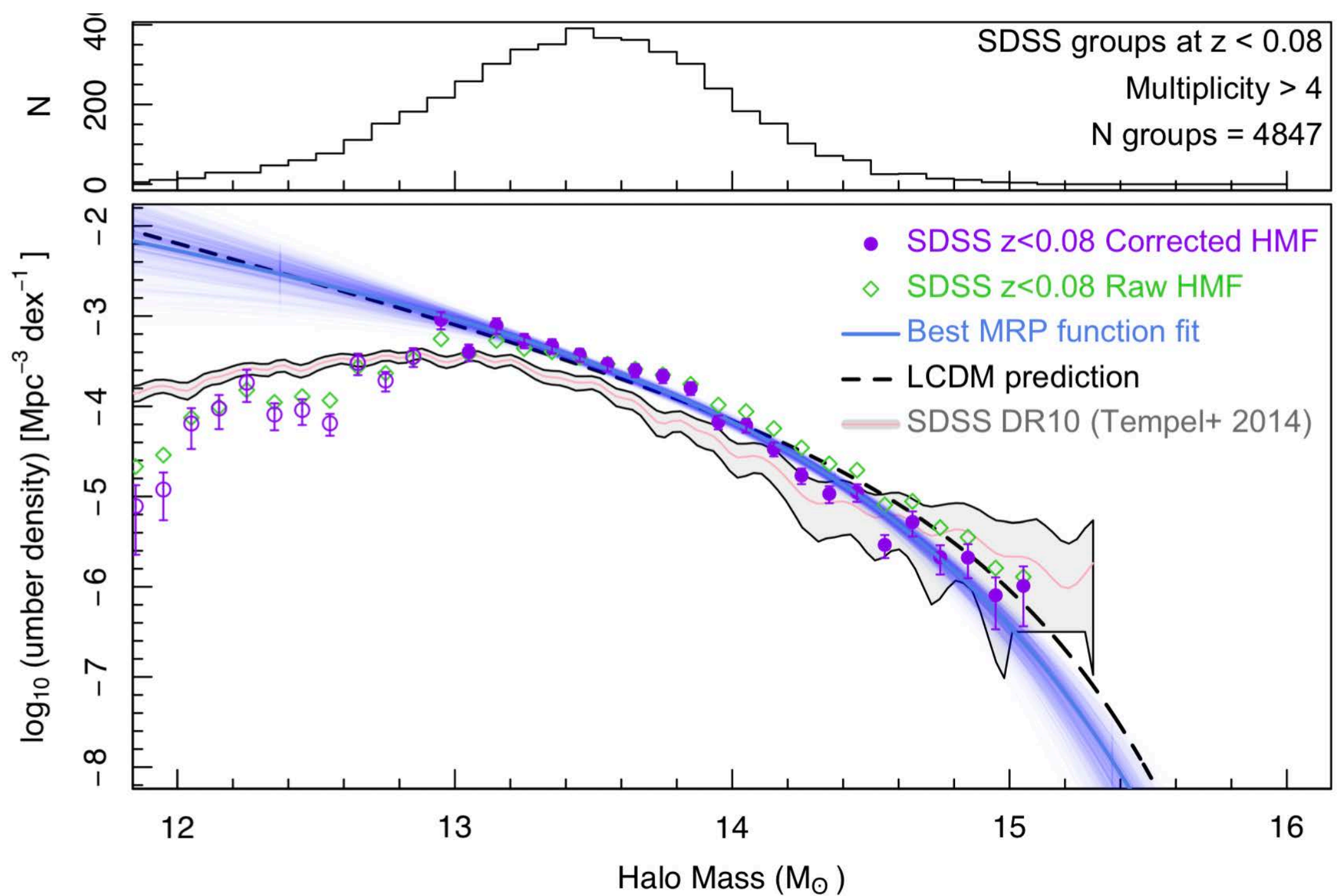
Marini et al. 2025, Popesso et al. 2025

22 estimates of masses





Estimated group masses



Estimating group masses:

observed properties of groups

$$\sigma_v^2 = \frac{1}{(1 + z_m)^2(n - 1)} \sum_{i=1}^n (v_i - v_{\text{mean}})^2$$

Radial velocity dispersion in the group.

$$v = cz$$

$$\sigma_r^2 = \frac{1}{2n(1 + z_m)^2} \sum_{i=1}^n (r_i)^2$$

Group extent in the sky:

r_i in co-moving coordinates,

$1/2n$ since Rayleigh distribution

Dynamical mass estimate

- From virial theorem (no free scaling parameters)

$$T = \frac{M_{\text{tot}} \sigma_v^2}{2}, \quad U = G \frac{M_{\text{tot}}^2}{R_g}, \quad 2T = U$$

T kinetic energy
 P potential energy

$$M_{\text{vir}} = 2.325 \frac{R_g}{\text{Mpc}} \left(\frac{\sigma_v}{100 \text{ km s}^{-1}} \right)^2 10^{12} M_{\odot},$$

R_g Gravitational radius, which is directly linked (e.g. assuming NFW profile) to the group size in the sky plane

σ_v Group velocity dispersion measured using galaxy redshifts

Estimating group masses: virial theorem

$$M_{\text{tot}} = 2.324 \cdot R_g \sigma_V^2$$

Mass in units of $10^{12} M_{\text{sun}}$

R_g in units of Mpc

σ_V in units of 100 km/s

$$\sigma_V = \sqrt{3} \sigma_{V1D}$$

Velocity dispersion.

Gravitational radius (R_g):

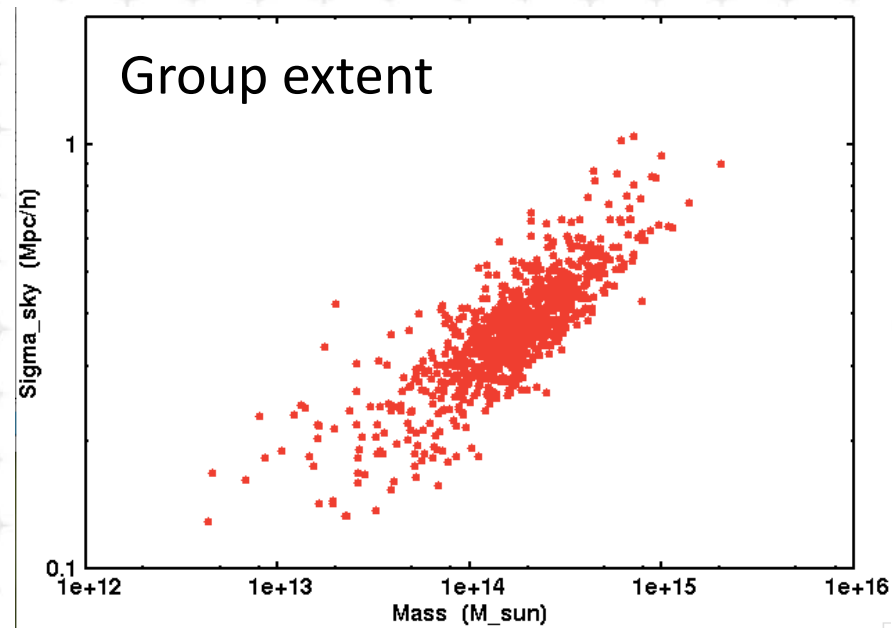
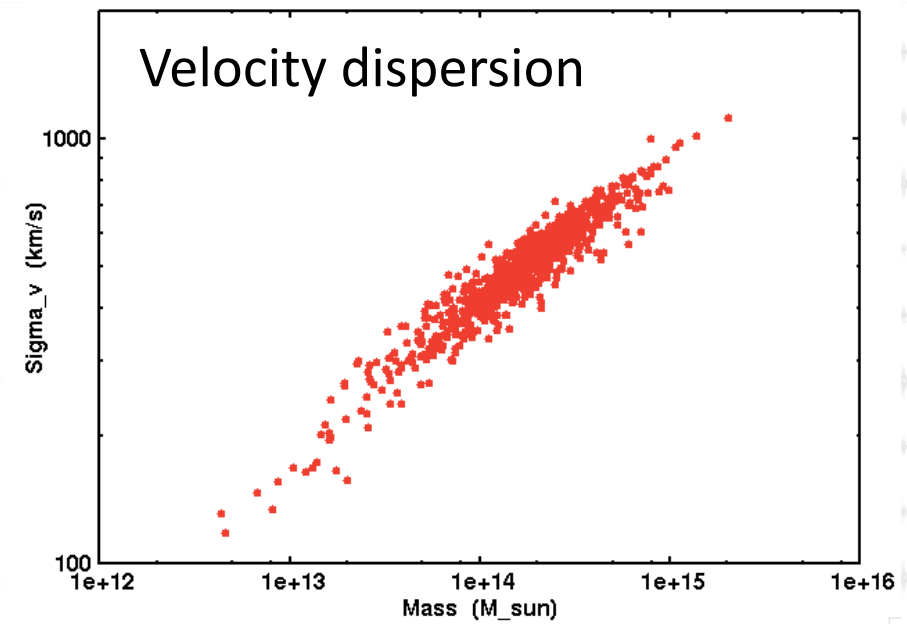
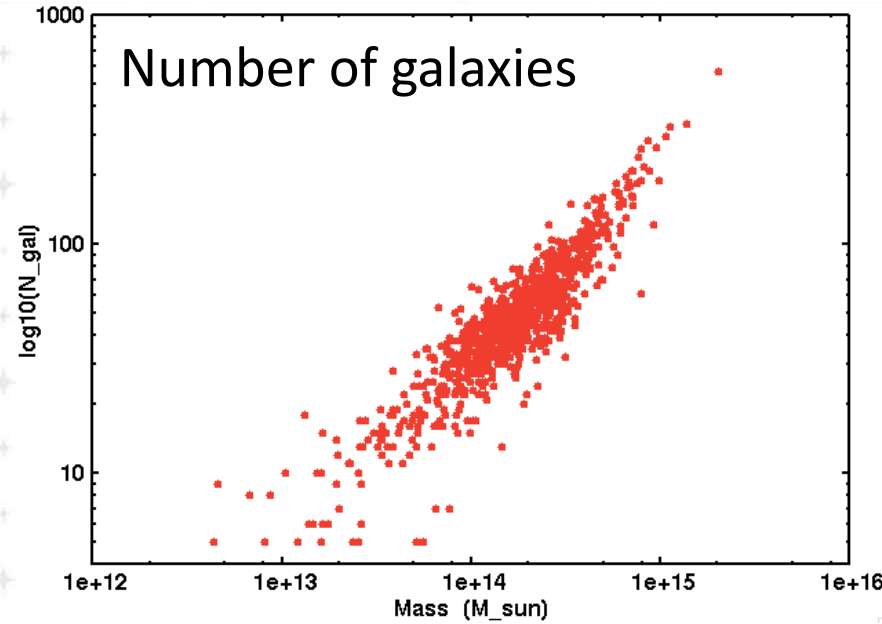
$$\frac{1}{R_g} = \frac{4\pi}{M^2} \int_0^\infty \frac{M(r)}{r} \rho(r) r^2 dr$$

Estimating group masses:

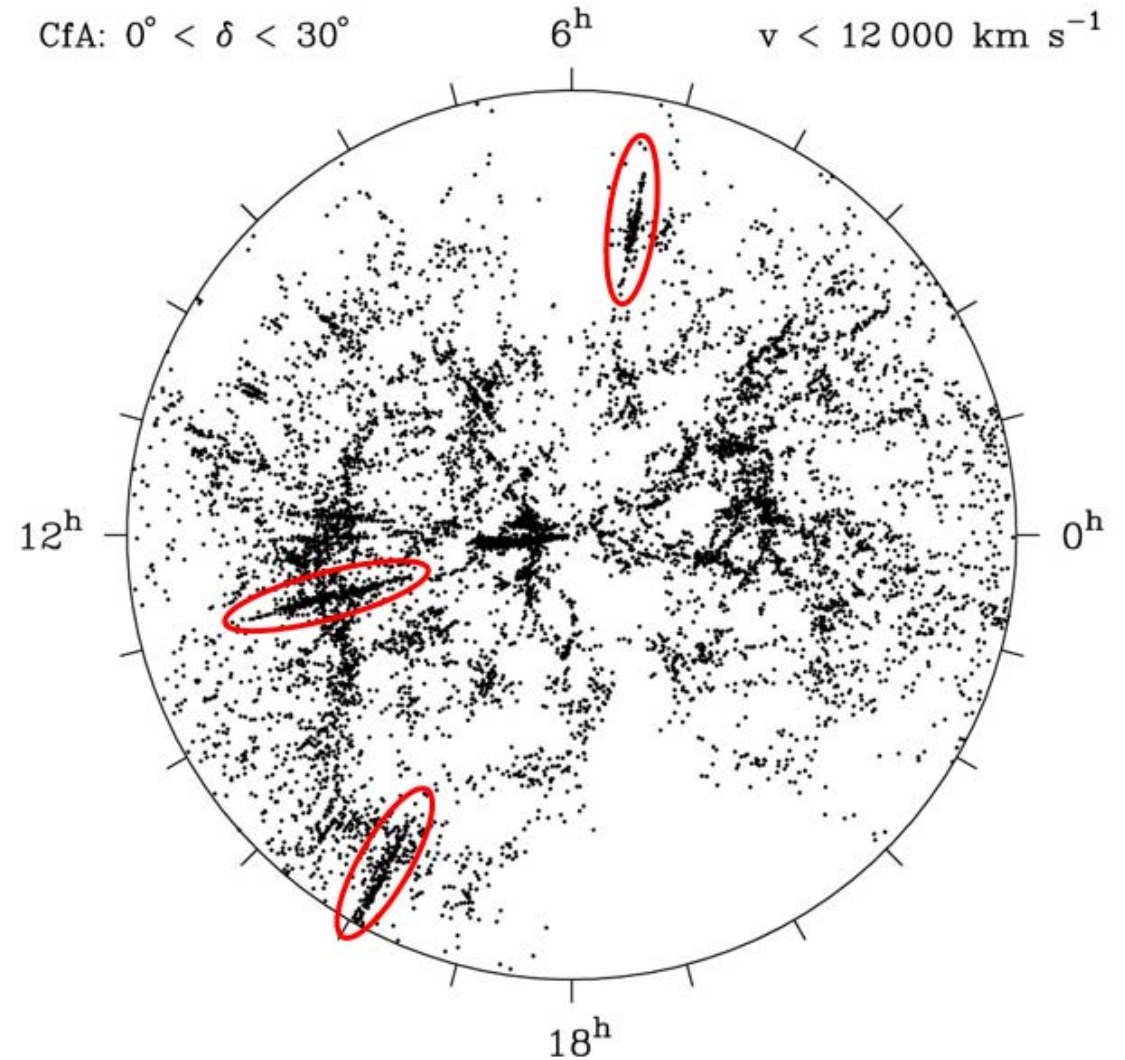
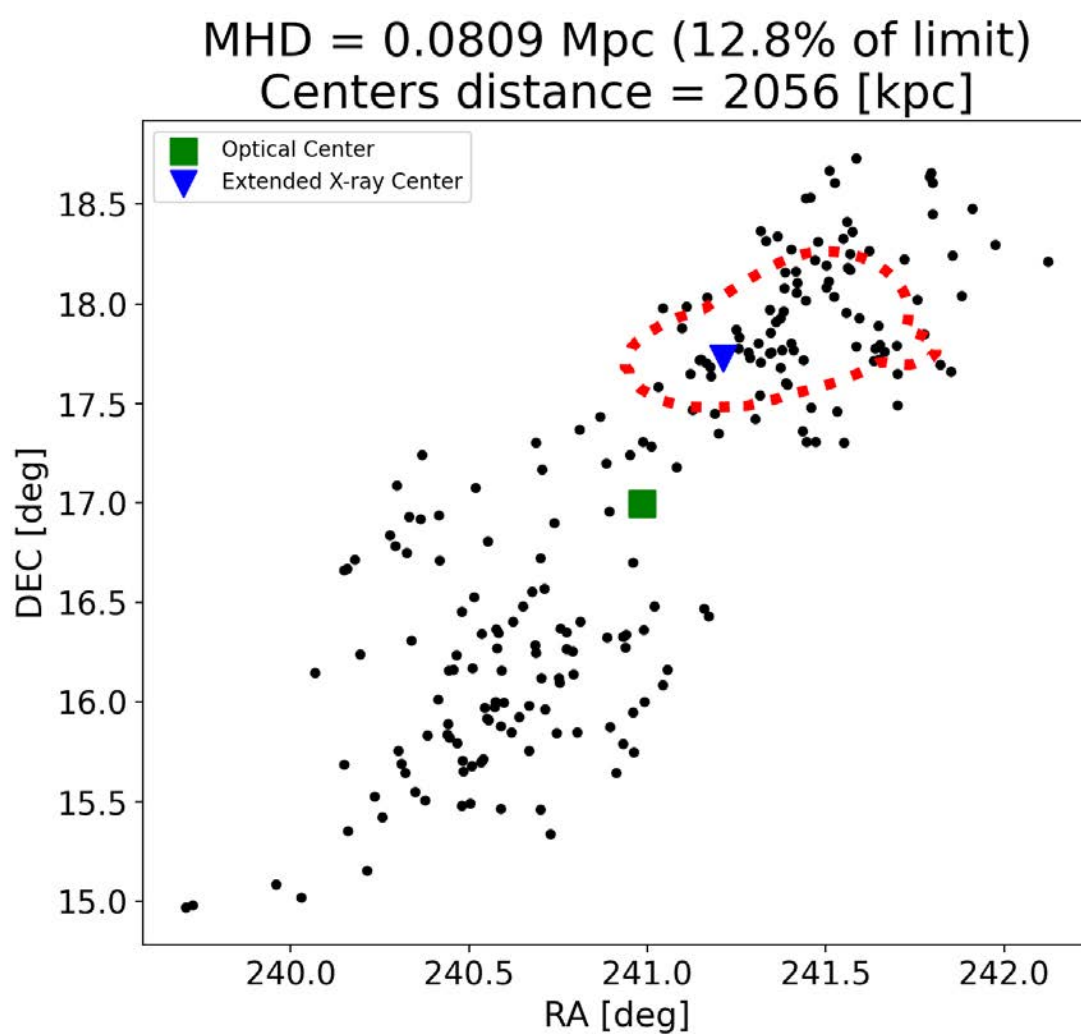
gravitational radius vs group extent in the sky

- ◆ We assume NFW profile.
- ◆ Mass-concentration relation from Maccio et al. (2008).
- ◆ $R_g = f(M_{200})$.
- ◆ For given mass M_{200} , we found R_g/σ_R using NFW profile.
- ◆ Using this relation we transfer the observed group extent in the sky to gravitational radius R_g .
- ◆ We calculate the observed group mass using virial theorem.
- ◆ The final mass is found iteratively.

Groups in LC1

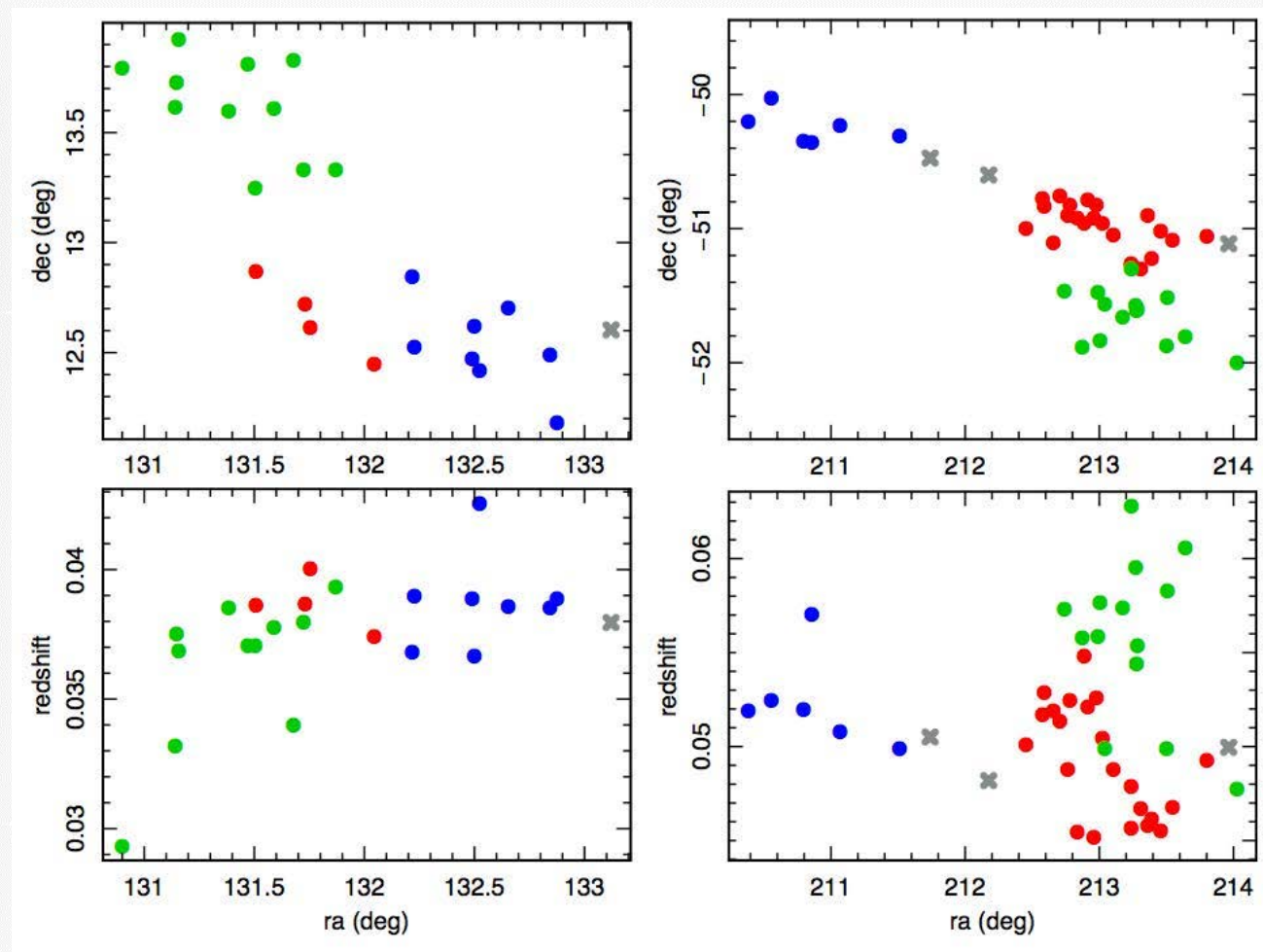


Merged Groups and Fingers-of-God

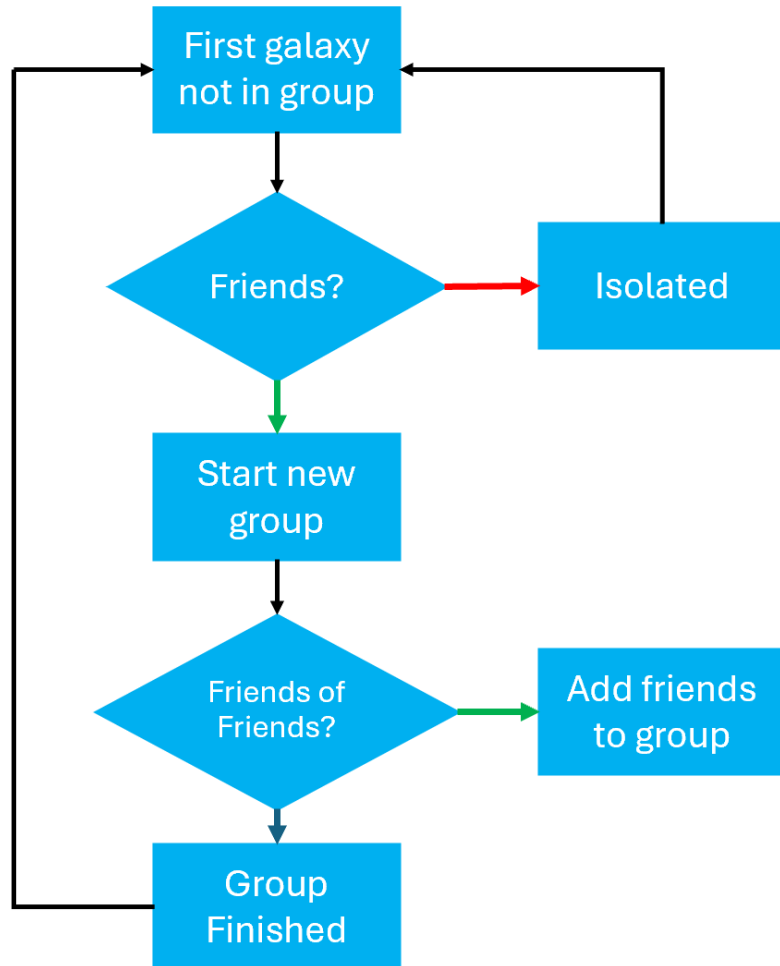




Improving Friends-of-Friends algorithm



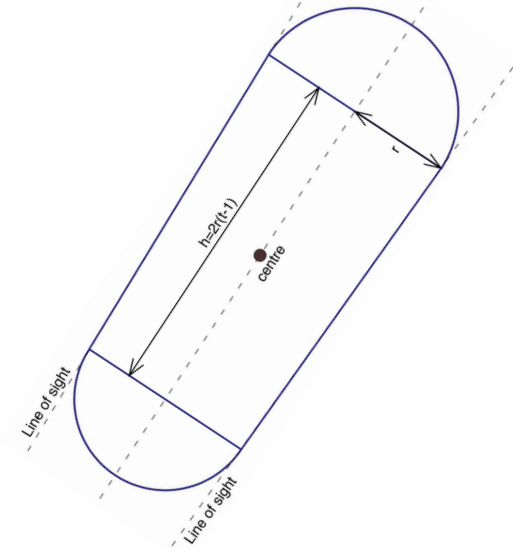
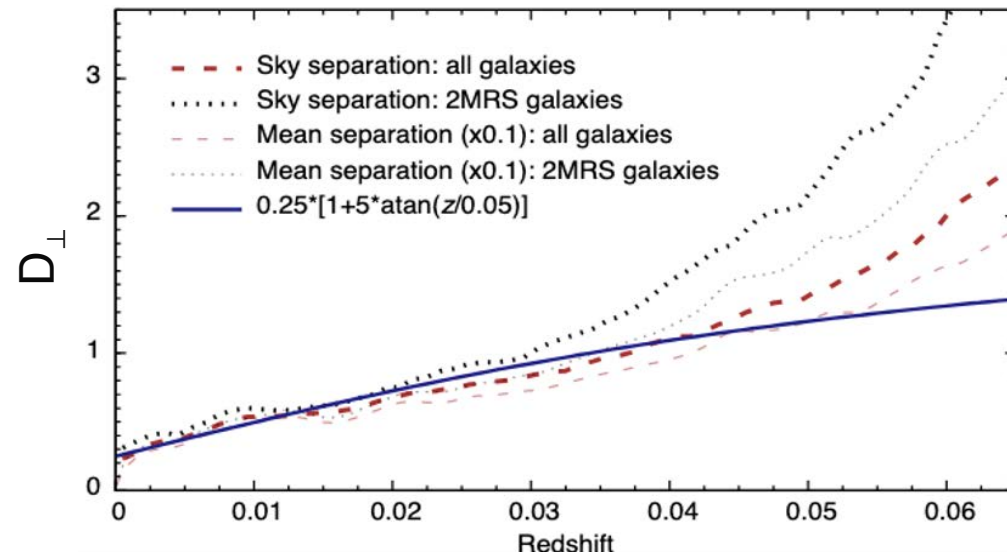
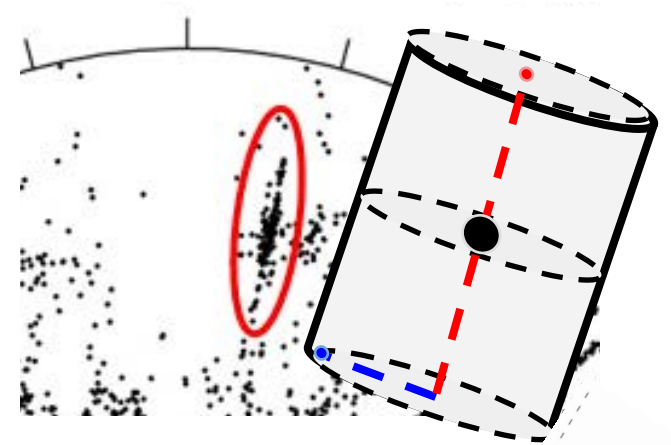
Friends-of-Friends Parameters



Used parameters

$$D_{\perp}$$

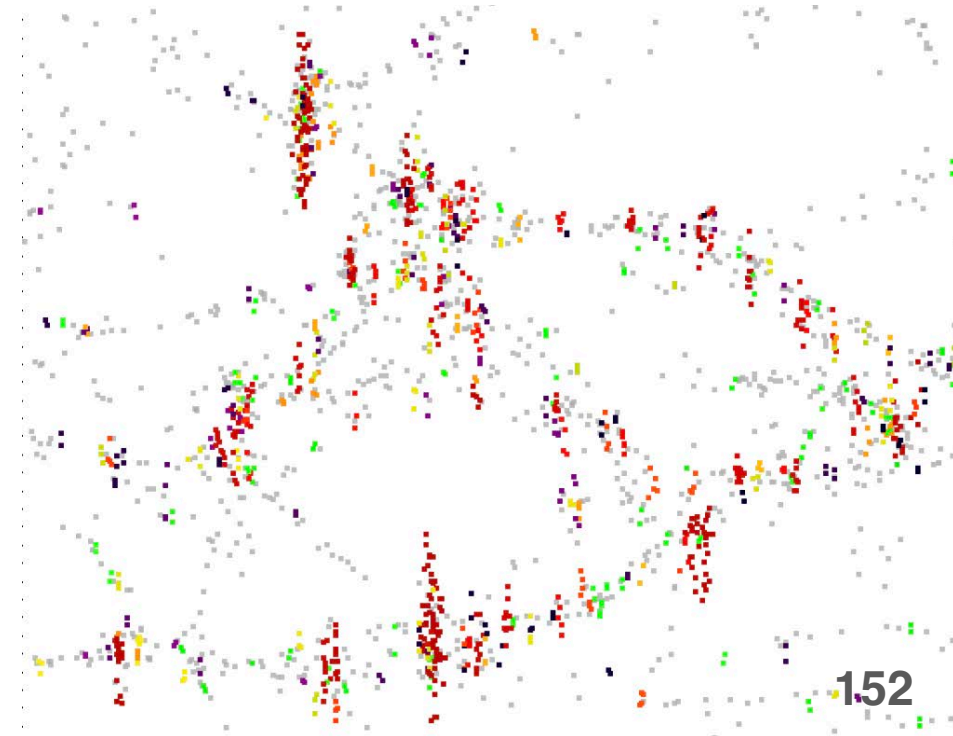
$$R = D_{\parallel} / D_{\perp}$$



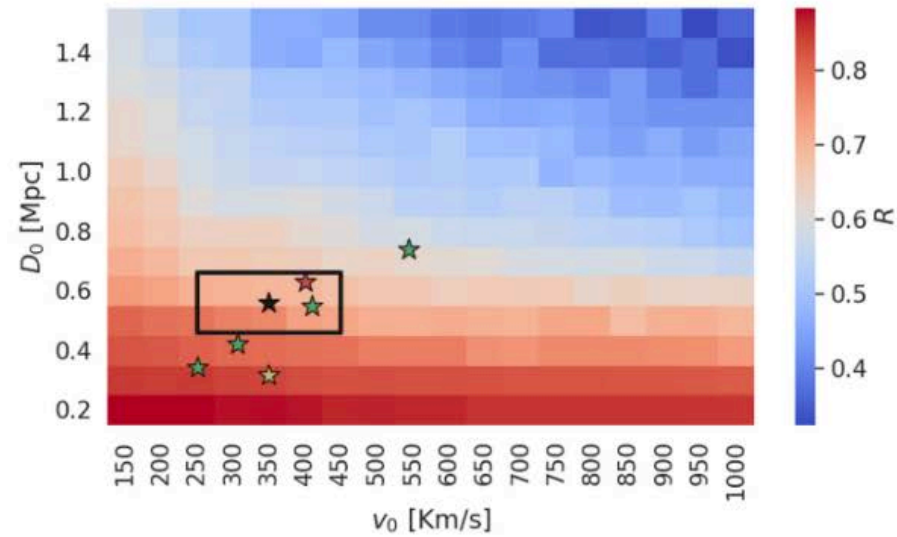
Friend-of-Friend group finder

- Linking length depends only on the mean number density of galaxies
- Different linking lengths in the sky plane and along the line of sight.
- 10x larger linking length along the line of sight

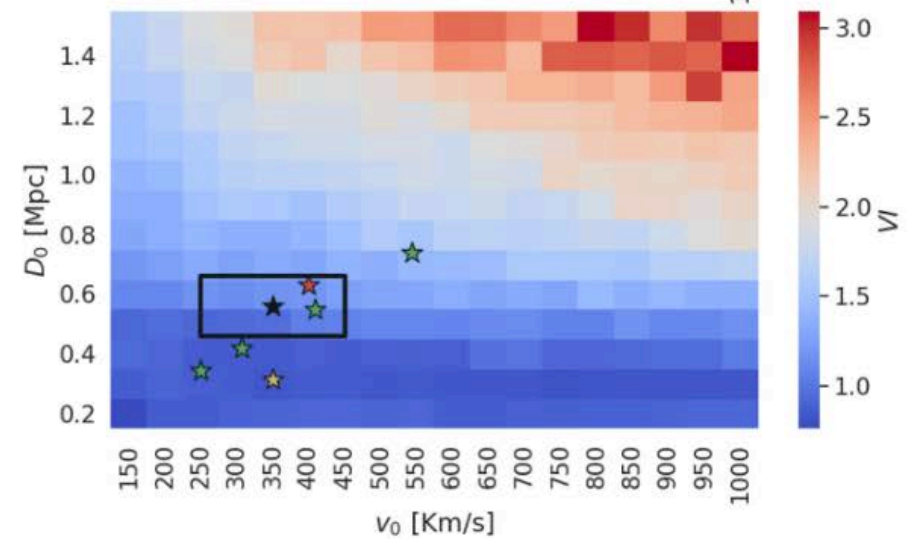
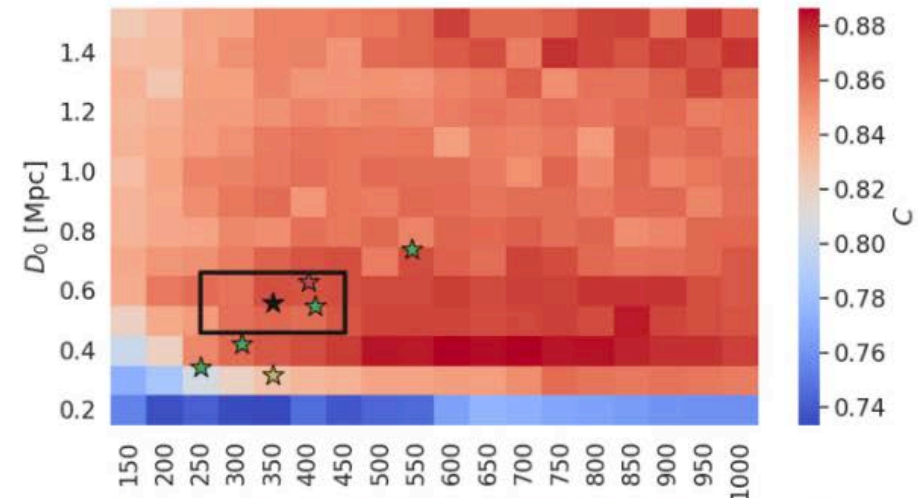
$$LL \approx 0.1 \cdot \left(\frac{Volume}{N_{gal}} \right)^{1/3}$$

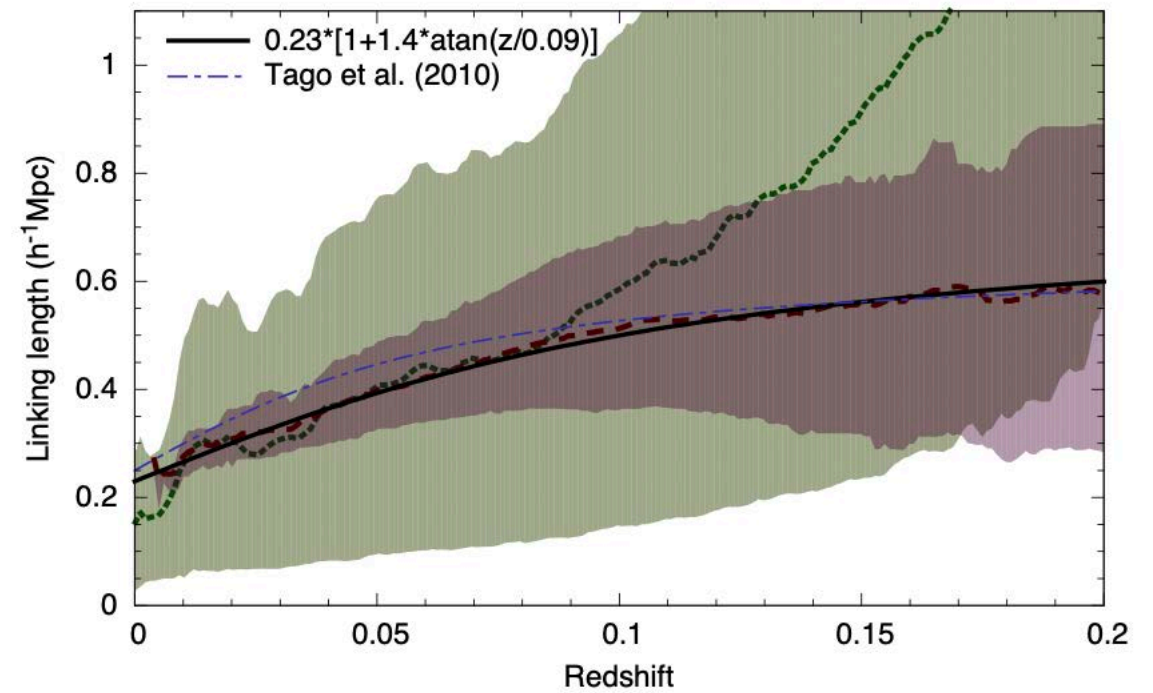
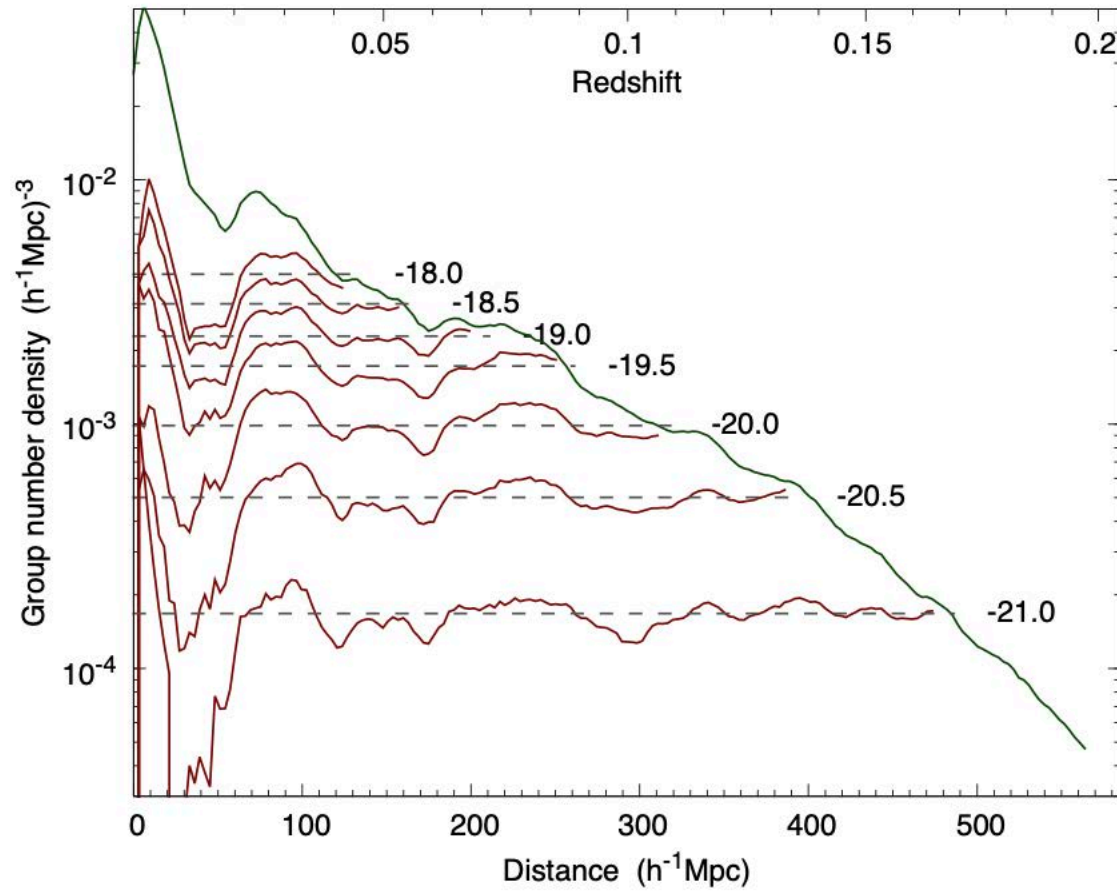


Lambert+2020 on the *not* so shallow 2MRS



- ★ Huchra & Geller, (1982)
- ★ Ramella et al., (1987) & Crook et al., (2007) HDC
- ★ Trasarti-Battistoni, (1998)
- ★ Crook et al., (2007) LDC
- ★ Tago et al., (2012) & Nurmi et al., (2013)
- This Work





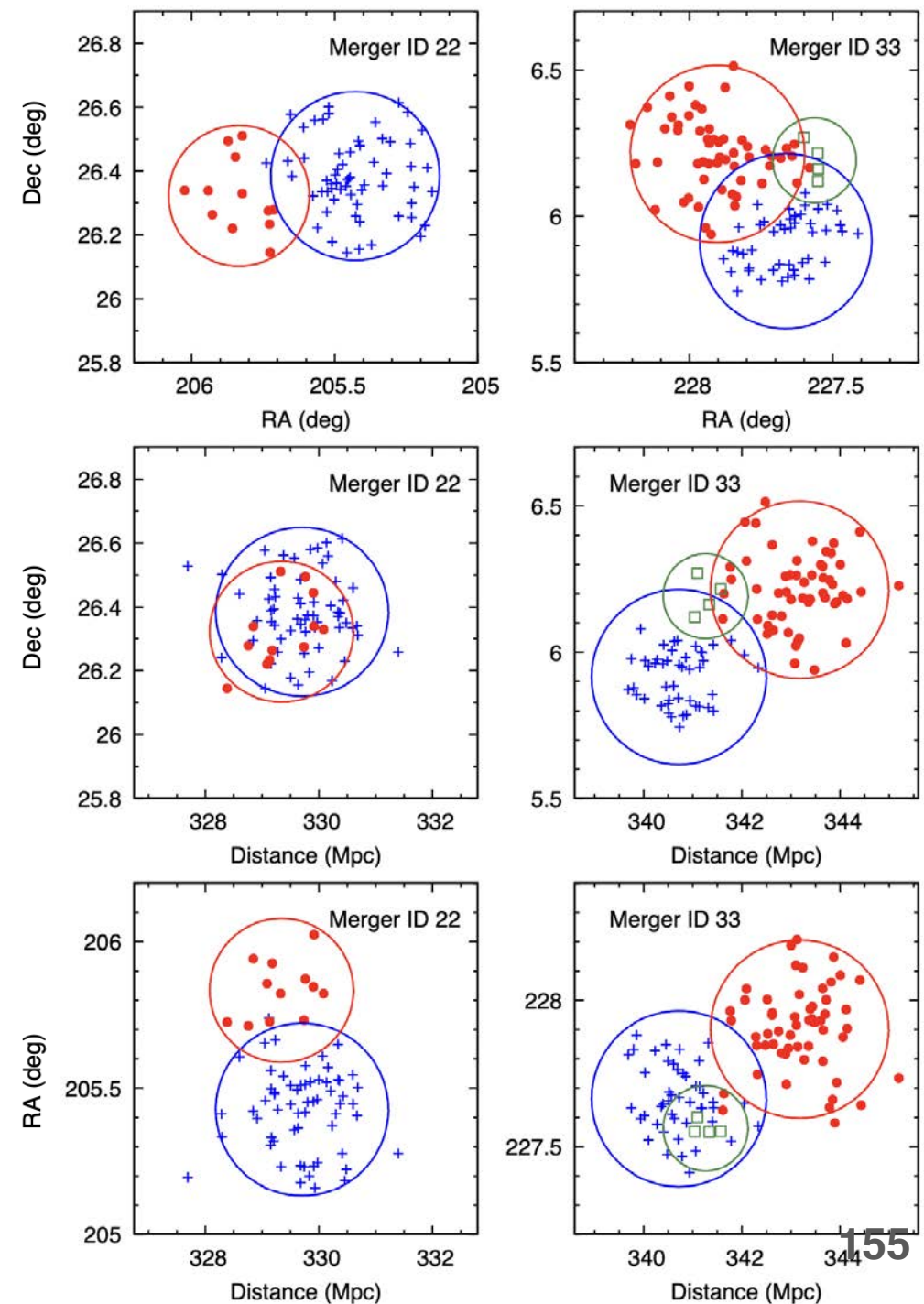
Linking length

Group refinement

- Often merging or closeby groups are taken as one group in FoF
- Multimodality analysis (mclust in R)
- Group membership refinement is based on estimates of the virial radius (in the sky plane) and escape velocity (along the line of sight) of the system.

$$\sigma_v^2 = \frac{1}{(1 + z_m)^2(n - 1)} \sum_{i=1}^n (v_i - v_{\text{mean}})^2,$$

$$\sigma_{\text{sky}}^2 = \frac{1}{2n(1 + z_m)^2} \sum_{i=1}^n (r_i)^2,$$

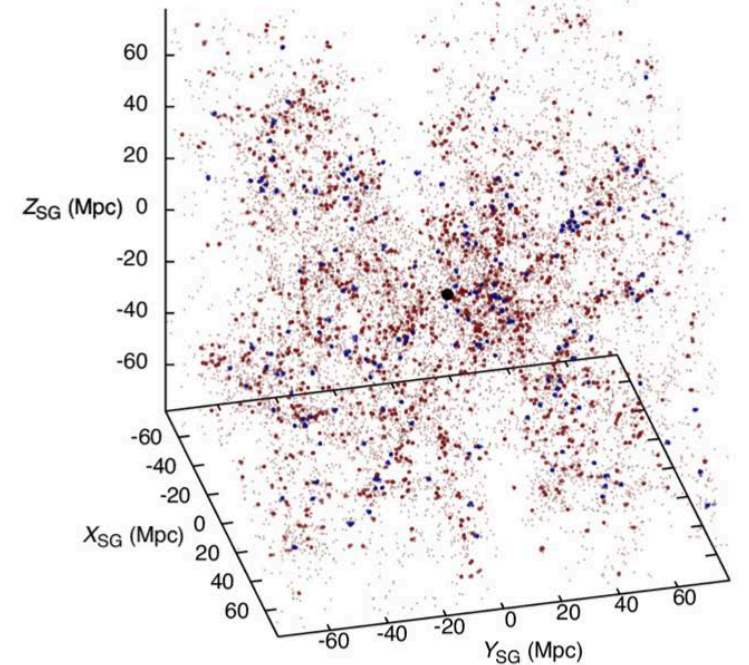
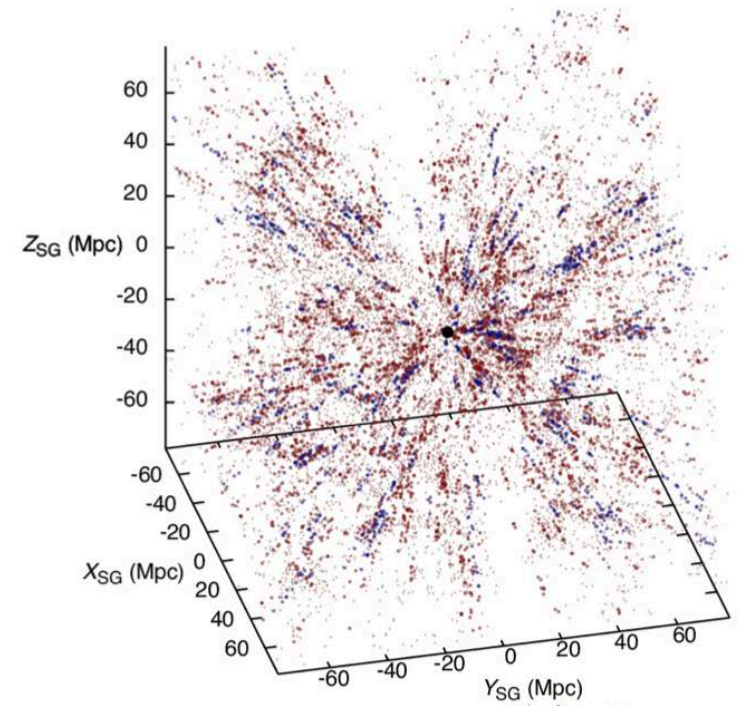


$$d_{\text{gal}} = d_{\text{group}} + \left(d_{\text{gal}}^* - d_{\text{group}} \right) \frac{\sigma_{\text{sky}}}{\sigma_v/H_0},$$

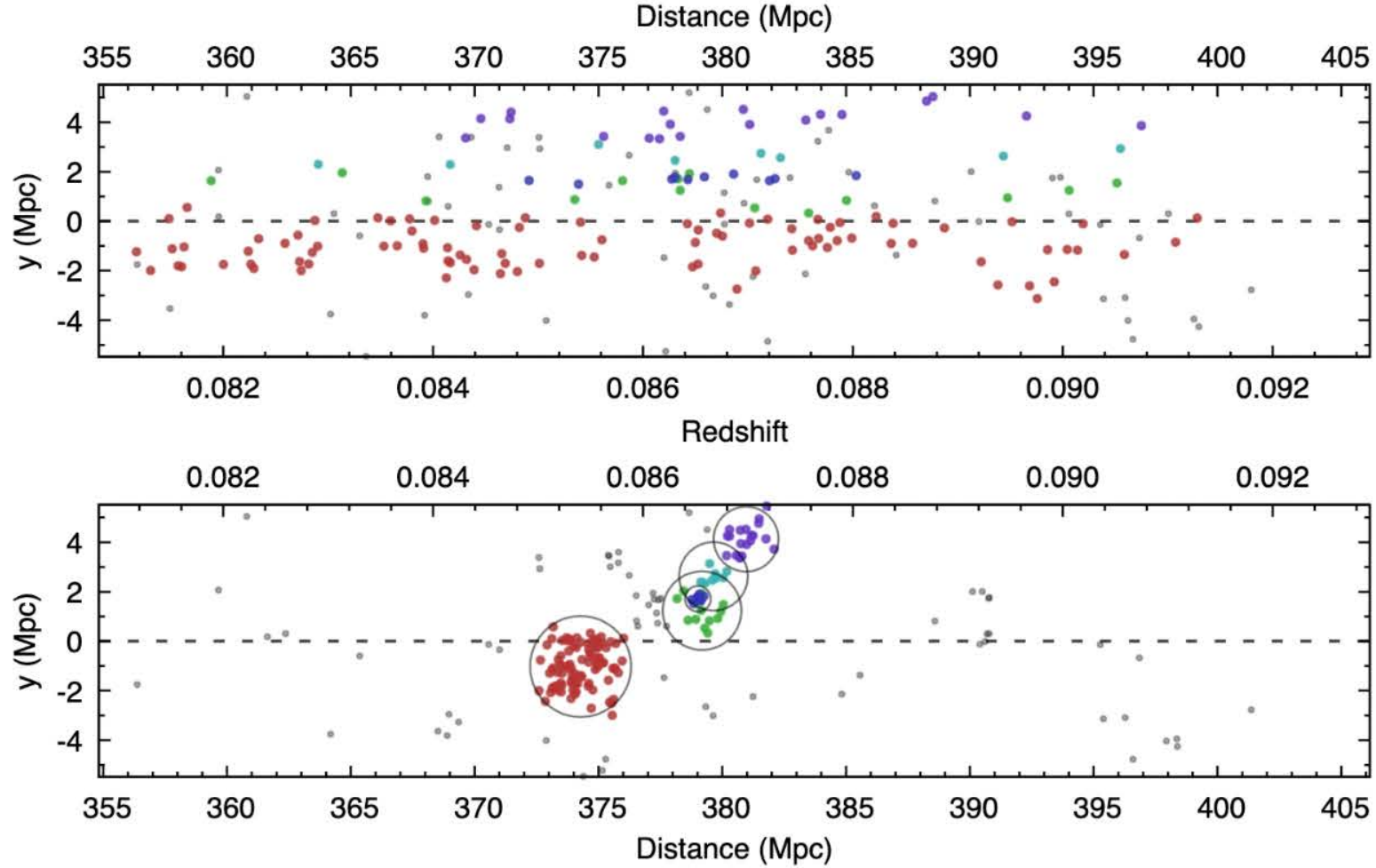
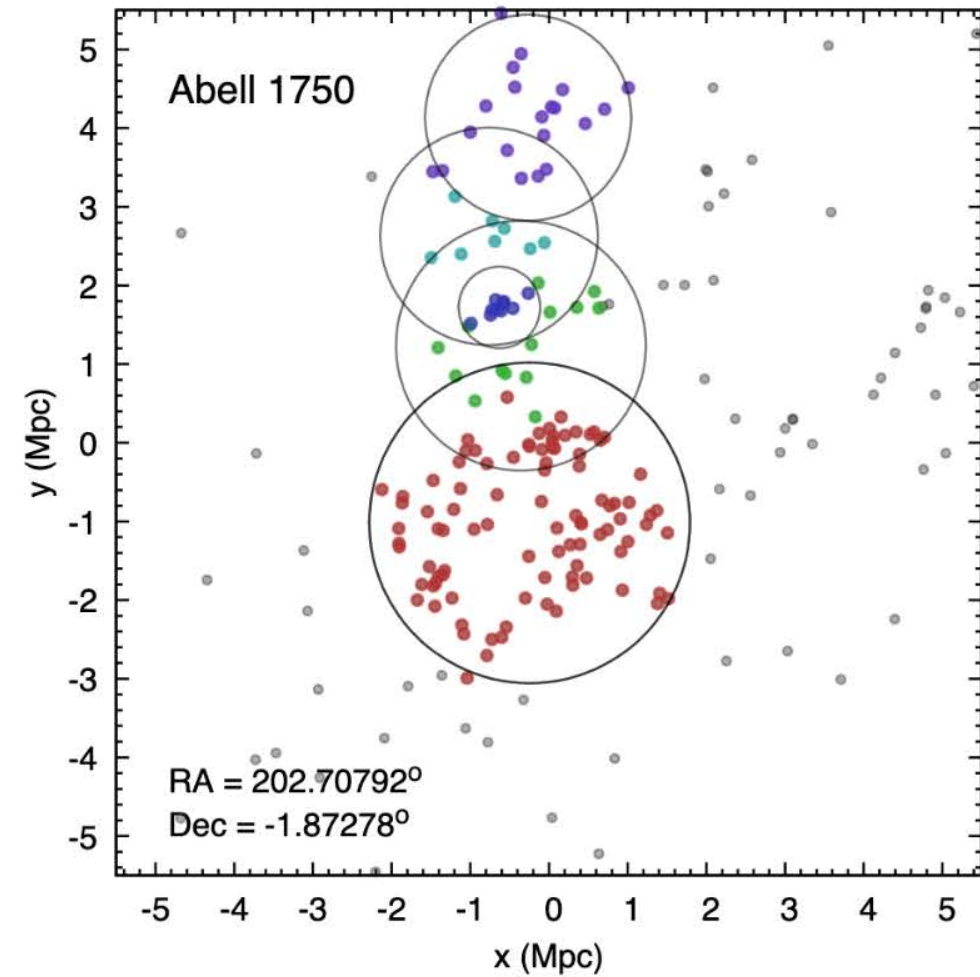
$$d_{\text{gal}} = d_{\text{group}} + \left(d_{\text{gal}}^* - d_{\text{group}} \right) \frac{d_{LL}(z)}{|v_1 - v_2|/H_0},$$

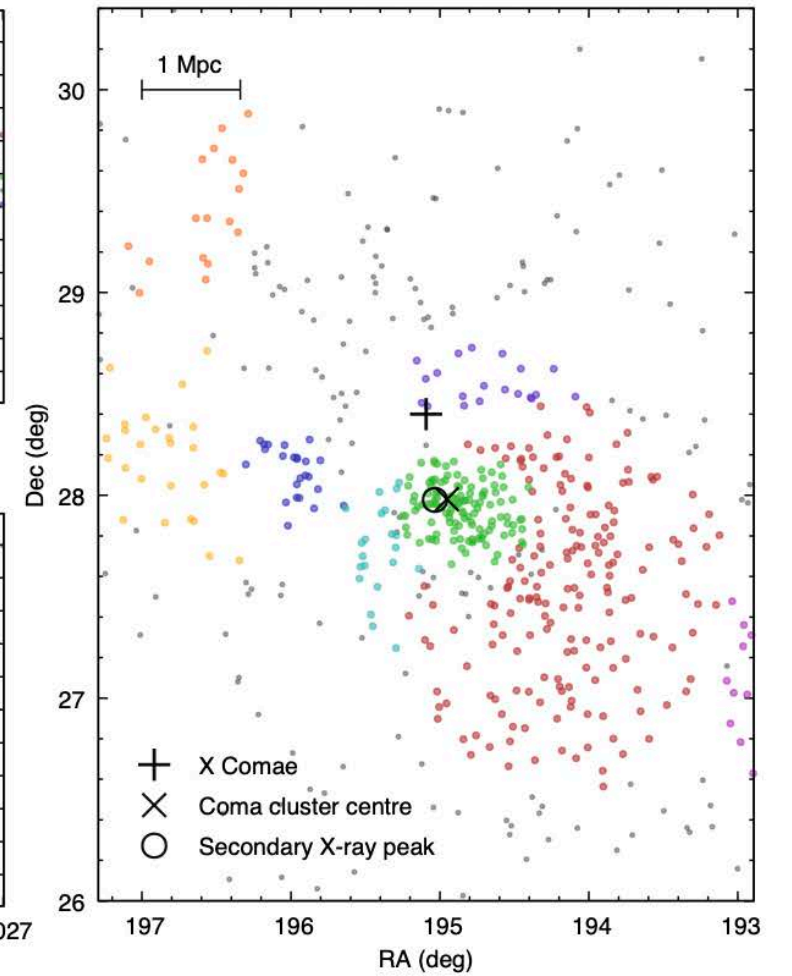
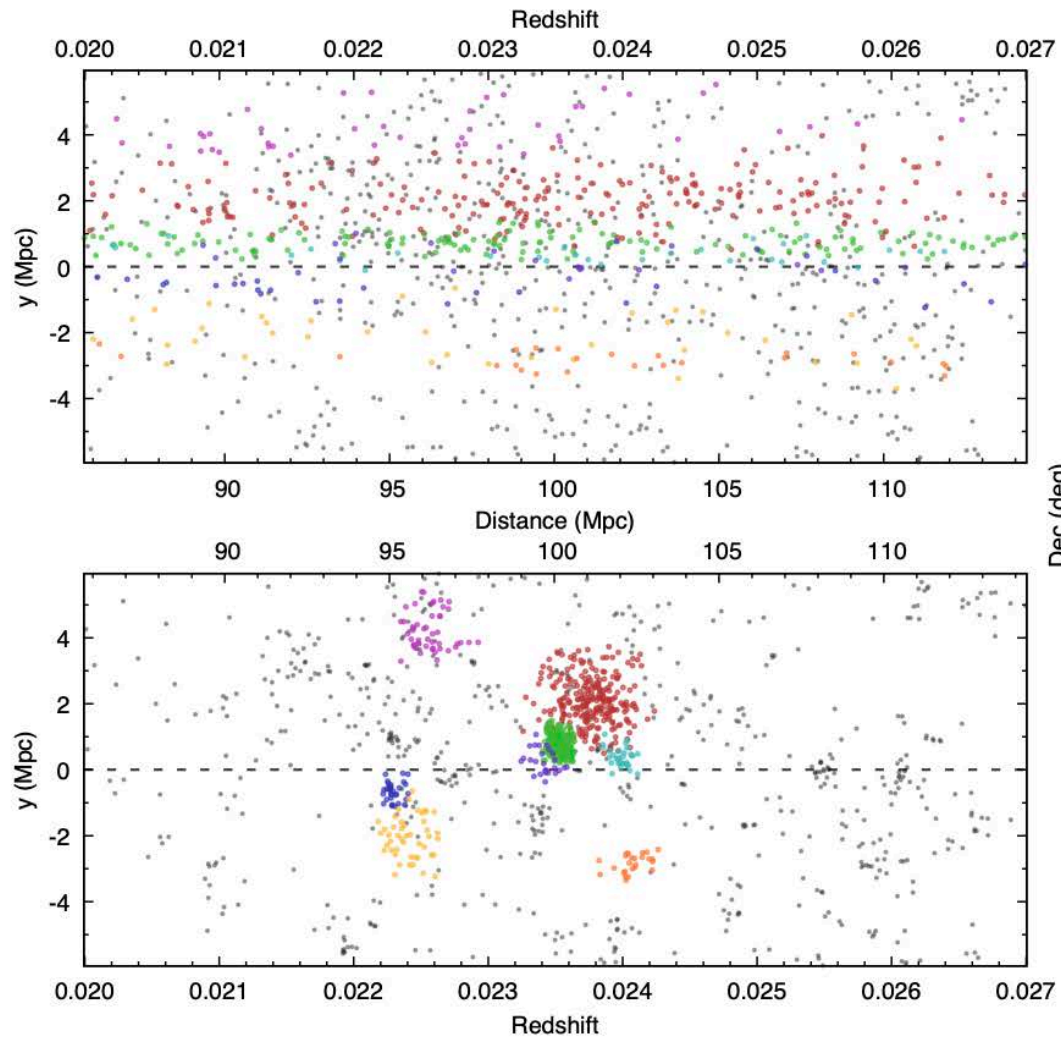
if $|v_1 - v_2|/H_0 > d_{LL}(z)$.

Suppressing FoG effect



Correction for the redshift space distortions





Coma in SDSS

Measuring group properties - centre

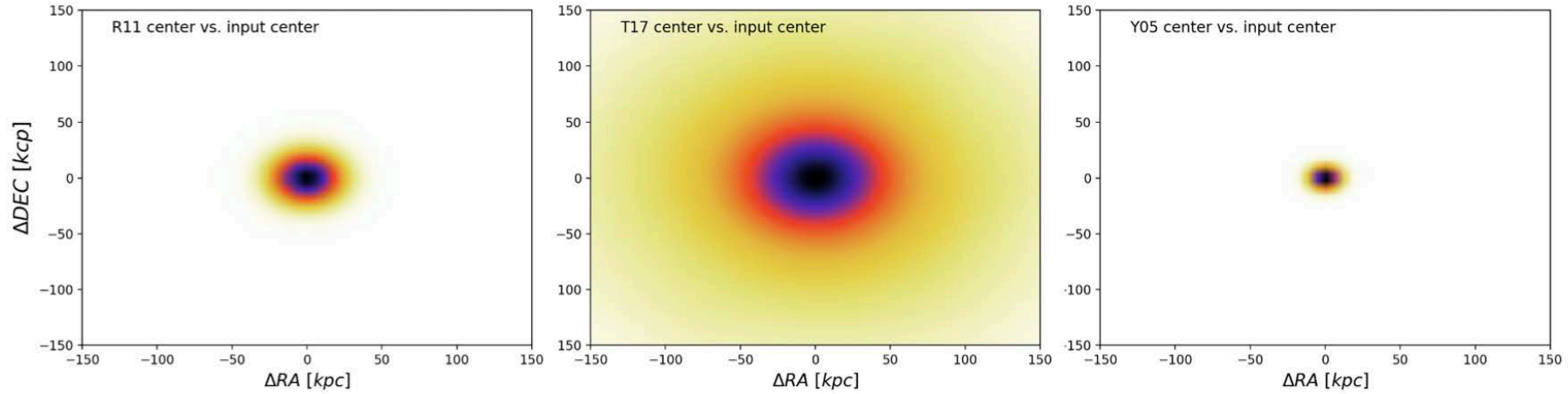


Fig. 6. The figure shows the difference in ΔRA and ΔDEC , estimated in kpc, between the center of the detected optical group and the center of the input halo (left panel), the coordinates of the eSASS X-ray detection and the center of the input halo (central panel), and the center of the detected optical group and of the eSASS X-ray detection.

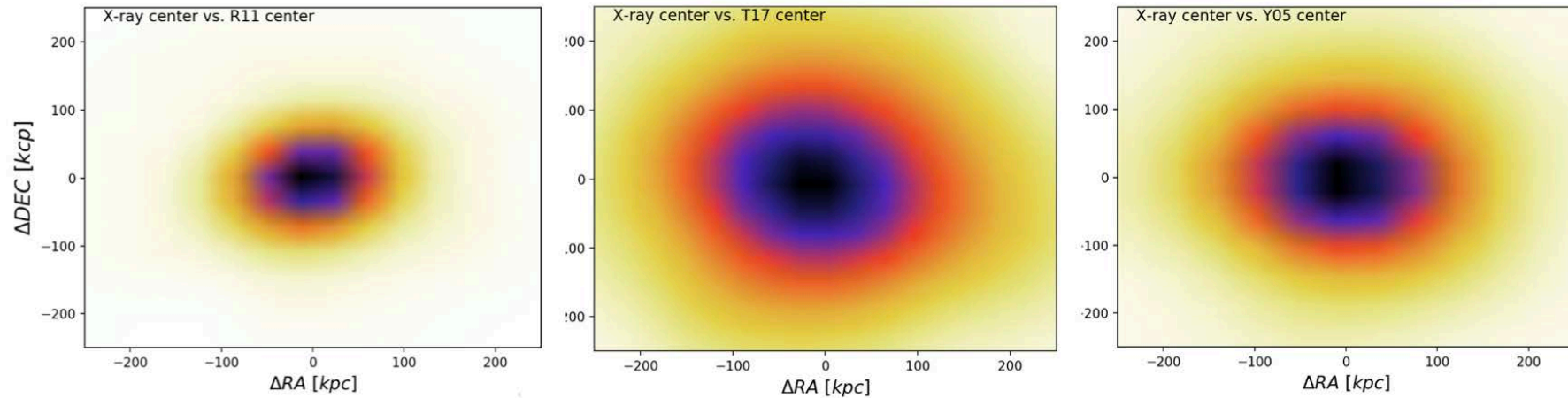
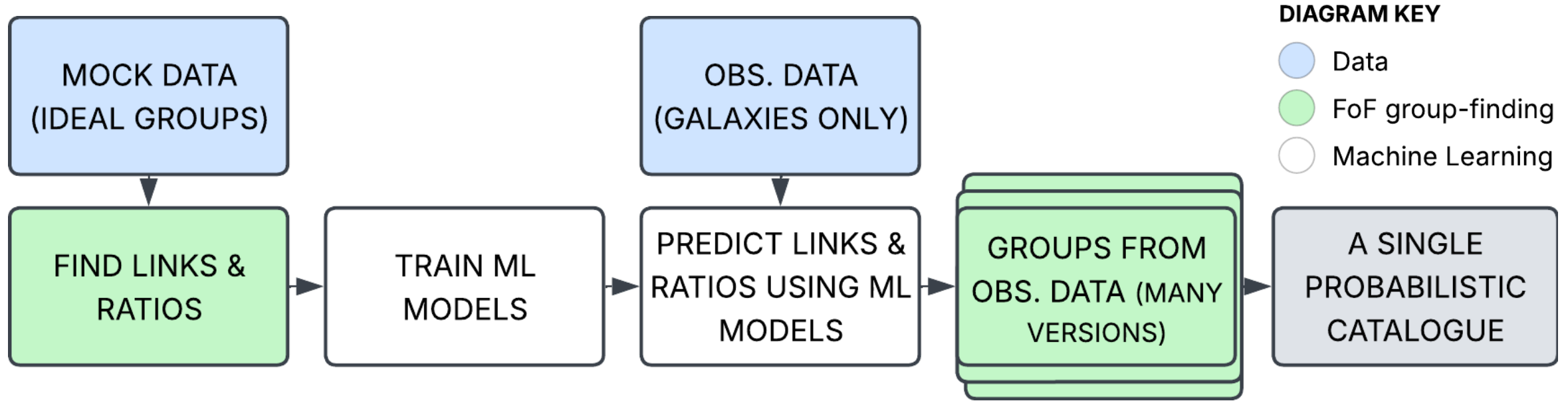


Fig. 7. The figure shows the difference in ΔRA and ΔDEC , estimated in kpc, between the center of the detected optical group and the center of the input halo (left panel), the coordinates of the eSASS X-ray detection and the center of the input halo (central panel), and the center of the detected optical group and of the eSASS X-ray detection.

The Current Group-Finder Pipeline



Two components: finding D_{\perp} , R and training ML model

Improvements

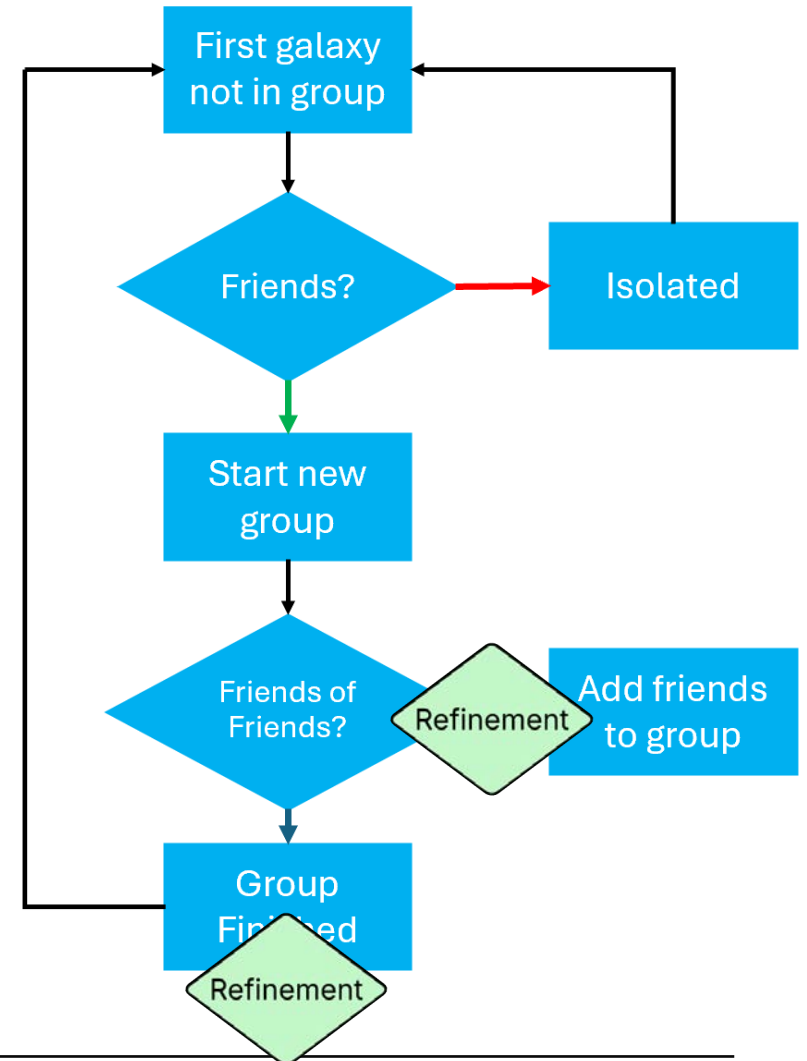
Merged groups: refinement part of FoF

Accuracy: unique D_{\perp} , R for all galaxies

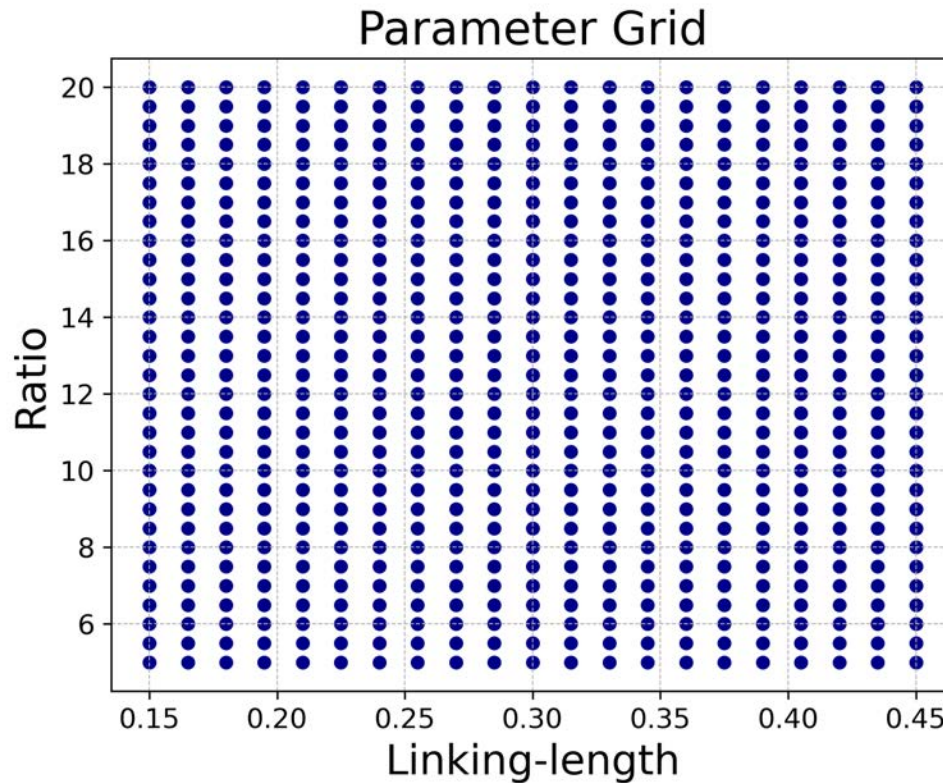
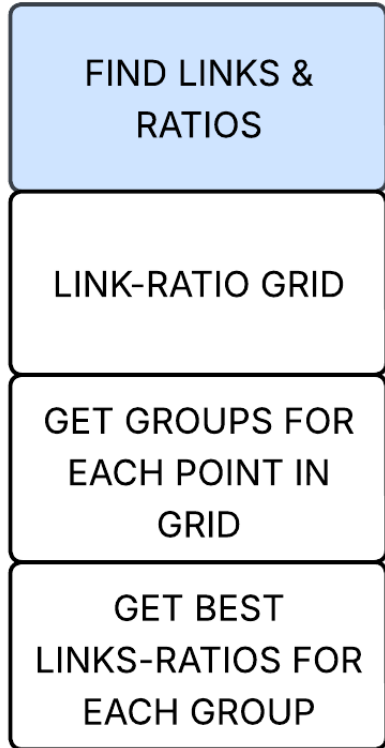
Niche: ML component

Universality: optimisable for *almost* any dataset

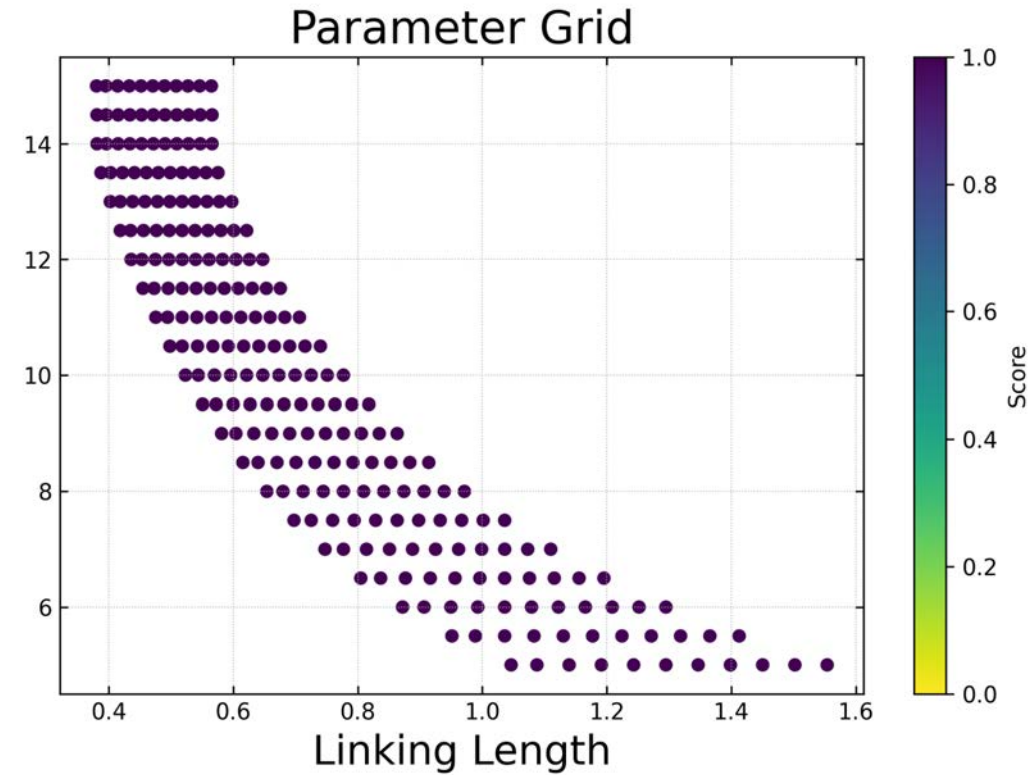
Output: probabilistic catalogue.. TBD



Finding D_{\perp} , R for Mock Groups



Unique to each group



$$\text{Score} = \frac{N_{gal}^2(\text{mock} \cap \text{FoF})}{N_{gal}(\text{mock})N_{gal}(\text{FoF})}$$

ML Model

Training (XGBRegressor)

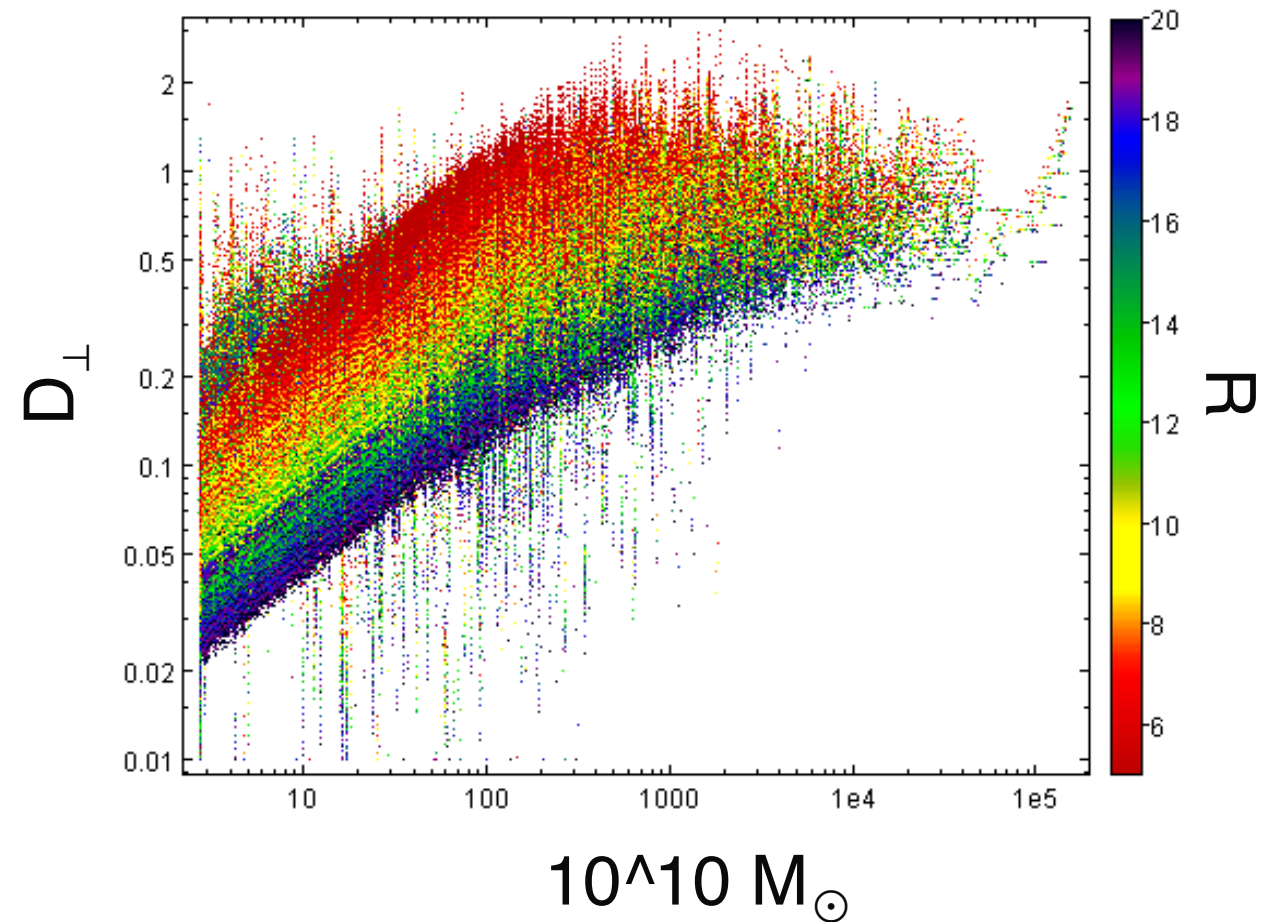
Inputs: Group mass, Ngal, Z, mag

Outputs: D_{\perp} , R

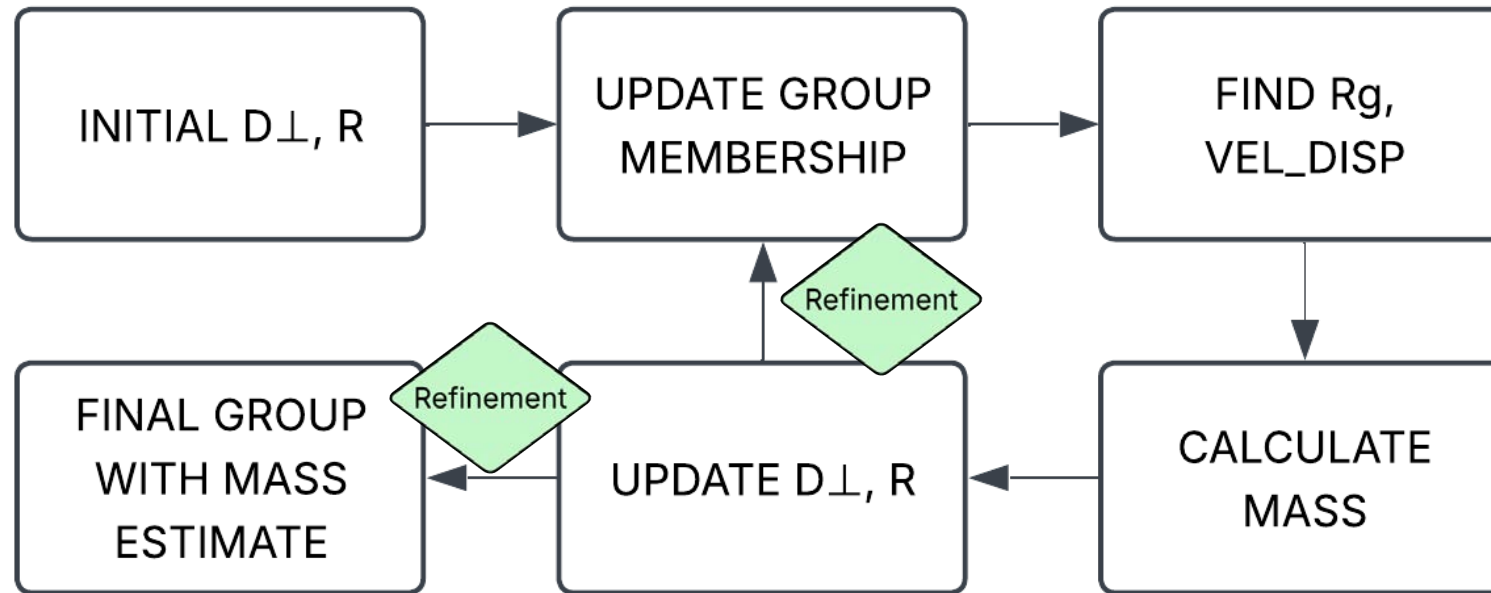
Predicting

D_{\perp} , R for a wide range of possible

Ngal & group masses



Mass Estimation Inside FoF



Dynamical mass

$$M_{tot} = 2.325 \times 10^{12} \frac{R_g}{\text{Mpc}} \left(\frac{\sigma_v}{100 \text{ km s}^{-1}} \right)^2 M_{\odot}$$

Slide credit:
Trystan Lambert

The WAVES-TWG4 Open Invitational



FRANKENSTEIN

- The perfect group finder
- Highly optimized for WAVES and consequently for 4HS too.
- Massive benefit to the community too.

JOIN US!!



UNIVERSITY OF TARTU

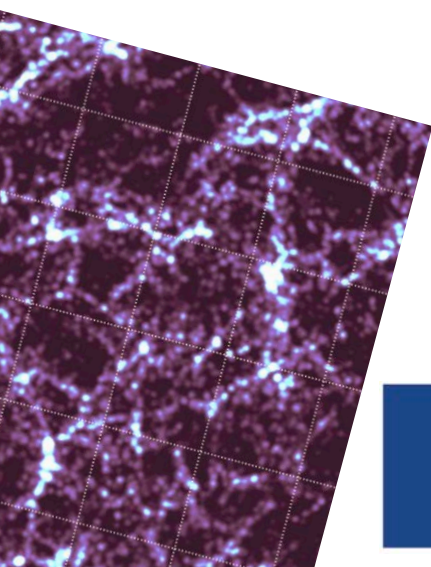


Co-funded by
the European Union



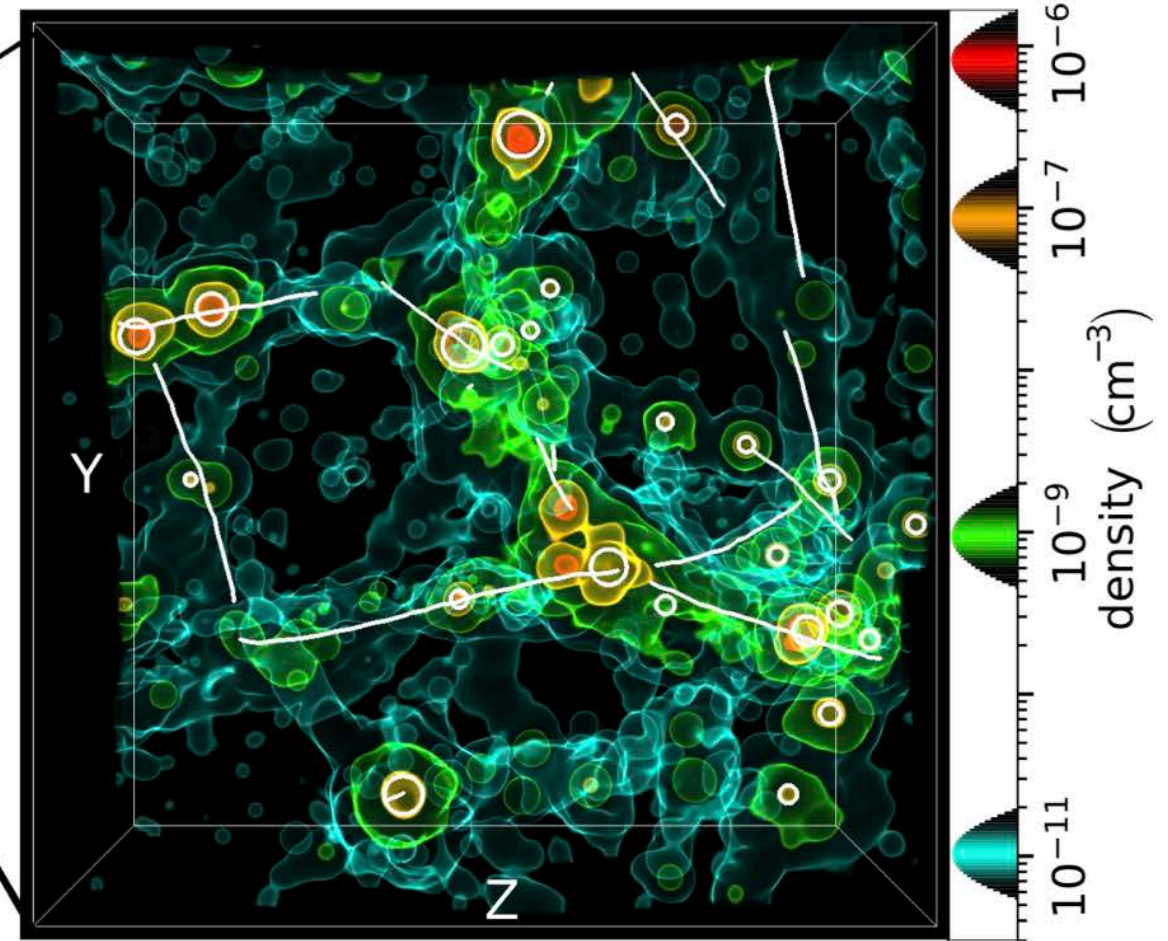
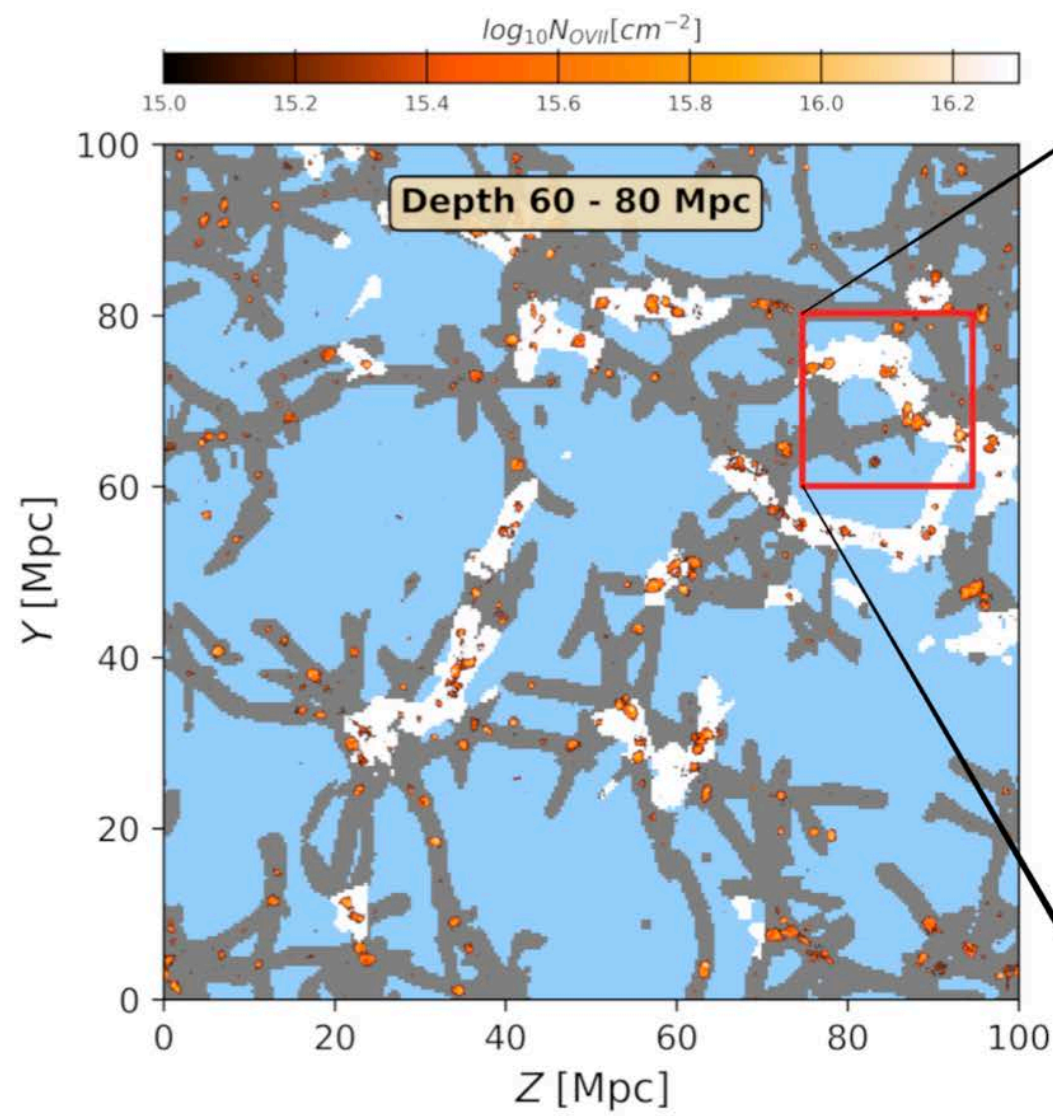
Investing
in your future

Filaments in the Cosmic Web



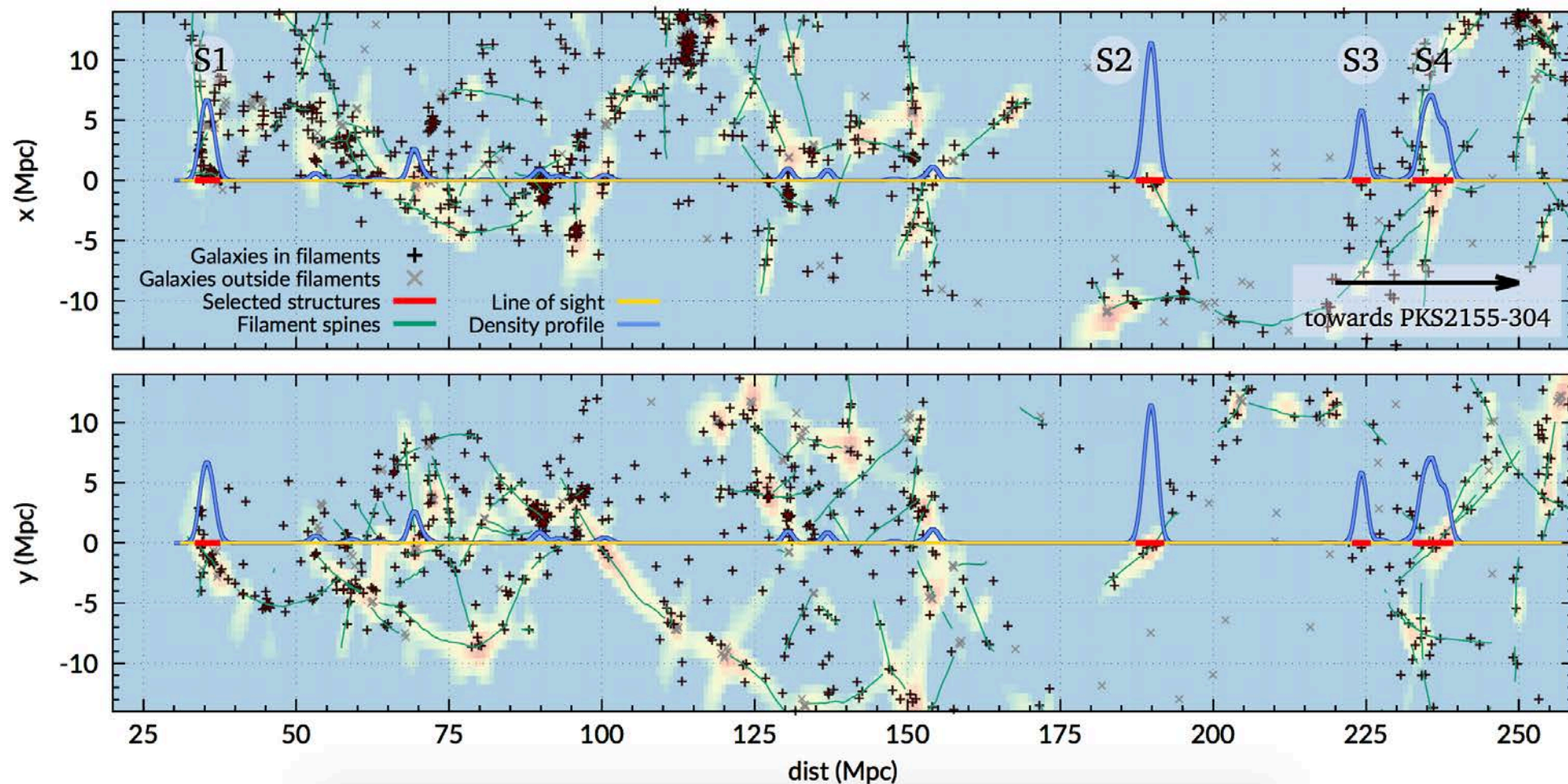
Funded by
the European Union







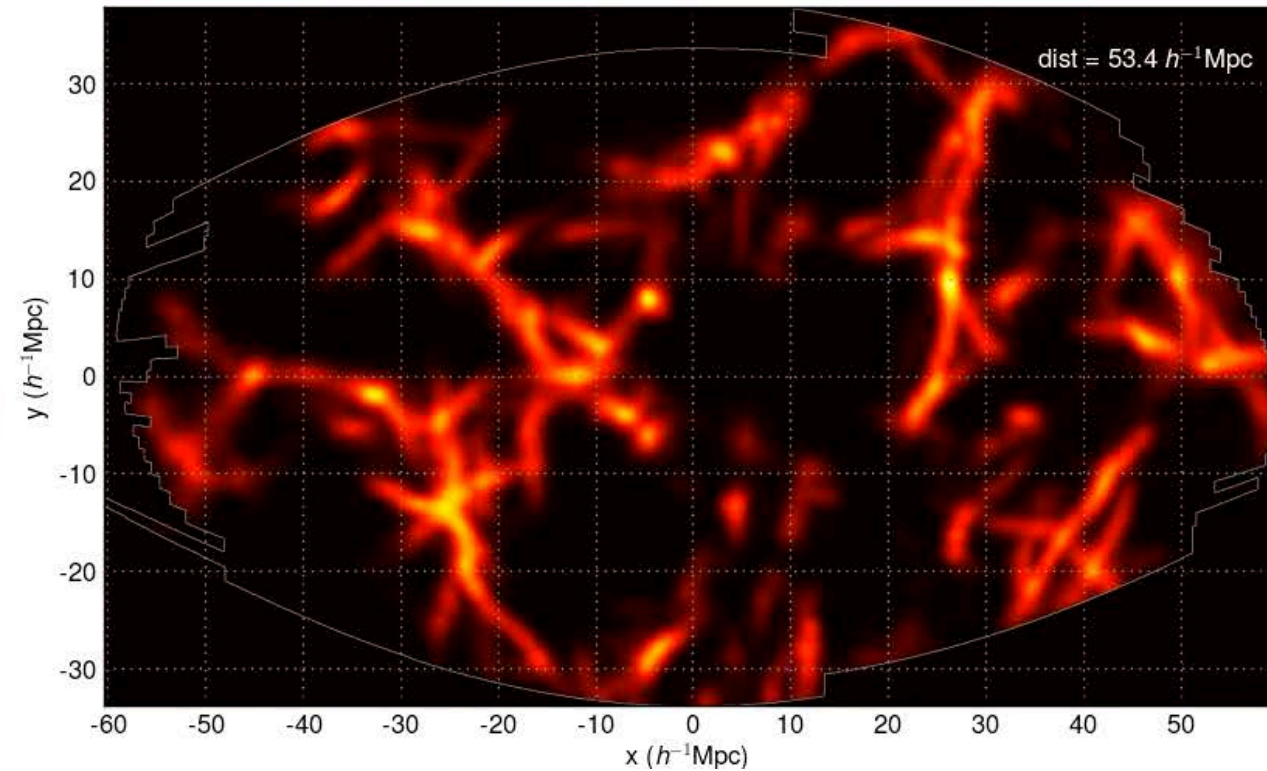
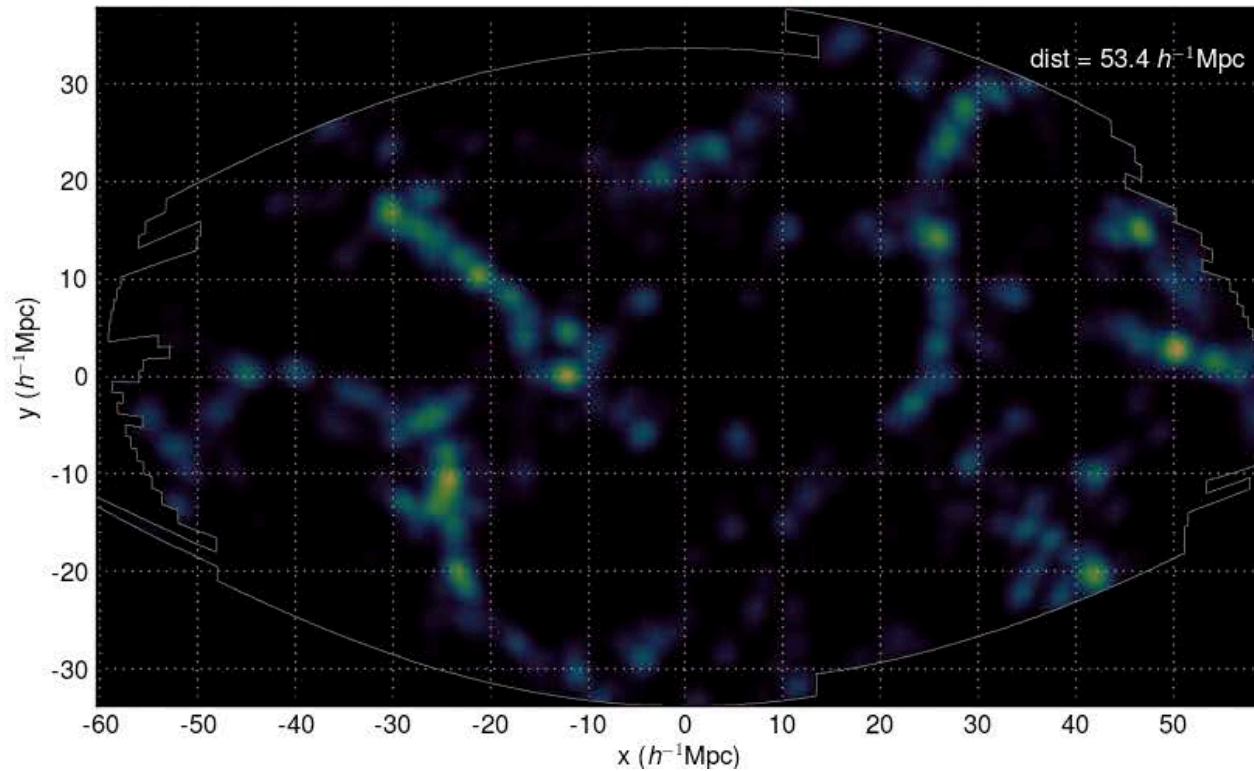
Hunting for WHIM (warm hot intergalactic medium)



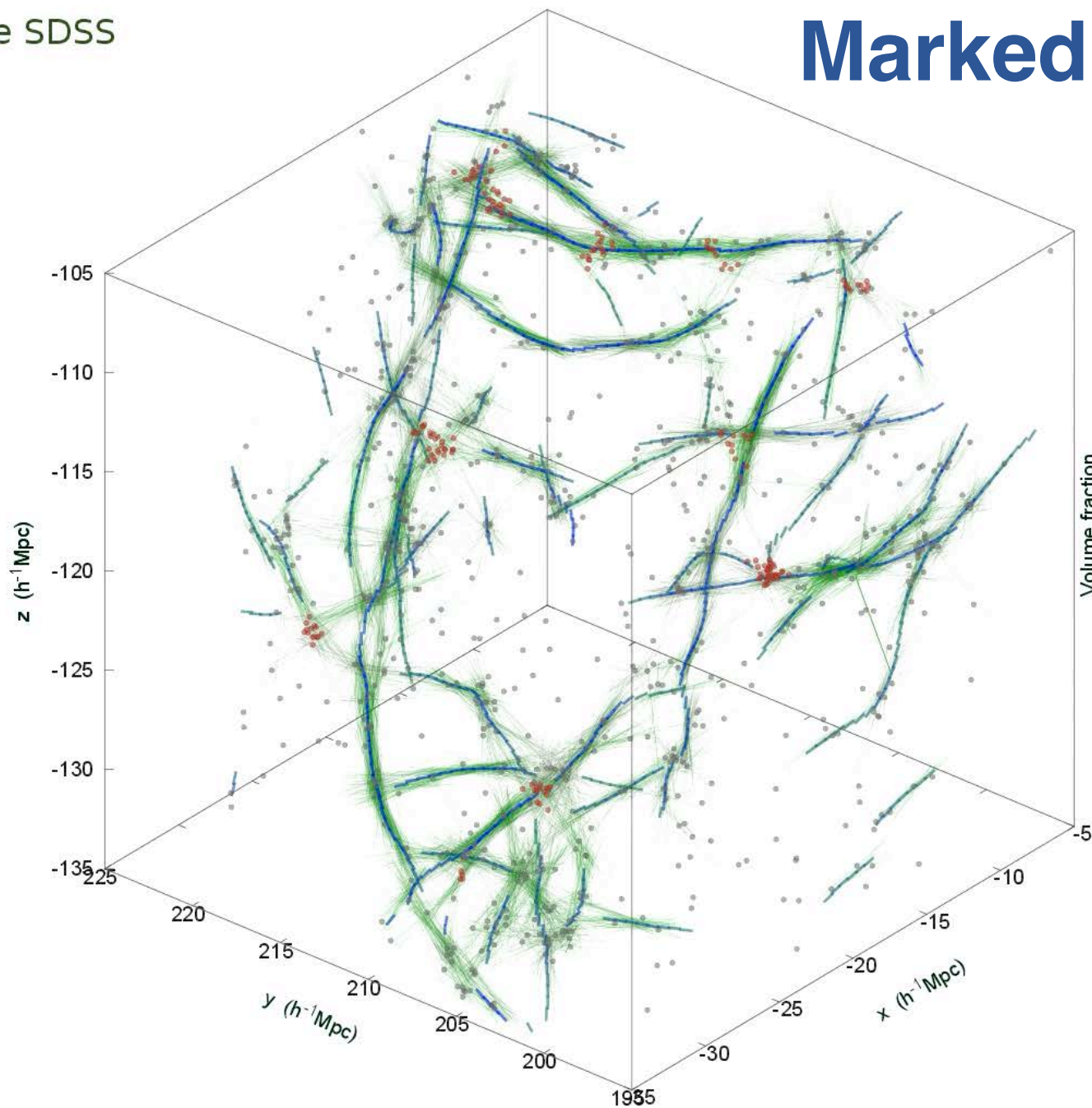
Why do we care about the cosmic web?

Galaxy filaments

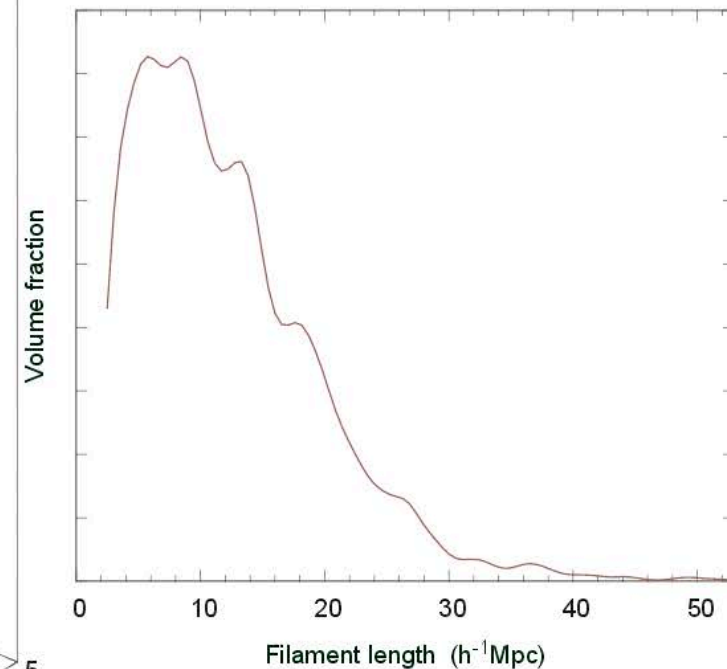
Marked point process for filamentary network detection



- Extracted filaments
- Connected cylinders
- Galaxies
- Galaxies in groups



Filament length distribution:
whole SDSS volume



Marked point process (Bisous model)

- ✦ The key idea is to see the filamentary network as an object point process.
- ✦ Cylinders are simplest objects to define a piece of filament.
- ✦ Interactions help to form a network.
- ✦ Metropolis-Hastings algorithm (together with simulated annealing) to sample probability distribution.

Stoica et al. (2003, 2005)

Stoica, Martinez, Saar (2007, 2010)

Tempel et al. (2014, 2016)

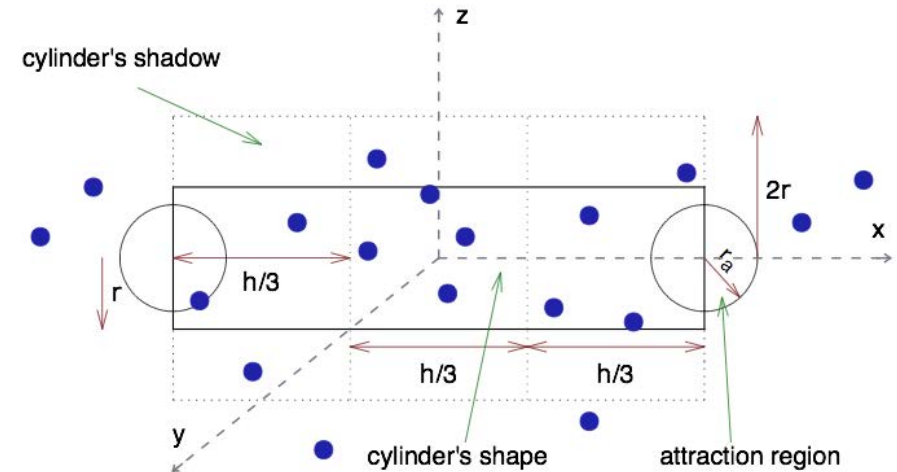


Figure 1. Two-dimensional projection of a cylinder with its shadow within a pattern of galaxies. The attraction regions are shown as spheres. The exact shape of the cylinder, its shadow and attraction regions depend on the model.

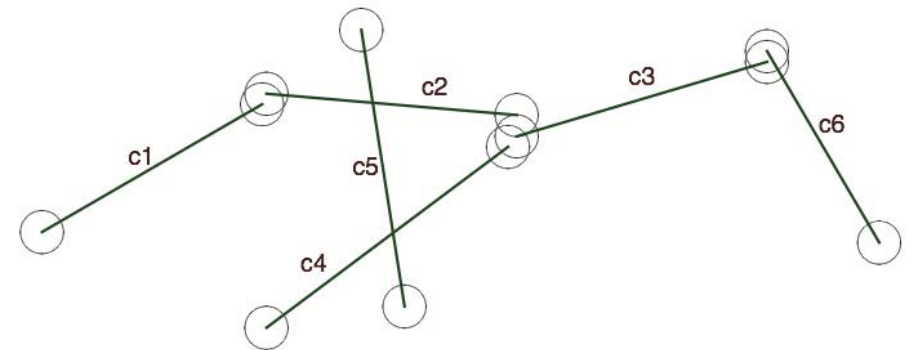


Figure 2. Two dimensional representation of cylinder configuration: attraction regions are shown with spheres. In this configuration: 71



Marked point process

Probability density that depends on the underlying data (position of galaxies) and the detected network (filamentary pattern)

Bisous model (Candy model)

The probability density for a marked point process based on random cylinders can be written

$$p(\mathbf{y}|\theta) = \frac{\exp[-U(\mathbf{y}|\theta)]}{\alpha} \quad (4)$$

where α is the normalising constant, θ is the vector of the model parameters and $U(\mathbf{y}|\theta)$ is the energy function of the system. Here, \mathbf{y} is the configuration of cylinders.

Following these two ideas the energy function given by (4) can be specified as:

$$U(\mathbf{y}|\theta) = U_d(\mathbf{y}|\theta) + U_i(\mathbf{y}|\theta), \quad (5)$$

where $U_d(\mathbf{y}|\theta)$ is the data energy (see Sect. 3.4) and $U_i(\mathbf{y}|\theta)$ is the interaction energy (see Sect. 3.5) associated to the first and second assumptions above, respectively. In fact, it is perfectly reasonable to think that the data energy is the reason that the cylinders in the galaxy field are positioned just so, and that the interaction energy is the main factor which causes the cylinders to form filamentary patterns.



Marked point process

Metropolis-Hastings algorithm to sample from probability density:

$$p(\mathbf{y}|\theta) = \frac{\exp[-U(\mathbf{y}|\theta)]}{\alpha}$$

- birth (uniform, connected)
- death
- change

$$\min \left\{ 1, \frac{p_d}{p_b} \frac{d(\mathbf{y} \cup \{\zeta\}, \zeta)}{b(\mathbf{y}, \zeta)} \frac{p_n(\mathbf{y} \cup \{\zeta\})}{p_n(\mathbf{y})} \right\}$$

$$b(\mathbf{y}, \zeta) = \frac{p_1}{v(K)} + p_2 b_a(\mathbf{y}, \zeta)$$

Simulated annealing:

$$p_n(\mathbf{y}) \propto [p(\mathbf{y})]^{T_n}$$

$$T_n = \frac{1}{\log(n+1)}$$

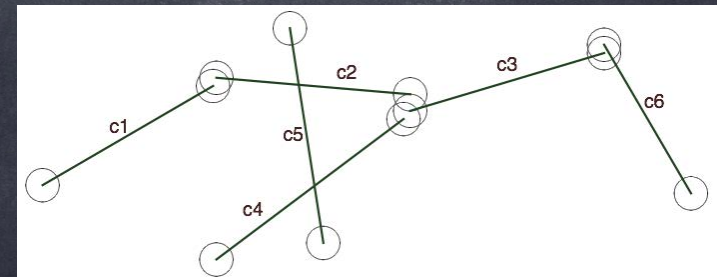


Figure 2. Two dimensional representation of cylinder configuration: attraction regions are shown with spheres. In this configuration:



Bisous model

Data energy:

$$U_d(\mathbf{x}|\theta) = - \sum_{x \in \mathbf{x}} [\log(p_{vu}(x)p_{vh}(x)) - \sigma^2(x)] , \quad (27)$$

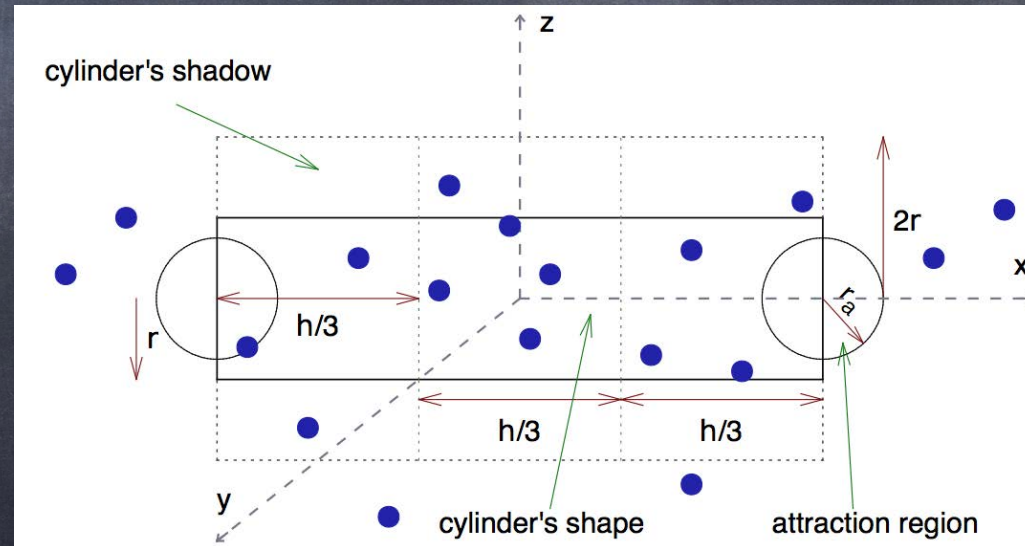
Hypothesis testing to test the “uniformity” of a filament and to test the “locally high density” in a filament.

$$p_{vu} = \mathbf{P}[X|X + \tilde{X}, p(\rho_u)] \leq \alpha_u, \quad (21)$$

$$p_{vh} = \mathbf{P}[X|X + \tilde{X}, p(\rho_h)] \leq 1 - \alpha_h. \quad (24)$$

Cylinder concentration:

$$\sigma^2 = \frac{1}{n-2} \sum_{j=1}^n d_j^2, \quad (25)$$

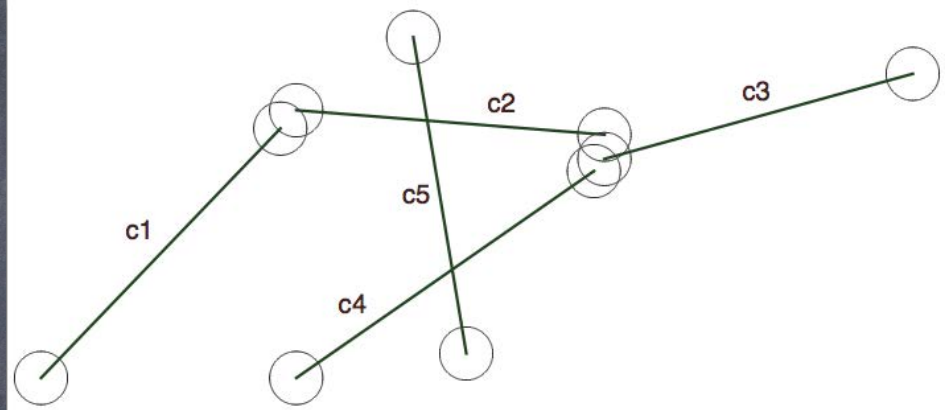




Bisous model

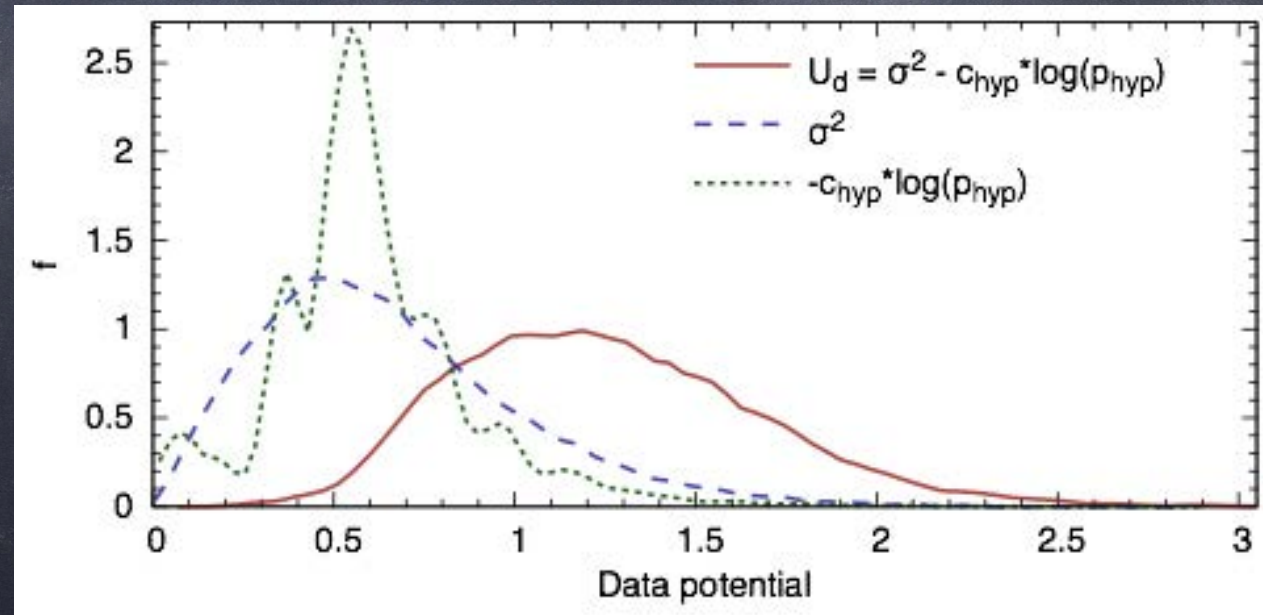
Interaction energy:

Repulsive cylinders,
0,1,2-connected cylinders



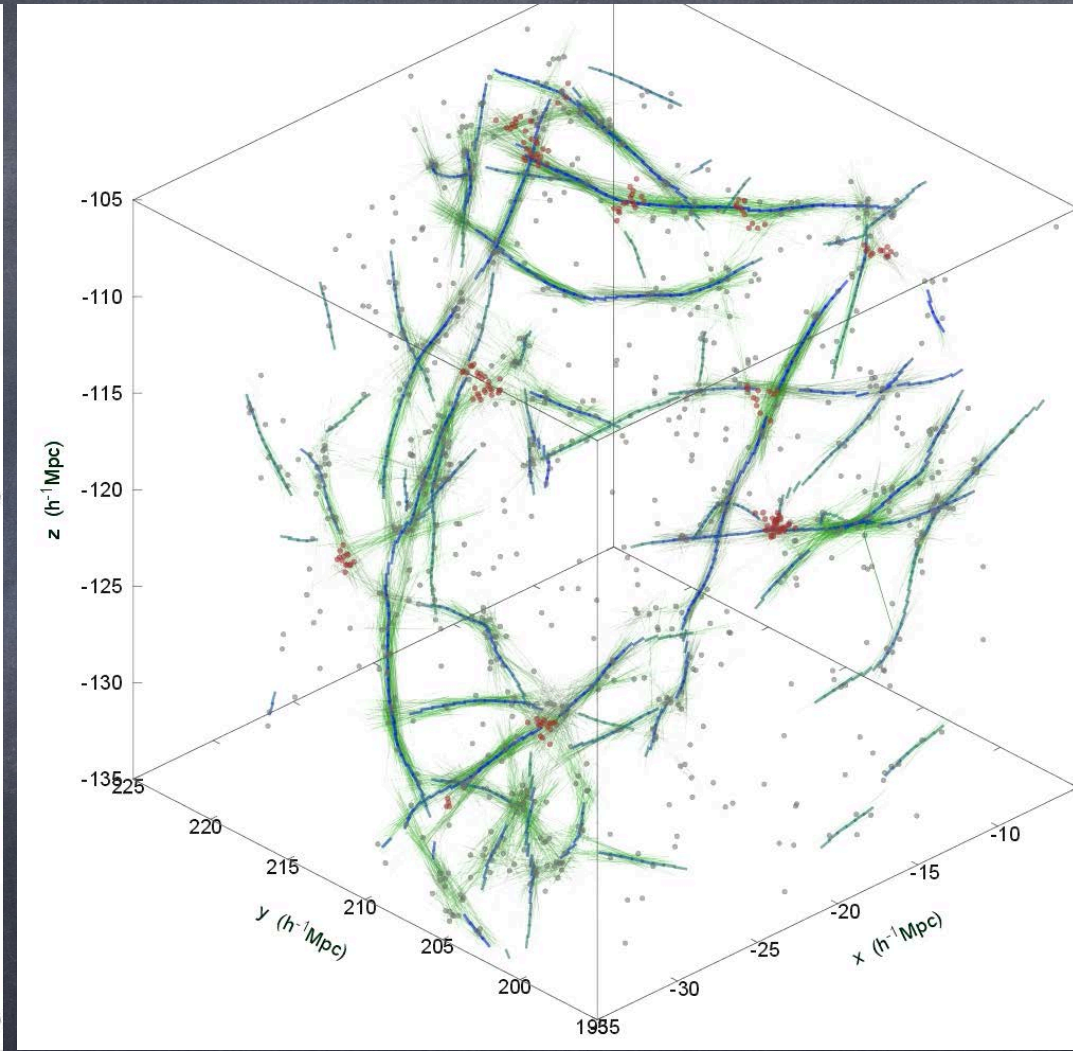
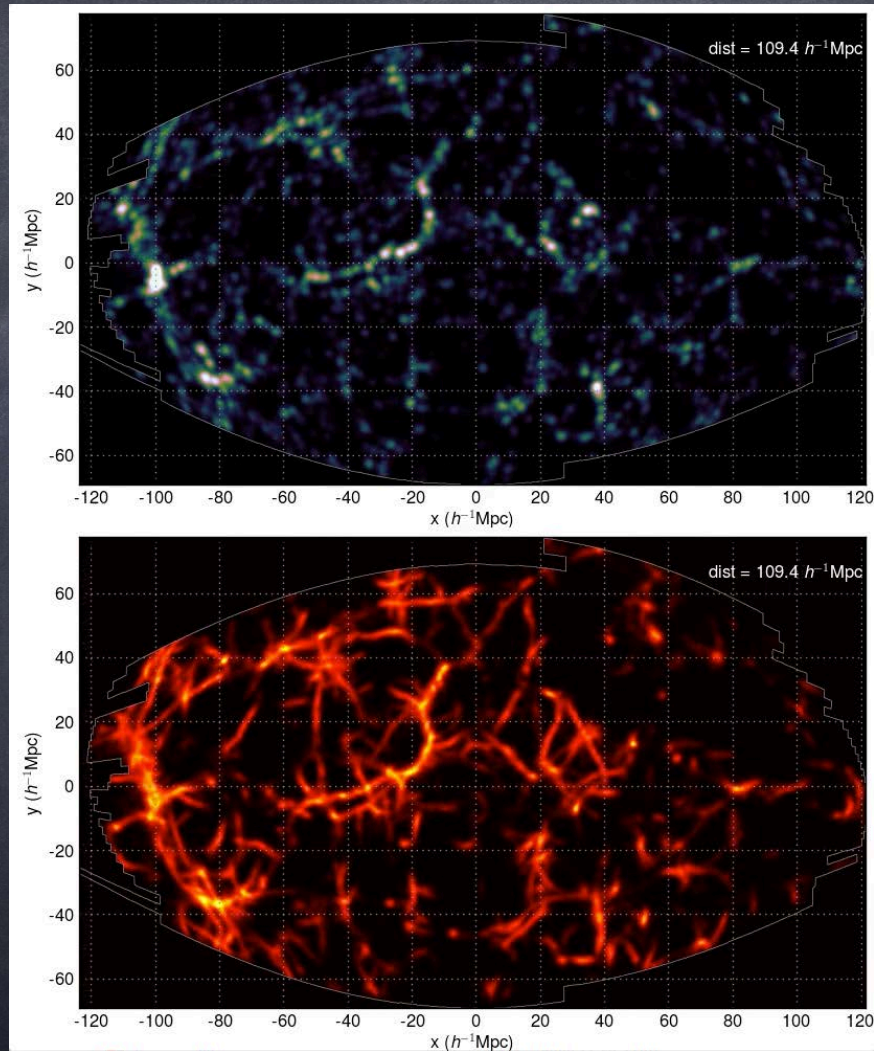
$$U_i(\mathbf{y}|\theta) = -n_k(\mathbf{y}) \log \gamma_k - \sum_{s=0}^2 n_s(\mathbf{y}) \log \gamma_s, \quad (29)$$

Data energy:





Results: detected filaments





Extracting single filaments

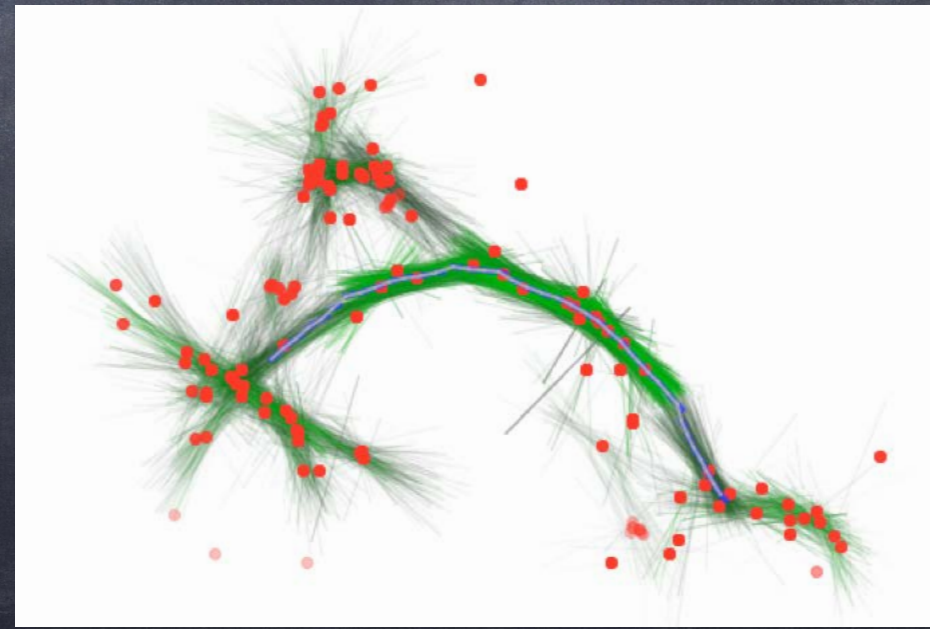
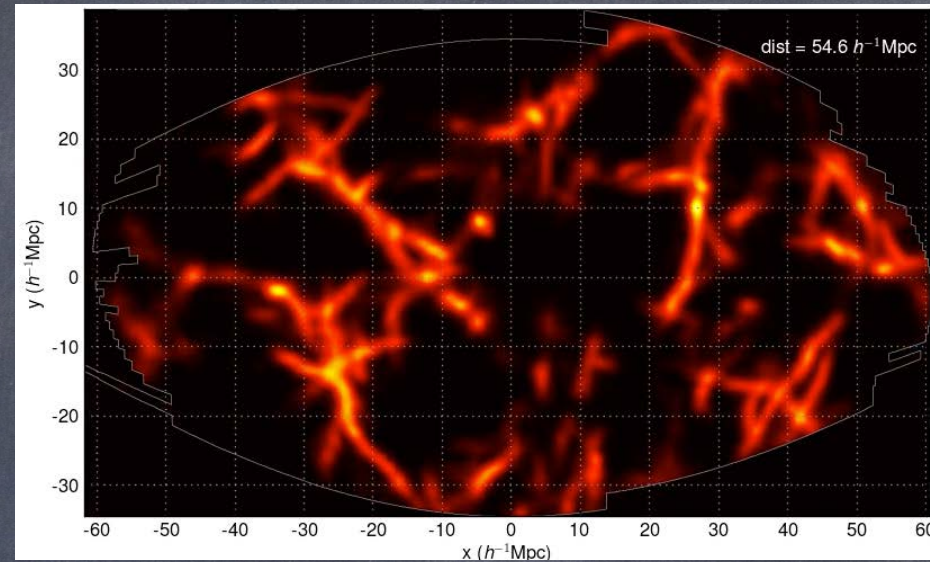
- Set of simulations (50 simulations):
100000x200000 moves!
- $50 \times 30 = 1500$ realizations



- Density field of filaments
- Orientation field of filaments

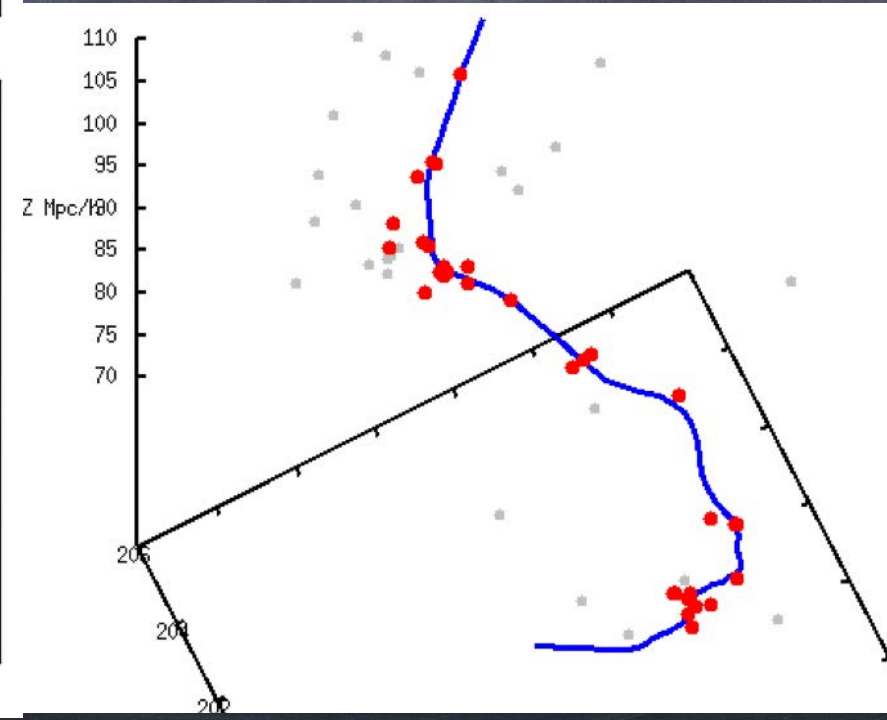
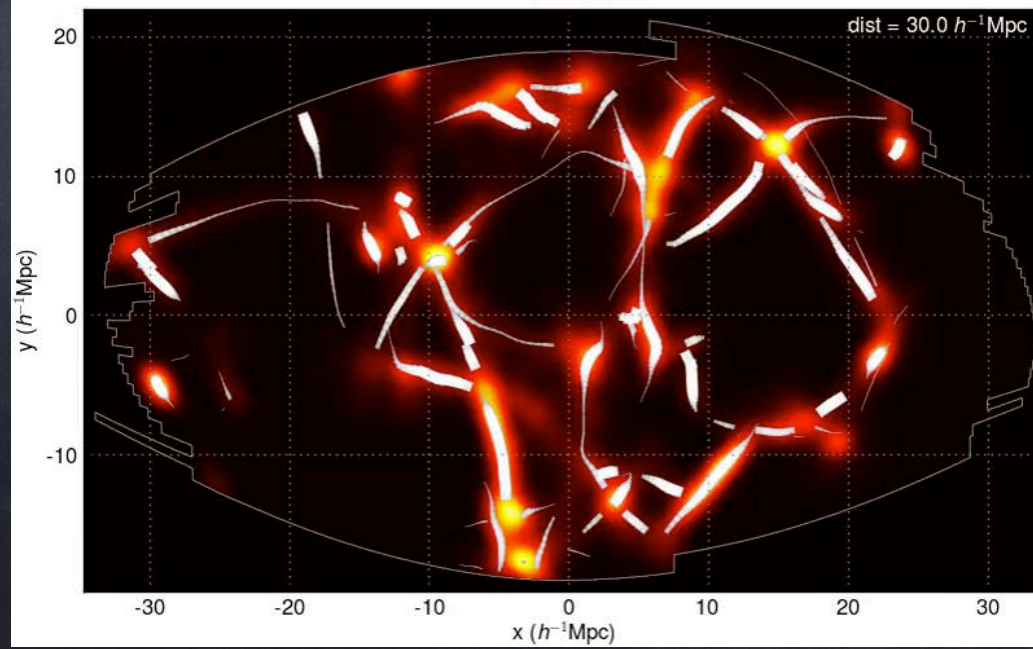
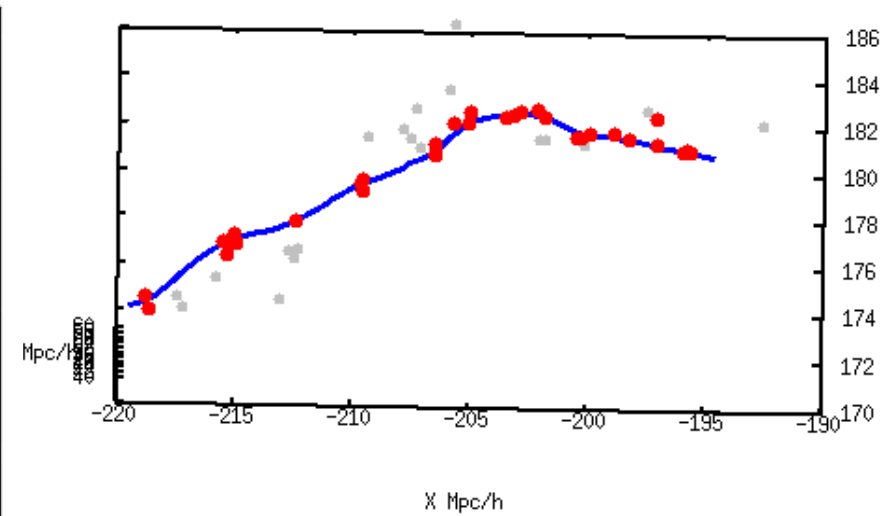
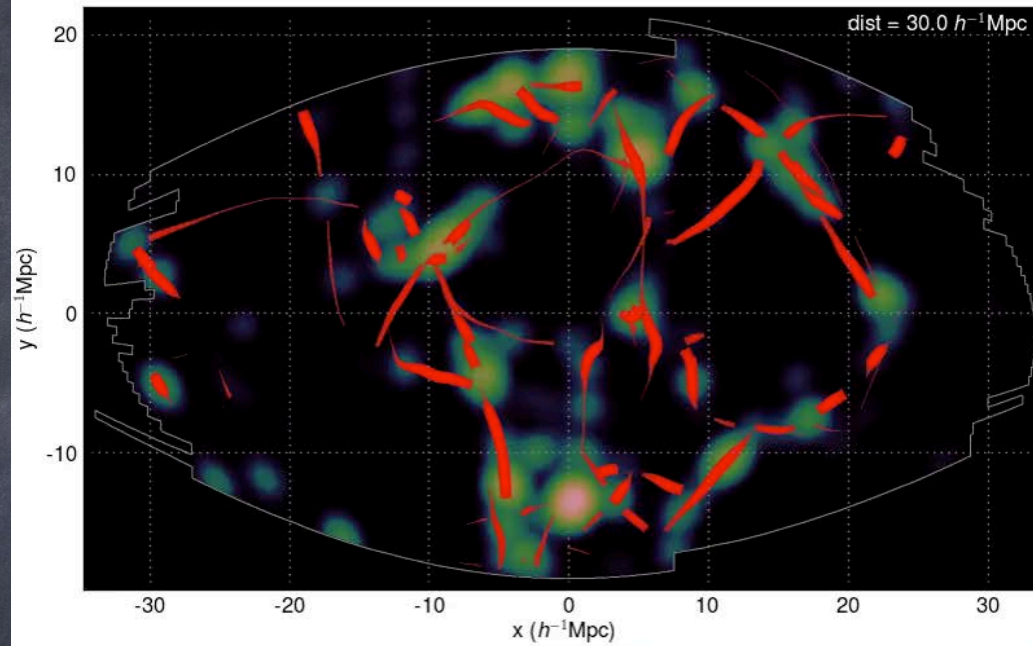


Single filaments





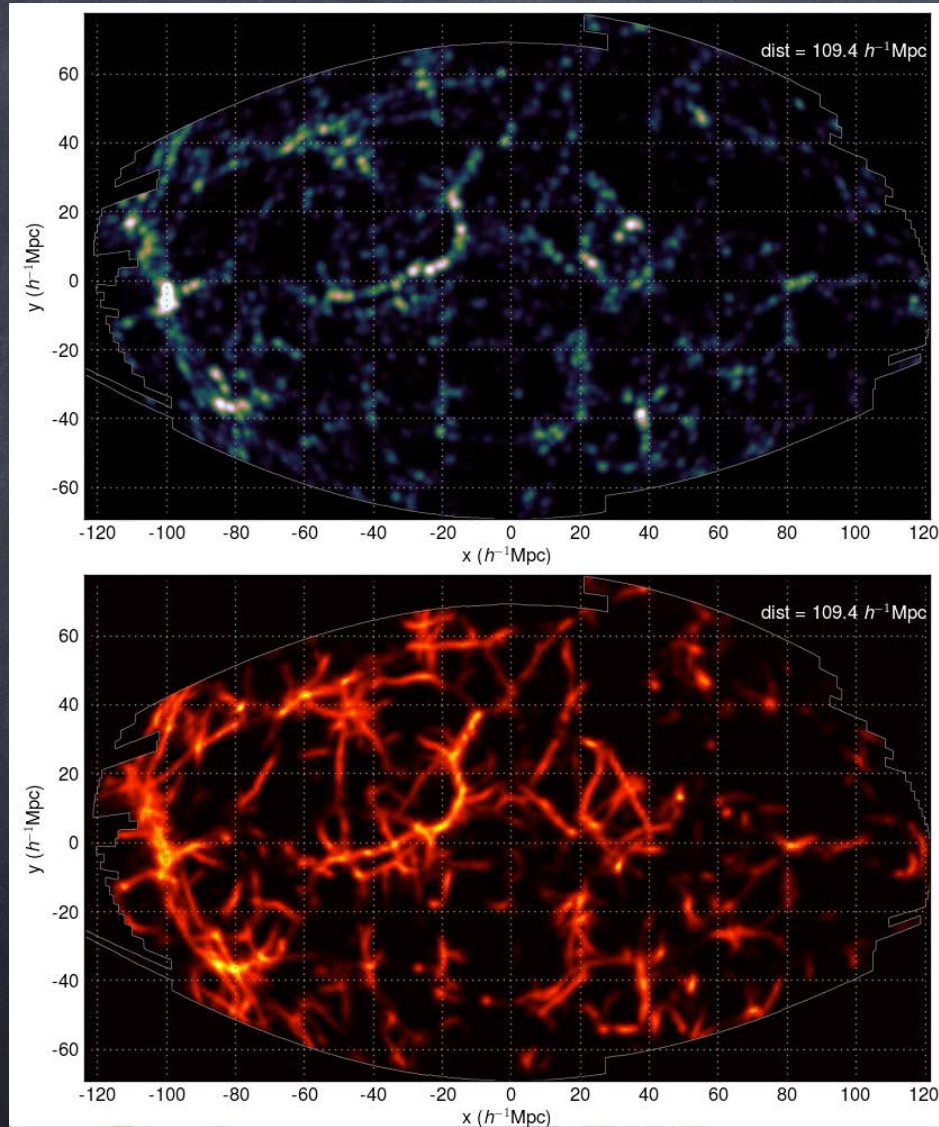
Detected filament spines





TARTU OBSERVATORY
space research centre

Detected filamentary pattern



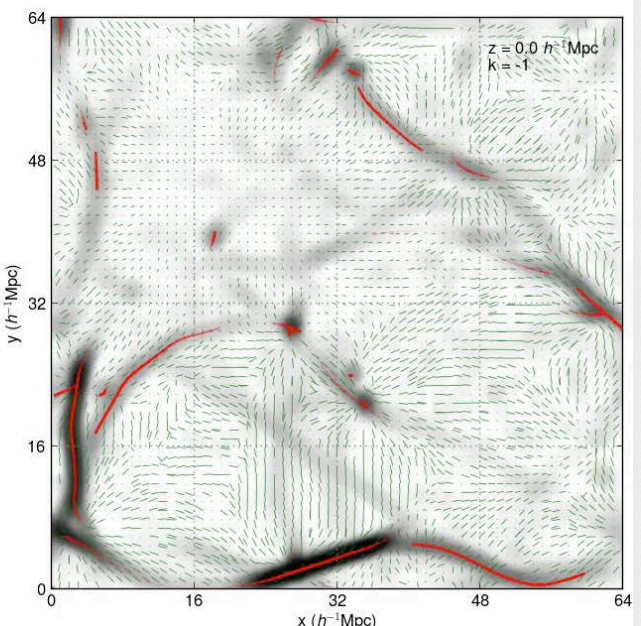
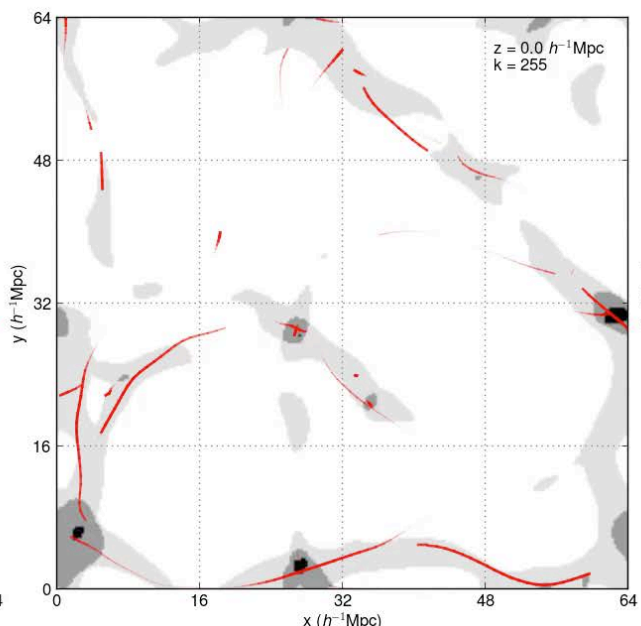
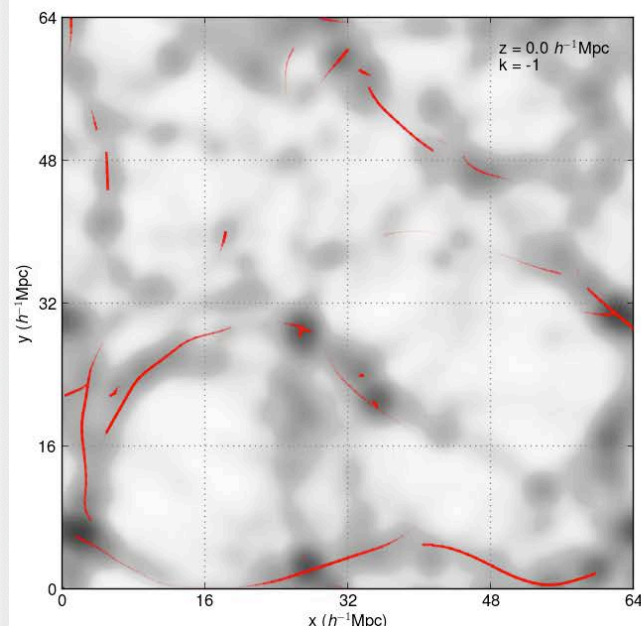
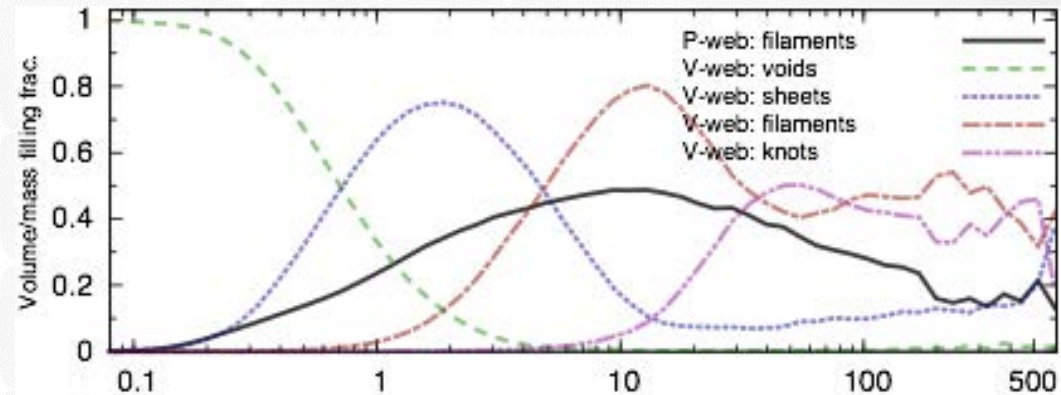
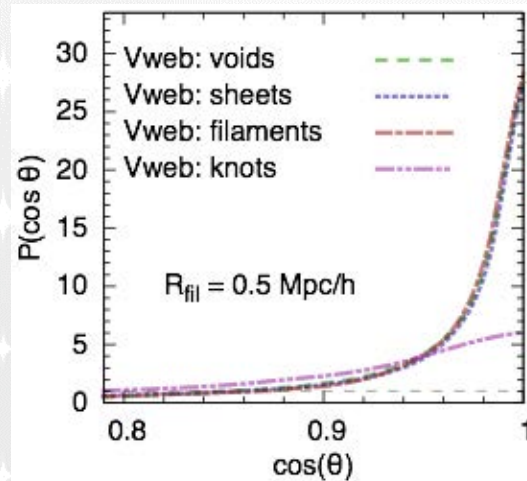
Juhan Liivamägi



Toni Tuominen

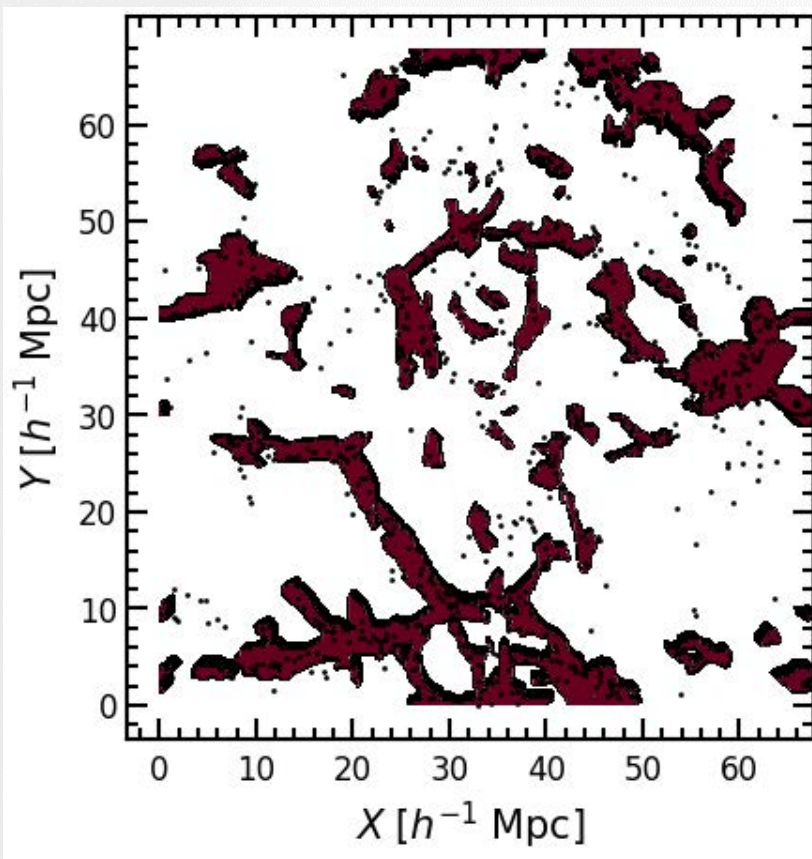
Orientation of cosmic web filaments with respect to the underlying velocity field

Tempel, Libeskind, Hoffmann et al. (2014)

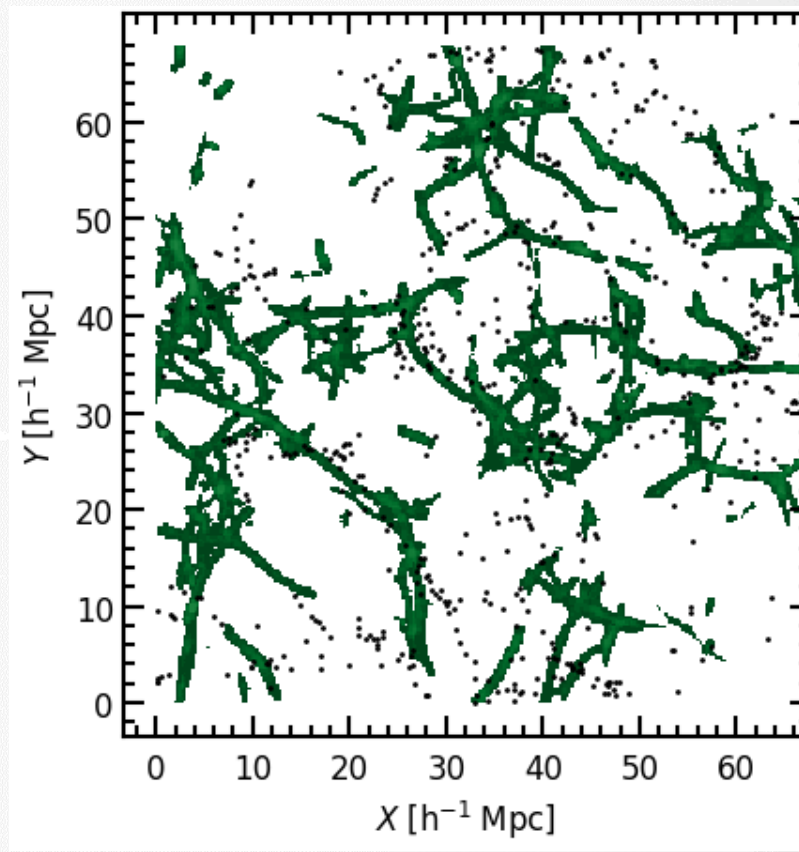


Filaments in Eagle simulation: Bisous vs Nexus

Nexus: Dark Matter



Bisous: galaxies

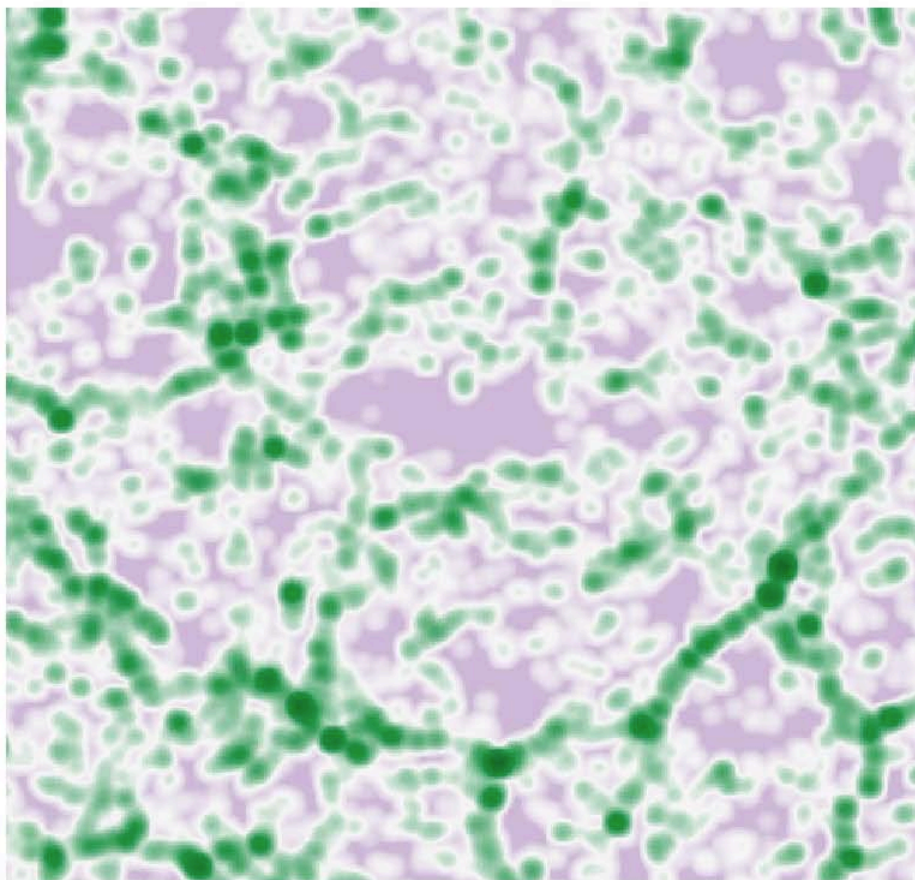




TARTU OBSERVATORY
space research centre

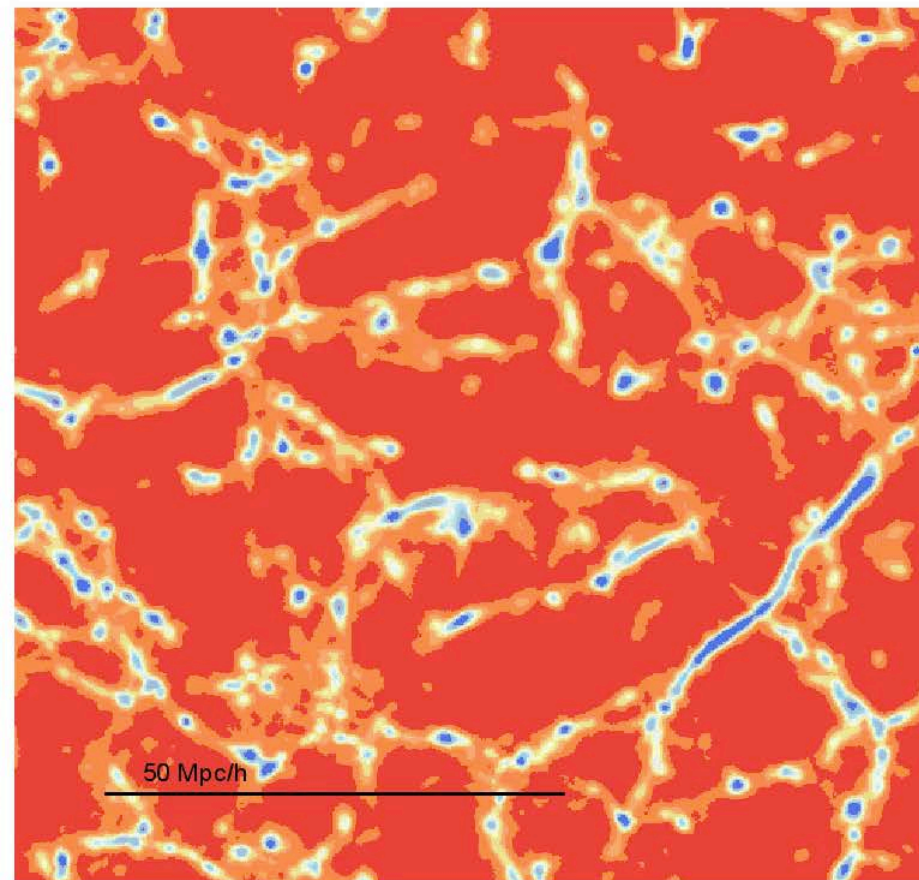
Bolshoi simulation

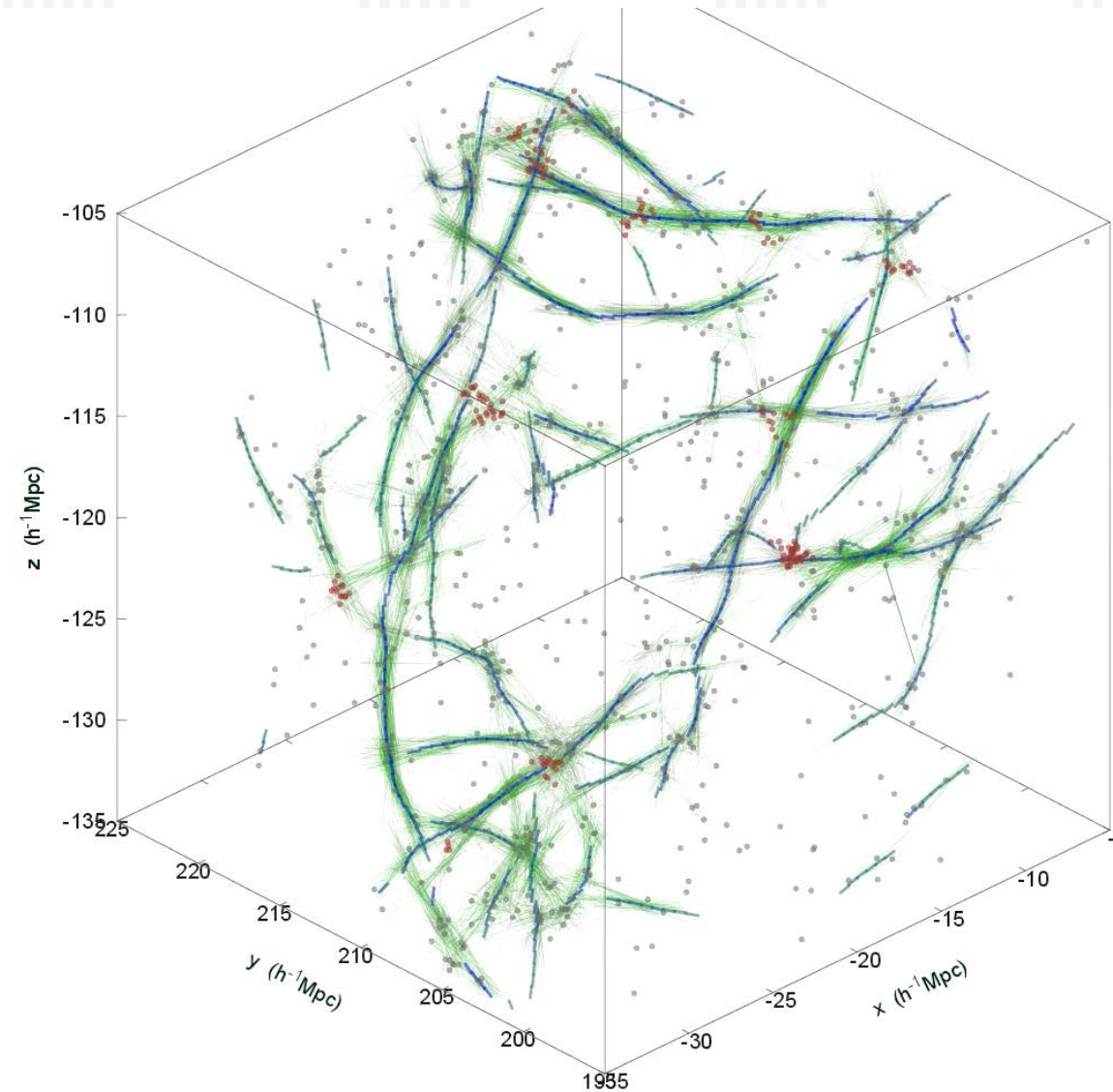
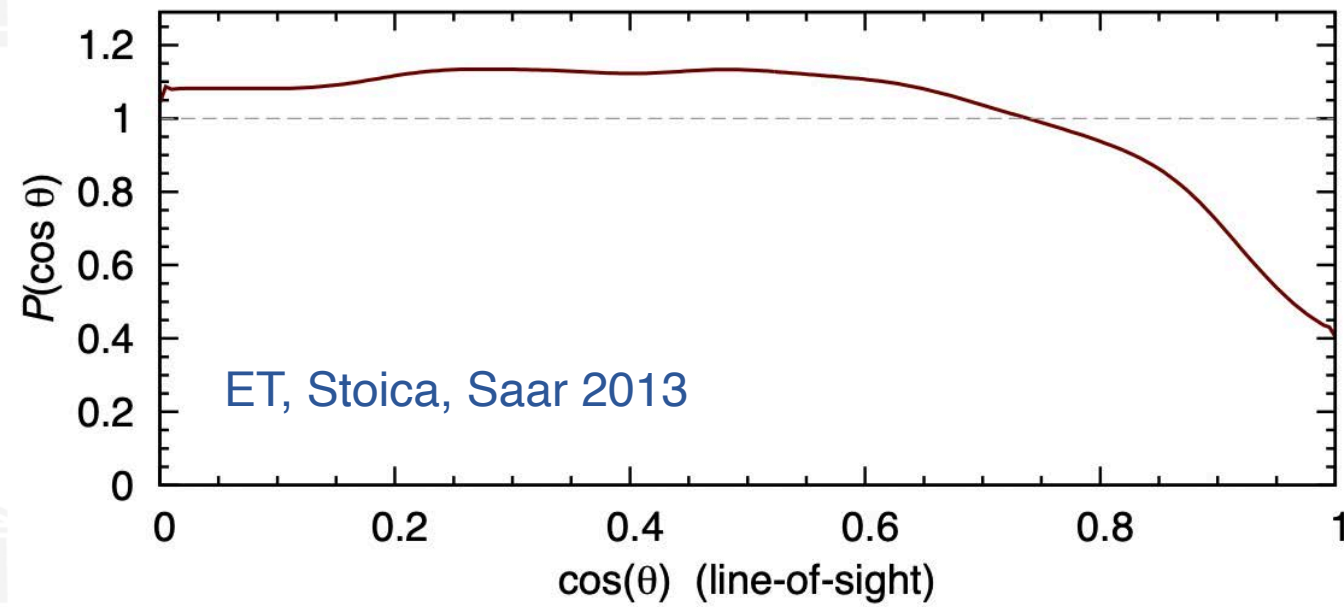
Density map



$z = 1.11$

Filament visit map



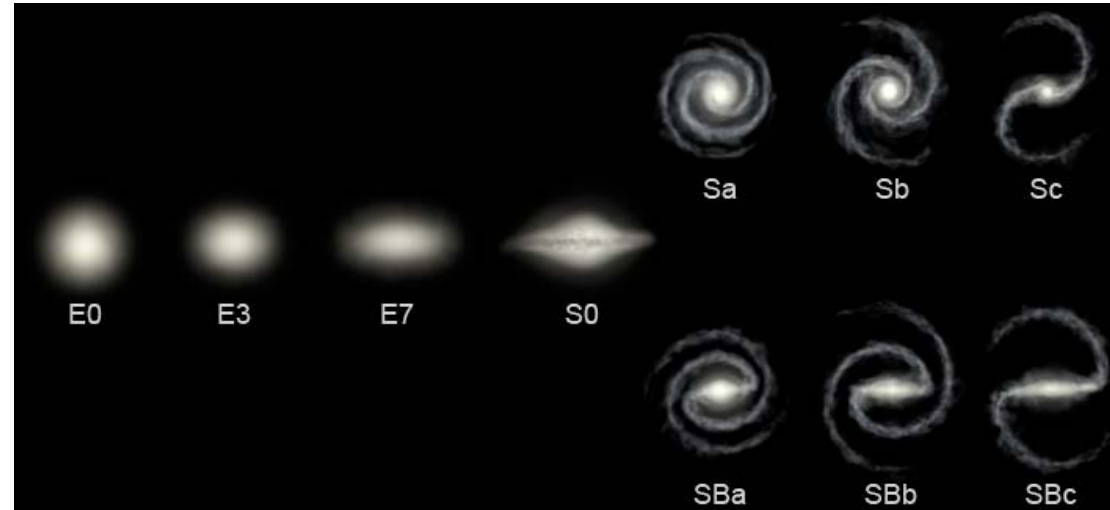


Redshift space distortions

Filament orientation is not uniform

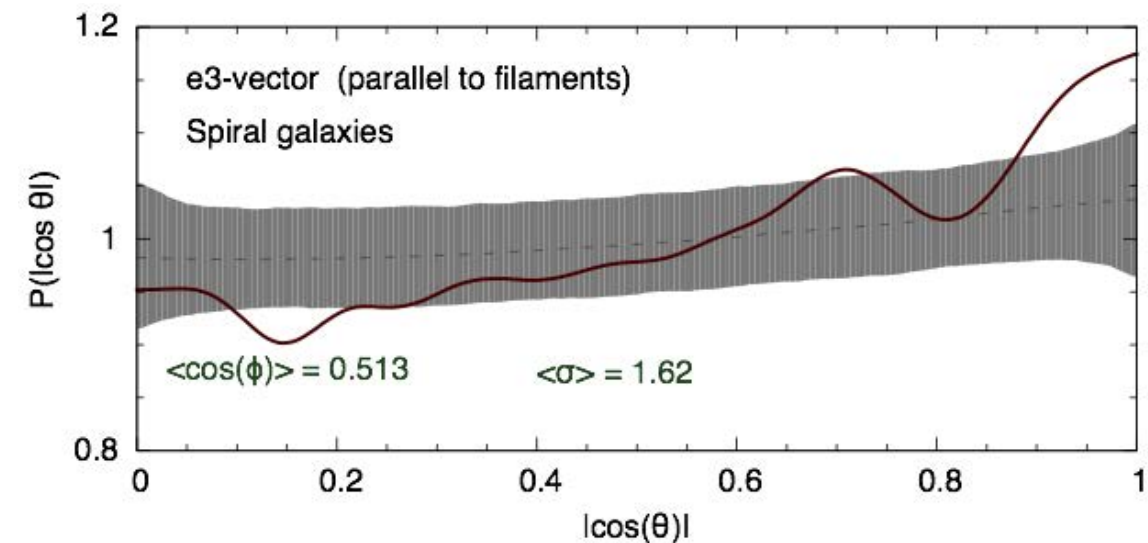
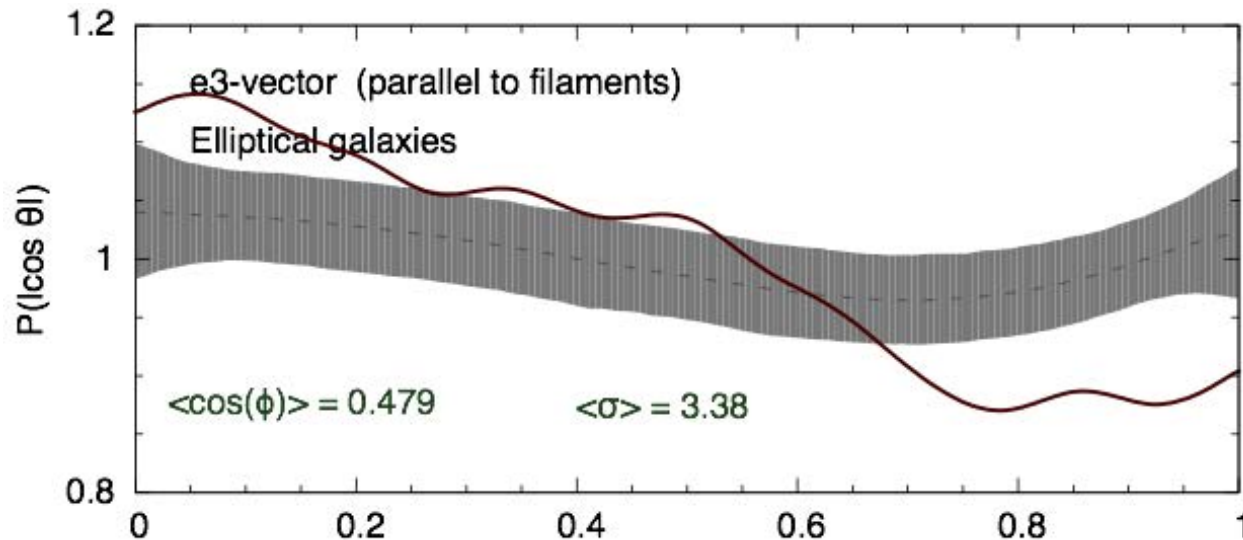
Bisous model for filament detection:
ET et al. 2014, 2016

Galaxy filament alignment



Ellipticals

Spirals

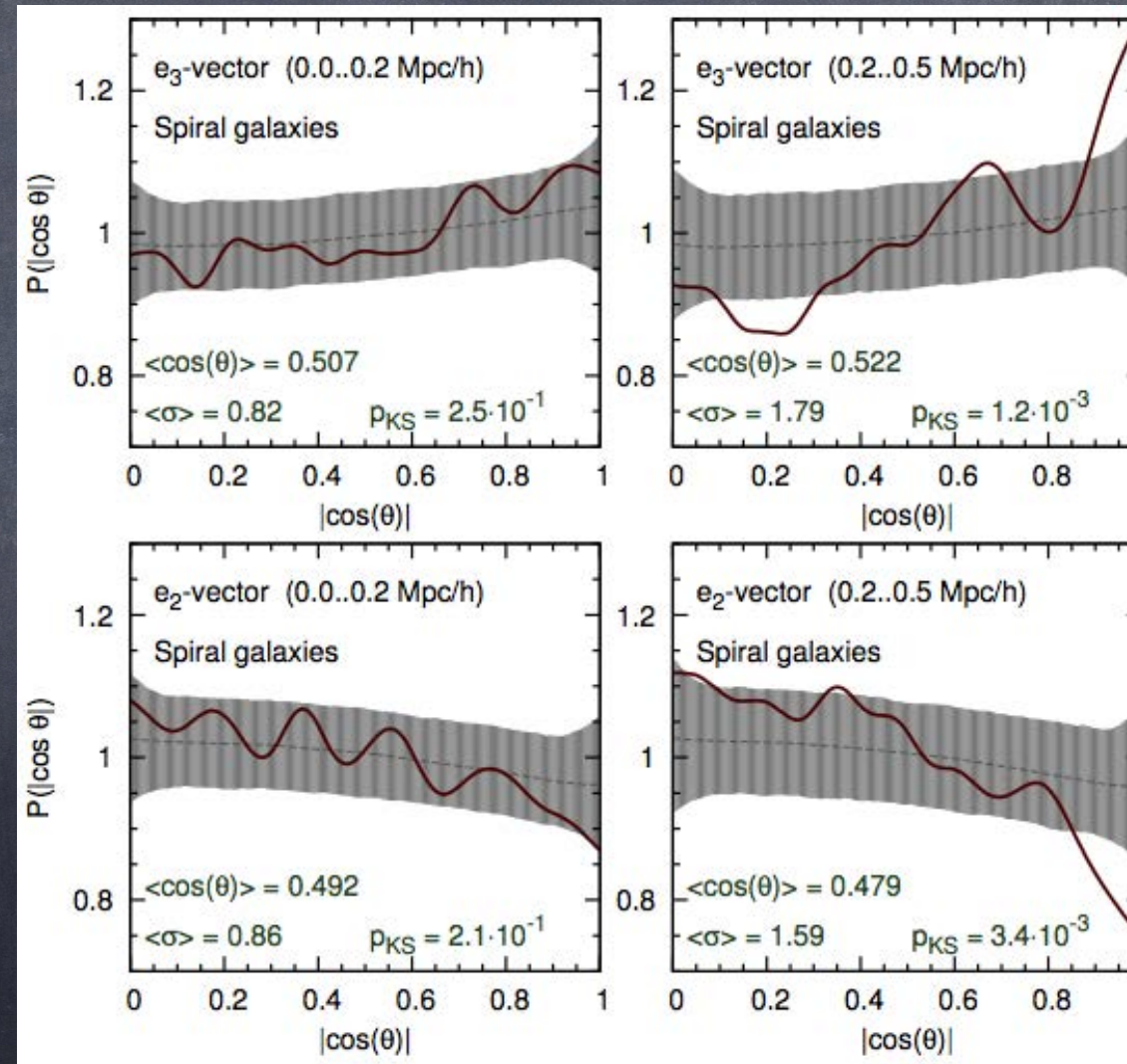




Filaments and galaxy formation

Inner part

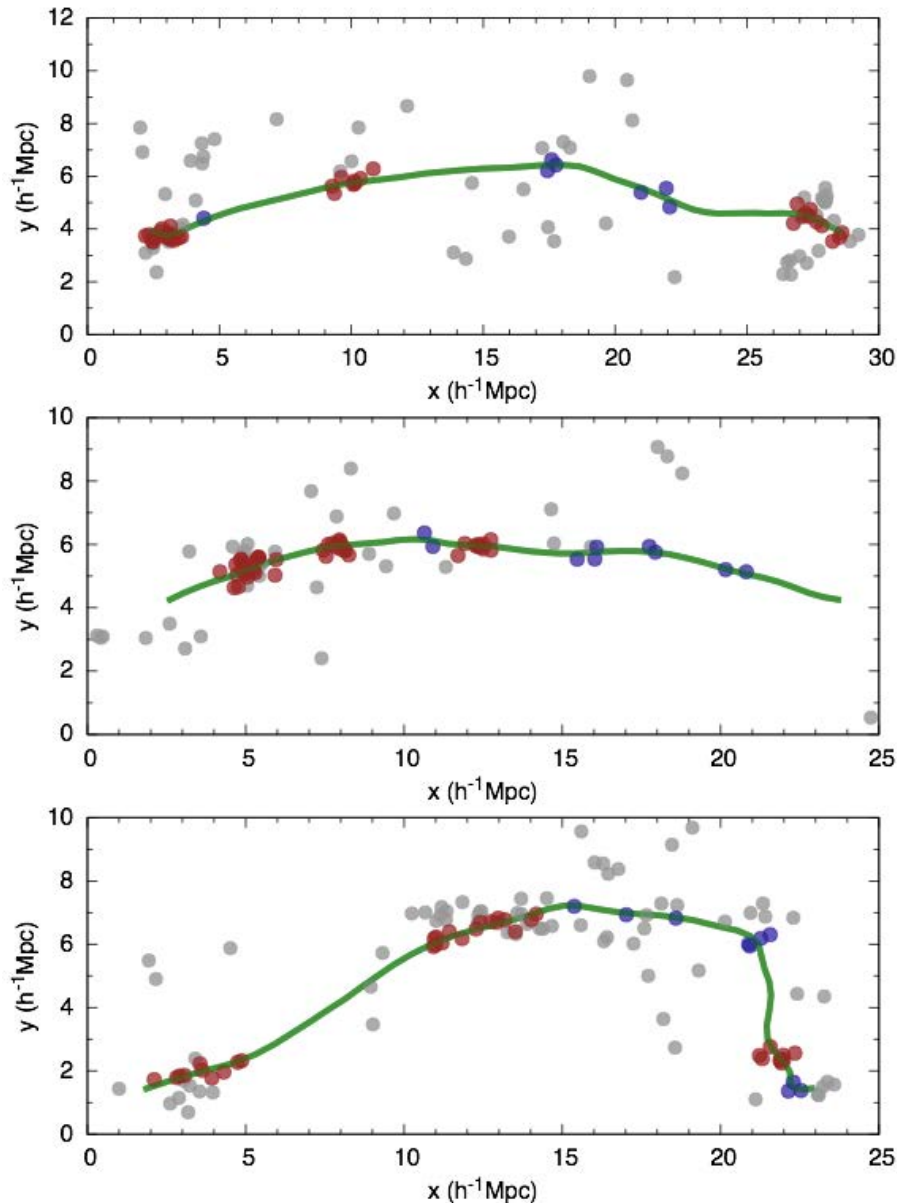
Outer part



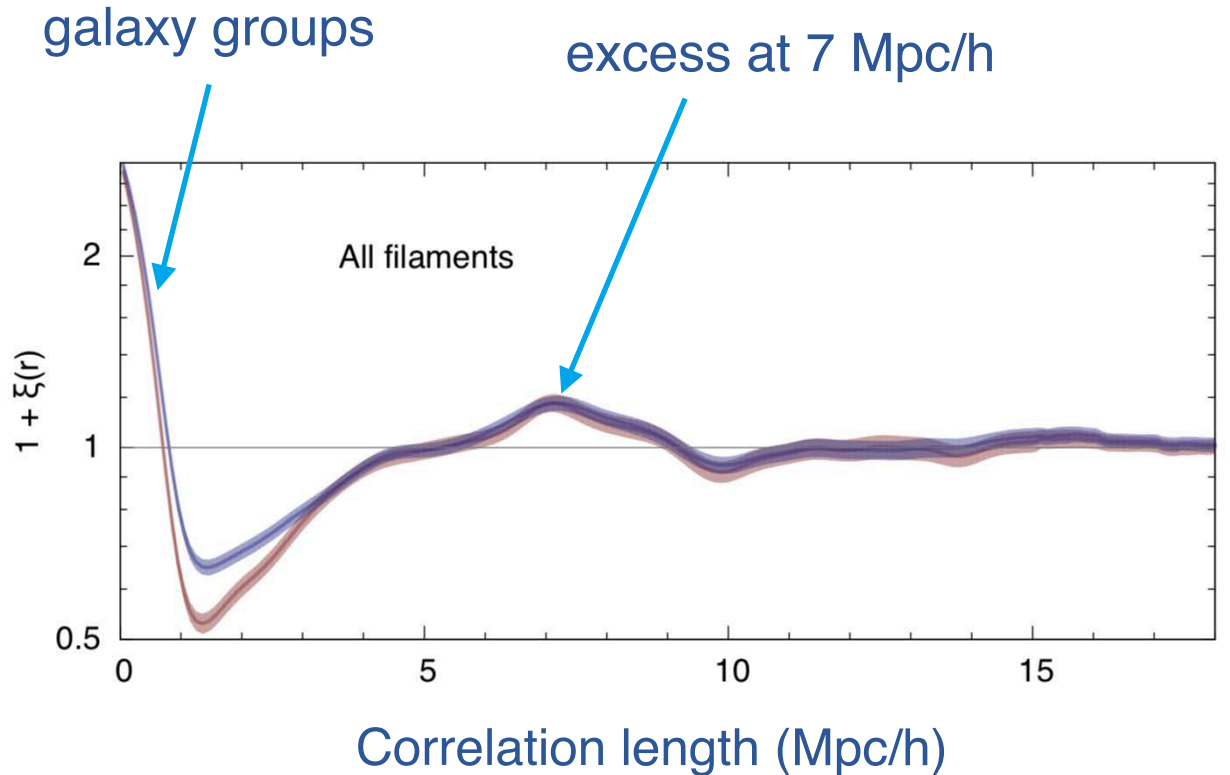
Galaxy filaments as pearl necklaces

Tempel et al. (2014)

Examples of filaments and their spines

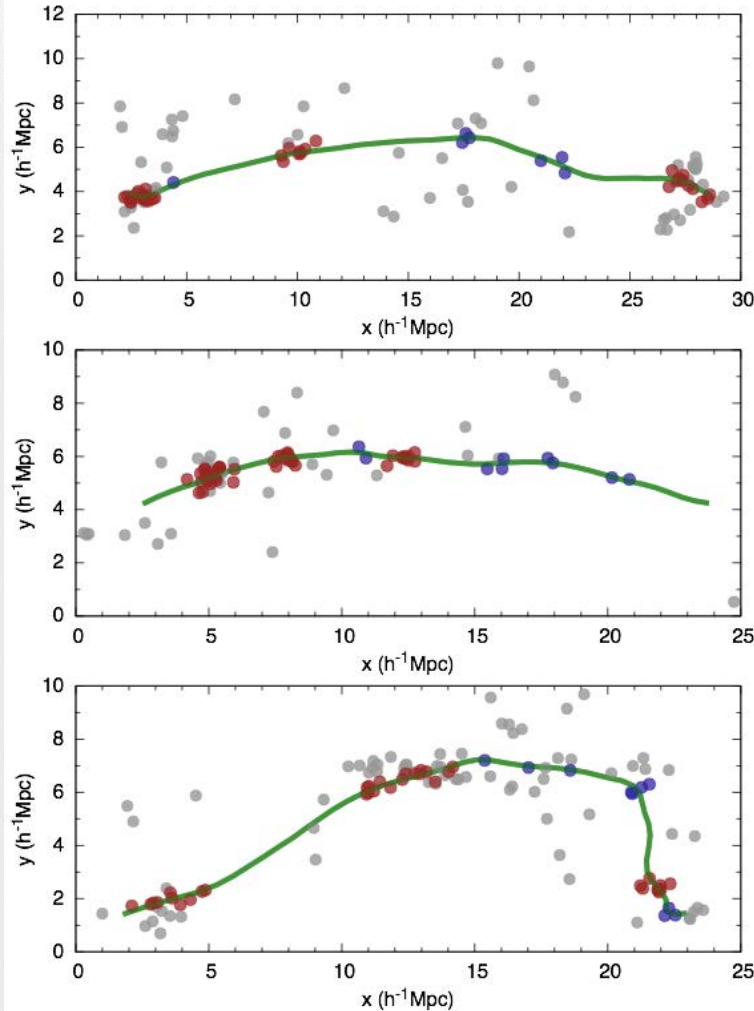


Pair correlation function along the filaments





Data and methods



Pair correlation function:

$$\widehat{\xi}(r) = 1 + \frac{DD(r)}{RR(r)} - 2\frac{DR(r)}{RR(r)},$$

Rayleigh Z-squared statistics:

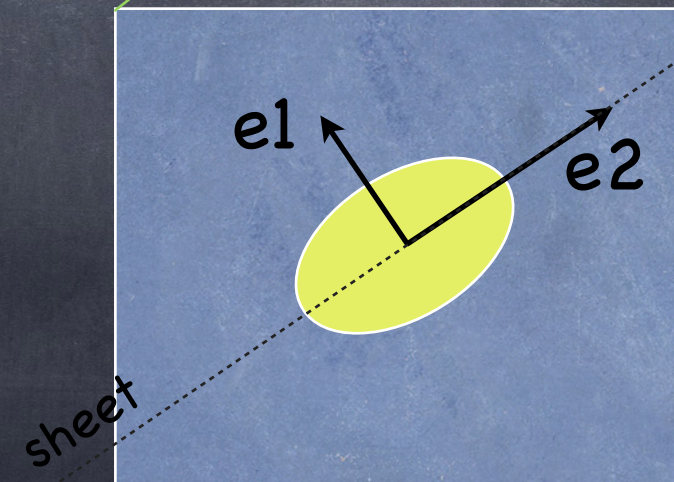
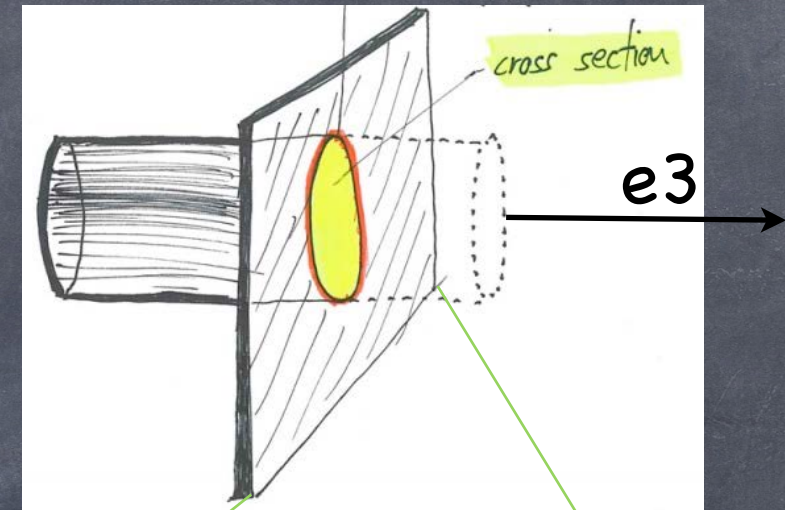
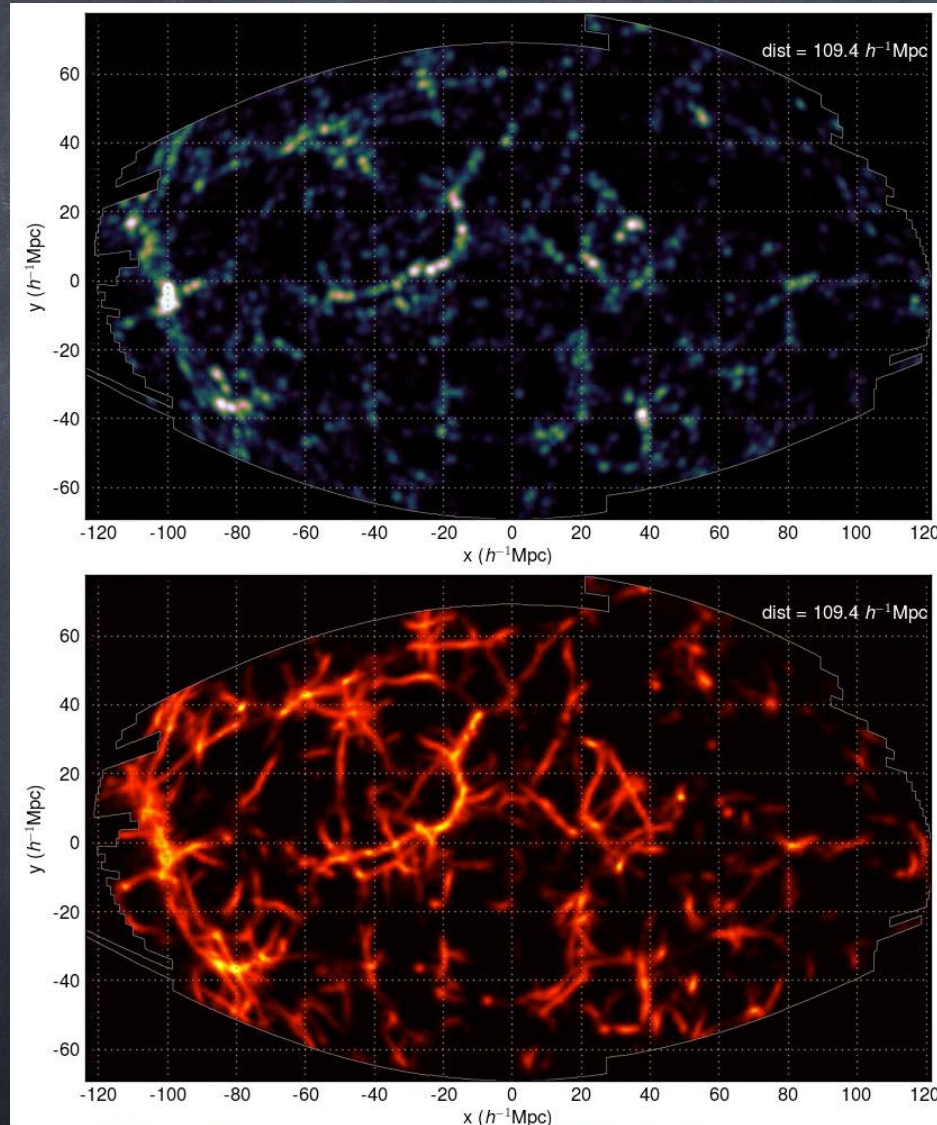
The algorithm works as following. For each filament, we produce a periodogram using the Z_1^2 (Rayleigh statistics),

$$Z_1^2 = \frac{2}{N} \left[\left(\sum_{j=1}^N \cos \phi_j \right)^2 + \left(\sum_{j=1}^N \sin \phi_j \right)^2 \right], \quad (4)$$

where N is the number of galaxies in a filament and $\phi_j = 2\pi l_j/d$ is the phase value for a galaxy j for a fixed period d ; l_j is a galaxy j distance along the filament spine from the beginning of the filament.



Detected filamentary pattern: sheet orientation



Galaxy pairs align with galactic filaments

Tempel & Tamm (2015)

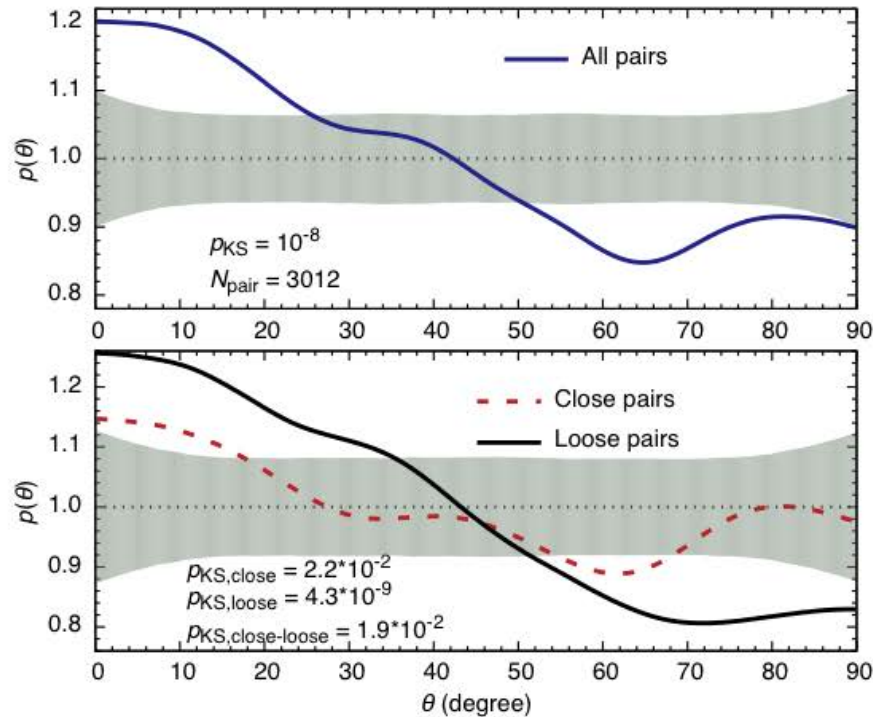
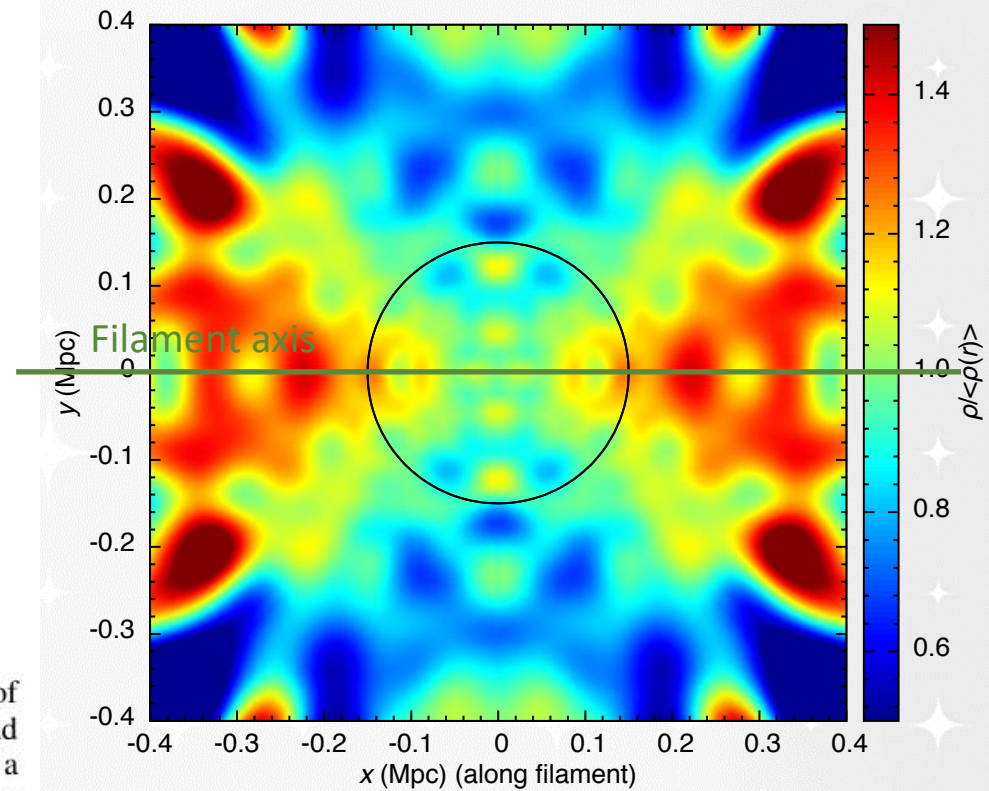
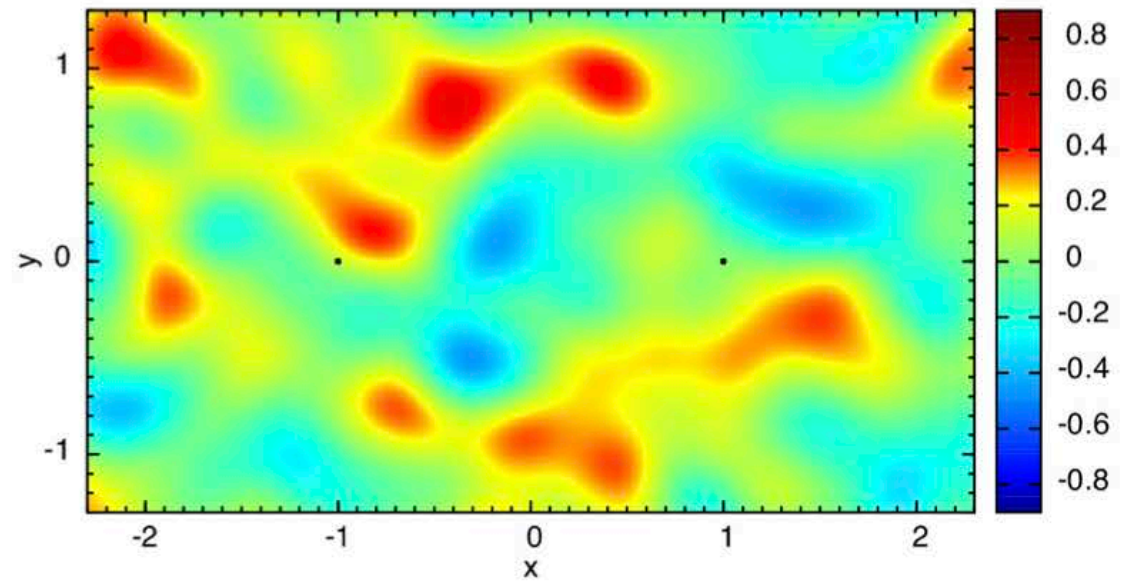
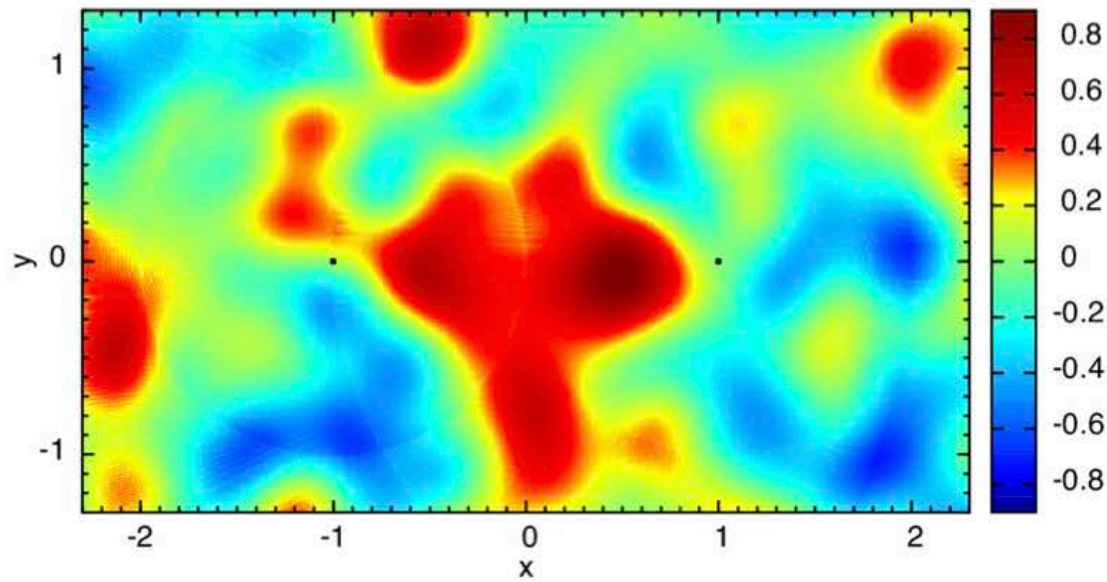
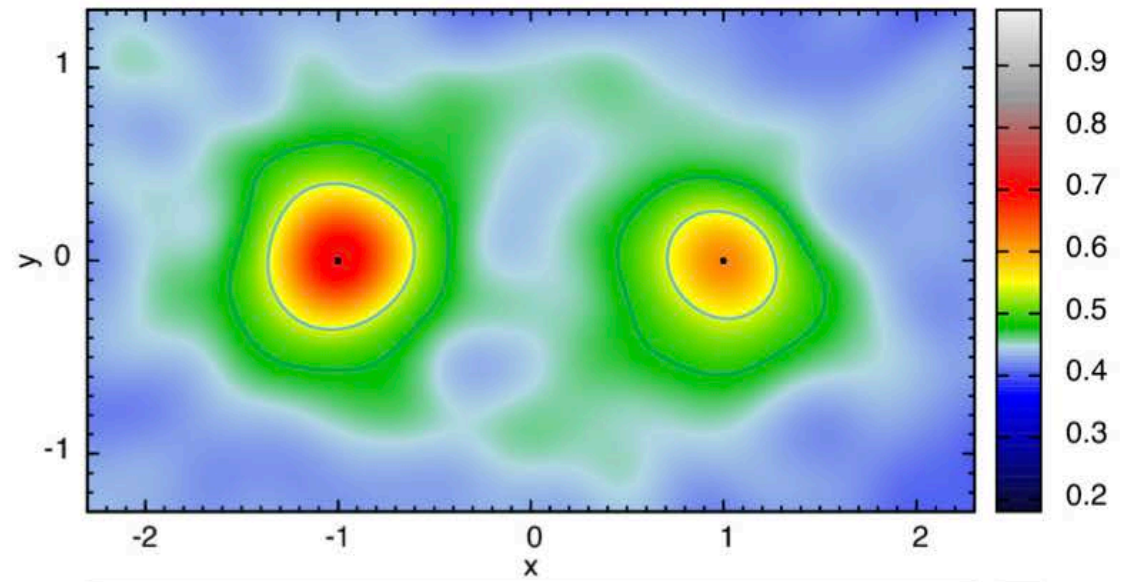
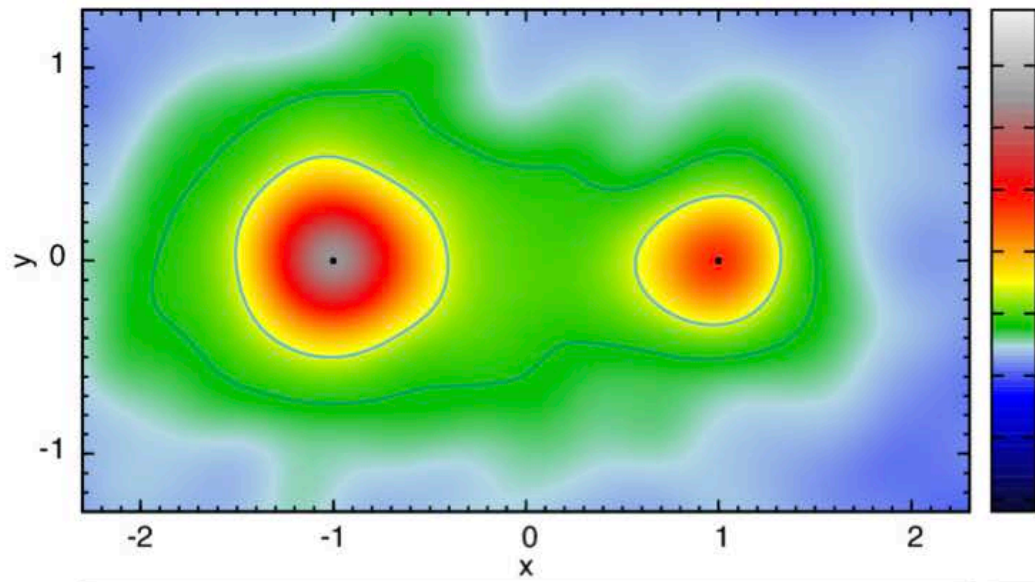


Fig. 2. *Upper panel:* probability distribution function (blue solid line) of the projected (in the plane of the sky) angles between galaxy pairs and their host filaments. The KS-test value that the sample is drawn from a uniform distribution is 10^{-8} . The filled area shows the 95% confidence region for a randomised distribution of 3012 pairs. *Lower panel:* the same as in the upper panel for two equal-size subsamples: close pairs ($d_{sep} < 0.3$ Mpc; red dashed line) and loose pairs ($d_{sep} > 0.3$ Mpc; black solid line).

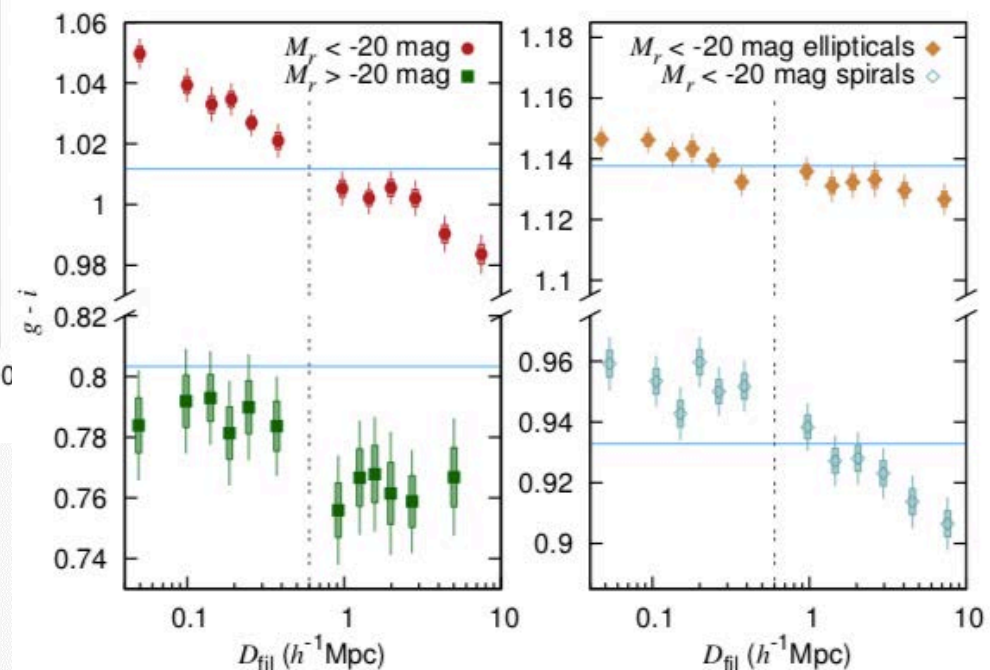
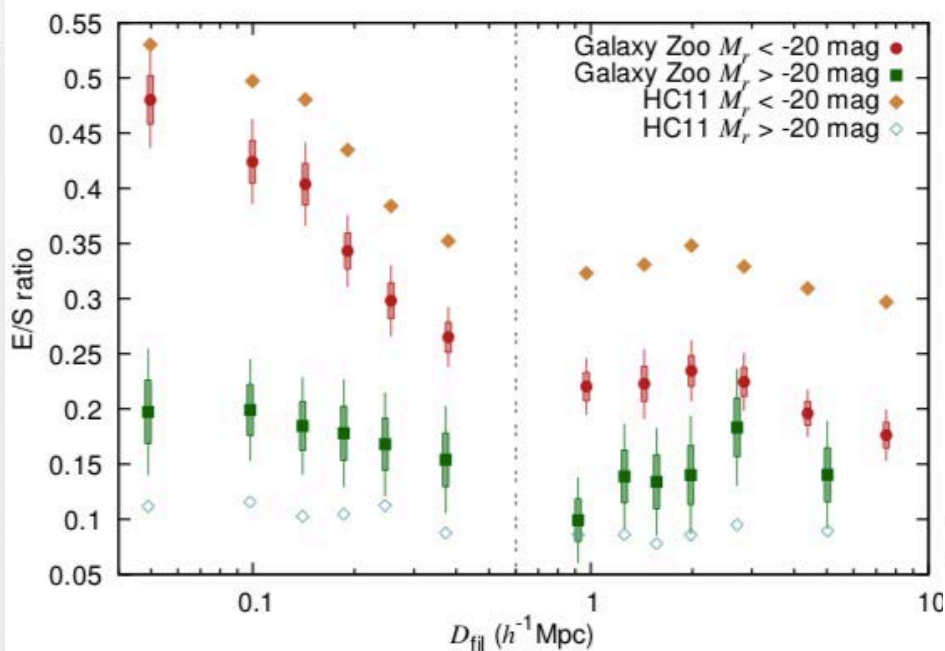




Satellite galaxies

Galaxy properties in filament environment

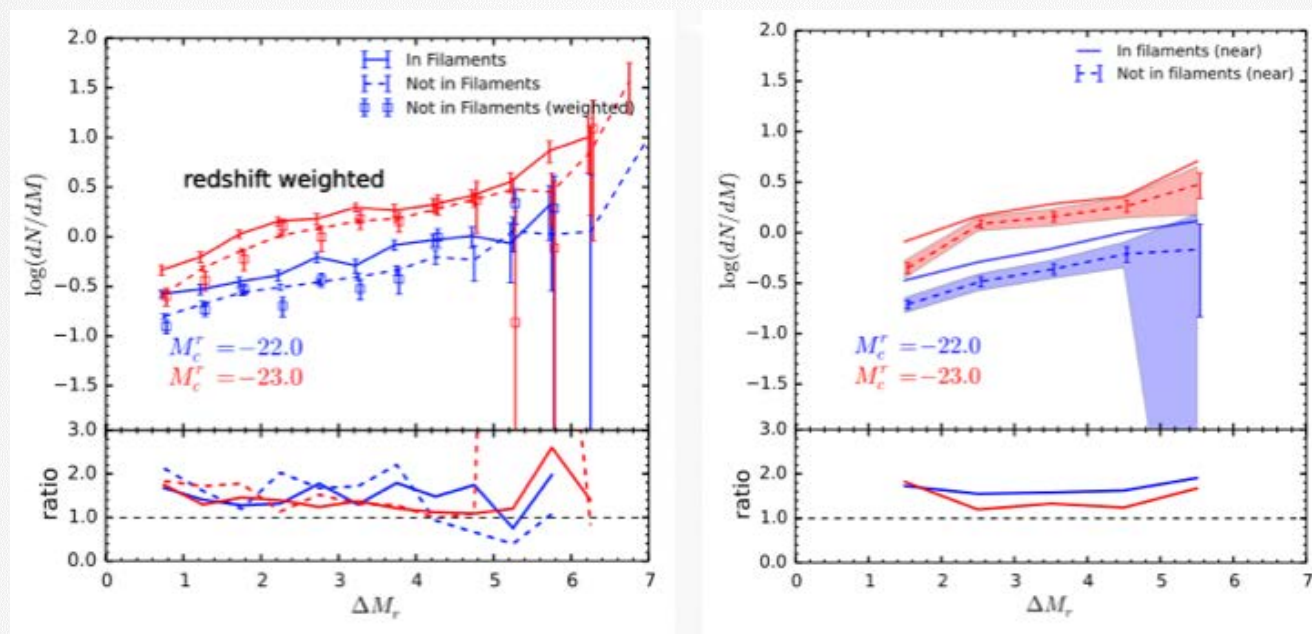
Kuutma, Tamm & Tempel (2017)



Galaxies in filaments have more satellites: the influence of the cosmic web on the satellite luminosity function in the SDSS

Guo, Tempel & Libeskind (2015)

Number of satellites

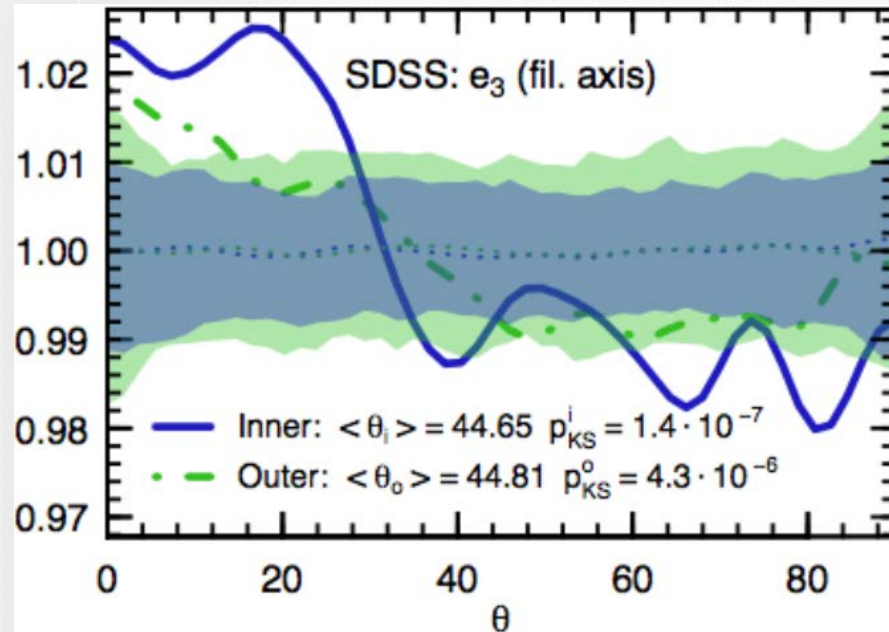


Satellite luminosity with respect to central galaxy

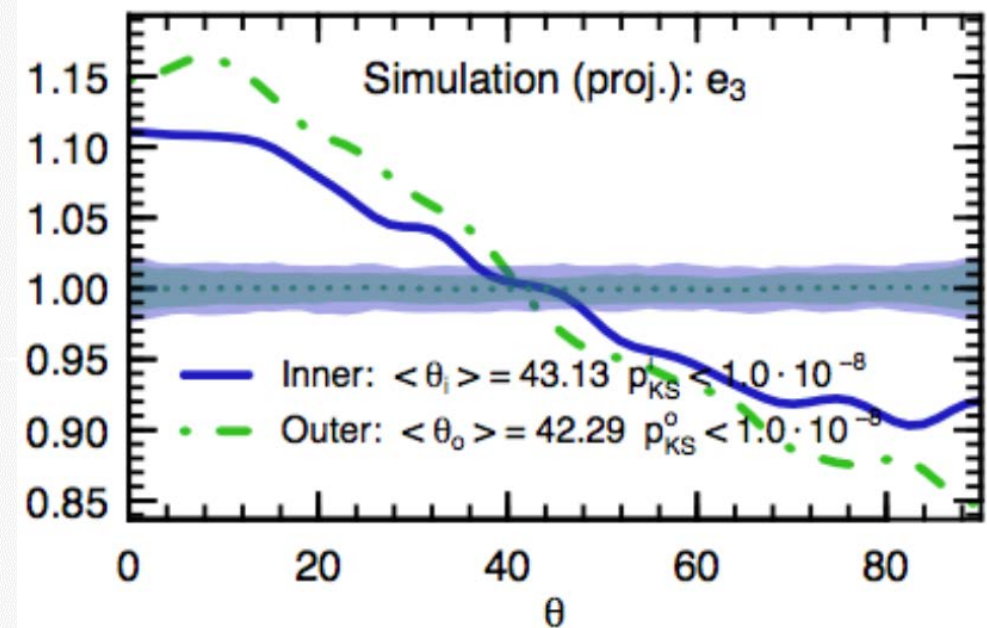
The alignment of satellite galaxies and cosmic filaments: observations and simulations

Tempel, Guo, Kipper, Libeskind (2015)

SDSS observations



Millennium simulation



Angle between the satellite position and filament axis

Intrinsics of the alignment signal

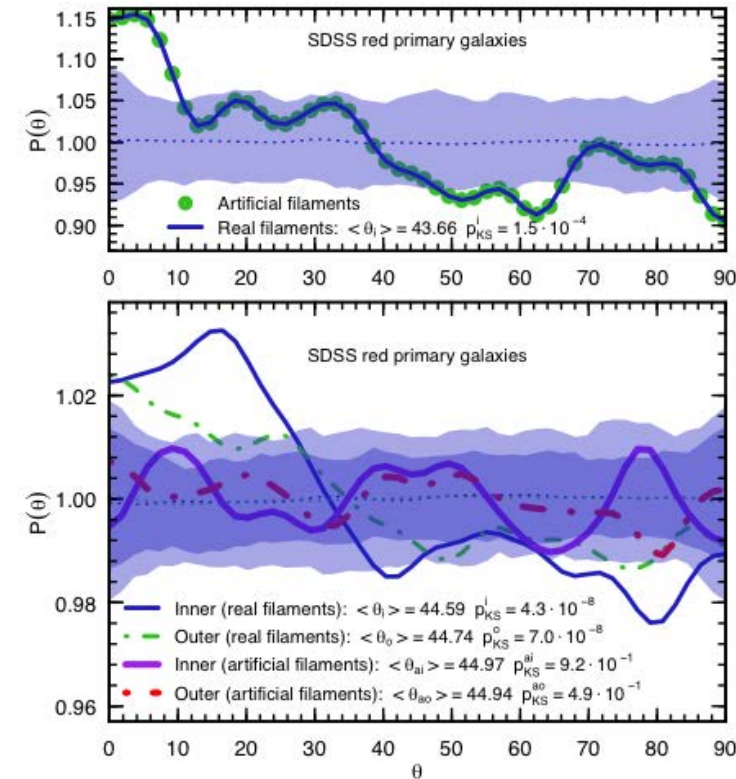
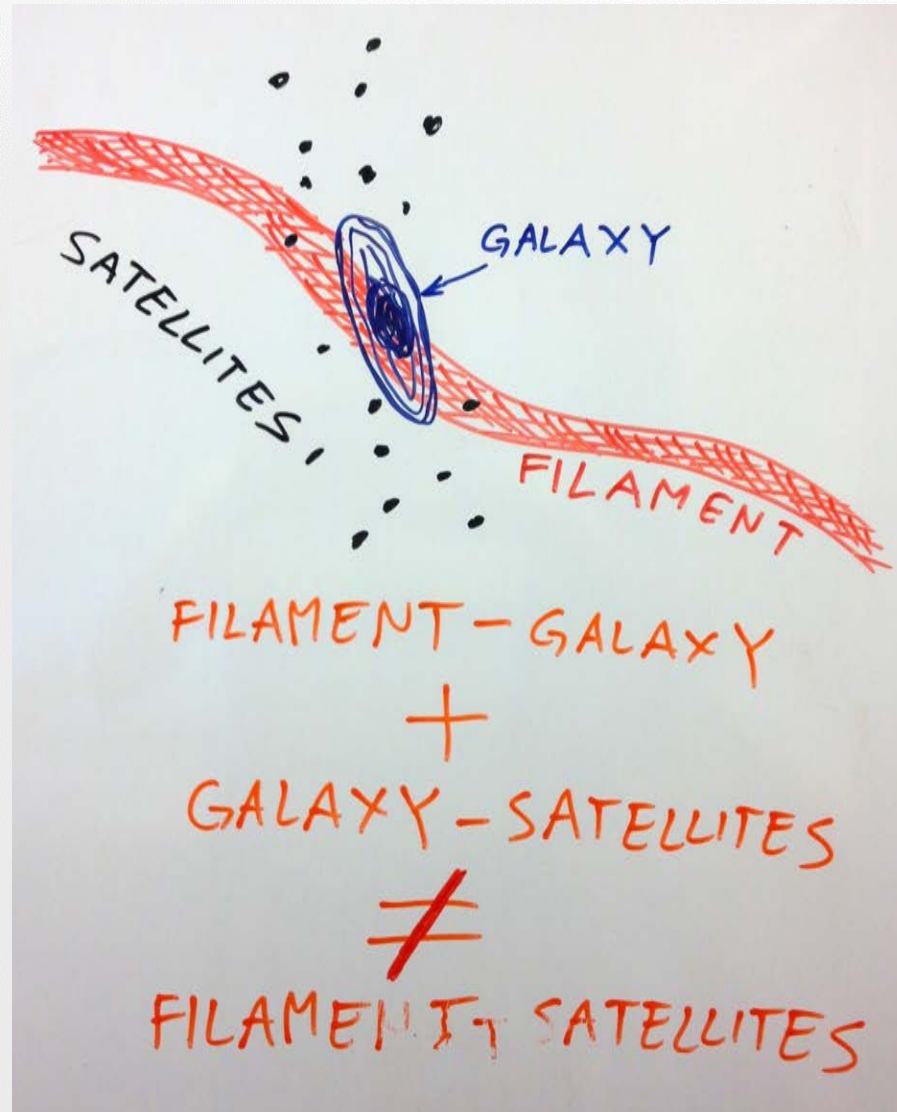
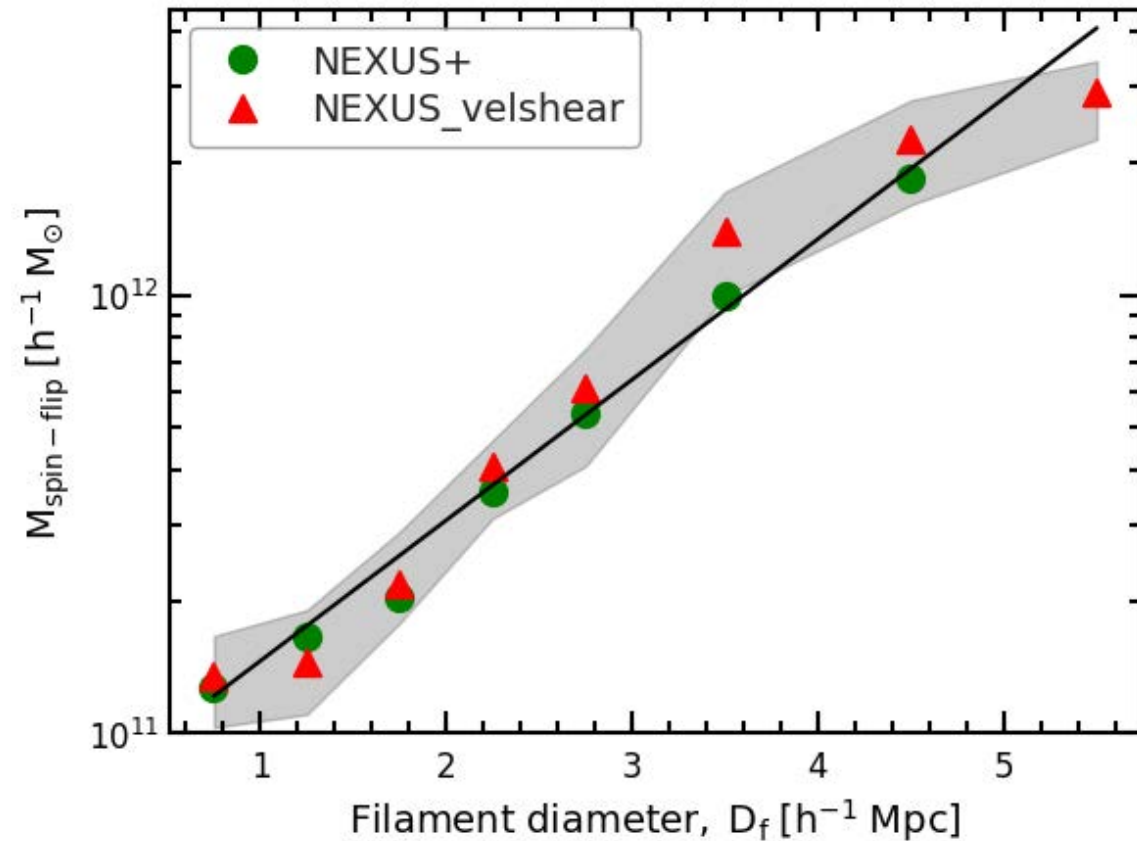
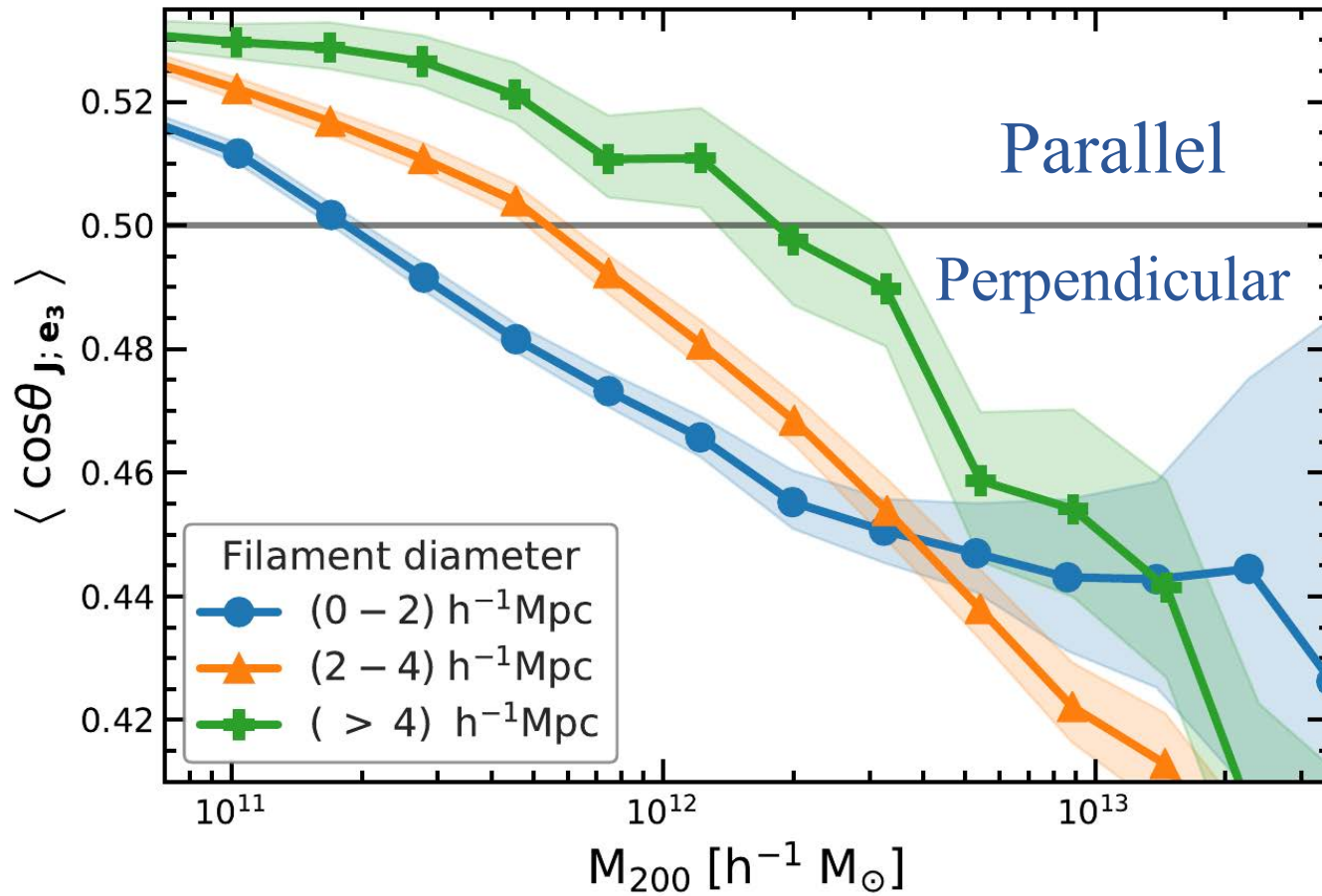


Figure 7. Test the intrinsic of the filaments between the filament axes and anisotropic distribution of satellites. *Top panel:* the alignment between real/artificial filament axes and the major axis of red primaries. *Bottom panel:* the alignments between anisotropic distribution of satellites with artificial filament axes (thick red and purple lines) and with real filament axes (thin blue and green lines).



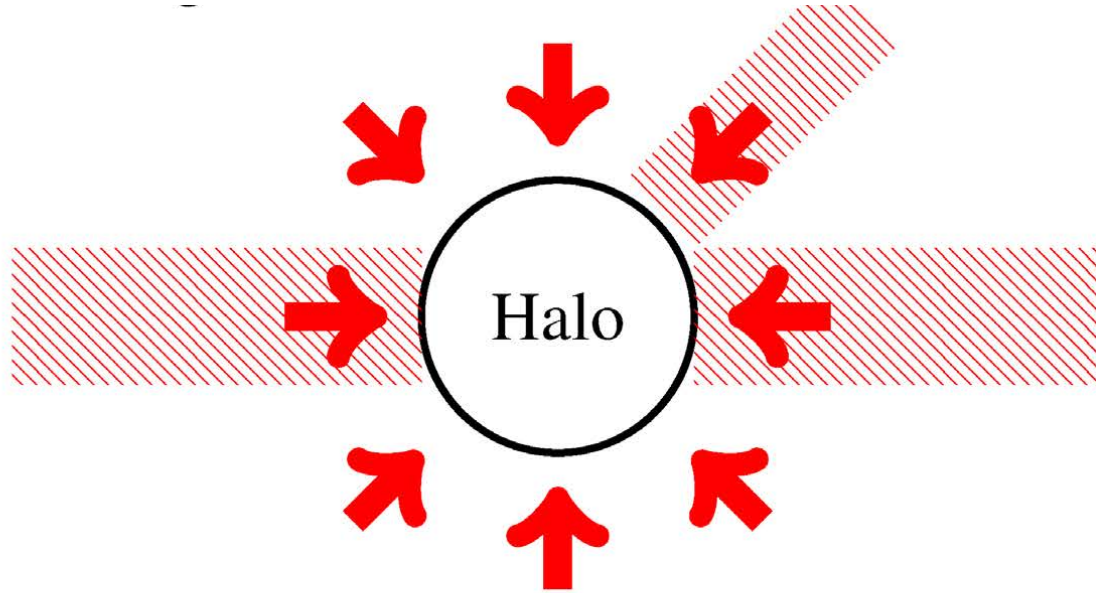
TARU FILAMENT

Alignment dependence on filament properties



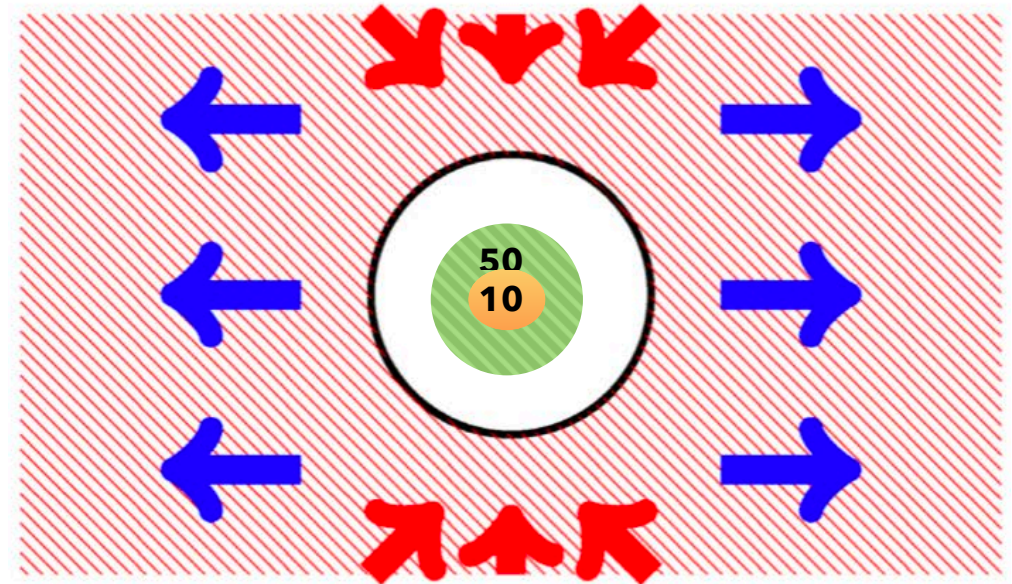
Late time accretion

ACCRETING HALO

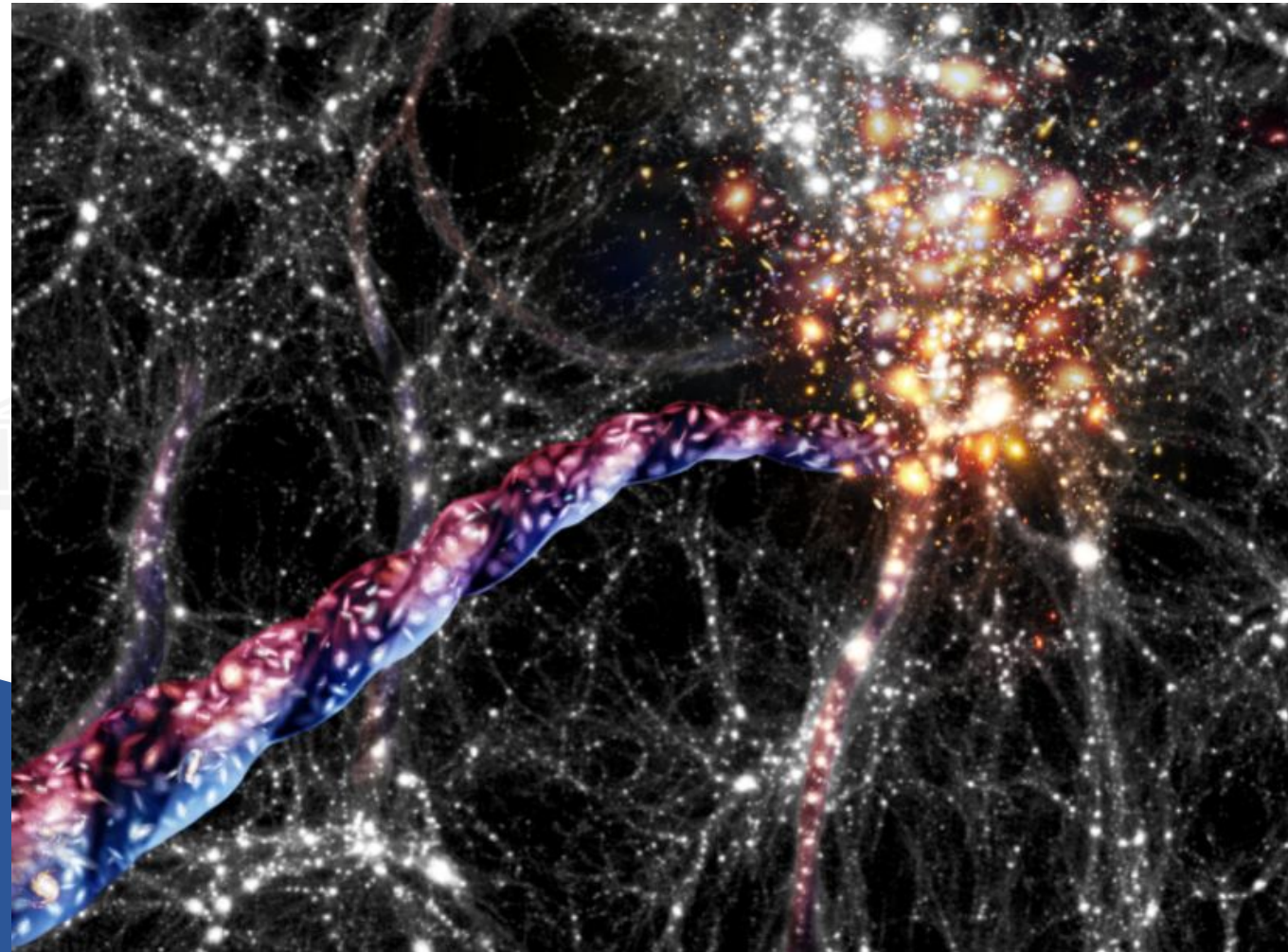
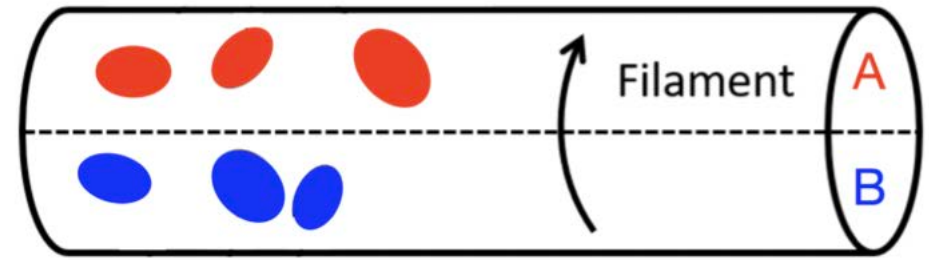
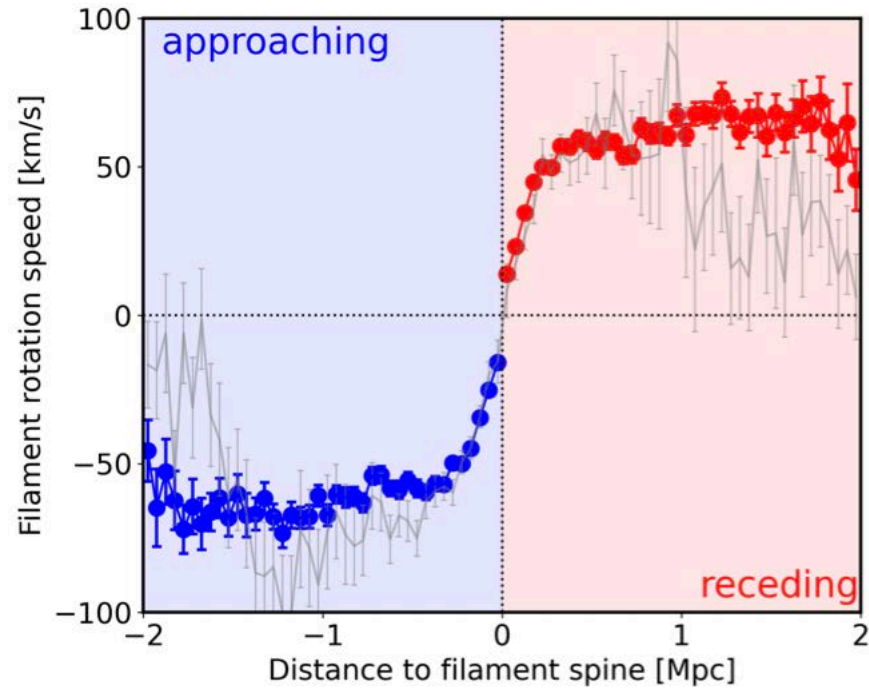


- Thin filament
- Accretion - perpendicular spin

STALLED HALO



- Thick filament
- Accretion - parallel spin



Rotating filaments



UNIVERSITY OF TARTU

Science in Tartu Observatory



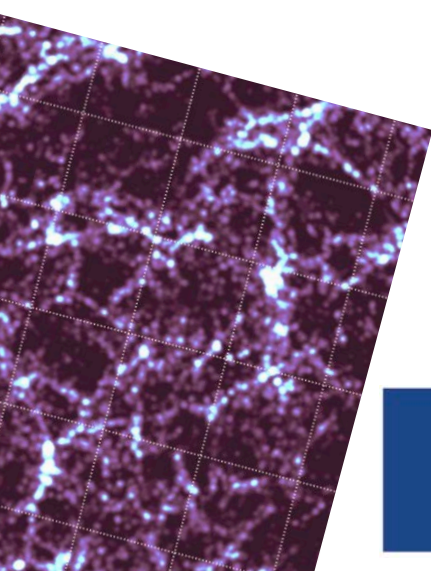
Co-funded by
the European Union



Investing
in your future



Funded by
the European Union





4MOST - 4-metre Multi-Object Spectroscopic Telescope



Cosmic Web & Galaxies @ Tartu Observatory

Photo-z (TOPz)
SED fitting

target selection
CIGALE templates
template fitting
k-correction
e-correction
galaxy properties
spec-z + photo-z

4MOST ProbSF
survey simulator

Visit Planner
4MOST scheduler
Probabilistic fibre-target assignment
Survey optimisation
Selection function
Statistical analysis

mFoF groups
mass estimation

Group detection
(incl. ProbSF)
Group membership
Group masses and mass uncertainties
ML approach
Local Environment

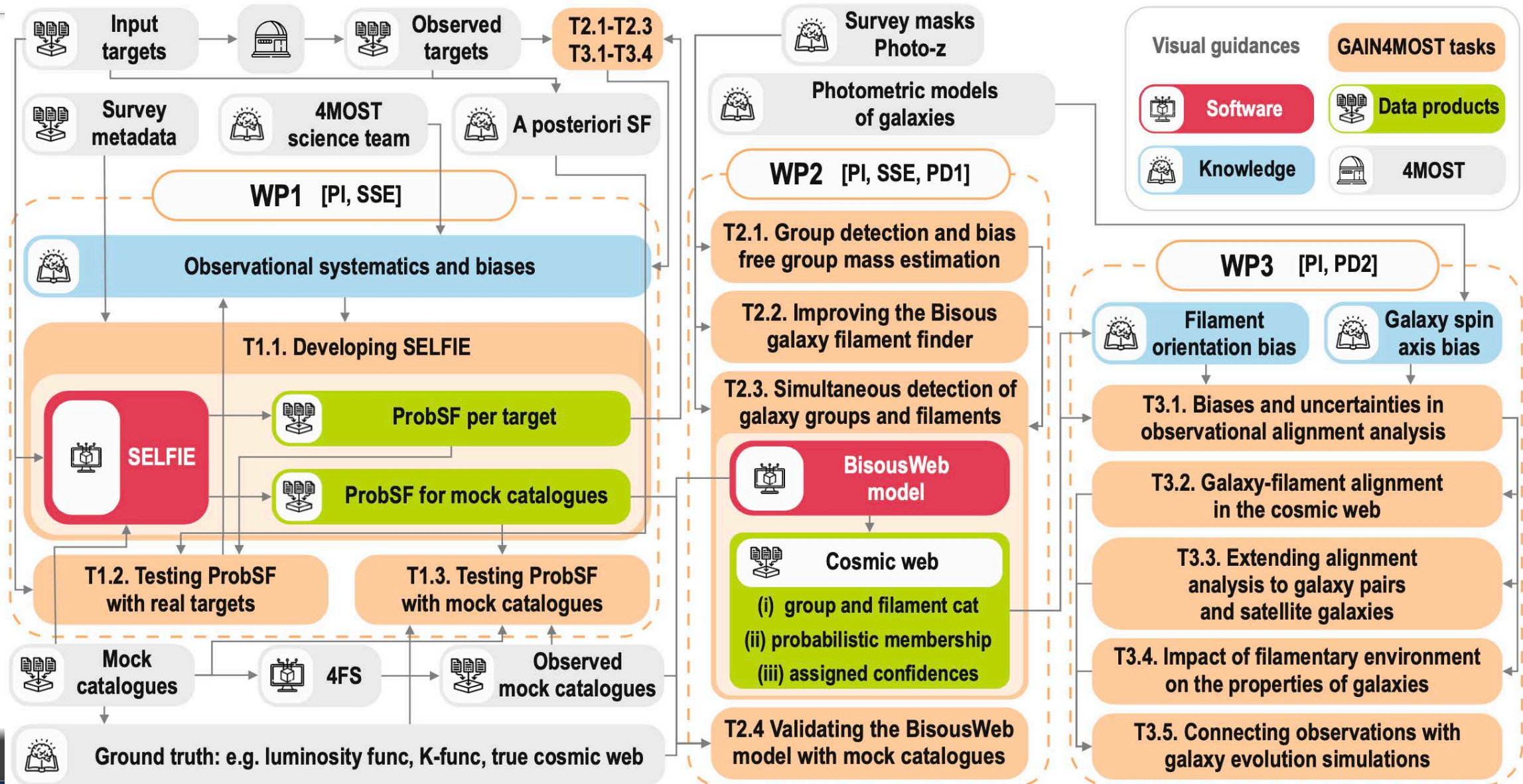
BisousWeb
galaxy filaments

Filament detection
Marked point process approach
Filament-group connectivity
Filament properties
Cosmic Web

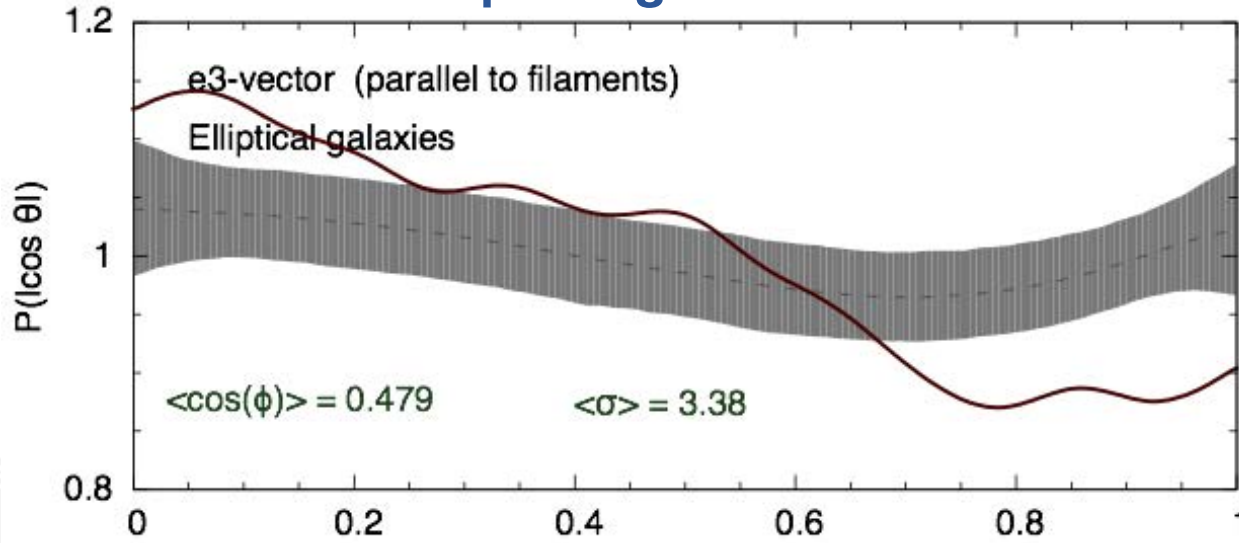
Weighted Galaxy Matching

Scaled flux matching
Galaxy-environment connection
Simulations vs observations
Understanding galaxy evolution

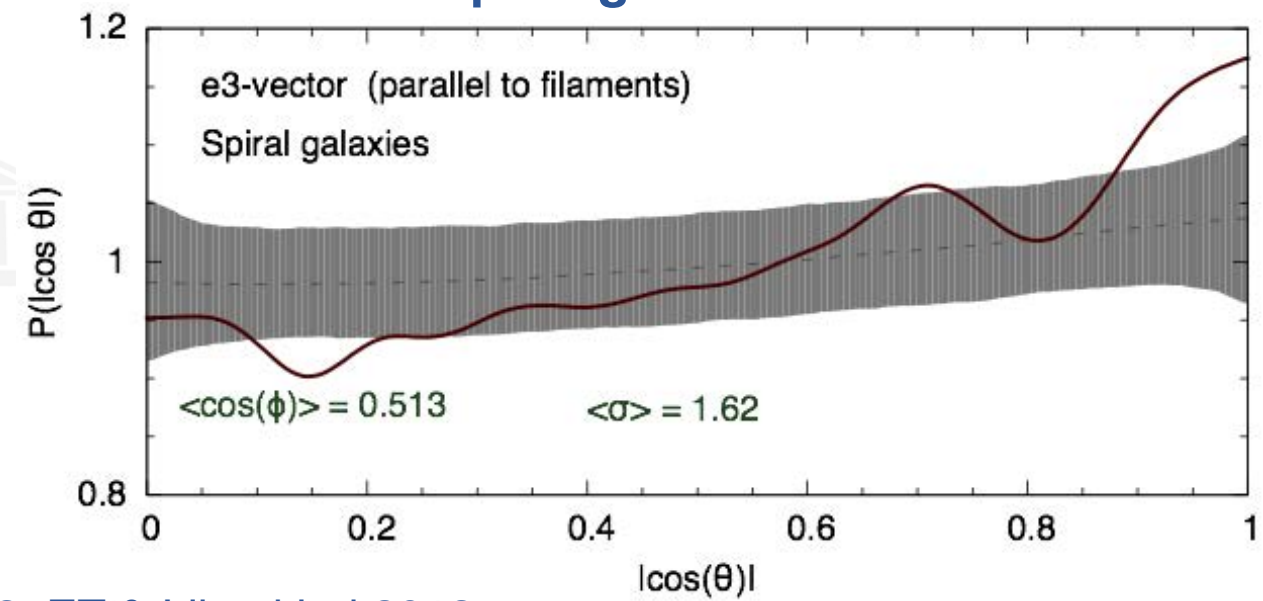
GAIN4MOST: Galaxy-filament Alignments IN 4MOST



Elliptical galaxies



Spiral galaxies



ET, Stoica & Saar 2013; ET & Libeskind 2013

Cosmic Web and Galaxy Evolution

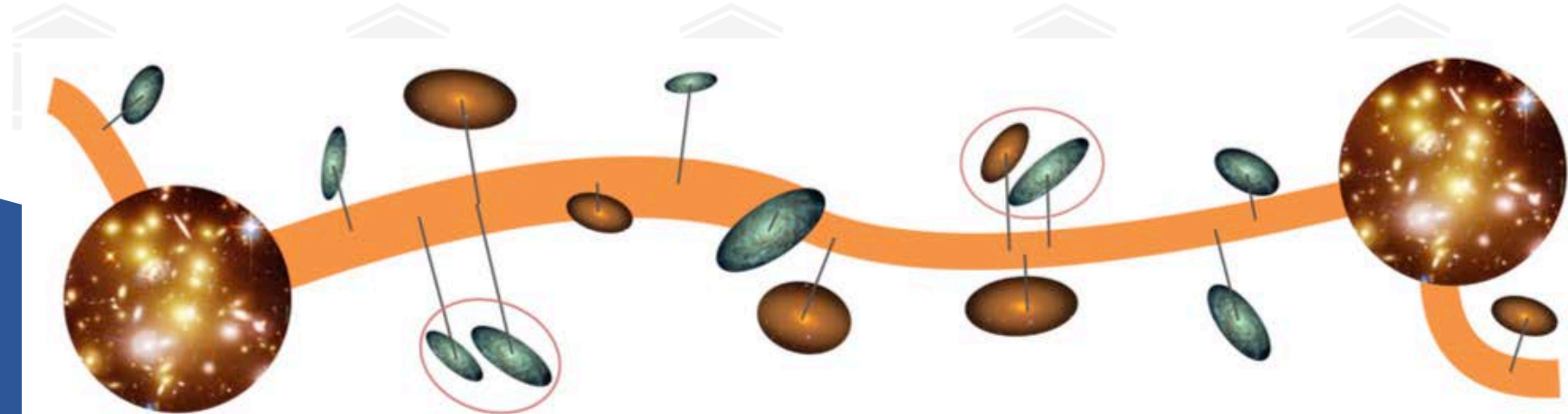
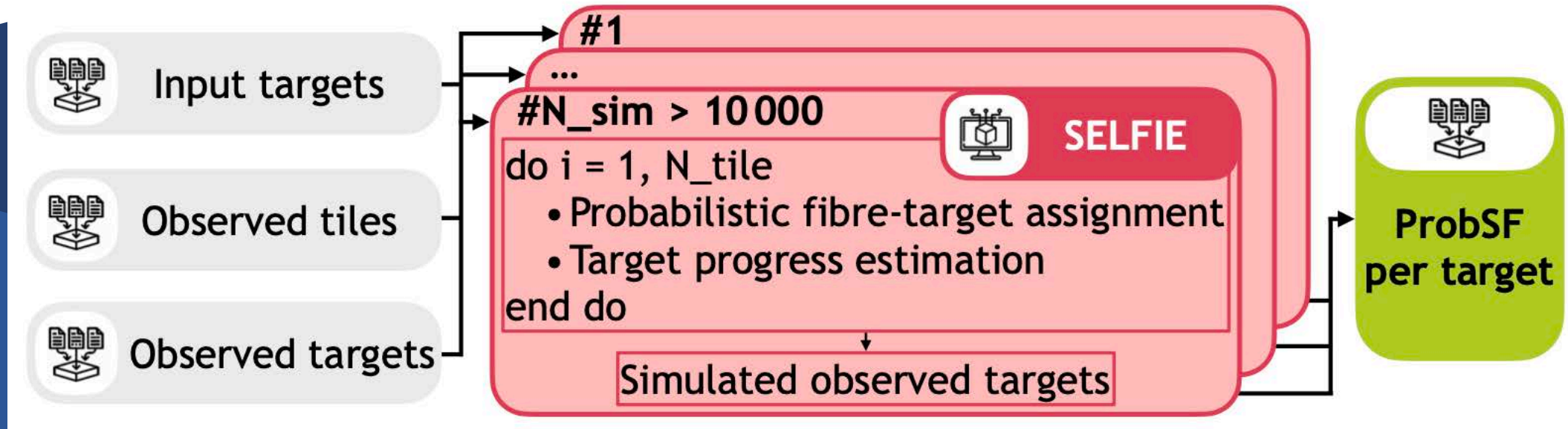
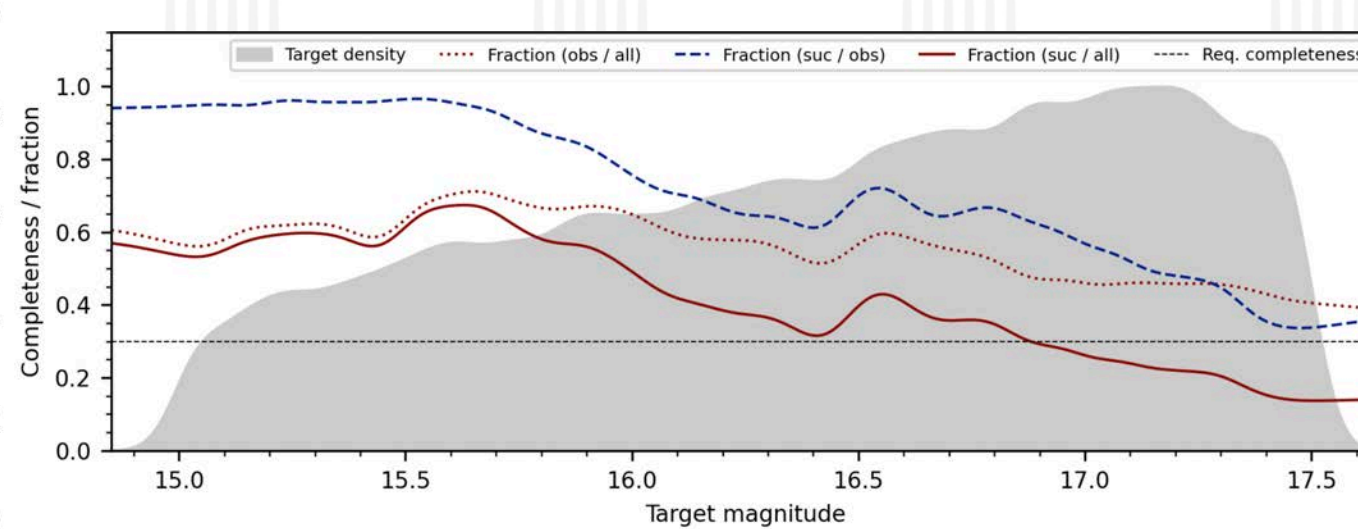
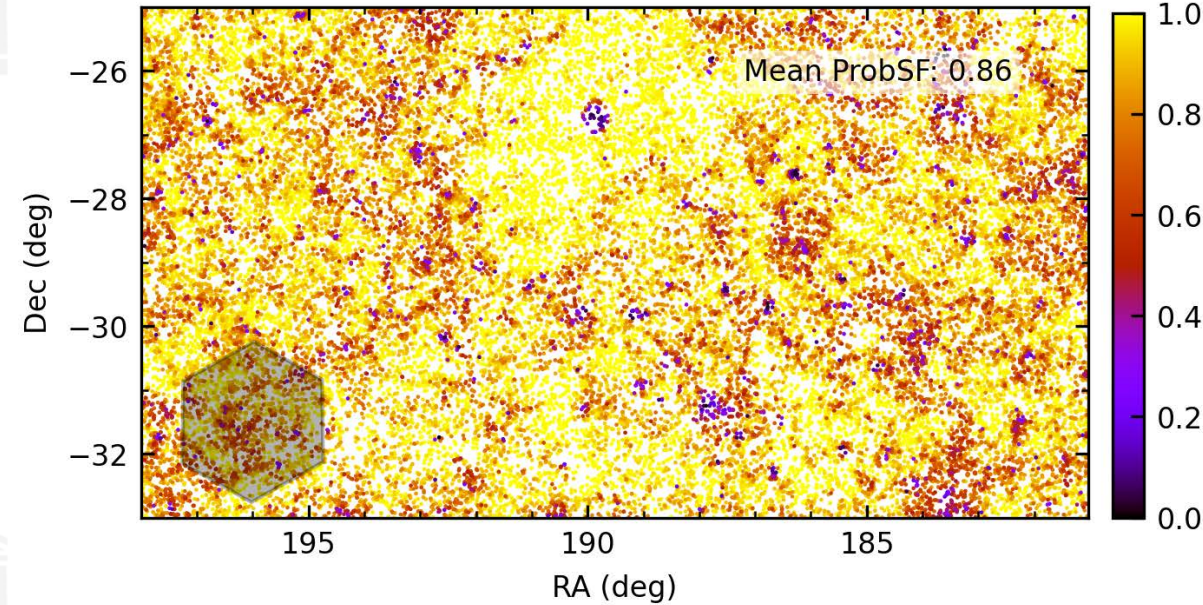


Fig. 4. A schematic illustration of galaxy-filament and galaxy-galaxy alignment in a filament that connects two clusters.



Probabilistic selection function

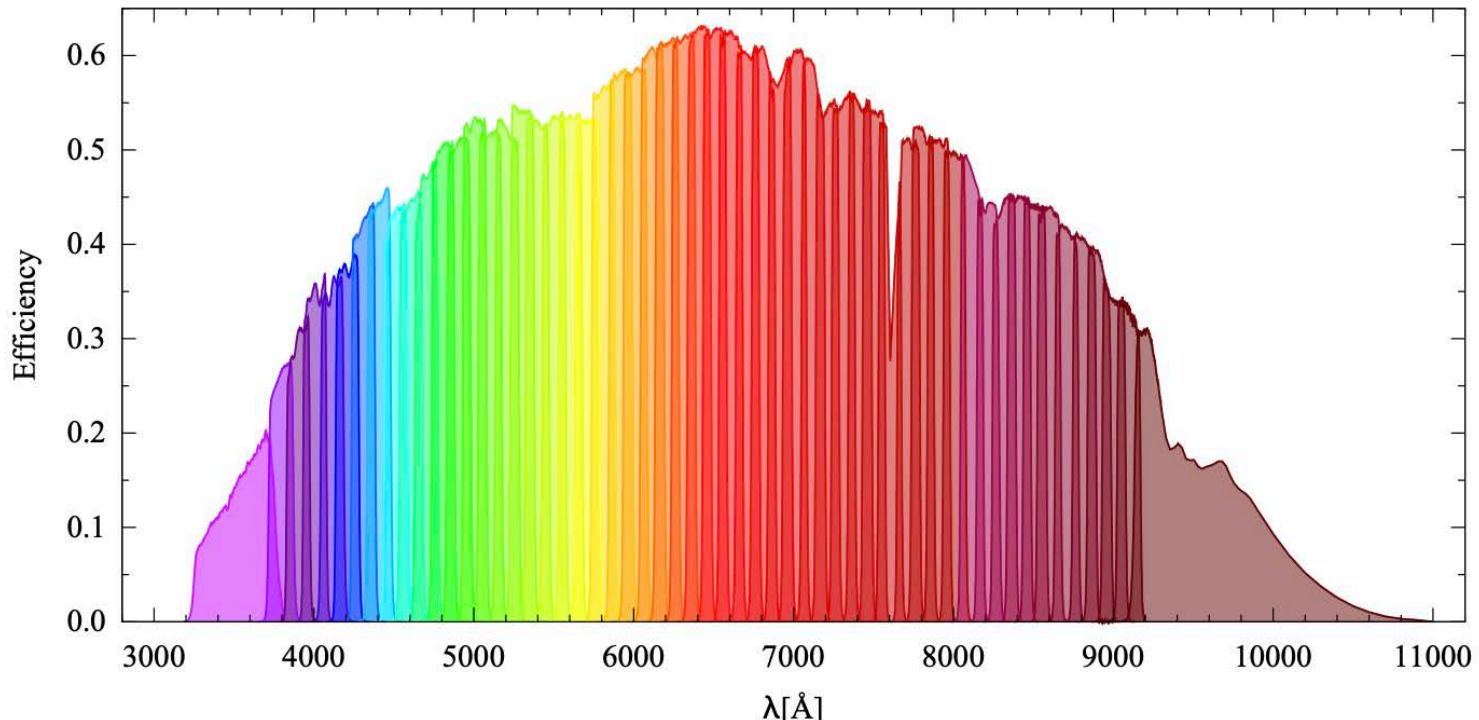
4MOST survey simulations

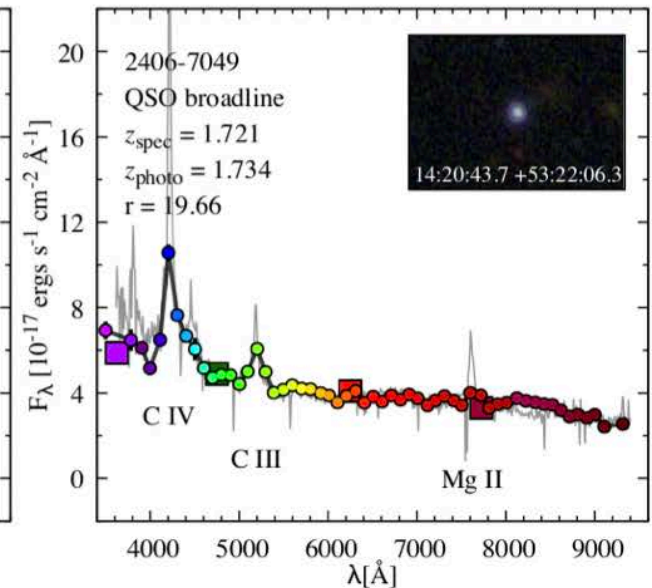
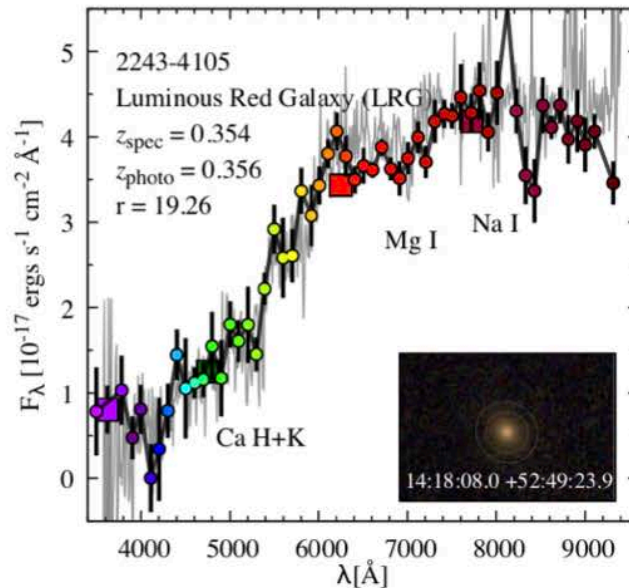
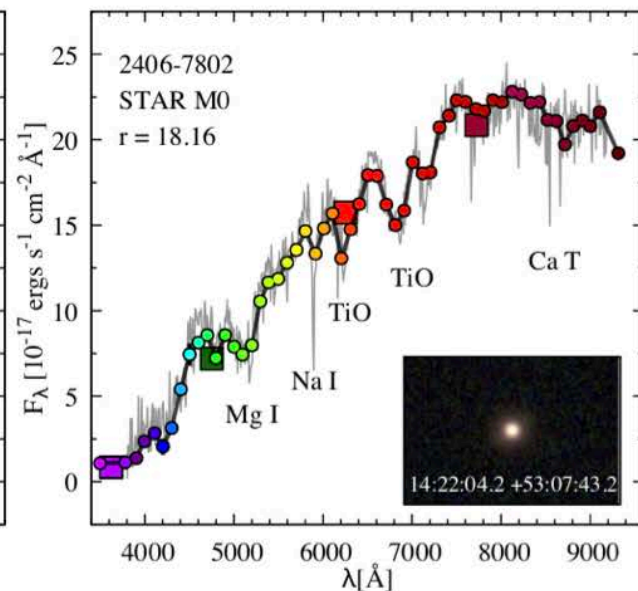
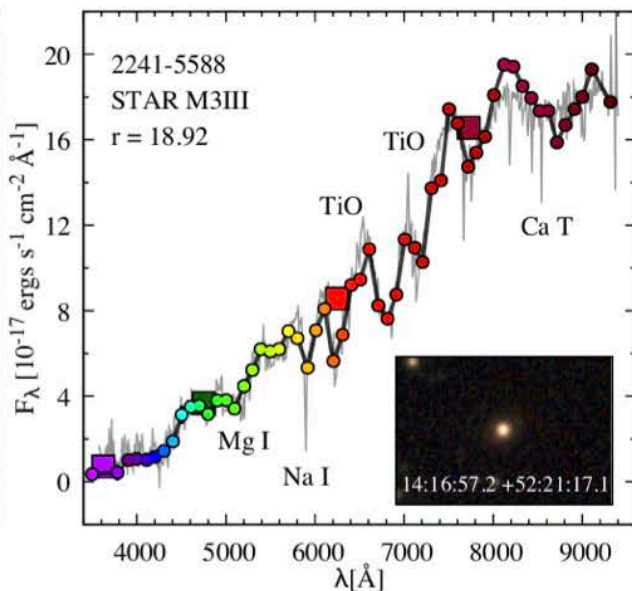
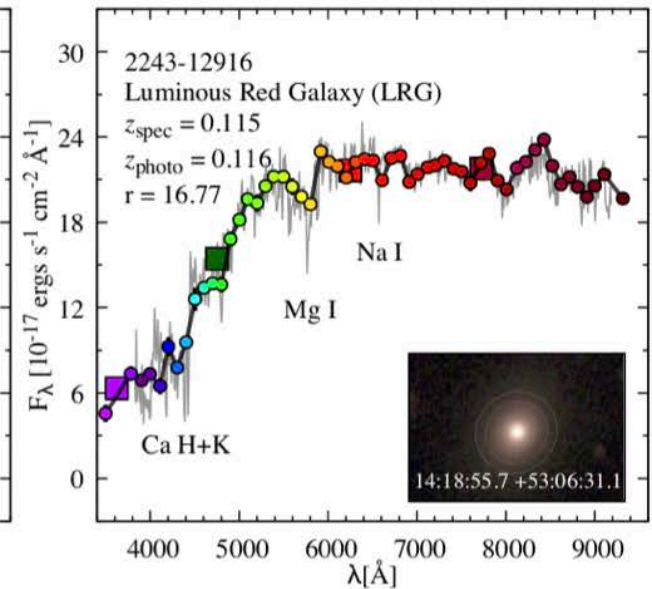
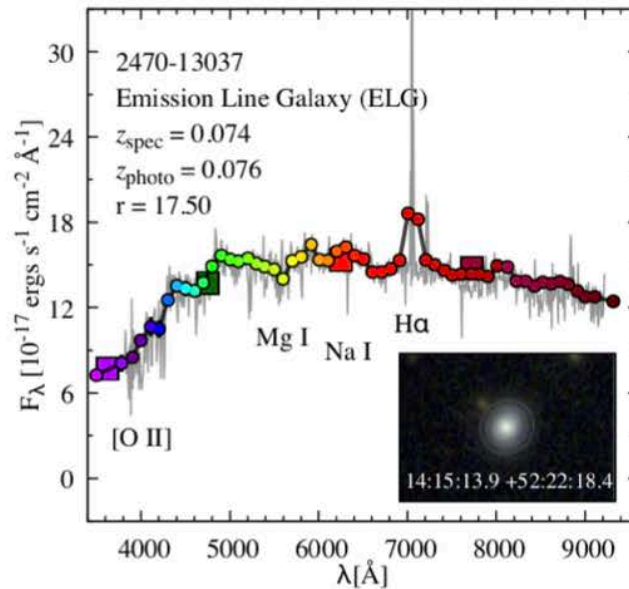
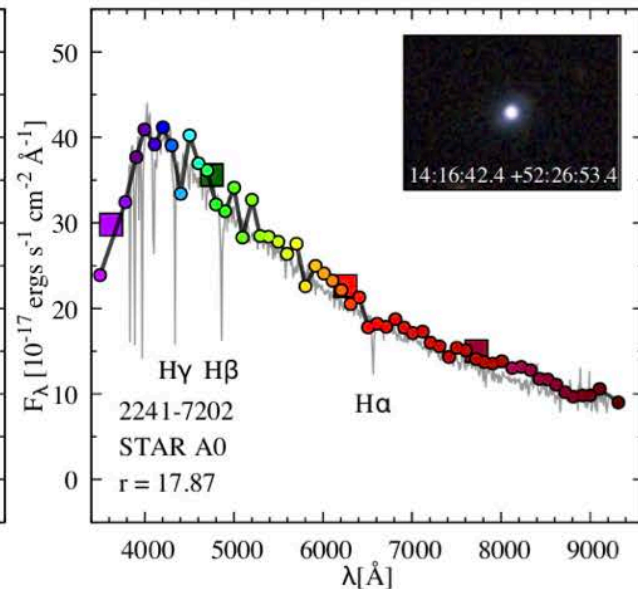
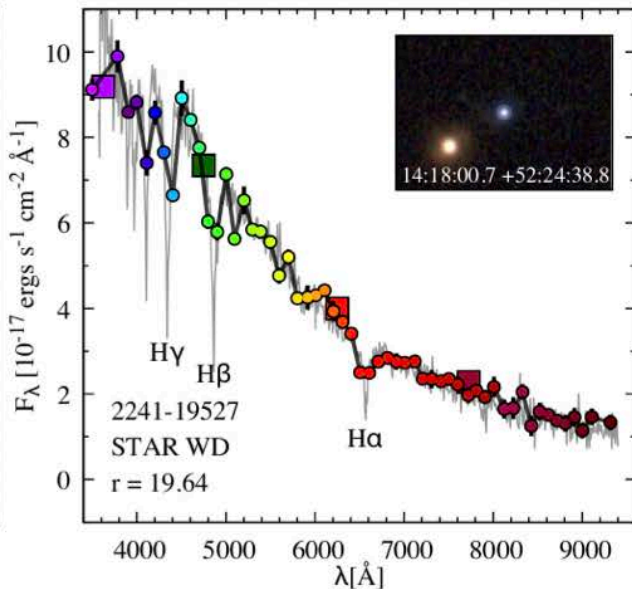
J-PAS – Javalambre Physics of the Accelerating Universe Astrophysical Survey



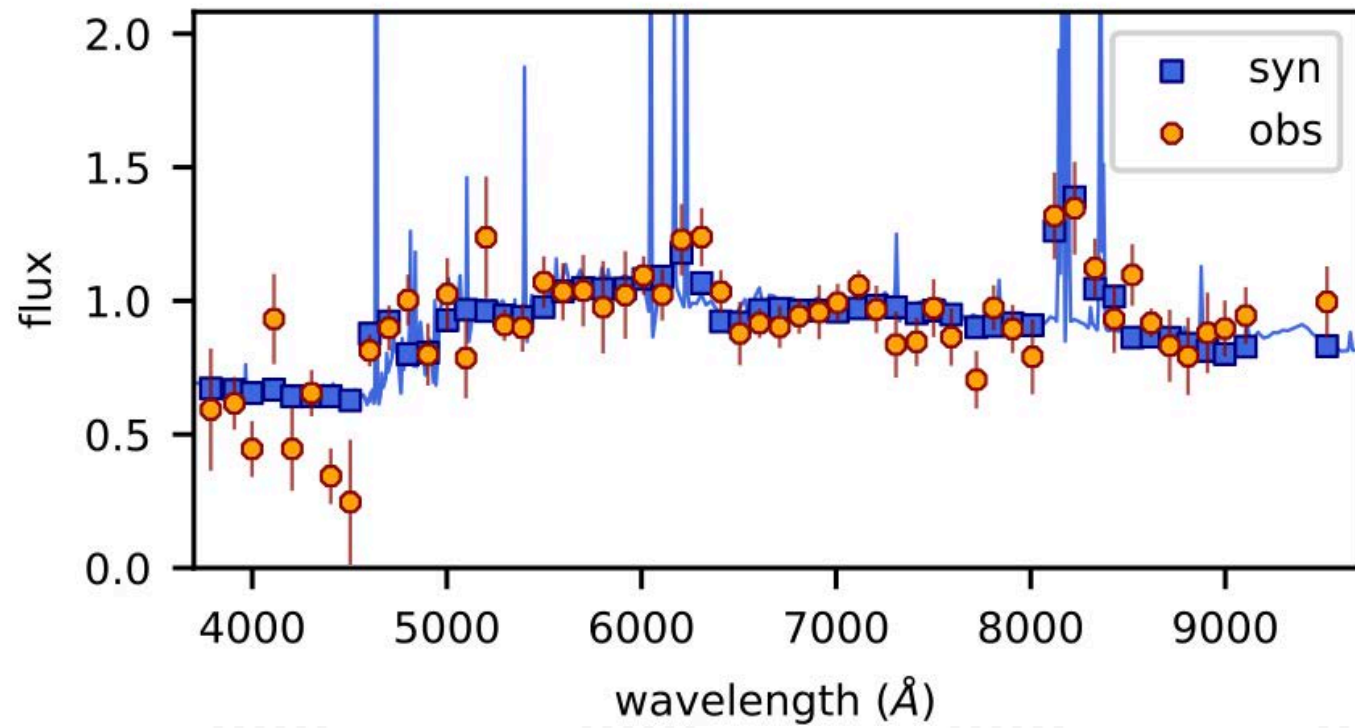
J-PAS – Javalambre Physics

of the Accelerating Universe Astrophysical Survey

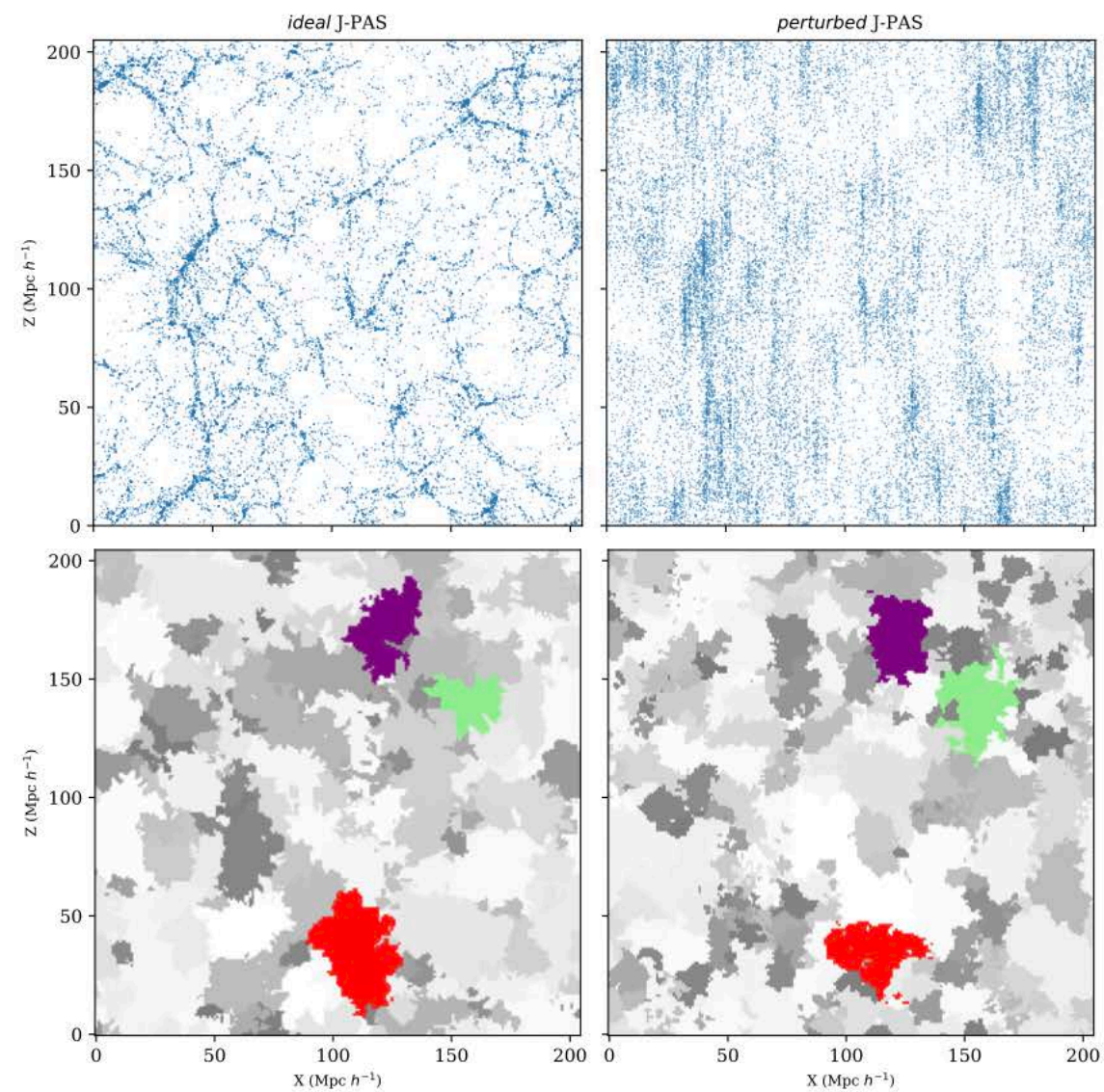
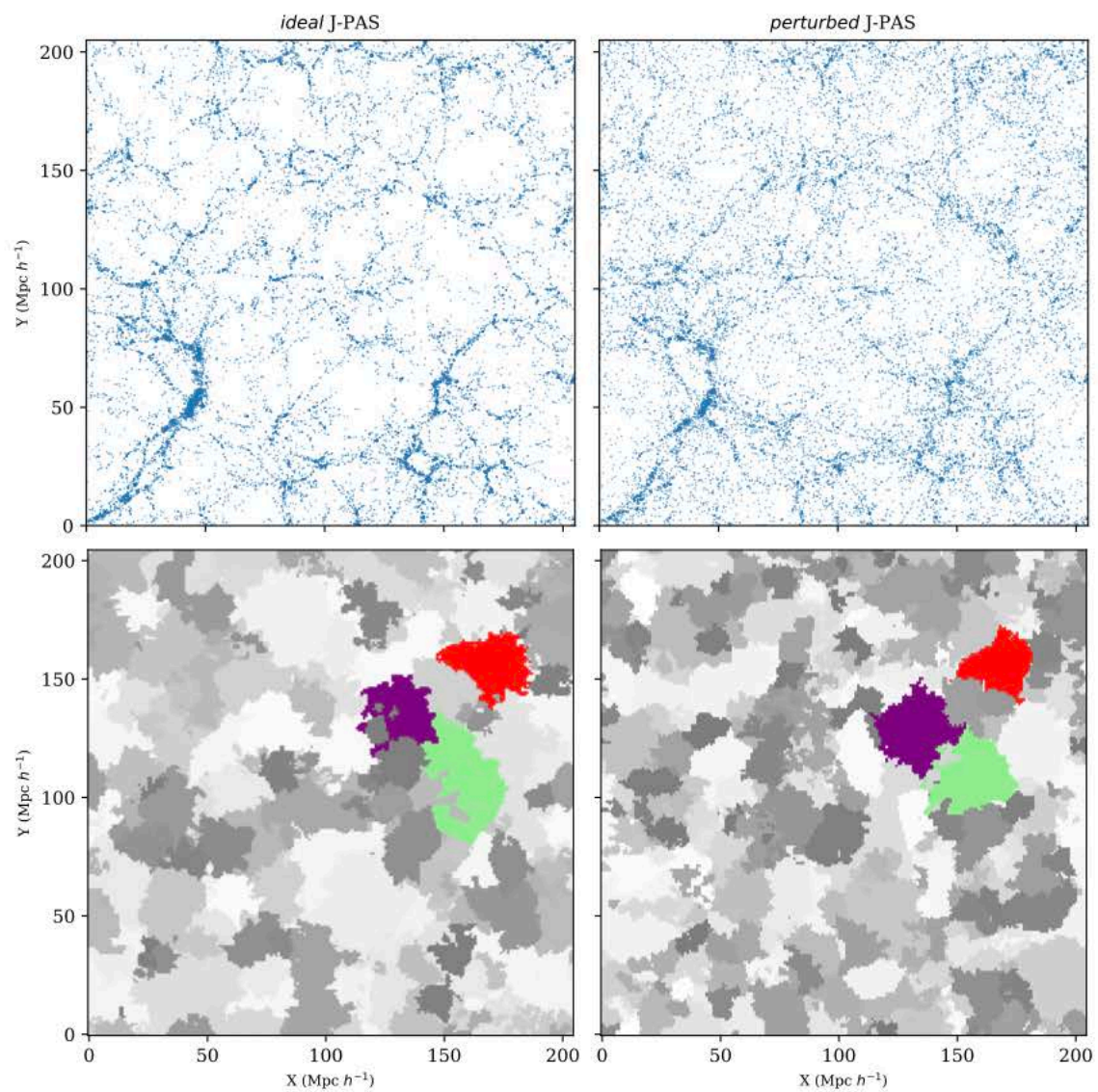




$z_{\text{spec}}=0.244$ $z_{\text{phot}}=0.246$



J-PAS reality





UNIVERSITY OF TARTU

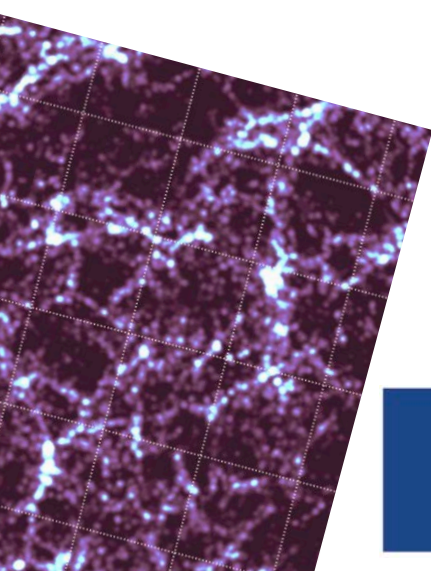
Measuring distances - photometric redshifts



Co-funded by
the European Union



Investing
in your future



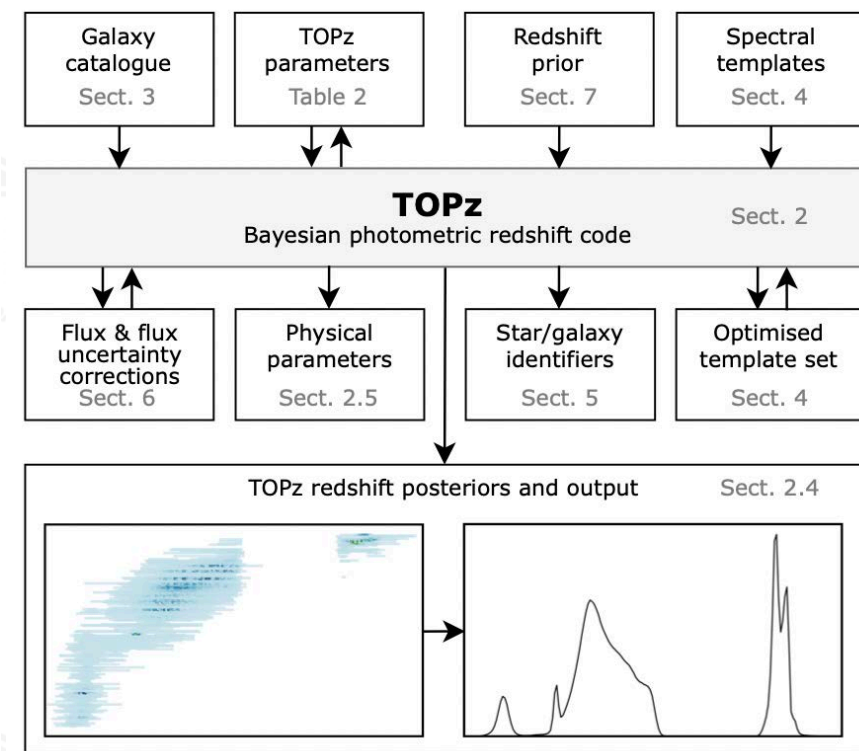
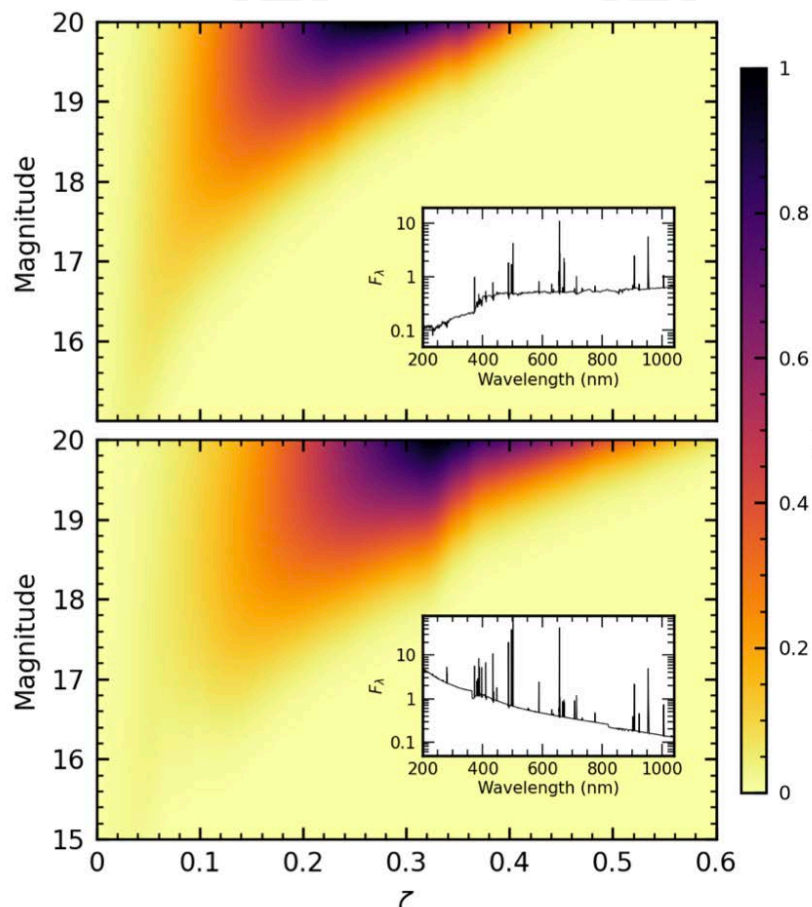
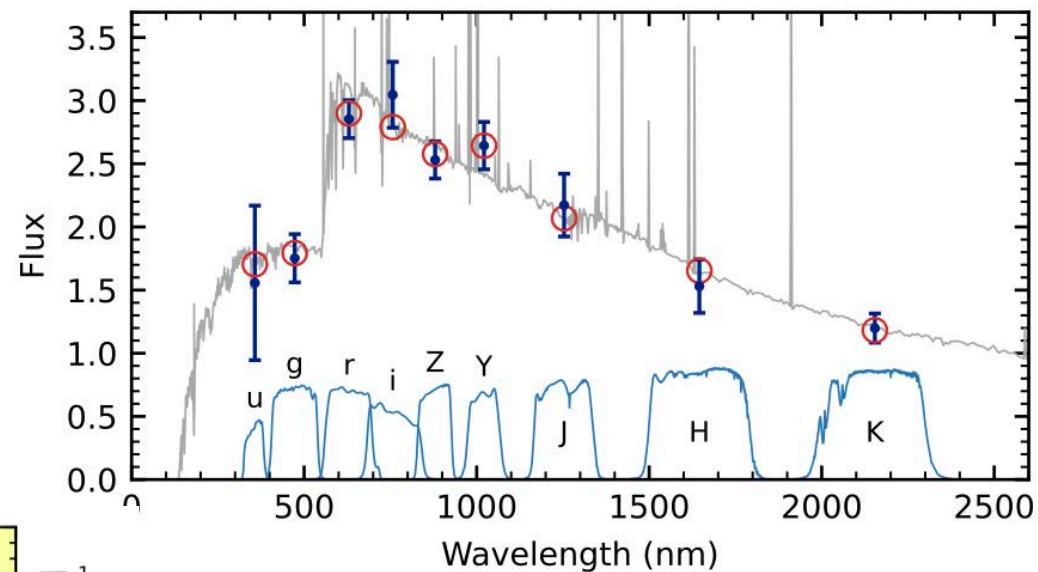
Funded by
the European Union

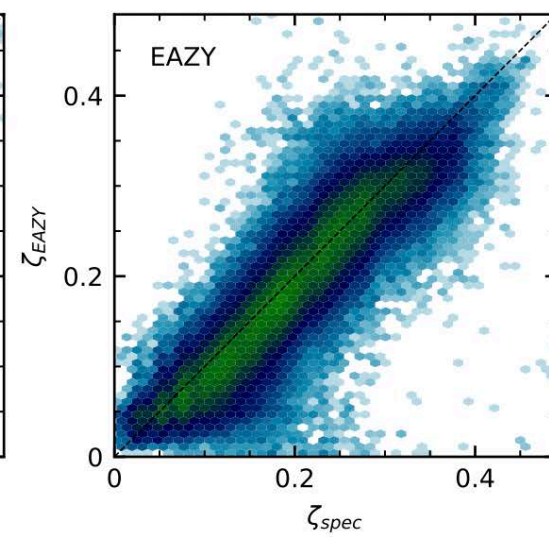
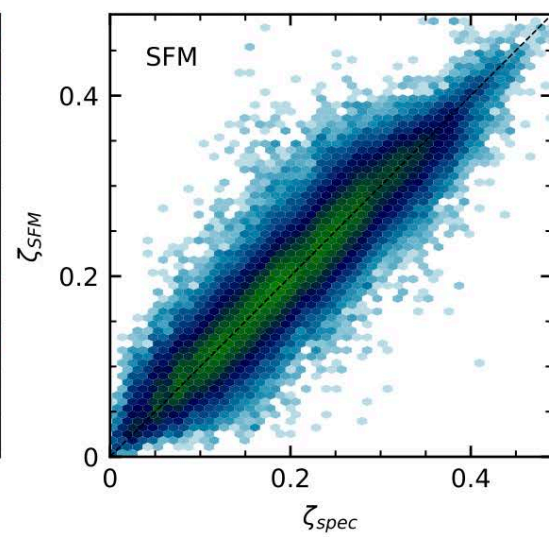
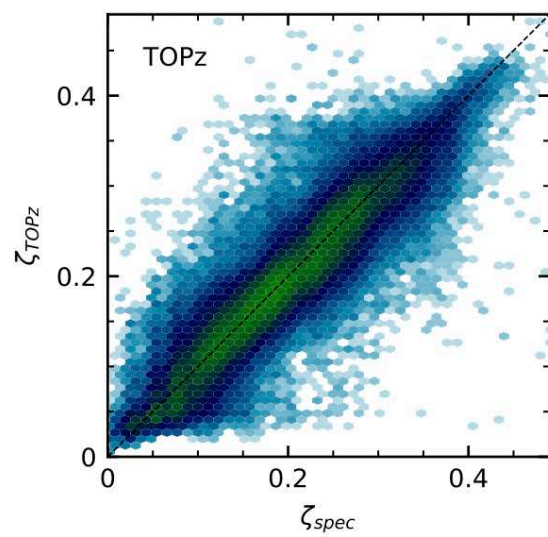
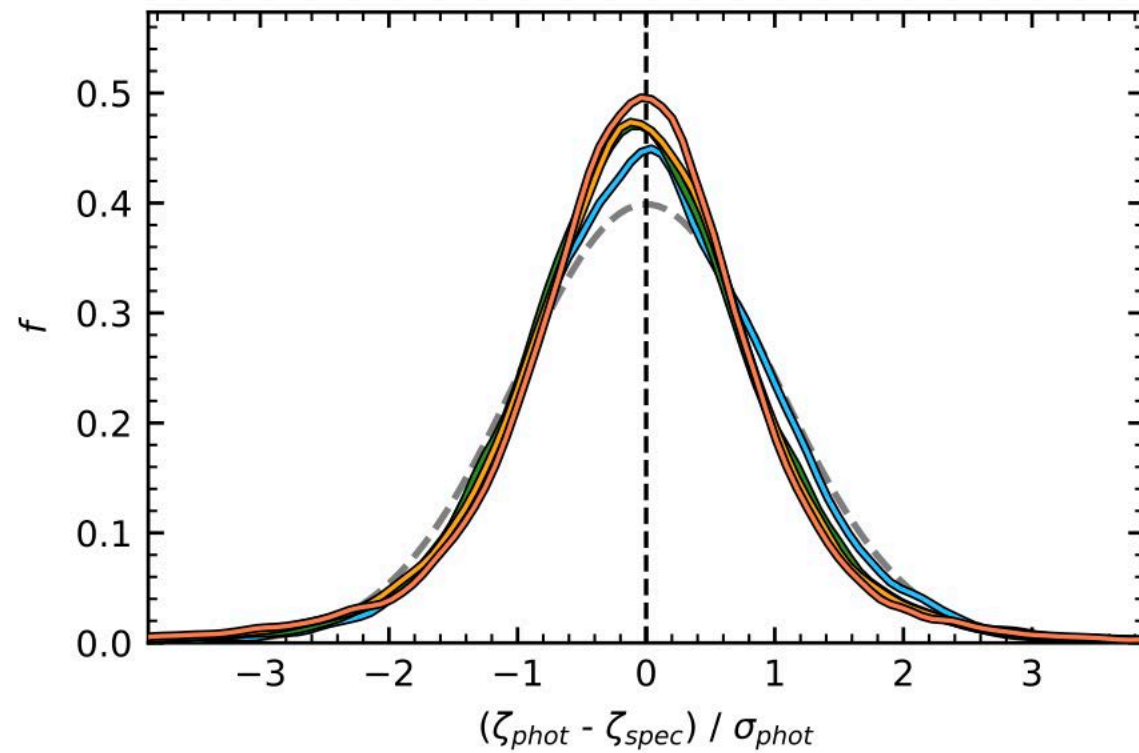
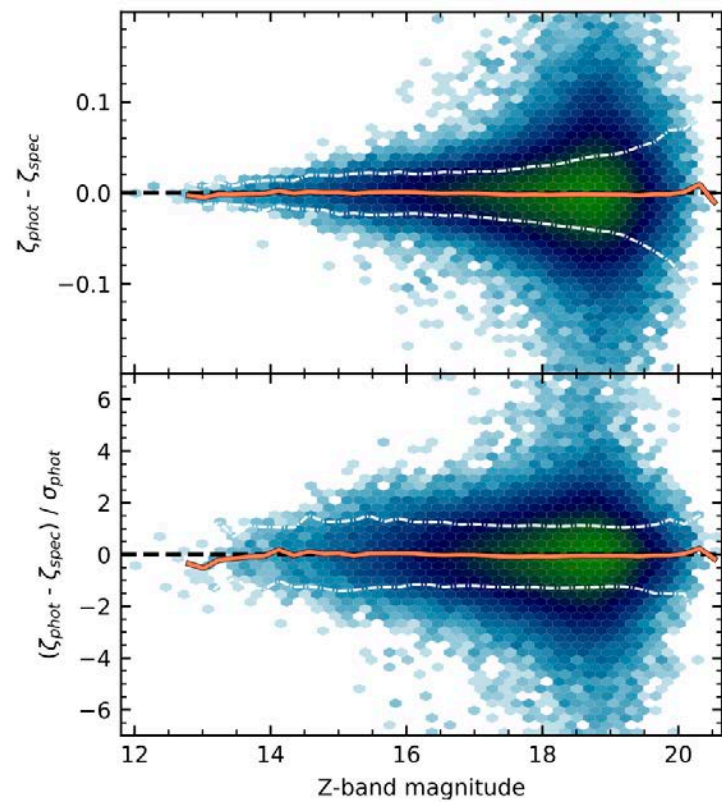


$$p(\zeta | F, m_0) = \sum_{T \in \mathbf{T}} p(\zeta, T | F, m_0) \propto \sum_{T \in \mathbf{T}} p(\zeta, T | m_0) p(F | \zeta, T), \quad (1)$$

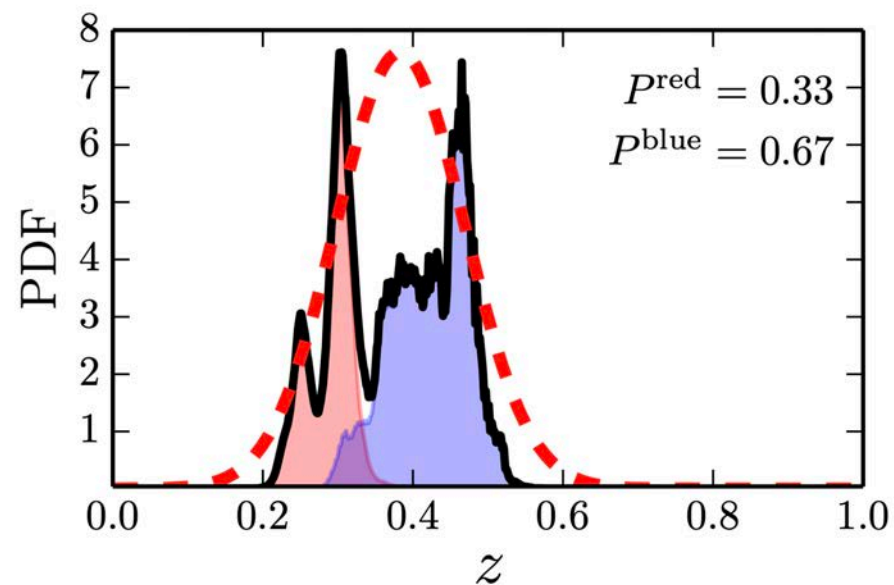
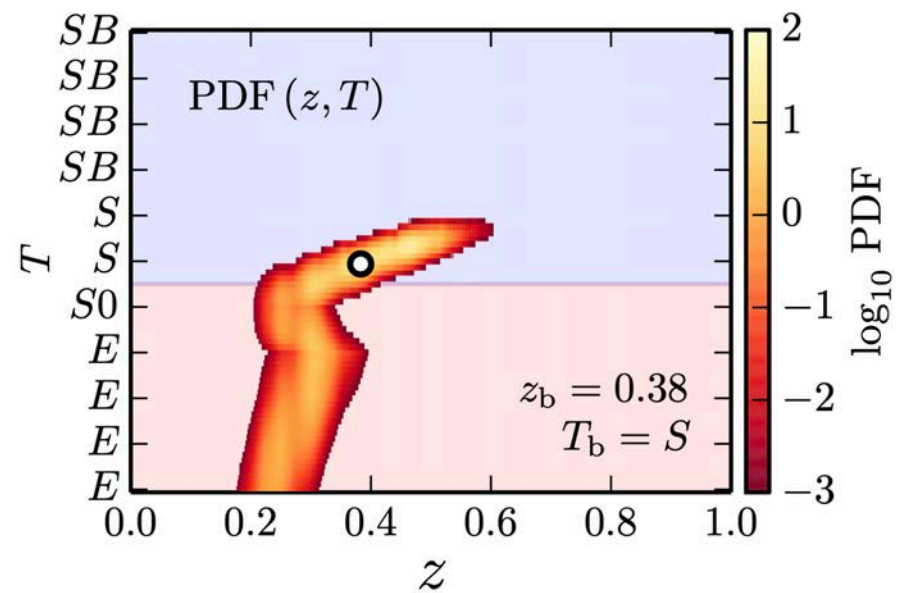
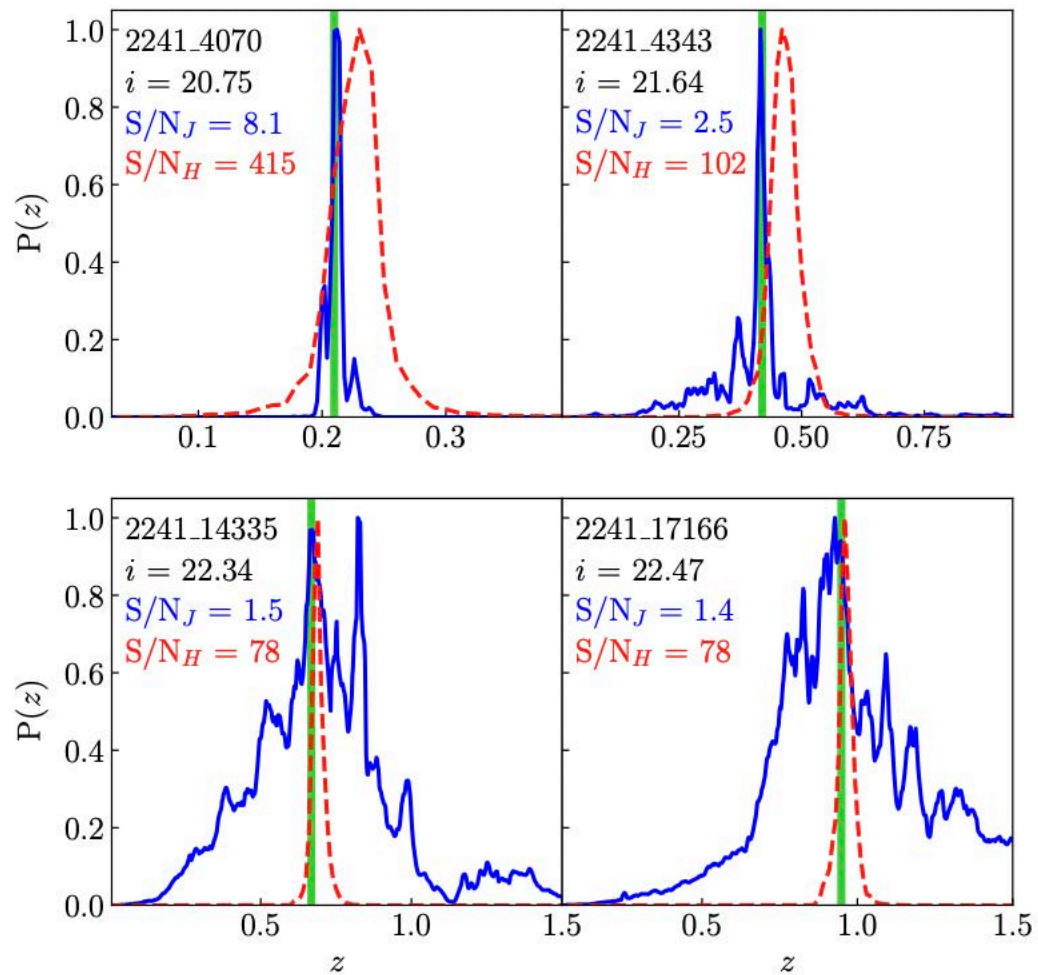
$$p(F | \zeta, T) \propto \frac{1}{\sqrt{F_{\text{TT}}}} \exp \left[-\frac{\chi^2(\zeta, T, a_m)}{2} \right],$$

$$F_{T\alpha} = \frac{\int f_{T,\zeta}(\lambda) W_\alpha(\lambda) d\lambda}{\int W_\alpha(\lambda) d\lambda},$$

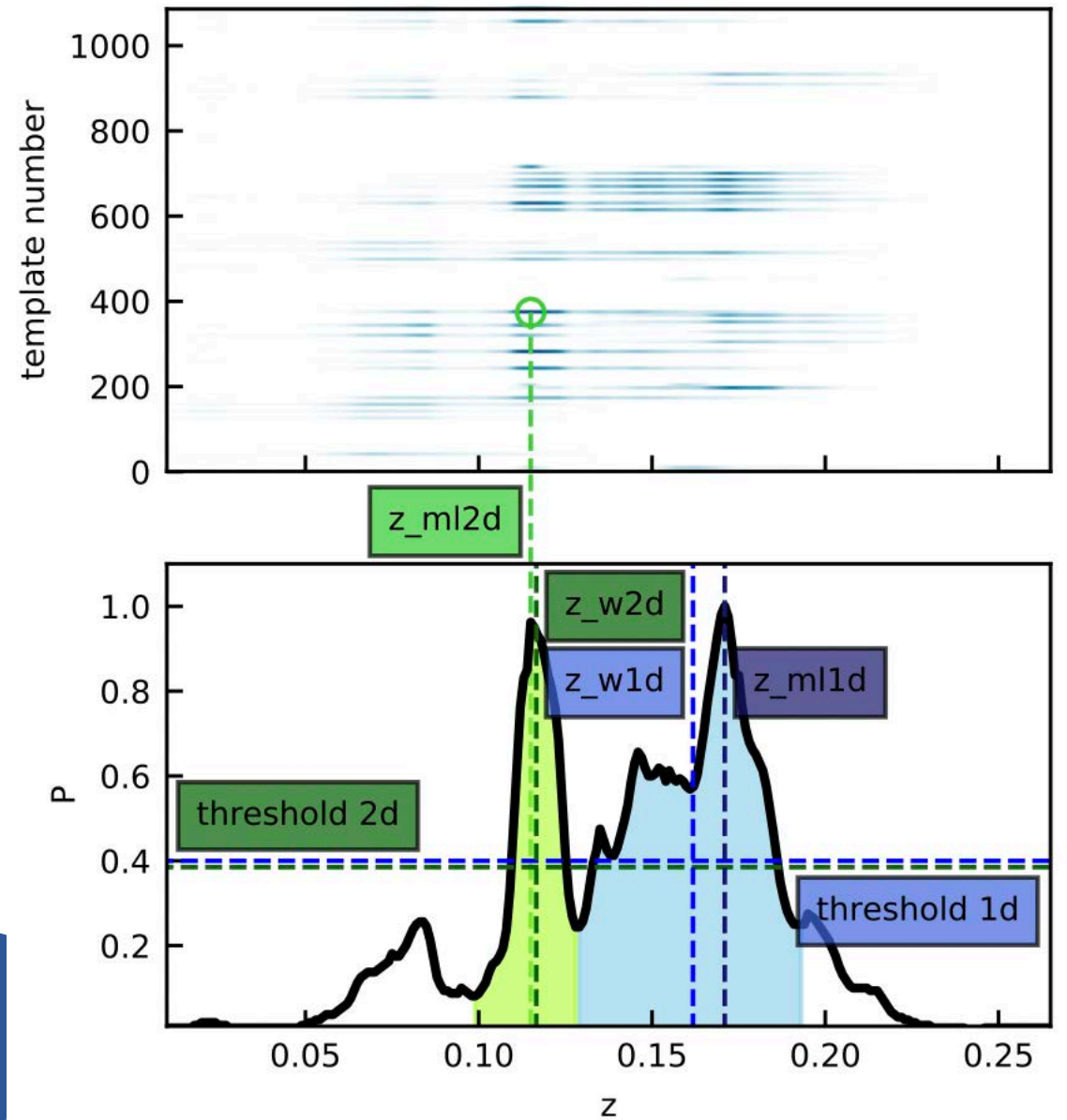


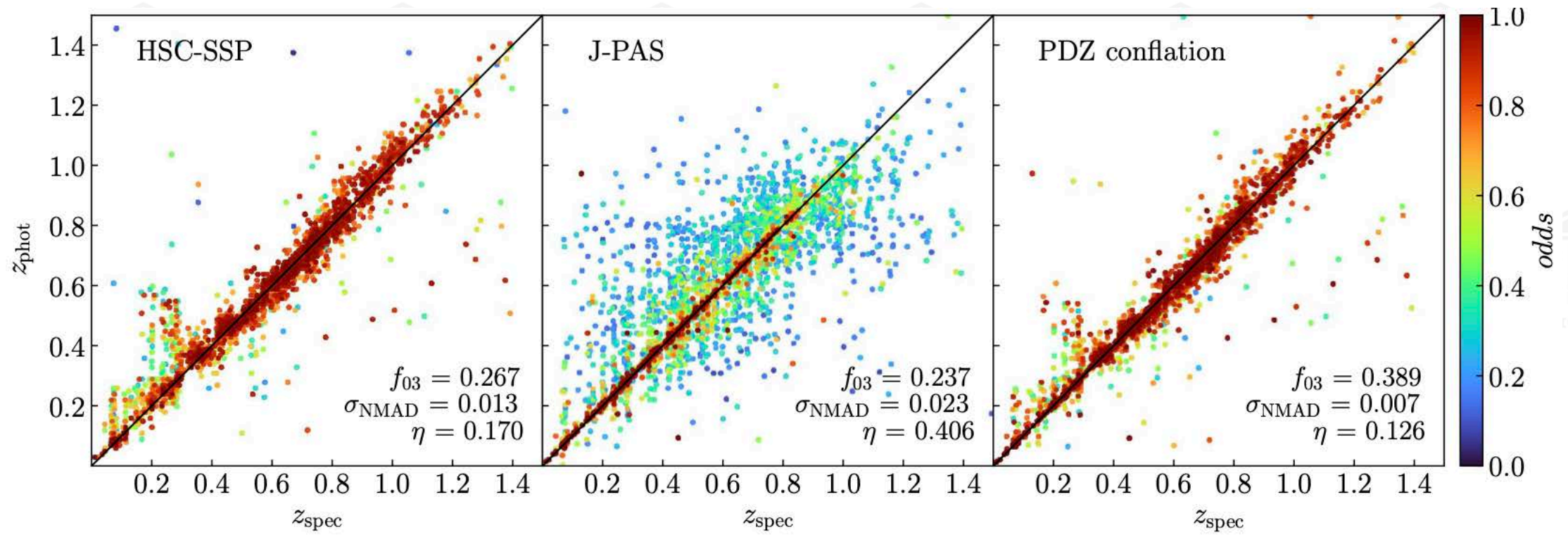


J-PAS — Javalambre Physics of the Accelerating Universe Astrophysical Survey

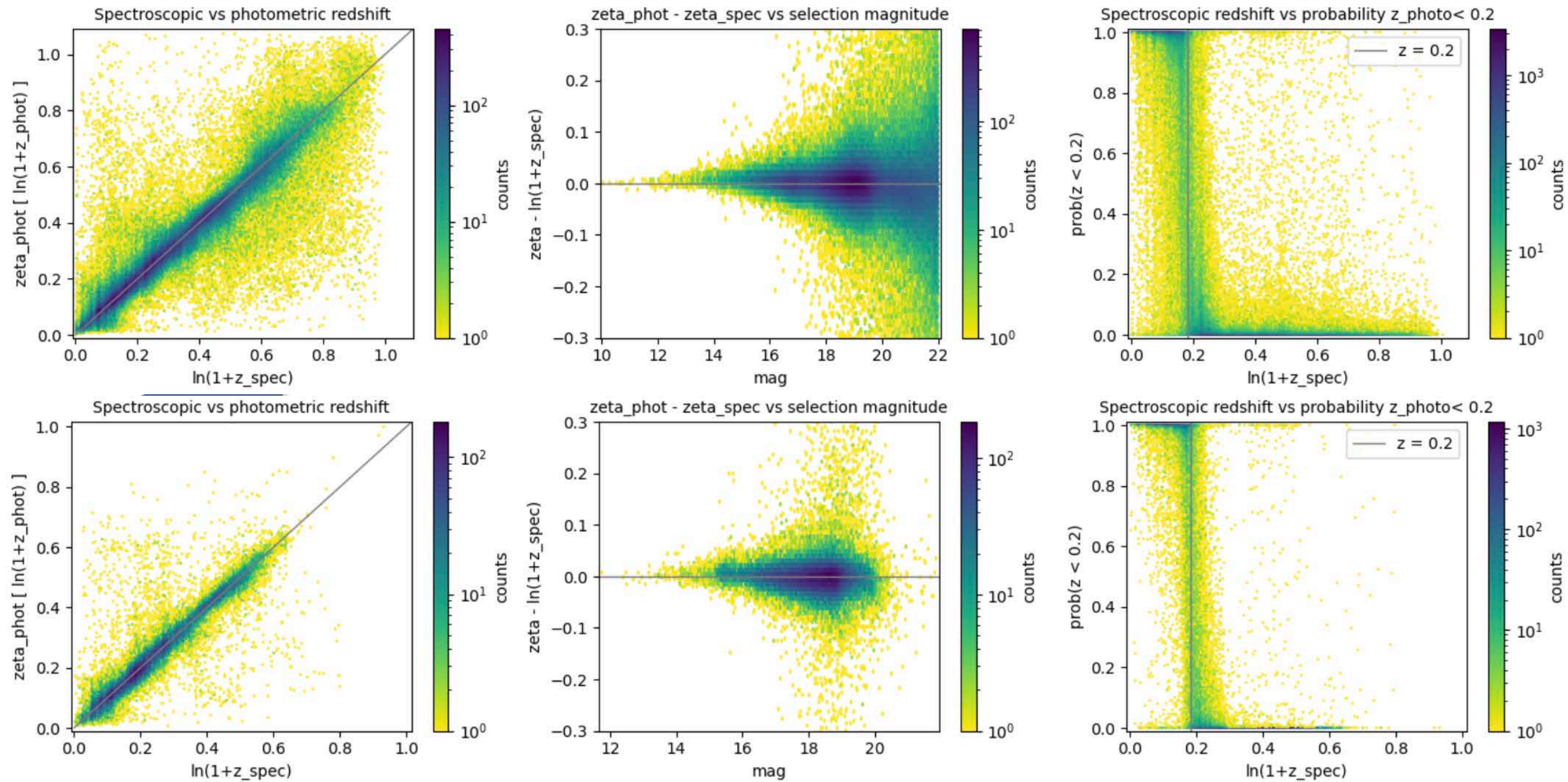


J_PAS





J_PAS



WAVES North: with prior



UNIVERSITY OF TARTU

Extra slides



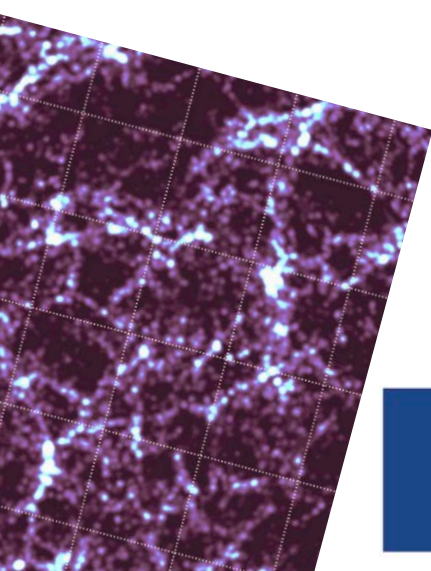
Co-funded by
the European Union



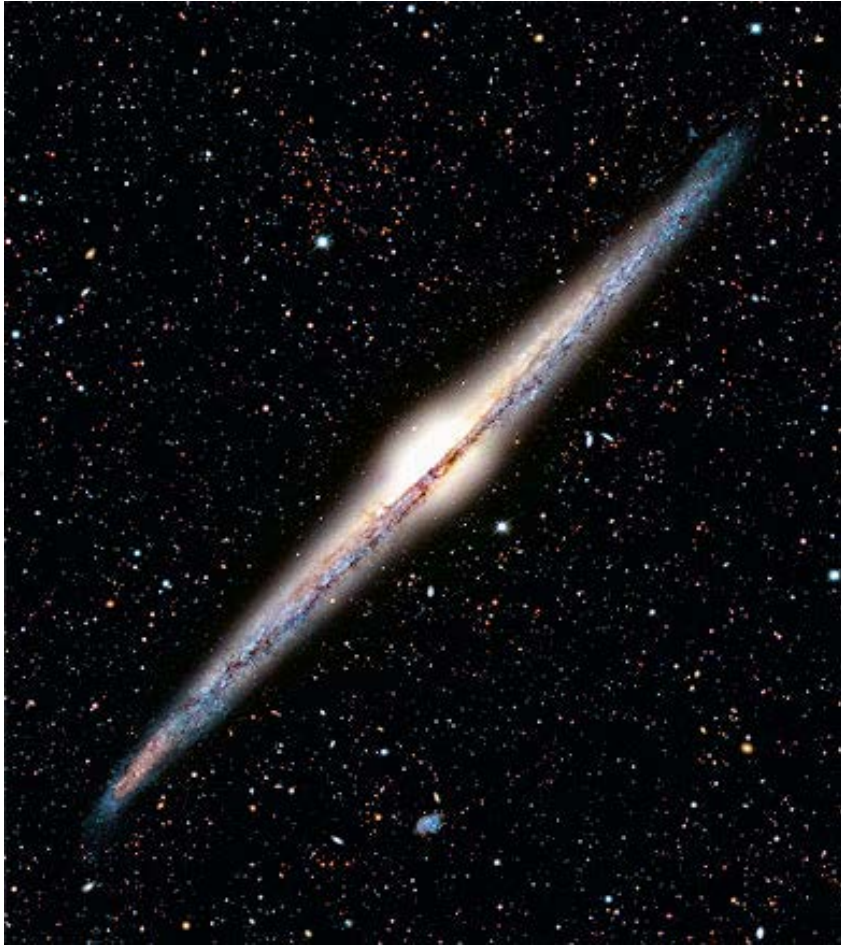
Investing
in your future



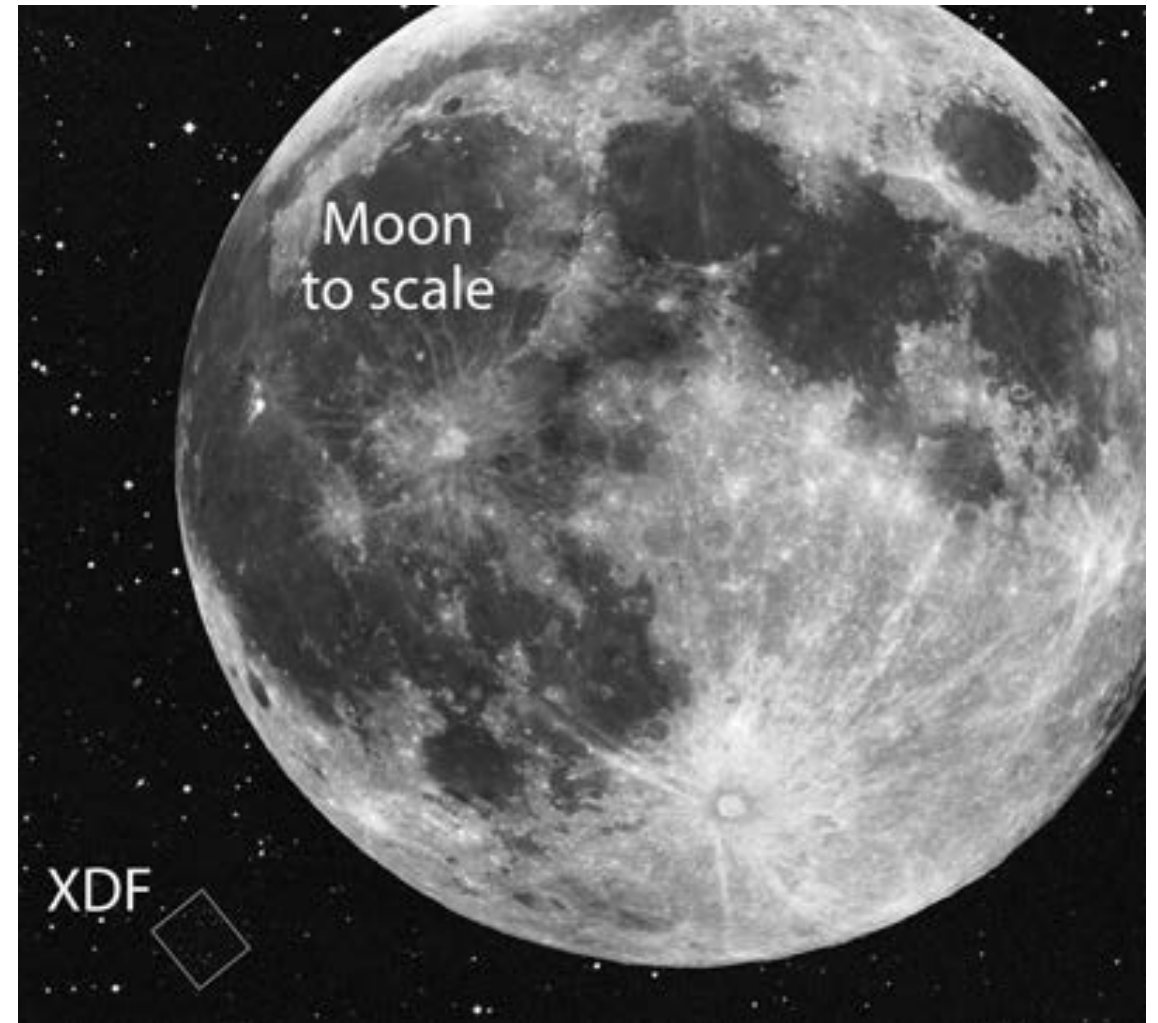
Funded by
the European Union



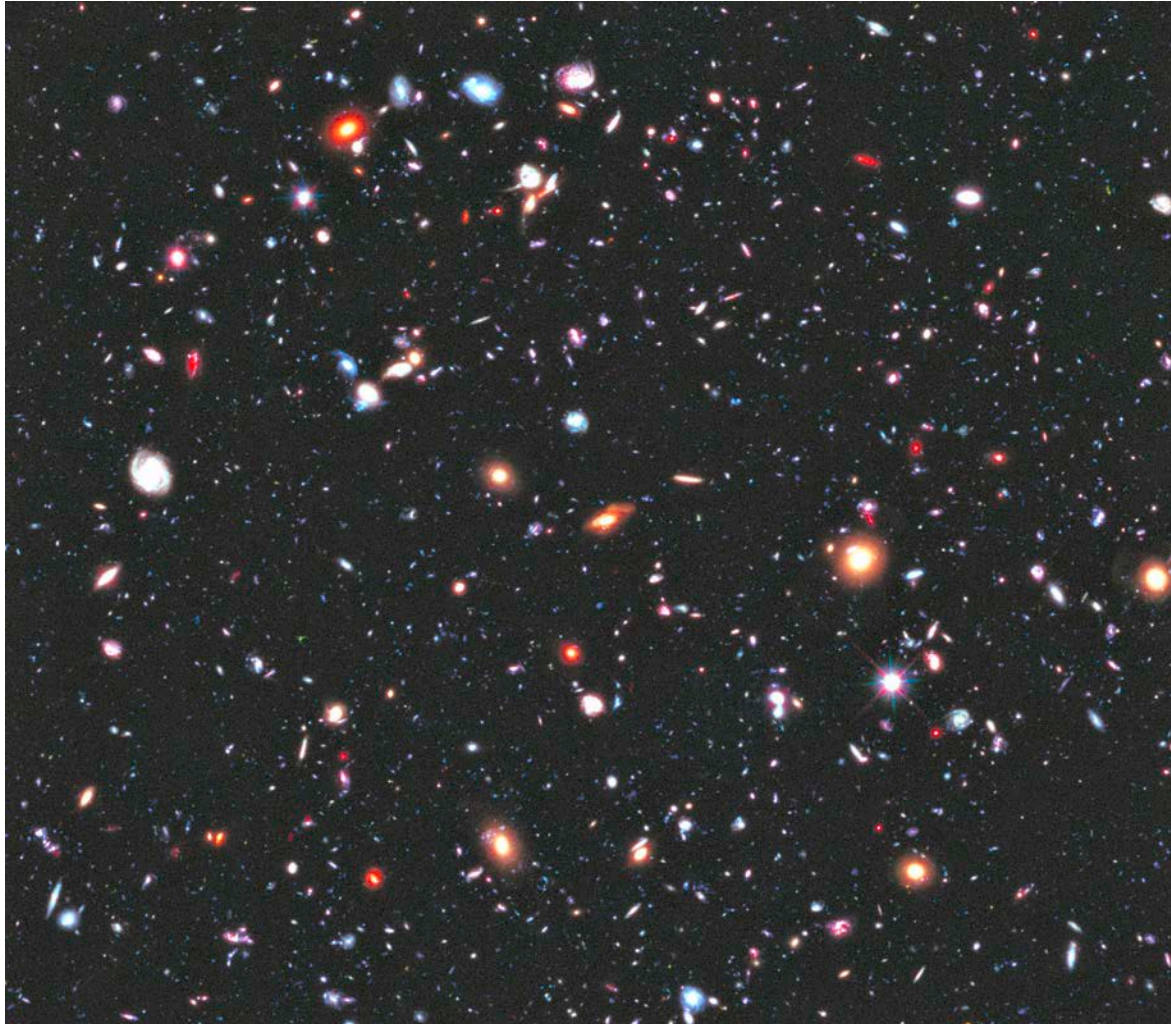
Is this the same galaxy?



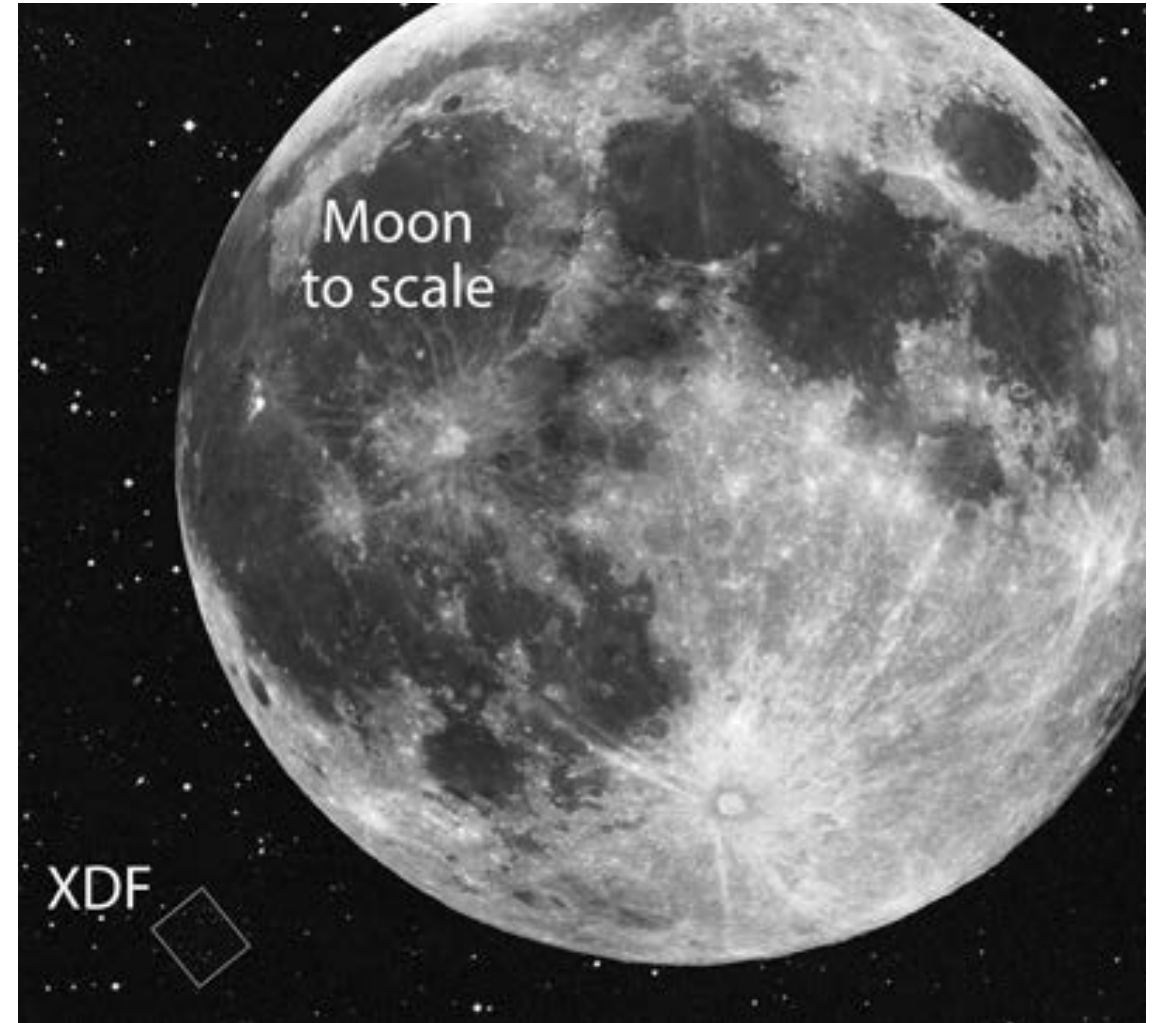
How empty is Universe?









How empty is Universe?



Source: ESA/Hubble



The Origin of the Solar System Elements

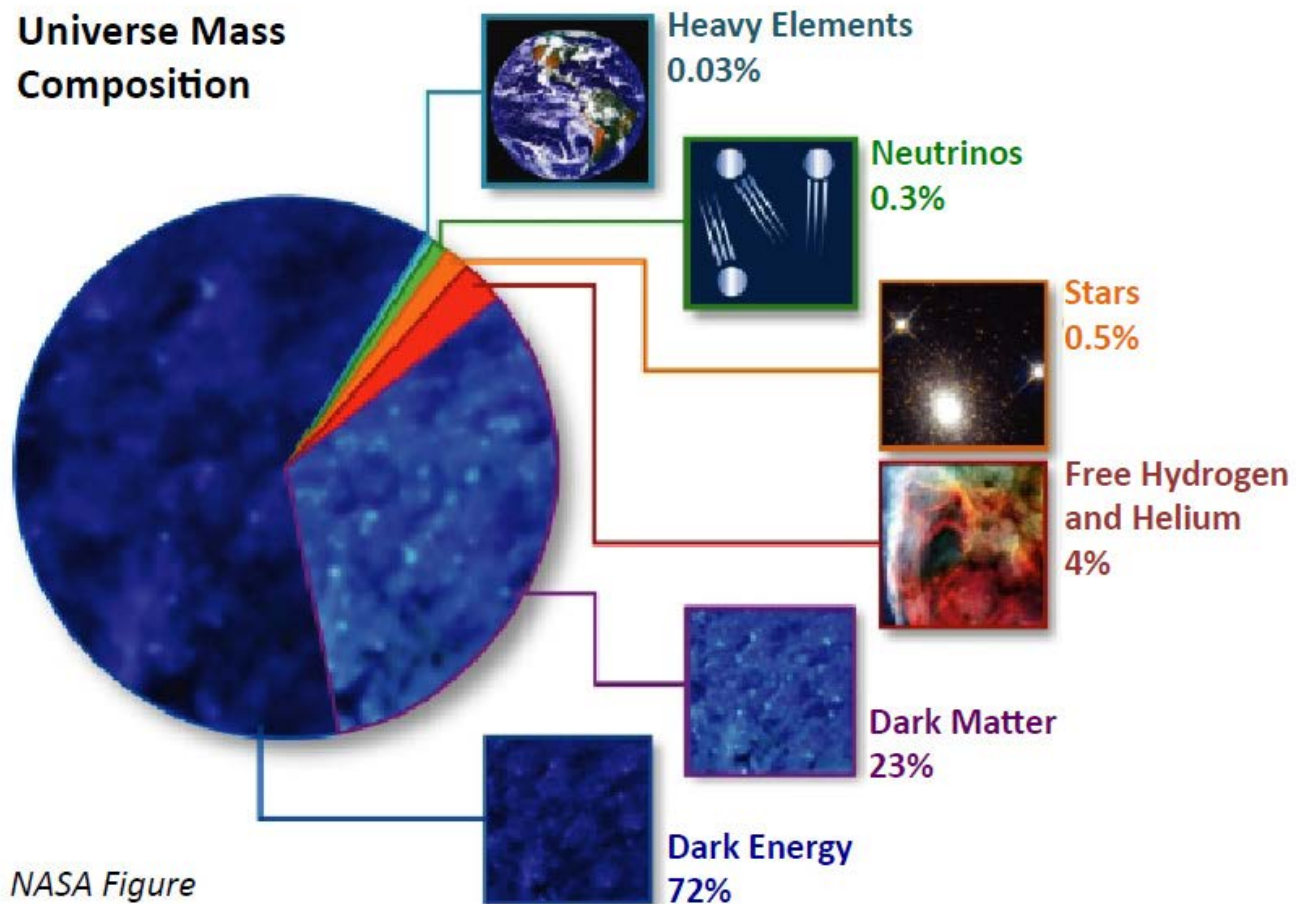
1 H	big bang fusion 						cosmic ray fission 						2 He											
3 Li	4 Be	merging neutron stars 						exploding massive stars 						5 B	6 C	7 N	8 O	9 F	10 Ne					
11 Na	12 Mg	dying low mass stars 						exploding white dwarfs 						13 Al	14 Si	15 P	16 S	17 Cl	18 Ar					
19 K	20 Ca	21 Sc	22 Ti	23 V	24 Cr	25 Mn	26 Fe	27 Co	28 Ni	29 Cu	30 Zn	31 Ga	32 Ge	33 As	34 Se	35 Br	36 Kr							
37 Rb	38 Sr	39 Y	40 Zr	41 Nb	42 Mo	43 Tc	44 Ru	45 Rh	46 Pd	47 Ag	48 Cd	49 In	50 Sn	51 Sb	52 Te	53 I	54 Xe							
55 Cs	56 Ba			72 Hf	73 Ta	74 W	75 Re	76 Os	77 Ir	78 Pt	79 Au	80 Hg	81 Tl	82 Pb	83 Bi	84 Po	85 At	86 Rn						
87 Fr	88 Ra																							
		57 La	58 Ce	59 Pr	60 Nd	61 Pm	62 Sm	63 Eu	64 Gd	65 Tb	66 Dy	67 Ho	68 Er	69 Tm	70 Yb	71 Lu								
		89 Ac	90 Th	91 Pa	92 U																			

Graphic created by Jennifer Johnson

Astronomical Image Credits:
ESA/NASA/AASNova

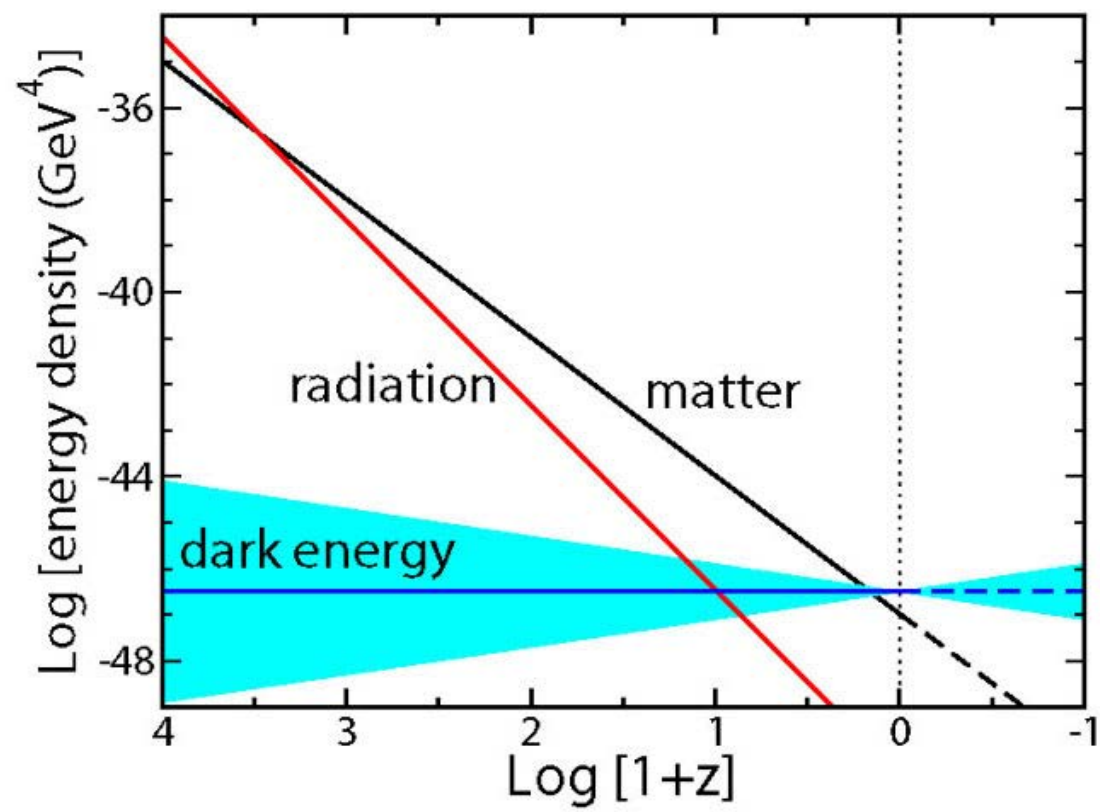
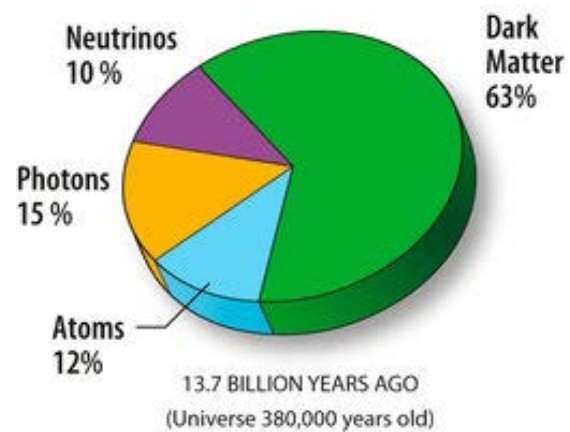
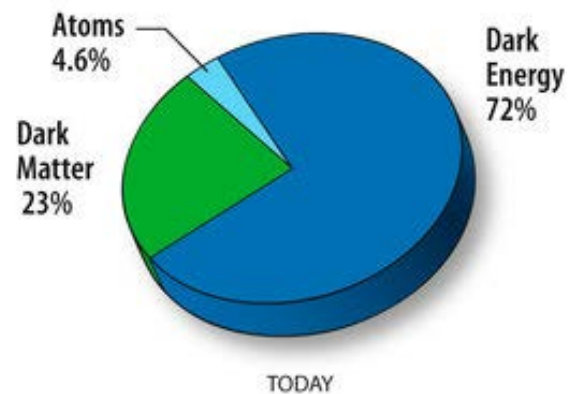
How dark is the Universe?

Universe Mass
Composition

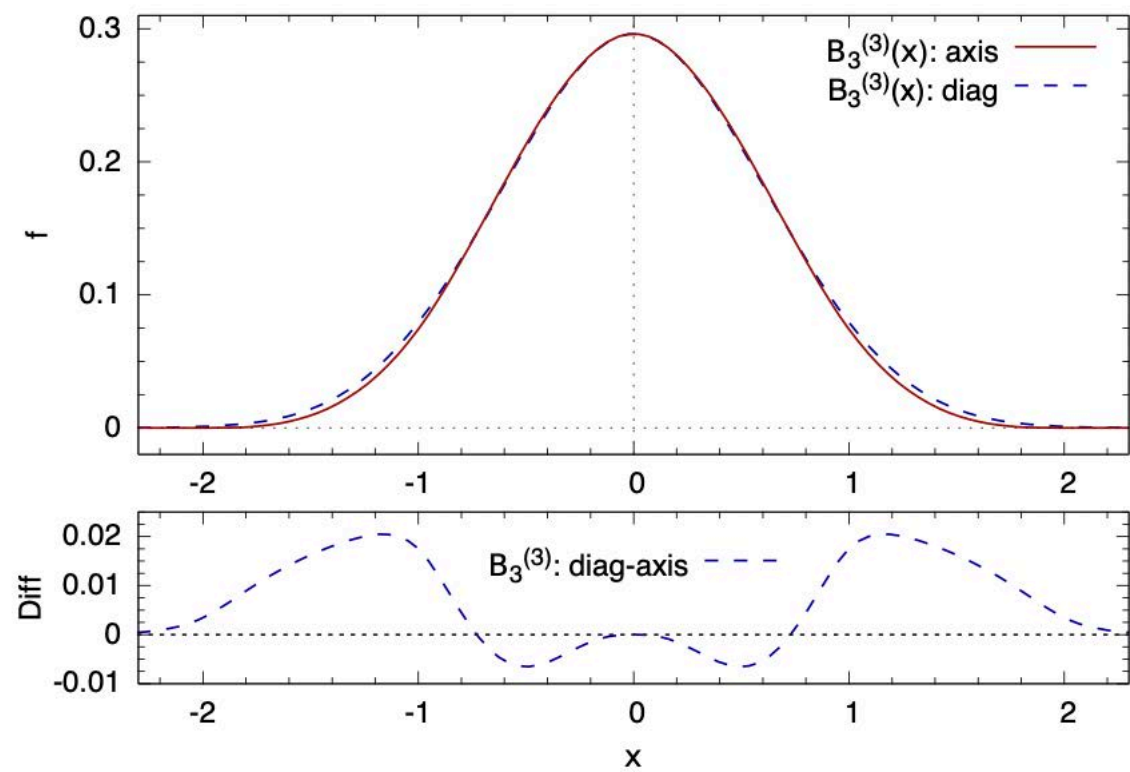


NASA Figure

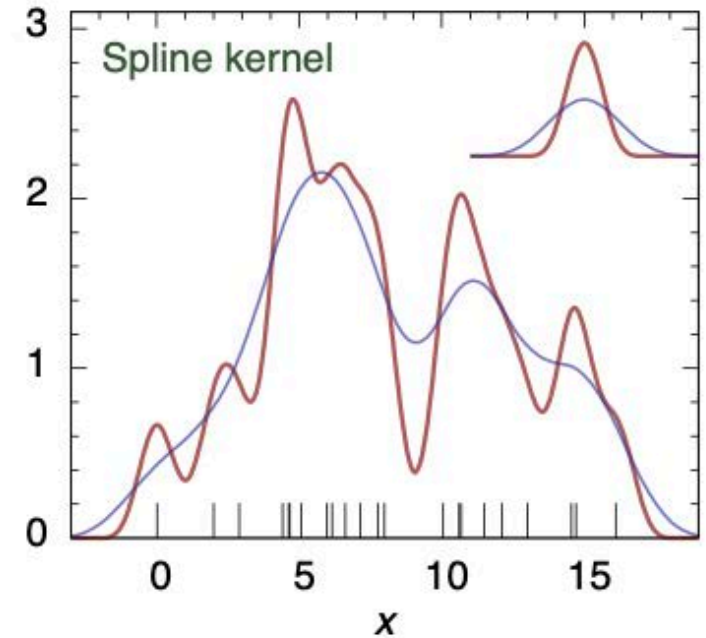
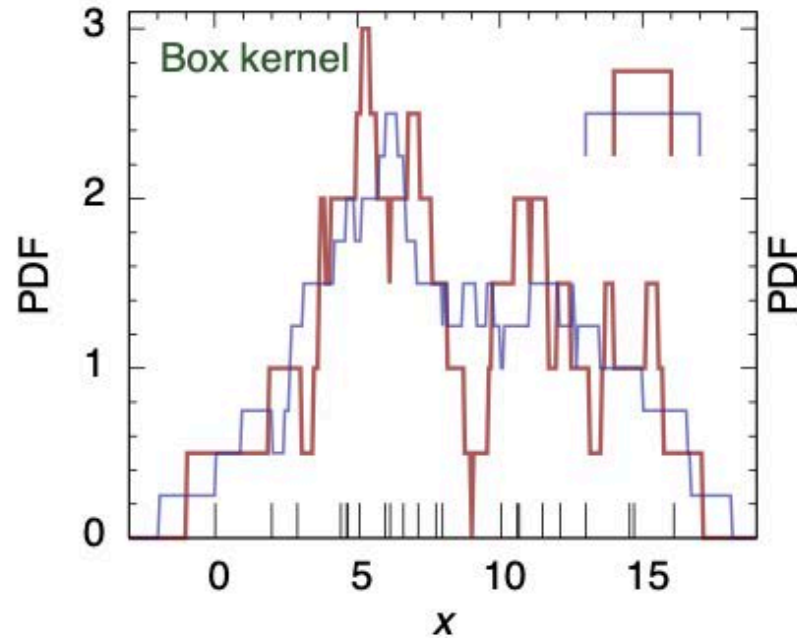
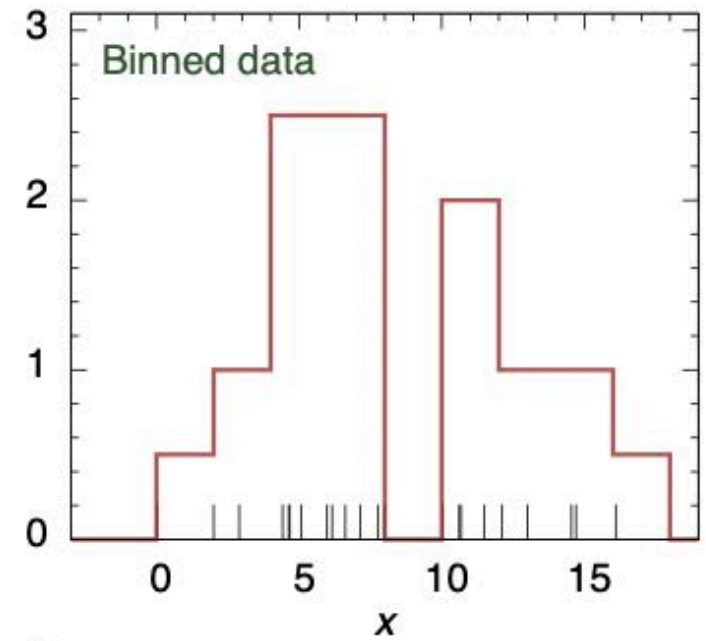
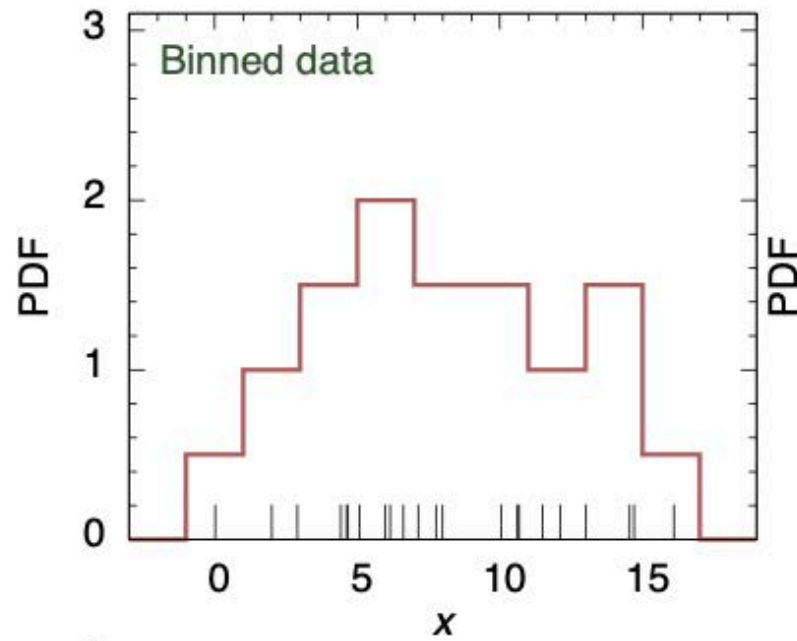
How dark is the Universe?



$$B_3(x) = \frac{|x-2|^3 - 4|x-1|^3 + 6|x|^3 - 4|x+1|^3 + |x+2|^3}{12}.$$



Distributions



Random part of the
sky

